Studies on Pd based catalysts for the electro-oxidation of alcohols

by

ROSHIMA K

Registration No: 10CC17A39002

A thesis submitted to the

Academy of Scientific & Innovative Research

for the award of the degree of

DOCTOR OF PHILOSOPHY

in

SCIENCE

Under the supervision of

Dr. K. G. NISHANTH

CSIR-National Institute for Interdisciplinary Science and Technology (CSIR-NIIST)

Thiruvananthapuram-695019

Academy of Scientific and Innovative Research

AcSIR Headquarters, CSIR-HRDC campus

Sector 19, Kamla Nehru Nagar,

Ghaziabad, U.P. – 201 002, India

July-2023

Dedicated to my beloved Family,

Friends &

God Almighty…

CSIR-NATIONAL INSTITUTE FOR INTERDISCIPLINARY SCIENCE & TECHNOLOGY (CSIR-NIIST)

Council of Scientific & Industrial Research
Thiruvananthapuram - 695 019

Dr. K. G. Nishanth
Senior Scientist
Centre for Sustainable Energy Technologies

Email: nishanthkg@niist.res.in
Mob: 9656728857

CERTIFICATE

This is to certify that the work incorporated in this Ph.D. thesis entitled, "***Studies on Pd based catalysts for the electro-oxidation of alcohols***", submitted by **Mrs. Roshima K** to the Academy of Scientific and Innovative Research (AcSIR), in partial fulfillment of the requirements for the award of the Degree of ***Doctor of Philosophy in Science***, embodies original research work carried-out by the student. We, further certify that this work has not been submitted to any other University or Institution in part or full for the award of any degree or diploma. Research materials obtained from other sources and used in this research work have been duly acknowledged in the thesis. Images, illustrations, figures, tables etc., used in the thesis from other sources, have also been duly cited and acknowledged.

Roshima K

Dr. K G Nishanth

(Research supervisor)

Thiruvananthapuram

July 2023

STATEMENTS OF ACADEMIC INTEGRITY

I, **Roshima K**, a Ph.D. student of the Academy of Scientific and Innovative Research (AcSIR) with Registration No. 10CC17A39002 hereby undertake that, the thesis entitled "***Studies on Pd based catalysts for the electro-oxidation of alcohols***" has been prepared by me and that the document reports original work carried out by me and is free of any plagiarism in compliance with the UGC Regulations on "Promotion of Academic Integrity and Prevention of Plagiarism in Higher Educational Institutions (2018)" and the CSIR Guidelines for "Ethics in Research and in Governance (2020)".

Roshima K

July 2023

Thiruvananthapuram

It is hereby certified that the work done by the student, under my supervision, is plagiarism free in accordance with the UGC Regulations on "Promotion of Academic Integrity and Prevention of Plagiarism in Higher Educational Institutions (2018)" and the CSIR Guidelines for "Ethics in Research and in Governance (2020)".

Dr. K G Nishanth

July 2023

Thiruvananthapuram

DECLARATION

I, Roshima K, bearing AcSIR Registration No.10CC17A39002 declare: that my thesis entitled, "***Studies on Pd based catalysts for the electro-oxidation of alcohols***" is plagiarism free in accordance with the UGC Regulations on "Promotion of Academic Integrity and Prevention of Plagiarism in Higher Educational Institutions (2018)" and the CSIR Guidelines for "Ethics in Research and in Governance (2020)".

I would be solely held responsible if any plagiarized content in my thesis is detected, which is violative of the UGC regulations 2018.

Roshima K

July 2023

Thiruvananthapuram

ACKNOWLEDGEMENTS

First and foremost, I have great pleasure in expressing my deepest gratitude towards my research supervisor, Dr K G Nishanth**,** for suggesting the research problem and guiding me throughout my research work. I thank him for his constant guidance, continuous encouragement and great patience during the course of my research leading to the successful completion of this work on time.

My sincere thanks to:

- Dr C. Anandharamakrishnan and Dr A. Ajayaghosh, present and former Directors of the CSIR-National Institute for Interdisciplinary Science and Technology, for letting me avail the laboratory facilities.
- Dr K. Karunakaran, Dr C.H Suresh and Dr Luxmi Varma, present and former AcSIR program coordinators at CSIR-NIIST, for the help during the academic procedures of AcSIR.
- Dr Narayanan Unni K N, present Head of C-SET, Dr S Ananthakumar, Dr M. Ravi, Dr S. Savitri and Dr. Harikrishna Bhatt, present and former Heads of MSTD, for allowing me to conduct my research at MSTD.
- DAC members (Dr S Ananthakumar, Dr Saju Pillai and Dr Pratish K P) for their valuable suggestions and fruitful discussions throughout my research programme.
- Mr. A Peer Muhammed for XPS, Mr. Harish Raj V for FESEM, Mr. Kiran Mohan for HRTEM.
- Dr. Subrata Das and his students (Ms. Shisina, Mr. Thejas K K, Ms. Malini Abraham, Ms. Sreevalsa, Mr. Renjith) for PXRD measurements.
- All scientists, technical and non-technical staffs, friends and seniors from MSTD and CSTD for their support and help during this journey.
- Mr. C K Chandrakanth, Mr. Kiran Mohan and Mr. Kiran J S for their constant motivation and inspiration during my course of PhD work.
- My wonderful lab mates Mr. Thejus P K, Mrs. Nithyaa J, Ms. Krishnapriya K V, Ms. Meera Sebastian and Ms. Dipannita Ganguly for their advices, suggestions, support and memorable days in the laboratory. My heartfelt gratitude to Mr. Thejus P K and Mrs. Nithyaa J for being my backbone during my research life. A special thanks to

Ms. Krishnapriya K V for the great companionship in all the academic procedures as we started our research programme together.

- Mrs. Surya Suma Kuttan, Ms. Vyshnapriya, Mrs. Nimisha G, Ms. Devika Surendran for their lovely companionship and friendly atmosphere in the laboratory.
- All my hostel mates for making my stay at scholars hostel memorable.
- All my respected teachers from school to till now for teaching me to dream big and fight life with hard work and courage.
- My beloved friends Dr. Swathi V C, Mr. Lijin Rajan, Mr. Deepak Joshy, Mrs. Meghana Mary Thomas, Mr. Vipin G Krishnan, Mrs. Aparna P N, Ms. Jinu joji and Ms. Sabitha Ann Jose for their immense support and irreplaceable friendship.
- Council of Scientific and Industrial Research (CSIR) and Academy of Scientific and Innovative Research (AcSIR), for the financial assistance and academic facilities respectively

I am forever profoundly grateful to my beloved parents and my sister, Kavya R. Their incredible support, motivation, hard work, sacrifice, love and prayers gave wings to my dreams and move me forward in life. I am extremely grateful to my father-in-law and mother-in-law for their endless love, care and encouragement during the last stages of my research life. The unconditional love and care of my partner Adv. Atul Sohan gave me strength to complete my research work. I also greatly acknowledge my whole family for their constant support, love and encouragement to achieve my goals. I extended my thanks to all my dear friends.

Above all, I am grateful to the Almighty for the never ending blessings throughout my life...

Roshima K

TABLE OF CONTENTS

LIST OF ABBREVIATIONS

DAFCs	Direct Alcohol Fuel Cells
IEA	International Energy Agency
T.O.E	Tonnes of Oil Equivalent
AFC	Alkaline Fuel Cell
PEMFC	Polymer Electrolyte Membrane Fuel Cell
DMFC	Direct Methanol Fuel Cell
PAFC	Phosphoric Acid Fuel Cell
MCFC	Molten Carbonate Fuel Cell
SOFC	Solid Oxide Fuel Cell
PEM	Proton Exchange Membrane
AEM	Anion Exchange Membrane
MOR	Methanol Oxidation Reaction
DEFC	Direct Ethanol Fuel Cell
EOR	Ethanol Oxidation Reaction
VC	Vulcan Carbon
CNT	Carbon Nano Tubes
SWNT	Single Walled Nano Tubes
MWNT	Multiple Walled Nano Tubes
NP	Nickel Phosphate
NH	Nickel Hydroxide.
PXRD	Powder X-ray Diffraction
SEM	Scanning Electron Microscopy
TEM	Transmission Electron Microscopy
XPS	X-ray Photoelectron Spectroscopy
ICPMS	Inductively Coupled Plasma Mass Spectrometry

CV	Cyclic Voltammetry
ECSA	Electrochemical Surface Area
EIS	Electrochemical Impedance Spectroscopy
NW	Nickel tungstate
WO	Tungten oxide
NO	Nickel oxide
1D	One Dimensional
SMSI	Strong Metal Support Interaction
Ni NW	Nickel Nanowire
FWHM	Full Width at Half Maximum
EDS	Energy dispersive X-ray spectroscopy
PdAu NW	PdAu Nanowire

LIST OF FIGURES

Chapter 1

Chapter 2

Chapter 3

Chapter 4

Chapter 5

LIST OF SCHEMES

Chapter 2

Chapter 3

Chapter 4

Chapter 5

LIST OF TABLES

PREFACE

The steady growth of world energy demand is driving the development of alternative energy sources. Fuel cell technology has emerged as an alternative and promising energy source where chemical energy directly converts to electrical energy. Among the different types of fuel cells, the simplicity and adaptability of the liquid fuel has made direct alcohol fuel cells (DAFCs) more appealing to portable applications. However, to improve the commercial viability of DAFCs, there are several scientific issues, viz. alcohol crossover, sluggish electrode kinetics and durability, which must be addressed with concurrent improvements in performance characteristics. The insufficient activity of the anode catalysts towards the alcohol oxidation reaction is one of the main drawbacks of DAFCs. Pt metal is widely used as anode catalyst for several decades and is considered to be the best catalyst for anode reactions. The high cost and scarcity of this precious metal remained as an obstacle for the wide scale fabrication of fuel cell. The similar properties, fifty times more abundant and comparatively low cost of palladium metal have gained greater attention as a suitable alternative to platinum. The Pd based catalysts are highly active in alkaline medium, unlike Pt based catalysts. The catalytic activity of Pd can be further enhanced by the incorporation of stable cost effective metals. At present, the research focus is on further enhancement in catalytic activity with reduced Pd content. In the view of above, the different strategies were adapted such as carbon supported Pd, non-carbon based supported Pd, metal alloying and morphology tuning. The thesis aims to develop efficient Pd based catalyst for electro-catalytic alcohol oxidation by reducing the amount of Pd metal.

The thesis comprises of five chapters. Chapter 1 gives a brief introduction to fuel cells, different types of fuel cells and alkaline fuel cells. The chapter details the development of various Pd based catalyst towards alcohol electro-oxidation. The chapter 2 and 3 discuss the development of surface modified carbon supported Pd catalysts and Pd modified one dimensional nano-architecture catalysts were discussed in chapter 4 and 5.

Transition metal phosphates emerge as a potential class of material for many potential electrochemical applications owing its many benefits such as abundance, environmental friendliness and low cost. The second chapter explores the excellent electro-chemical properties of nickel phosphate (NP) as a promoter for alcohol oxidation. Novel NP modified carbon supported Pd was synthesized through a wet chemical method at room temperature. In the presence of NP, homogeneous, well-dispersed Pd particles with reduced size were

observed. Approximately, seven-fold increment in the catalytic efficiency towards methanol oxidation and three fold increment towards ethanol oxidation than unmodified carbon supported pure Pd were achieved. Mass activity of 804.67 and 772.96 mA/mg $_{Pd}$ exhibited by Pd@5%NP/VC for methanol oxidation and ethanol oxidation reaction, respectively. The improved electrochemical property and increased surface area by the combination of Pd with nickel phosphorous compound and supporting carbon material imparted an excellent catalytic efficiency to the synthesized catalyst.

The electronic coupling effect through interfacial engineering between noble metal and transition metal tungstates is considered as an effective strategy to enhance the electrocatalytic activity. In this chapter a new hybrid electrocatalyst consisting of Pd nanoparticle supported on $NiWO_4$ nanocrystals modified carbon was developed for efficient alcohol electro-oxidation reaction. The synthesised catalyst exhibited well dispersed homogeneous Pd particles. Approximately, ten-fold (1202.48 mA/mg$_{Pd}$) and six fold (1508.24 mA/mg$_{Pd}$) increments in the catalytic efficiency towards methanol and ethanol electro- oxidation reaction were obtained. The electronic modification and improved surface area by the combination of Pd with nickel tungstate-carbon support imparted excellent catalytic efficiency for synthesized catalyst.

The fourth chapter describes a cost effective one-dimensional (1D) nano structured electro-catalyst for improved alcohol oxidation reaction. Pd modified Ni nanowire catalyst towards alcohol electro oxidation were prepared by galvanic replacement reaction. Exclusive nano-wire morphology achieved through a wet chemical reduction method without employing any capping agents or surfactants. The Pd modified Ni wires prepared through galvanic replacement reaction. Pd modified Ni nano-wires exhibited a supreme catalytic activity and durability towards alcohol electro-oxidation. The distinctive 1D morphology and strong metal support interaction (SMSI) between Pd and Ni NW along with the bifunctional effects of Pd and Ni attributed to the enhanced catalytic activity. The 10wt% Pd modified Ni nano wire exhibited a mass activity of 1118.35 mA/mg $_{Pd}$ towards methanol oxidation. The amount of precious Pd metal was reduced by 90 wt% with enhanced catalytic efficiency. Ethanol electro-oxidation study showed an improved catalytic activity with mass activity of 1479.79 mA/mg $_{Pd.}$

The fifth chapter includes PdAu nano wires with excellent electro-catalytic activity towards methanol and ethanol oxidation. Ultrathin one-dimensional PdAu nanowires were

prepared rapidly through one step process in which $HAuCl_4$ and H_2PdCl_4 were reduced in the presence of α-naphthol ethanol and $NaBH_4$ solution. Among the prepared catalysts, the 10 wt% Pd contained PdAu nano wire catalyst imparted greater catalytic activity, which exhibited ten times enhancement in activity towards methanol as well as six times higher activity towards ethanol than that of the pure Pd catalyst. A mass activity of 2256.9 and 2932.5 mA/mg_{Pd} obtained for methanol and ethanol oxidation respectively. Eventually, the amount of Pd metal reduced to 90wt% without compromising its catalytic efficiency. Distinctive properties of one-dimensional Au were attributed to the improved catalytic activity. The amount of Pd metal employed was reduced in all the synthesized catalysts without compromising its catalytic efficiency. Further the catalytic activity of the synthesised catalysts were compared with that of commercial Pt/C. The developed Pd based catalysts imparted better catalytic performance than commercial Pt/C towards methanol (806.50 mA/mg_{Pt}) as well as ethanol (875.38 mA/mg_{Pt}) electro-oxidation. Among the prepared catalysts the 10%PdAu catalyst exhibited supreme catalytic activity towards methanol and ethanol oxidation.

Chapter 1

Introduction

1.1 Abstract

In the field of fuel cells, the selection and the development of an efficient catalyst are very vital; consequently, the controllable production of catalysts with a variety of sizes and shapes has attracted extensive interest in this area. Even though the DAFCs (Direct Alcohol Fuel Cells) are known as a promising energy source for fulfilling the inevitable energy demands especially in portable electronic devices, the efficiency of catalysts is still not satisfactory. Until now, Pt has been viewed as the most efficient catalyst for anode reactions. But, the expensive and limited supply of Pt extremely interrupted the large scale manufacturing of DAFC. As an alternative, Pd is considered as a potential candidate owing to its similar properties and availability. Especially, Pd exhibits outstanding activity and stability in alkaline medium. However, it is indeed necessary to reduce the Pd usage because of its cost and at the same time, the activity needs to be further improved. In this regards, the thesis aims to develop highly efficient cost effective Pd based catalysts by reducing the amount of Pd.

1.2 Energy crisis

Global energy demand is everlasting for sustainable development. As the population grows, there is a tremendous rise in energy consumption. The world population is about to reach 9 billion by 2050 and 10 billion by 2100. The International Energy Agency (IEA), Paris, estimated that global energy consumption was climbed from roughly 12 billion Tonnes of Oil Equivalent (T.O.E.) in 2009 to 17-18 billion T.O.E. by 2035. The global energy demand heavily relies on non-renewable fossil fuels for several decades.[1–3] **Figure 1.1** depicts the current status of energy consumption.[4]

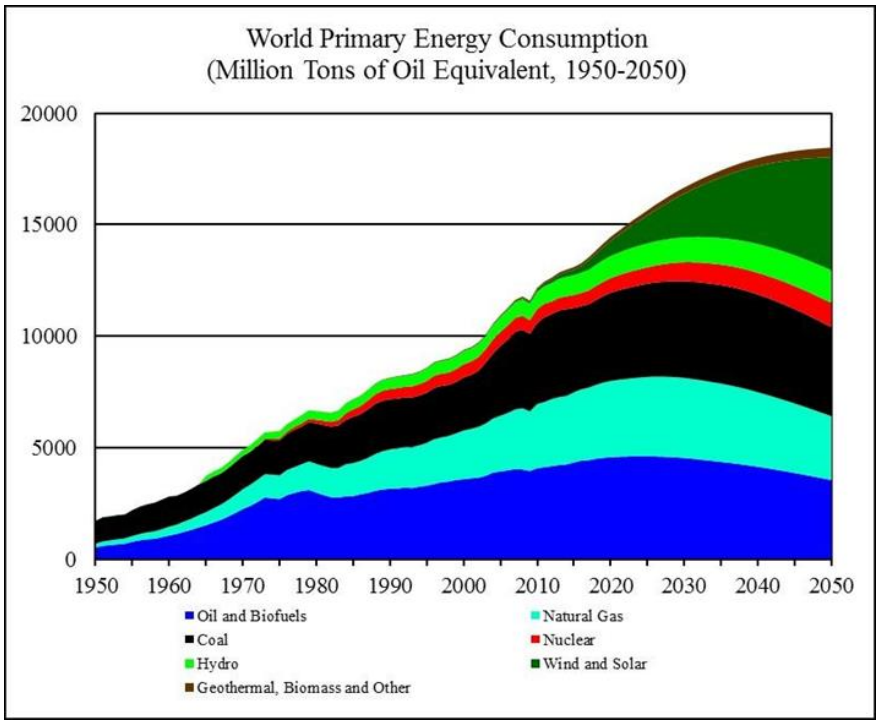

Figure 1.1 World Primary Energy Consumption in million tonnes of oil equivalents.[4]

The world economy and ecosystem will be significantly impacted by energy use and production that depend on fossil fuels. The ongoing industrial revolution has almost outsourced fossil fuel resources, which propelled the need for alternative reliable energy sources. Electrochemical reactions have emerged as a potential alternative energy source since they are very sustainable and environmentally friendly.

1.3 Fuel Cell

Fuel cells are electrochemical devices which can directly convert chemical energy to electrical energy.[5,6] The innovation of fuel cells as an energy conversion system emerged long

ago in the middle of the 19th century. Although the principle was discovered by Christian Friedrich Schönbein, the concept of the Fuel cell was invented by Sir William Robert Grove in 1839. Grove immersed two platinum electrodes on one end in sulphuric acid solution and other two ends in separately sealed hydrogen and oxygen containers. A constant current was noticed to be flowing between the electrodes and the presence of water was found in the sealed containers along with the respective gases. Thus the electrochemical reactions between hydrogen and oxygen lead to electricity generation. It was known as gas battery, and the term Fuel Cell was introduced by British chemists Ludwig Mond and Charles Langer.[7–9] William W Jacques and Emil Baur were the leading researchers in the field of fuel cells in the late 19th and early 20th century. In 1896 Jacques developed the first fuel cell with practical applications and was the first to build a high power fuel cell system of 30 kW. Fransis Bacon, in 1958, developed the first alkaline fuel cell, which later used in the Apollo spacecraft. The first Polymer Electrolyte Membrane Fuel Cell was created by Willard Thomas Grubb and Leonard Niedrach towards the end of 1950 and used by NASA in the Gemini space programme. Since 1970, interest in using fuel cells in automobiles has increased, and since 2007 they have started to commercialize. Fuel cells are considered to be one of the oldest energy conversion technologies. However, their development was prolonged during their first century because of the unrestricted abundance of primary energy sources. Due to the rise in electricity use at the turn of the 20th century, the conversion of chemical energy into electrical energy had more significance.[10,11] Fuel cells produce electricity as long as we supply fuel and oxidants which applied for portable, stationary and transportation applications.[12–14]

1.4 Working Principle of Fuel Cell

Fuel cells can directly convert the electrochemical reaction of hydrogen from hydrogen-containing fuel and oxygen from the air to electricity. It consists of two electrodes, anode (positive electrode) and cathode (negative electrode), and an electrolyte between them. The basic structure of the fuel cell is depicted in **Figure. 1.2**. Electrochemical reactions take place at the electrodes and produce electricity as long as the reactants are supplied.

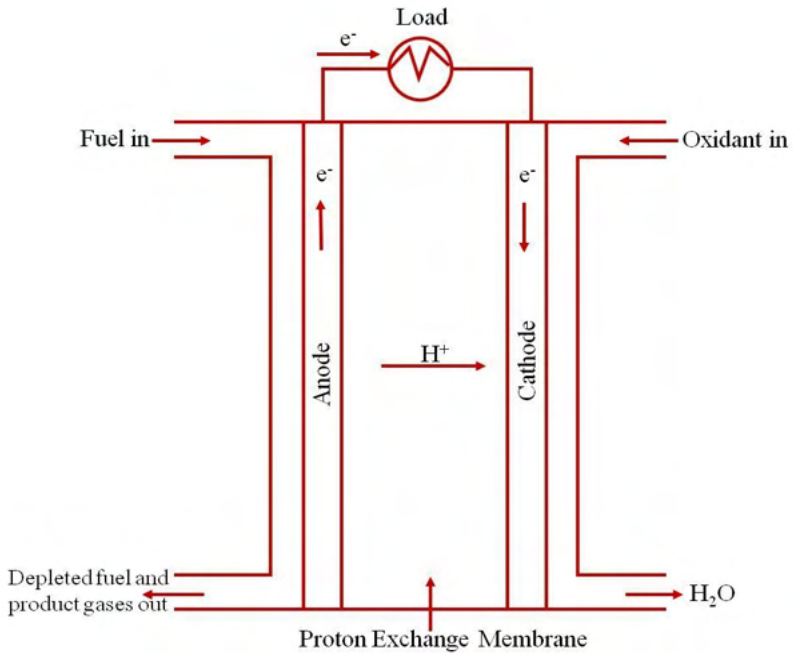

Figure 1.2 Fuel cell operation diagram

Oxidation of fuel takes place at the anode, and reduction of oxygen will undergo on cathode. The transportation of the ions takes place through the electrolyte. The electrodes were connected to an external circuit; during these reactions, electrons flow through the circuit. Fuel cell with a proton conducting electrolyte, oxidation of hydrogen occurs at the anode, and the protons move towards the cathode through the electrolyte. The electrode reactions are given below.[15–19]

$$\text{Anode:} \quad H_2 \rightarrow 2H^+ + 2e^- \tag{1.1}$$

$$\text{Cathode:} \quad 1/2\ O_2 + 2H^+ + 2e^- \rightarrow H_2O \tag{1.2}$$

$$\text{Overall reaction:} \quad H_2 + 1/2\ O_2 \rightarrow H_2O \tag{1.3}$$

The reaction product water is formed at the cathode in the case of proton exchange fuel cells, whereas it can be formed at the anode in the case of anion conducting electrolyte.

1.5 Classification of Fuel Cell

Fuel cells can be classified into different types depending on the electrolyte employed. Based on the operating temperature, fuel cell is also categorized into low temperature and high temperature fuel cell. Alkaline Fuel Cells (AFC), Polymer Electrolyte Membrane Fuel Cells (PEMFC), Direct Methanol Fuel Cells (DMFC) and Phosphoric acid fuel cells (PAFC) come under low temperature fuel cells. High temperature fuel cells consist of molten carbonate (MCFC) and solid oxide fuel cells (SOFC).[20–22] Details of the different types of fuel cells are given in **Table 1.1**.

Table 1.1 Different types of fuel cells

Fuel Cell	Operating temp. (˚C)	Anode reaction	Cathode reaction	Charge carrier
AFC	<100	$H_2+2OH^- \rightarrow 2H_2O+2e^-$	$1/2O_2+H_2O+2e^- \rightarrow 2OH^-$	OH^-
PEMFC	60-120	$H_2 \rightarrow 2H^+ +2\ e^-$	$1/2O_2+2H^+ +2e^- \rightarrow H_2O$	H^+
DMFC	60-120	$CH_3OH+H_2O \rightarrow CO_2+ 6H^+ +6e^-$	$3/2O_2+6H^+ +6e^- \rightarrow 3H_2O$	H^+
PAFC	160-220	$H_2 \rightarrow 2H^+ +2\ e^-$	$1/2O_2+2H^+ +2e^- \rightarrow H_2O$	H^+
MCFC	600-800	$H_2+CO_3^{2-} \rightarrow H_2O+ CO_2+2e^-$	$1/2O_2+CO_2+2e^- \rightarrow CO_3^{2-}$	CO_3^{2-}
SOFC	800-1000	$H_2+O^{2-} \rightarrow H_2O + 2e^-$	$1/2O_2+2e^{--} \rightarrow O^{2-}$	O^{2-}

1.6 Direct Alcohol Fuel Cell (DAFC)

Alcohols are used as the fuel in DAFC, which is an exception in the classification of fuel cells as its classification is not based on the electrolyte employed. Alcohols have received greater attention as an alternative fuel because of its several advantages over conventional fuel hydrogen. Production, storage and transportation are serious concerns related to hydrogen. Hydrogen fuel is flammable and needs to be stored under high pressure.

Generally, at room temperature alcohols are at liquid state. Unlike hydrogen, handling and transportation of alcohols are safe and can be stored in convenience. Moreover, alcohols

have high energy density than that of hydrogen. Basic structure of DAFC consists of an anode, a cathode and an electrolyte separating them. DAFC can generally operate under acidic medium and alkaline medium. Type of electrolyte used and the transporting ion through the electrolyte are different in these two systems. Proton exchange membrane (PEM) is used as the electrolyte in acid fuel cells, where Nafion is the most popular PEM. The electrolyte used in alkaline DAFC is either liquid or solid. Through the anion exchange membrane (AEM), the hydroxyl ions formed at the cathode reach the anode.[14,23–27] Schematic representation of DAFC is shown in **Figure 1.3**.

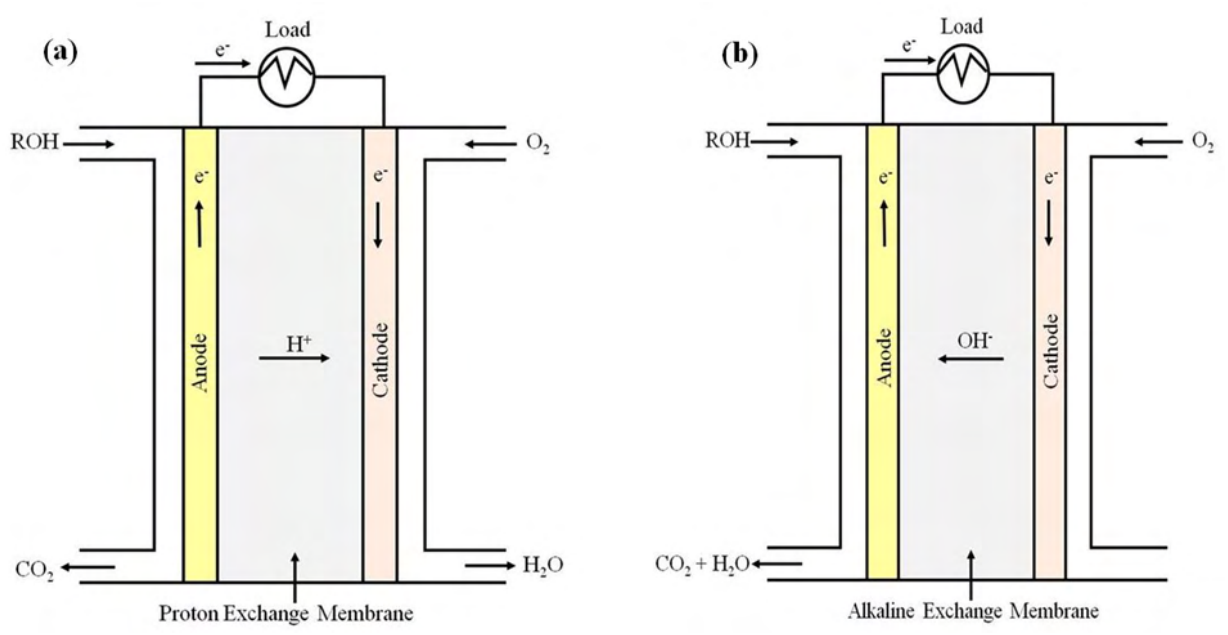

Figure 1.3 Schematic representation of DAFC: (a) PEM-FC, (b) alkaline AEM-DAFC.

General reactions in DAFC which employ an acid electrolyte are,[27]

$$\text{Anode: } C_nH_{2n+1}OH + (2n-1)\,H_2O \rightarrow nCO_2 + 6nH^+ + 6ne^- \quad (1.4)$$

$$\text{Cathode: } 3n/2\,O_2 + 6nH^+ + 6ne^- \rightarrow 3n\,H_2O \quad (1.5)$$

$$\text{Overall cell reaction: } C_nH_{2n+1}OH + 3n/2\,O_2 \rightarrow nCO_2 + (n+1)\,H_2O \quad (1.6)$$

Electrode reactions in DAFC employing anion exchange membrane as an electrolyte are,[27]

$$\text{Anode: } C_nH_{2n+1}OH + 6n\,OH^- \rightarrow nCO_2 + (4n+1)\,H_2O + 6ne^- \quad (1.7)$$

Cathode: $3n/2\ O_2 + 3n\ H_2O + 6ne^- \rightarrow 6n\ OH^-$ (1.8)

Overall cell reaction: $C_nH_{2n+1}OH + 3n/2\ O_2 \rightarrow nCO_2 + (n+1)\ H_2O$ (1.9)

1.6.1 Direct Methanol Fuel Cell (DMFC)

DMFC are most popular in the fuel cell family, and extensive research works are focused on this area. Excellent properties of methanol make DMFC a promising alternative power source. The renewable liquid methanol can be directly fed to the anode without any pre-reforming process. Methanol has advantages such as high electrochemical activity, effectiveness, biodegradability and low cost. The fuel can be easily treated, and it simplifies the fuel cell system.[28–35] Methanol also possesses a high energy density of 4.82 $kWhL^{-1}$ which is much higher than hydrogen (0.53 $kWhL^{-1}$). Methanol is slightly toxic therefore safety measurements should be taken in fuel cell technologies. The simplest alcohol, methanol consisting of only one carbon, can quickly oxidize at the anode. DMFC can convert the energy stored in the methanol directly to electricity.[36–40]

The reaction process in acid based DMFC is given below.[33]

Anode reaction:

$$CH_3OH + H_2O \rightarrow CO_2 + 6H^+ + 6e^- \quad (1.10)$$

Cathode reaction:

$$3/2\ O_2 + 6H^+ + 6e^- \rightarrow 3H_2O \quad (1.11)$$

Overall reaction:

$$CH_3OH + 3/2O_2 \rightarrow CO_2 + 2H_2O \quad (1.12)$$

The reaction process involved in the alkaline based DMFC is shown below.[33]

Anode reaction:

$$CH_3OH + 6OH^- \rightarrow CO_2 + 5H_2O + 6e^- \quad (1.13)$$

Cathode reaction:

$$3/2O_2 + 3H_2O + 6e^- \rightarrow 6OH^- \quad (1.14)$$

Overall reaction:

$$CH_3OH + 3/2O_2 \rightarrow CO_2 + 2H_2O \quad (1.15)$$

1.6.2 Mechanism of Methanol Oxidation Reaction (MOR)

Based on electro-oxidation mechanism on different catalysts, the reaction mechanism of MOR in acidic and alkaline media can be briefly summarized as follows,

1.6.2(a) Mechanism of MOR in acidic medium

The oxidation mechanism of methanol can be summarized as follows.[41]

1) Methanol is adsorbed on the catalyst surface.
2) Methanol dissociates, and the C-H bond oxidises on the catalyst surface.
3) H_2O is adsorbed on the surface of the catalyst and activated by the catalysts, thus OH^-_{ads} is formed.
4) The CO molecules generated during the C-H bond oxidation get oxidized to CO_2 by the OH^-_{ads}.

General methanol oxidation on Pt catalyst surface occurs through a series of steps.

$$CH_3OH + Pt(s) \rightarrow Pt\text{-}CH_2OH + H^+ + e^- \quad (1.16)$$

$$Pt\text{-}CH_2OH + Pt\ (s) \rightarrow Pt_2\text{-}CHOH + H^+ + e^- \quad (1.17)$$

$$Pt_2\text{-}CHOH + Pt\ (s) \rightarrow Pt_3\text{-}CHO + H^+ + e^- \quad (1.18)$$

$$Pt_3\text{-}CHO \rightarrow Pt_2\text{-}CO + Pt\ (s) + H^+ + e^- \quad (1.19)$$

$$Pt_2\text{-}CO + H_2O \rightarrow Pt\text{-}COOH + Pt\ (s) + H^+ + e^- \quad (1.20)$$

$$Pt\text{-}COOH \rightarrow Pt\ (s) + CO_2 + H^+ + e^- \quad (1.21)$$

1.6.2(b) Mechanism of MOR in alkaline medium

The MOR mechanism in the alkaline medium can be described as follows.[41]

1) Methanol, as well as OH^- adsorbed on the catalyst surface
2) Dissociation of methanol to various carbonaceous intermediates takes place.
3) Through the activation of surface adsorbed H_2O molecule, OH^- and OH_{ads} are formed.
4) The intermediates are oxidized by the OH^- and OH_{ads} species to CO_2.

MOR mechanism on Pt catalyst surface in an alkaline medium described as follows.

$$Pt + OH^- \rightarrow Pt\text{-}OH + e^- \quad (1.22)$$

$$Pt\text{-}CH_3OH + OH^- \rightarrow Pt\text{-}(CH_3O) + H_2O + e^- \quad (1.23)$$

$$Pt\text{-}(CH_3O) + OH^- \rightarrow Pt\text{-}(CH_2O) + H_2O + e^- \quad (1.24)$$

$$Pt\text{-}(CH_2O) + OH^- \rightarrow Pt\text{-}(CHO) + H_2O + e^- \quad (1.25)$$

$$Pt\text{-}(CHO) + Pt\text{-}OH + 2OH^- \rightarrow 2Pt + CO_2 + 2H_2O + 2e^- \quad (1.26)$$

1.6.3 Direct Ethanol Fuel Cell (DEFC)

Ethanol is another promising liquid fuel in the development of fuel cells. Ethanol is less toxic than methanol, and it can be produced to a large extent from agricultural products. It is the major renewable biofuel produced from the fermentation of biomass. Ethanol has an energy density of 6.34 $kWhL^{-1}$ which is higher than methanol. Compared to an equal amount of methanol, ethanol can provide more energy and hence more power can be generated. It is the smallest alcohol with C-C bond and is difficult to cleave. The oxidation of ethanol can generate 12 electrons.[42–51]

The electrode reactions in DEFC are as follows.

Reactions occurring in acid medium.[49]

Anode reaction:

$$C_2H_5OH + 3H_2O \rightarrow 2CO_2 + 12\,H^+ + 12e^- \quad (1.27)$$

Cathode reaction:

$$3O_2 + 12\,H^+ + 12e^- \rightarrow 6H_2O \quad (1.28)$$

Overall reaction:

$$C_2H_5OH + 3O_2 \rightarrow 2CO_2 + 3H_2O \quad (1.29)$$

Reaction processes involved in alkaline DEFC.[49]

Anode reaction:

$$C_2H_5OH + 12OH^- \rightarrow 2CO_2 + 9H_2O + 12e^- \quad (1.30)$$

Cathode reaction:

$$3O_2 + 6\,H_2O + 12e^- \rightarrow 12OH^- \quad (1.31)$$

Overall reaction:

$$C_2H_5OH + 3O_2 \rightarrow 2CO_2 + 3H_2O \quad (1.32)$$

1.6.4 Mechanism of Ethanol Oxidation Reaction (EOR)

Ethanol electro-oxidation follows a complicated mechanism. Complete oxidation of ethanol molecule to CO_2 involves cleavage of the C-C bond, multiple dehydrogenation and oxidation steps and can release 12 electrons. The incomplete oxidation of ethanol can lead to acetic acid by delivering 4 electrons or to acetaldehyde by providing 2 electrons without breaking the C-C bond. The two pathways are named as C1 and C2 pathways, according to the number of carbon atoms in the products.[46,52] $PtRhSnO_2$, Au@PtIr/C, Au@AuPd catalysts exhibit $12e^-$ ethanol oxidation.

1.6.4(a) Mechanism of EOR in acidic medium

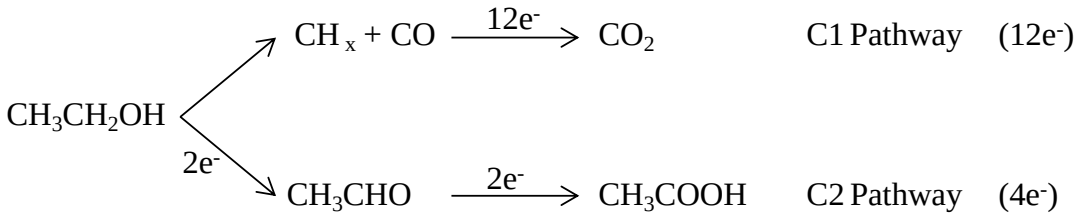

C1 Pathway

$$CH_3CH_2OH + 3H_2O \rightarrow 2CO_2 + 12\,H^+ + 12e^- \quad (1.33)$$

$$CH_3CH_2OH + 5H_2O \rightarrow 2HCO_3^- + 14\,H^+ + 12e^- \quad (1.34)$$

$$CH_3CH_2OH + 5H_2O \rightarrow 2CO_3^{2-} + 16\,H^+ + 12e^- \quad (1.35)$$

C2 Pathway

$$CH_3CH_2OH + H_2O \rightarrow CH_3COOH + 4\,H^+ + 4e^- \quad (1.36)$$

$$CH_3CH_2OH \rightarrow CH_3CHO + 2\,H^+ + 2e^- \quad (1.37)$$

1.6.4(b) Mechanism of EOR in alkaline medium

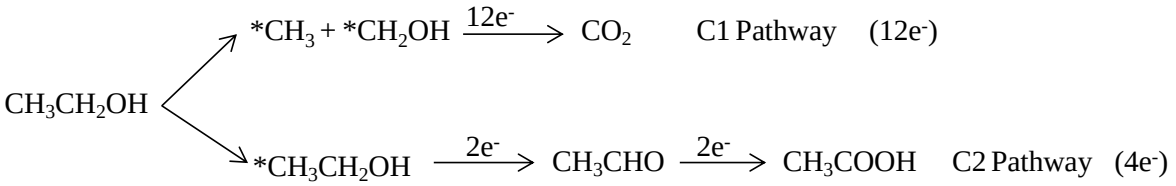

1.7 Major Challenges in DAFC

1.7.1 Sluggish electrode reaction

The electrode reactions are an important parameter and critical factor in fuel cell performance. The slow reaction kinetics can reduce the performance of the fuel cell system. Compared to the hydrogen oxidation in the PEM fuel cell, the rate of alcohol oxidation in the anode is relatively slow in DAFC. The poor alcohol oxidation kinetics leads to a high activation over potential, which reduces the cell's power density and efficiency. The electrodes should provide high catalytic activity, porosity and high conductivity. Pt based catalysts use in the anode and cathode for commercial application. To overcome the slow electrode kinetics DAFC require higher catalyst loading. Pt based catalysts are highly expensive, thus a high catalyst loading will lead to more cost for the fuel cell. Development of highly active electrode catalysts is necessary to overcome the slow electrode kinetics. [33,53–56]

1.7.2 Fuel crossover

Fuel crossover is another issue associated with DAFC. The movement of liquid fuel from the anode to the cathode side through the membrane electrolyte is termed as fuel crossover. Liquid fuel has a concentration gradient on both sides of the electrodes and this concentration difference will cause the transport of fuel from higher concentration to lower concentration, which is from anode to cathode. This will result in the loss of some of the total fuel that needs to be oxidized at the anode for effective electricity production.[57–62] The primary factor causing the fuel diffusion in DAFC is the electro-osmotic drag associated with proton migration through the membrane. The fuel cross-over creates a reduction in fuel consumption, deceleration in cathode activity, excess heat generation, decrease in cell potential and reduction in overall cell function. The type of fuel, concentration of the fuel and operating condition of the fuel system affect the fuel crossover. The fuel crossover will increase with respect to the fuel concentration. At the

same time, the reduced fuel concentration decreases the efficiency of the cell. Determination of optimum concentration is needed to ensure best performance. The presence of fuel impedes the effective electro-reduction kinetics of oxygen at the cathode. In order to counter the effect of fuel crossover, development of better alcohol impermeable membrane and alcohol tolerant oxygen reduction catalysts were necessary.[63–66]

1.7.3 CO poisoning

CO poisoning is one of the significant concerns encountered with the performance of the DAFC system. During the alcohol oxidation reaction, CO species generate as an intermediate and hinder the further reaction kinetics by blocking the active sites of the catalyst. This is known as CO poisoning, one of the worst catalyst deactivating processes.[67–71] CO poisoning remains as a significant hurdle to the activity of the anode catalyst. The CO intermediate can limit the anodic reaction rate, and the slow anode kinetics can decrease cell efficiency. The adsorbed CO molecule should be removed sufficiently for the catalyst to function properly. Enormous efforts have been devoted to mitigating the CO poisoning. The CO molecules can be eliminated through the oxidation process. Alloying with oxophilic materials is a strategy that helps to oxidize the CO intermediates through bifunctional effects. Presence of hydroxyl groups facilitates CO oxidization. High catalyst loading and improved catalyst surface area are other solutions to the sluggish anode kinetics, but it will make the fuel cell expensive. Thus highly active CO tolerant anode catalysts are required to improve cell performance. [72–75]

1.7.4 High cost

The biggest obstacle for the full-fledged commercialization of fuel cells across all power levels is its high cost. The manufacturing cost of DAFC exceeds both PEMFC and Li-ion batteries. The high cost is mainly due to using expensive noble metal catalysts as anode and cathode. The expensive membrane employed also contributes to the high cost. In commercial application, DAFC utilizes Pt based catalysts as both anode and cathode. Reduction in catalyst loading results in decreased cell performance. The effectiveness of the catalyst should be improved to make up for the low catalyst loading.[25,33,56,76–78]

In order to overcome all these hurdles, the development of electrocatalyst which enhance the electrode kinetics for alcohol oxidation, alcohol tolerant catalyst with high activity towards

oxygen reduction and electrolytic membrane with high ionic conductivity and low alcohol crossover are necessary. The thesis focuses on the development of electrocatalyst for anode reaction where the oxidation of alcohol is taking place.

1.8 Electrocatalyst for alcohol oxidation reactions

Fuel cell structure consists of anode and cathode electrodes interconnected with an electrolyte. The electrochemical reactions take place at the interface between the electrode and electrolyte. Catalysts are inevitable components at the electrodes that speed up the electrochemical reaction kinetics at the electrode-electrolyte interface. Catalysts play a crucial role in chemical reactions. The catalysts which take part in electrochemical reactions are referred to as electrocatalysts. The activity and stability of electrocatalyst directly affect fuel cells' performance and service life. The most significant challenge for DAFC is the development of active, robust and low cost electrocatalysts.[79–82] Tremendous efforts were devoted to find out excellent catalysts for fuel cell application. Extensive studies over the decades have found Pt as the outstanding catalyst for anode reaction. However, the high cost, limited supply, and CO adsorbate poisoning of the precious metal hampered its wide-scale application. In this regard, the similar properties and relative abundance of palladium have gained greater attention as an appropriate alternative to platinum. Palladium is fifty times abundant and relatively cheaper than Pt metal, however, it is still an expensive noble metal. It is essential to have a highly efficient and cost-effective electrocatalyst for the large-scale production of DAFC, where the search for an appropriate electrocatalyst is still in pursuit.[46,76,78,83–86]

1.9 Pd based anode catalysts

Pd based catalysts have emerged as potential replacement for Pt metal as anode catalyst in DAFC. Relative abundance and low cost compared to Pt attracted the Pd metal. The real attraction of Pd metal is that it can be highly active in oxidation of various substrates at alkaline environment, where non noble metal is also sufficiently stable for electrochemical application. A number of non-noble metals are also stable in alkaline media and thus enable the incorporation of them with Pd.[87–89] Despite being more abundant than Pt, Pd metal is also precious. Consequently, it is necessary to reduce the amount of Pd owing to its very high cost, and simultaneously, the activity also needs to be improvised. For the past few years, researchers put

efforts into further reduction of Pd metal content so that the DMFC can be commercially more viable. In this view, the highly rated strategies adapted to improve palladium's performance using different carbon based support, non carbon based support, alloying with different metals and tuning variety of morphologies with high surface area.[90–92]

1.9.1 Pd supported on Carbon substrates

One of the highly rated strategies utilized to enhance catalytic activity is using supporting materials. The supported catalyst is an effective method to maximize the utilization of active area of precious metals. A suitable catalyst support should possess a large surface area, high conductivity, better porosity and stability. Usually carbon based supports are used in fuel cell applications. Vulcan carbon (VC), carbon nanotubes (CNT), multiwalled CNT, graphene, etc. are the different carbon based supporting materials. VC (carbon black) is the most commonly used supporting material in fuel cells for studies and commercial applications. Pyrolysis of hydrocarbons produces VC. It consists of spherical particles with a diameter less than 50 nm and a surface area of approximately 250 m^2/g. CNTs are one dimensional nanomaterials with unique structures and properties. The tubes were formed by rolled-up single sheets of hexagonally arranged carbon atoms. They are generally categorized into single walled nanotubes (SWNT) and multiple walled nanotubes (MWNT). MWCNT contains multiple concentric graphene tubes with a constant interlayer separation of 0.34 nm. Compared to commonly used carbon black, carbon nano tubes possess better conductivity, corrosion resistance, mechanical and electrochemical properties. Graphene is a two dimensional thin sheet of carbon atoms arranged in a hexagonal pattern. It possesses high surface area, electronic conductivity, electrochemical stability and electron transfer rate. Planar structure of graphene allows both the edge planes and basal planes to interact with the catalyst particle. Further the catalytic activity is elevated by introducing another metal or metals, binary or ternary metal compounds leading to the formation of Pd alloys or Pd over layer structures.[93–96] Several studies were carried out using Pd supported on different C-based supporting materials. Some of the literature reports were tabulated in **Table 1.2**.

Table 1.2 Pd based catalysts supported on different carbon based supporting materials

Catalyst	Support	Medium	Activity	Ref
Pd-Ni	Carbon	0.5M KOH + 0.6 M MeOH	7.64 mA/cm^2	97
Pd-Ni	Carbon	1 M NaOH + 1 M MeOH	530 mA/mg $_{Pd}$	
Pd-Ni	MWCNT	0.5M NaOH +1 M MeOH	482.2 mA/mg $_{Pd}$	98
Pd_3Mo	VC	1M KOH + 1 M MeOH	71.2 mA/cm^2	99
Pd_3Mo	VC	1M KOH + 1 M EtOH	121.2 mA/cm^2	
Pd_7Ir	VC	1M KOH + 1 M EtOH	0.103 A /cm^2	100
Pd	(NiO/MgO- CNT)	1M KOH + 1 M EtOH	98.20 mA/cm^2	101
Pd	TiO_2-MWCNT	0.5M NaOH +1 M MeOH	41.60 mA/cm^2	102
Pd	TiO_2-MWCNT	0.5M NaOH +1 M EtOH	49.49 mA/cm^2	
$Pd_{90}Au_{10}$	CNT	1M KOH + 1 M EtOH	1050.00 mA/mg$_{Pd}$	103
Cu@Pd	SnO_2- Gr	0.5M NaOH +1 M EtOH	60.28 mA/cm^2	104
40%Pd-5%Ru	GNS	1M KOH + 1 M MeOH	71 mA/cm^2	105
Pd-Ag (1:1)	RGO	1M KOH + 1 M MeOH	630 mA/mg$_{Pd}$	106
Pd-Ag (1:1)	RGO	1M KOH + 1 M EtOH	1601 mA/mg$_{Pd}$	
Pd-Cu (1:1)	RGO	1M KOH + 1 M MeOH	1153.4 mA/mg$_{Pd}$	107
Pd-Cu (1:1)	RGO	1M KOH + 1 M EtOH	2105.4 mA/mg$_{Pd}$	
Pd-Co	RGO	1M KOH + 1 M EtOH	64.2 mA/cm^2	108
PdNi	EGO	0.1M NaOH +1 M EtOH	770.6 mA/mg$_{Pd}$	109
PdSn	SnO_2/C	1M KOH + 1 M EtOH	68.71 mA/cm^2	110
Pd	SnO_2-GNS	0.25M NaOH + 0.25 M EtOH	46.1 mA/cm^2	111
Pd	MWCNT	1M KOH + 1 M MeOH	10.82 mA/cm^2	112
Pd	MWCNT	0.5M NaOH +1 M MeOH	315.1 mA/mg$_{Pd}$	98
PdNi	MWCNT	0.5M NaOH +1 M MeOH	482.2 mA/mg$_{Pd}$	98
Pd	MWCNT	1M KOH + 1 M EtOH	0.663 A/mg$_{Pd}$	113
Pd	MWCNT	1M KOH + 1 M EtOH	9.615 mA/cm^2	114

Pd catalysts loaded on supporting materials enhance the utilization efficiency of Pd particles. Deterioration of the catalytic activity has been attributed to CO poisoning. Alloying Pd with another metal alters the surface electronic state, which may potentially reduce catalyst poisoning and boost catalytic activity and lifetime. Synergistic effect between the metals helps to alleviate CO poisoning. In addition, the carbon supporting materials were further modified with metal oxides as an alternative to increasing the activity and stability of the Pd based catalysts. The combination of oxide materials and carbon substrates can further improve the catalytic performance of Pd supported catalysts through electronic effect and bifunctional mechanism.

Moreover, the electronic coupling effect achieved by the interfacial engineering between Pd and the modified carbon supporting material is considered as an efficient approach to accelerate the intrinsic catalytic activity of Pd. In order to maximize the effectiveness of the catalyst, modification of carbon supporting materials by bimetallic compounds is being explored due to the intense interaction of two types of metals than monometallic compounds. Strong metal support interaction with Pd and supporting material can induce electronic alteration in Pd particles. The electronic modification can lead to a shift in the d band center of Pd, which results in prominent electro catalytic enhancement.[87–89,95,115,116]

An active catalyst needs to be adequately dispersed on convenient supporting material to obtain maximum catalyst utilization. The Vulcan XC-72 carbon offers a high dispersion of metal nanoparticles to enable electron transfer and impart a better catalytic performance. The production and functionalization of carbon supporting materials like CNT, graphene and reduced graphene oxide are tedious and hazardous. Owing to these, in the present thesis VC selected as the supporting material.

1.9.2 Morphology effect of Pd nanostructures

Morphology is another factor which greatly influences the activity of the catalyst. Catalytic performance of the nanostructures can be significantly controlled by the size and morphology. Exposed surface area of the nanostructures is governed by its shape. Catalysts with a variety of morphologies have been investigated, and the morphologies with high surface area got great attention.[117–119] You *et al.* developed a series of core@shell PdAg worm-like network catalysts. Optimized composition $Pd_{76}Ag_{24}$ exhibited superior performance for ethanol oxidation than commercial Pd/C. Mass activity increased 3.5 times than commercial Pd/C. Better activity could be attributed to the network structure, synergistic effect and particular core shell structure.[120] Sheng *et al.* fabricated porous octahedral PdCu nano cages catalyst via disproportionation and displacement method. Morphology of the prepared nano cages were controlled by tuning the molar ratio of the Pd and Cu precursor. Catalyst PdCu-5 having Pd/Cu precursor ratio of 1:5 resulted in a nanocage morphology and exhibited superior catalytic activity compared to the other catalysts and commercial Pd/C. A mass activity of 1090 mA/mg_{Pd} was obtained towards the methanol oxidation, which is 2.9 times higher than that of commercial Pd/C. High porosity and large surface area offered by the hollow and porous nano cage

morphology and the electronic effect between Pd and Cu contributed to the improved catalytic activity.[121] Chen *et al.* reported PdCu flower-like nano cages synthesized through galvanic and disproportionation reactions with corner etched Cu_2O octahedral as templates. H_2PdCl_4/Cu_2O with a molar ratio of 1:1 resulted in PdCu nano cages. As synthesized catalyst displayed high poison tolerance, high electrochemical surface area, good stability and great activity for methanol oxidation in alkaline media.[122] Hasan *et al.* prepared Ni nanowire supported three dimensional flowers-like Pd nanocatalyst. Large electrochemical surface area, excellent electrocatalytic activity, high stability and poisoning tolerance were shown by the novel catalyst for ethanol oxidation. The abundant grain boundaries and three-dimensional open nanostructure of the Pd nano flower helped to improve the activity. The open interspaces of the Ni core ensure alcohol access, and the branched shape and interspaces of the Pd nano flower imparted excellent efficiency.[123] Ding *et al.* investigated PdSn alloy nanosheet dendrites for the first time by an electrodeposition method. The catalyst with a high surface area exhibited excellent activity and long-term stability towards ethanol electro-oxidation. The promotional effects induced due to the dendrites structure like large specific surface area, fast charge transmission, large number of edges and corner atoms, special effects of 2D nanosheets and PdSn alloys helped to improve the performance.[124] Pd concave nanocubes developed by Xie *et al.* exhibited significant enhanced catalytic activity towards methanol oxidation than Pd/C and Pd nanocubes because of the unique morphology, which possess more active sites on the corners and edges.[125] Ma *et al.* obtained Pd nano flowers employing carrageenan as a novel capping agent that is essential for developing nanoflower structures and L ascorbic acid as a reducing agent. It has been discovered that Pd nanoflowers having the longest thorns demonstrated the most significant current density towards ethanol oxidation. In contrast, Pd nanoflowers having short thorns exhibited greater cycle stability.[126] Xiao *et al.* developed a bimetallic screw-like PdPt nanowire through a facile electrochemical synthesis route as a highly active MOR catalyst. The surface of the nanowires is immensely rough, bounded by high-index facets, and exhibits a high number of active sites. The catalyst composition Pd_1Pt_1 showcased a 5.4-fold enhancement in activity for MOR than that of commercial Pt/C.[127] Zhao *et al.* reported PdNi micro cages through a self- assembled growth as a highly effective and long-lasting electrocatalyst for MOR in an alkaline medium. The reaction circumstances were optimised to produce micro cages with a well-defined bicontinuous porous structure. The electrical conductivity, high porosity and atomically stepped surfaces of these

micro cages enable them to deliver a current density of 3.2 $mAcm^2_{Pd}$. The structure remained unaltered after a long term stability test.[128] Guo *et al.* synthesized high quality PdPt porous nano wires through the galvanic replacement method. Subsequent electro catalytic tests carried out have demonstrated superior properties towards MOR. $Pd_{21}Pt_{79}$ presented the best methanol oxidation efficiency, 1.45 times that of Pt/C.[129]

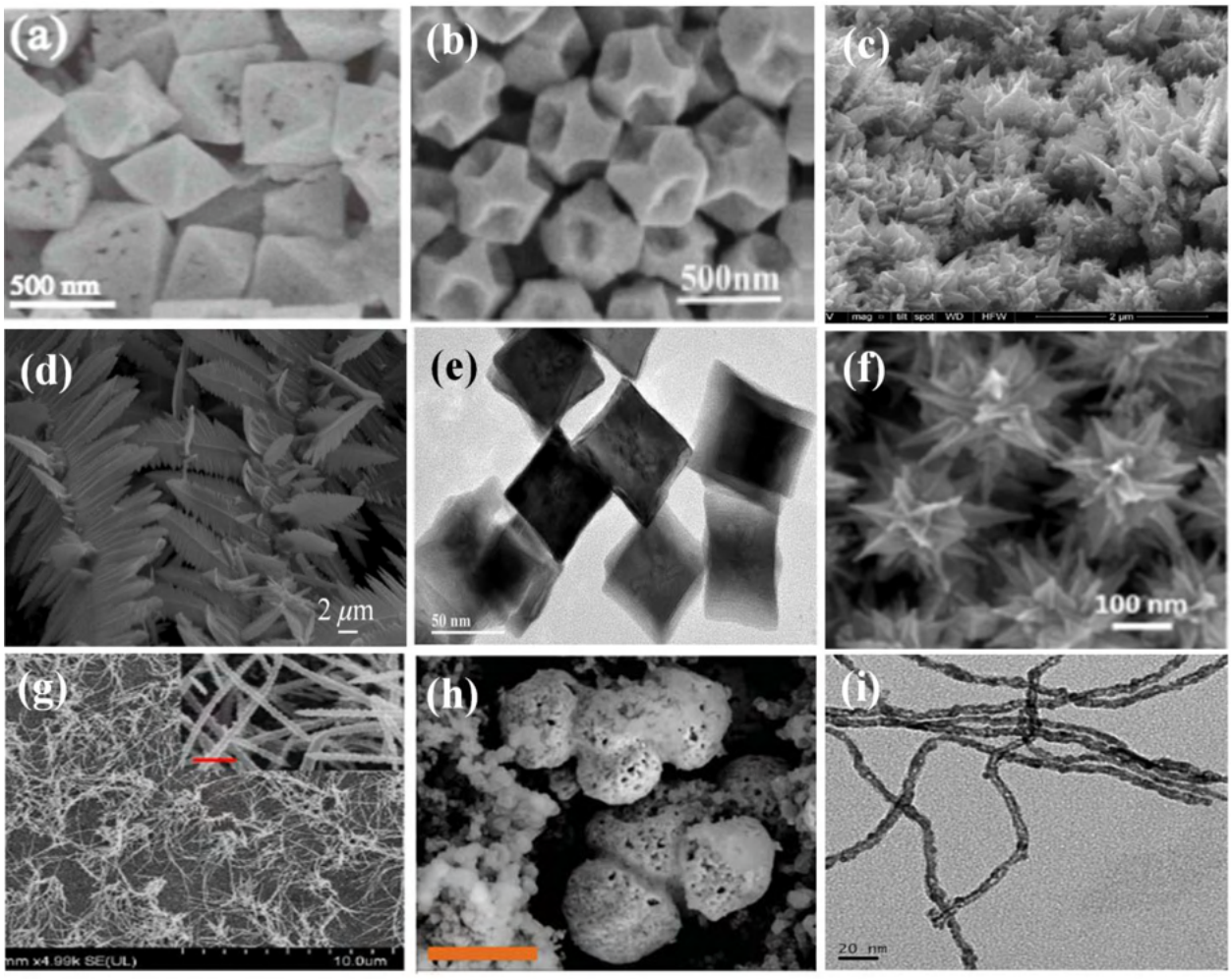

Figure 1.4 Electron micrographs of different reported catalysts.

((a) PdCu nanocage. Reproduced with permission.[121] Copyright 2018, The Royal Society of Chemistry (b) PdCu flower like nanocage. Reproduced with permission.[122] Copyright 2018, American Chemical Society (c) Ni nanowire supported Pd nano flower. Reproduced with permission.[123] Copyright 2012, Elsevier (d) PdSn alloy nano sheet dendrites[124] (e) TEM image of Pd concave nanocube[125], SEM image of (f) Pd nano flowers. Reproduced with permission.[126] Copyright 2018, American Chemical Society (g) PdPt nano wire. Reproduced with permission.[127] Copyright 2018, The Royal Society of Chemistry (h) PdNi microcage. Reproduced with permission.[128]Copyright 2018, The Royal Society of Chemistry (i) TEM image

of PdPt porous nano wire. Reproduced with permission.[129] Copyright 2020, American Chemical Society).

One dimensional nanostructure has emerged as a new class of material in various areas such as catalysis, optoelectronics, nano science, sensing, biological applications, etc. The unique structural features with high aspect ratios hold the key for its fascinating optical and electrical properties. The specific architecture possesses advantages like structural anisotropy, large surface area, increased flexibility and high conductance. The common issues associated with nano particles like dissolution, aggregation and Ostwald ripening can be controlled to an extent. The peculiar structure can promote the electron transport characteristic due to the path-directing effect of structural anisotropy. The easy transport of electrons associated with the 1D structure also favours the enhancement of catalytic activity. The structural robustness provides more active surface area to take part in the reaction and, in turn boost the activity.[130–134]

1.10 Objectives of the thesis

Although significant progress has been achieved in this area Pd based electro-catalysts towards alcohol oxidation reaction, still there is a need to further improve the alcohol oxidation activity and stability of the catalysts. Studies carried out in this thesis deal with the aforementioned issues associated with the development of electro-catalysts for alcohol oxidation reactions. The first two chapters discuss Pd particles supported on modified VC for improved alcohol oxidation reaction. Herein, chapter 2 describes the effect of nickel phosphate modified carbon supported Pd and chapter 3 presents bimetallic $NiWO_4$ as an efficient interface modulator for Pd towards enhanced electro-catalytic alcohol oxidation reactions. Chapter 4 and 5 deals with one dimensional architectures, Pd modified Ni nanowire and PdAu nanowire catalysts.

1.11 References

(1) Chu, S.; Majumdar, A. Opportunities and Challenges for a Sustainable Energy Future. *Nature* **2012**, *488* (7411), 294–303. https://doi.org/10.1038/nature11475.

(2) Pathak, S. Energy Crisis: A Review. *J. Eng. Res. Appl. www.ijera.com* **2014**, *4* (3), 845–851.

(3) Abdeen, M. O. The Energy Crisis, the Role of Renewable and Global Warming. *Greener J. Environ. Manag. Public Saf.* **2012**, *1* (1), 038–070. https://doi.org/10.15580/gjemps.2012.1.103012167.

(4) *World Energy 2017-2050: Annual Report | Seeking Alpha*. https://seekingalpha.com/article/4083393-world-energy-2017minus-2050-annual-report (accessed 2023-05-09).

(5) Maheshwari, K.; Sharma, S.; Sharma, A.; Verma, S. Fuel Cell and Its Applications : A Review. **2018**, *7* (06), 6–9.

(6) Smith, W. The Role of Fuel Cells in Energy Storage. **2000**.

(7) Appleby, A. J. From Sir William Grove to Today: Fuel Cells and the Future. **1990**, *29*, 3–11.

(8) Perry, M. L.; Fuller, T. F. An ECS Centennial Series Article A Historical Perspective of Fuel Cell Technology in the 20th Century. **2002**, 59–67. https://doi.org/10.1149/1.1488651.

(9) Segura, F.; Andu, J. M. Fuel Cells : History and Updating . A Walk along Two Centuries. **2009**, *13*, 2309–2322. https://doi.org/10.1016/j.rser.2009.03.015.

(10) Carrette, B. L.; Friedrich, K. A.; Stimming, U. Fuel Cells ± Fundamentals and Applications. **2001**, No. 1, 5–39.

(11) Lucia, U. Overview on Fuel Cells. *Renew. Sustain. Energy Rev.* **2014**, *30*, 164–169. https://doi.org/10.1016/j.rser.2013.09.025.

(12) Tasa, S. Fuel Cells as Energy Sources For. **2013**, *3* (November 2006), 492–494. https://doi.org/10.1115/1.2349534.

(13) Dufour, A. U. Fuel Cells – a New Contributor to Stationary Power. **1998**, *71*, 19–25.

(14) Fadzillah, D. M.; Kamarudin, S. K.; Zainoodin, M. A.; Masdar, M. S. ScienceDirect Critical Challenges in the System Development of Direct Alcohol Fuel Cells as Portable

Power Supplies : An Overview. *Int. J. Hydrogen Energy* **2018**, No. xxxx. https://doi.org/10.1016/j.ijhydene.2018.11.089.

(15) Mekhilef, S.; Saidur, R.; Safari, A. Comparative Study of Different Fuel Cell Technologies. *Renew. Sustain. Energy Rev.* **2012**, *16* (1), 981–989. https://doi.org/10.1016/j.rser.2011.09.020.

(16) Pan, Z. F.; An, L.; Zhao, T. S.; Tang, Z. K. Advances and Challenges in Alkaline Anion Exchange Membrane Fuel Cells. **2018**, *66*. https://doi.org/10.1016/j.pecs.2018.01.001.

(17) Pan, Z. F.; Chen, R.; An, L.; Li, Y. S. Alkaline Anion Exchange Membrane Fuel Cells for Cogeneration of Electricity and Valuable Chemicals. **2017**, *365*, 430–445. https://doi.org/10.1016/j.jpowsour.2017.09.013.

(18) Haile, S. M. Fuel Cell Materials and Components ଝ. **2003**, *51*, 5981–6000. https://doi.org/10.1016/j.actamat.2003.08.004.

(19) Kirubakaran, A.; Jain, S.; Nema, R. K. A Review on Fuel Cell Technologies and Power Electronic Interface. **2009**, *13*, 2430–2440. https://doi.org/10.1016/j.rser.2009.04.004.

(20) Acres, G. J. K. Recent Advances in Fuel Cell Technology and Its Applications. **2001**, *100*, 60–66.

(21) Singh, A.; Baredar, P.; Khare, H.; Kumar, A. *Fuel Cell : Fundamental , Classi Fi Cation , Application , and Environmental Impact*; Springer Singapore. https://doi.org/10.1007/978-981-10-7326-7.

(22) Review, A. B. New Perspectives on Fuel Cell Technology : **2020**.

(23) Nacef, M.; Affoune, A. M. Comparison between Direct Small Molecular Weight Alcohols Fuel Cells ' and Hydrogen Fuel Cell ' s Parameters at Low and High Temperature . Thermodynamic Study. *Int. J. Hydrogen Energy* **2010**, *36* (6), 4208–4219. https://doi.org/10.1016/j.ijhydene.2010.06.075.

(24) Abdullah, S.; Kamarudin, S. K.; Hasran, U. A.; Masdar, M. S.; Daud, W. R. W. Modeling and Simulation of a Direct Ethanol Fuel Cell : An Overview. *J. Power Sources* **2014**, *262*, 401–406. https://doi.org/10.1016/j.jpowsour.2014.03.105.

(25) Ong, B. C.; Kamarudin, S. K.; Basri, S. ScienceDirect Direct Liquid Fuel Cells : A Review. *Int. J. Hydrogen Energy* **2017**, 1–16. https://doi.org/10.1016/j.ijhydene.2017.01.117.

(26) Yu, E. H. Principles and Materials Aspects of Direct Alkaline Alcohol. **2010**, 1499–1528.

https://doi.org/10.3390/en3081499.

(27) Corti, H. R.; Gonzalez, E. R. *Direct Alcohol Fuel Cells*.

(28) Alias, M. S.; Kamarudin, S. K.; Zainoodin, A. M.; Masdar, M. S. ScienceDirect Active Direct Methanol Fuel Cell : An Overview. *Int. J. Hydrogen Energy* **2020**, No. xxxx. https://doi.org/10.1016/j.ijhydene.2020.04.202.

(29) Samimi, F.; Rahimpour, M. R. *Direct Methanol Fuel Cell*; Elsevier B.V., 2018. https://doi.org/10.1016/B978-0-444-63903-5.00014-5.

(30) Wee, J. A Feasibility Study on Direct Methanol Fuel Cells for Laptop Computers Based on a Cost Comparison with Lithium-Ion Batteries. **2007**, *173*, 424–436. https://doi.org/10.1016/j.jpowsour.2007.04.084.

(31) Aricò, A. S.; Srinivasan, S.; Antonucci, V. DMFCs : From Fundamental Aspects to Technology Development. **2001**, No. 2, 133–161.

(32) Junoh, H.; Jaafar, J.; Abdul, N.; Nordin, H. M.; Ismail, A. F.; Othman, M. H. D. Porous Polyether Sulfone for Direct Methanol Fuel Cell Applications : Structural Analysis. **2020**, No. March, 1–15. https://doi.org/10.1002/er.5921.

(33) Joghee, P.; Malik, J. N. REVIEW A Review on Direct Methanol Fuel Cells – In the Perspective of Energy and Sustainability. **2015**, 1–31. https://doi.org/10.1557/mre.2015.4.

(34) Environ, E.; Zhao, X.; Yin, M.; Ma, L.; Liang, L.; Liu, C.; Liao, J. Environmental Science Recent Advances in Catalysts for Direct Methanol Fuel Cells. **2011**, 2736–2753. https://doi.org/10.1039/c1ee01307f.

(35) Zainoodin, A. M.; Kamarudin, S. K.; Daud, W. R. W. Electrode in Direct Methanol Fuel Cells. *Int. J. Hydrogen Energy* **2010**, *35* (10), 4606–4621. https://doi.org/10.1016/j.ijhydene.2010.02.036.

(36) Demirbas, A. Direct Use of Methanol in Fuel Cells. **2008**, 529–535. https://doi.org/10.1080/15567030600817159.

(37) Olah, G. A. Beyond Oil and Gas : The Methanol Economy **. **2005**, 2636–2639. https://doi.org/10.1002/anie.200462121.

(38) Dillon, R.; Srinivasan, S.; Aricò, A. S.; Antonucci, V. International Activities in DMFC R & D : Status of Technologies and Potential Applications. **2004**, *127*, 112–126. https://doi.org/10.1016/j.jpowsour.2003.09.032.

(39) Lerhun, Â.; Delime, F.; Lamy, C.; Lima, A.; Coutanceau, C.; Le, J. Recent Advances in

the Development of Direct Alcohol Fuel Cells (DAFC). **2002**, *105*.

(40) Kumar, P.; Dutta, K.; Kundu, P. P. Enhanced Performance of Direct Methanol Fuel Cells : A Study on the Combined Effect of Various Supporting Electrolytes , Fl Ow Channel Designs and Operating Temperatures. https://doi.org/10.1002/er.3034.

(41) Tong, Y.; Yan, X.; Liang, J.; Dou, S. X. Metal-Based Electrocatalysts for Methanol Electro-Oxidation : Progress , Opportunities , and Challenges. **2019**, *1904126*. https://doi.org/10.1002/smll.201904126.

(42) An, L.; Zhao, T. S.; Li, Y. S. Carbon-Neutral Sustainable Energy Technology : Direct Ethanol Fuel Cells. **2015**, *50*, 1462–1468. https://doi.org/10.1016/j.rser.2015.05.074.

(43) Akhairi, M. A. F.; Kamarudin, S. K. ScienceDirect Review Article Catalysts in Direct Ethanol Fuel Cell (DEFC): An Overview. *Int. J. Hydrogen Energy* **2016**, 1–15. https://doi.org/10.1016/j.ijhydene.2015.12.145.

(44) Badwal, S. P. S.; Giddey, S.; Kulkarni, A.; Goel, J.; Basu, S. Direct Ethanol Fuel Cells for Transport and Stationary Applications – A Comprehensive Review. *Appl. Energy* **2015**, *145*, 80–103. https://doi.org/10.1016/j.apenergy.2015.02.002.

(45) Kamarudin, M. Z. F.; Kamarudin, S. K.; Masdar, M. S.; Daud, W. R. W. Review : Direct Ethanol Fuel Cells. *Int. J. Hydrogen Energy* **2012**, *38* (22), 9438–9453. https://doi.org/10.1016/j.ijhydene.2012.07.059.

(46) Wang, Y.; Zou, S.; Cai, W. Recent Advances on Electro-Oxidation of Ethanol on Pt- and Pd-Based Catalysts: From Reaction Mechanisms to Catalytic Materials. **2015**, 1507–1534. https://doi.org/10.3390/catal5031507.

(47) Chen, L.; Lu, L.; Zhu, H.; Chen, Y.; Huang, Y.; Li, Y.; Wang, L. Improved Ethanol Electrooxidation Performance by Shortening Pd–Ni Active Site Distance in Pd–Ni–P Nanocatalysts. **2017**, 1–9. https://doi.org/10.1038/ncomms14136.

(48) Yaqoob, L.; Noor, T. A Comprehensive and Critical Review of the Recent Progress in Electrocatalysts for the Ethanol. **2021**, 16768–16804. https://doi.org/10.1039/d1ra01841h.

(49) Monyoncho, E. A.; Woo, K.; Baranova, E. A. *Ethanol Electrooxidation Reaction in Alkaline Media for Direct Ethanol Fuel Cells*; 2019. https://doi.org/10.1039/9781788013895-00001.

(50) Xu, B. C.; Wang, H.; Shen, P. K.; Jiang, S. P. Highly Ordered Pd Nanowire Arrays as Effective Electrocatalysts for Ethanol Oxidation in Direct Alcohol Fuel Cells. **2007**,

510275, 4256–4259. https://doi.org/10.1002/adma.200602911.

(51) An, H.; Pan, L.; Cui, H.; Li, B.; Zhou, D.; Zhai, J.; Li, Q. Electrochimica Acta Synthesis and Performance of Palladium-Based Catalysts for Methanol and Ethanol Oxidation in Alkaline Fuel Cells. *Electrochim. Acta* **2013**, *102*, 79–87. https://doi.org/10.1016/j.electacta.2013.03.142.

(52) Electrocatalyst, P. S.; Liang, Z.; Song, L.; Deng, S.; Zhu, Y.; Stavitski, E.; Adzic, R. R.; Chen, J.; Wang, J. X. Direct 12-Electron Oxidation of Ethanol on a Ternary Au(Core)-PtIr(Shell) Electrocatalyst. **2019**. https://doi.org/10.1021/jacs.9b03474.

(53) Kamarudin, S. K.; Daud, W. R. W.; Ho, S. L.; Hasran, U. A. Overview on the Challenges and Developments of Micro-Direct Methanol Fuel Cells (DMFC). **2007**, *163*, 743–754. https://doi.org/10.1016/j.jpowsour.2006.09.081.

(54) Munjewar, S. S.; Thombre, S. B.; Mallick, R. K. Approaches to Overcome the Barrier Issues of Passive Direct Methanol Fuel Cell – Review. *Renew. Sustain. Energy Rev.* **2017**, *67*, 1087–1104. https://doi.org/10.1016/j.rser.2016.09.002.

(55) Tag, X.; Dx, D. X. X. A.; X, T. D. X. Advances and Challenges in Alkaline Anion Exchange Membrane Fuel Cells. **2018**, *66*. https://doi.org/10.1016/j.pecs.2018.01.001.

(56) Shaari, N. Progress and Challenges : Review for Direct Liquid Fuel Cell. **2021**, No. June 2020, 6644–6688. https://doi.org/10.1002/er.6353.

(57) Cruickshank, J.; Scott, K. The Degree and Effect of Methanol Crossover in the Direct Methanol Fuel Cell. **1998**, *70*, 40–47.

(58) Wang, R.; Zhang, W.; Gao, P. Thin Proton Exchange Membrane-Based Fuel Cells. **2014**, 16416–16423. https://doi.org/10.1039/c4ta03799e.

(59) Choi, S.; Sharma, P. P.; Shah, S. A.; Singh, R.; Kim, D.; Jin, K. Controlling Fuel Crossover in Open Electrochemical Cells by Tuning the Water Nanochannel for Power Generation. **2020**. https://doi.org/10.1021/acssuschemeng.0c01013.

(60) Dicks, A. *Fuel Cell Systems Explained*.

(61) Scott, K.; Taama, W.; Haslar, D. R. A.; Britain, G. Performance of a Direct Methanol Fuel Cell *. **1998**, *28* (August 1996), 289–297.

(62) Kamarudin, S. K.; Achmad, F.; Daud, W. R. W. Overview on the Application of Direct Methanol Fuel Cell (DMFC) for Portable Electronic Devices. *Int. J. Hydrogen Energy* **2009**, *34* (16), 6902–6916. https://doi.org/10.1016/j.ijhydene.2009.06.013.

(63) Qian, W.; Wilkinson, D. P.; Shen, J.; Wang, H.; Zhang, J. Architecture for Portable Direct Liquid Fuel Cells. **2006**, *154*, 202–213. https://doi.org/10.1016/j.jpowsour.2005.12.019.

(64) Heinzel, A. A Review of the State-of-the-Art of the Methanol Crossover in Direct Methanol Fuel Cells. **1999**, 70–74.

(65) Ramya, K.; Dhathathreyan, K. S. Direct Methanol Fuel Cells : Determination of Fuel Crosso v Er in a Polymer Electrolyte Membrane. **2003**, *542*, 109–115. https://doi.org/10.1016/S0022-0728(02)01476-6.

(66) Ahmed, M.; Dincer, I. A Review on Methanol Crossover in Direct Methanol Fuel Cells : Challenges and Achievements. https://doi.org/10.1002/er.1889.

(67) Valdes-lopez, V. F.; Mason, T.; Shearing, P. R.; Brett, D. J. L. Carbon Monoxide Poisoning and Mitigation Strategies for Polymer Electrolyte Membrane Fuel Cells – A Review. *44* (0).

(68) Christoffersen, E.; Liu, P.; Ruban, A.; Skriver, H. L.; Nørskov, J. K. Anode Materials for Low-Temperature Fuel Cells : A Density Functional Theory Study. **2001**, *131*, 123–131. https://doi.org/10.1006/jcat.2000.3136.

(69) Environ, E.; Rossmeisl, J.; Ferrin, P.; Tritsaris, G. A.; Nilekar, U.; Koh, S. Environmental Science Bifunctional Anode Catalysts for Direct Methanol Fuel Cells. **2012**, 8335–8342. https://doi.org/10.1039/c2ee21455e.

(70) Chem, J. M. Nano-Boron Carbide Supported Platinum Catalysts with Much Enhanced Methanol Oxidation Activity and CO Tolerance. **2012**, 9155–9160. https://doi.org/10.1039/c2jm30538k.

(71) Baschuk, J. J.; R, X. L. Carbon Monoxide Poisoning of Proton Exchange Membrane Fuel Cells. **2001**, *713* (April 2000), 695–713. https://doi.org/10.1002/er.713.

(72) Boaventura, M.; Sander, H.; Friedrich, K. A.; Mendes, A. Electrochimica Acta The Influence of CO on the Current Density Distribution of High Temperature Polymer Electrolyte Membrane Fuel Cells. *Electrochim. Acta* **2011**, *56* (25), 9467–9475. https://doi.org/10.1016/j.electacta.2011.08.039.

(73) Lee, M. J.; Kang, J. S.; Kang, Y. S.; Chung, D. Y.; Shin, H.; Ahn, Y.; Park, S.; Kim, M.; Kim, S.; Lee, K.; Sung, Y. Understanding the Bifunctional Effect for Removal of CO Poisoning : Blend of Platinum Nanocatalyst and Hydrous Ruthenium Oxide as a Model System. **2016**. https://doi.org/10.1021/acscatal.5b02580.

(74) Salgado, J. R. C.; Duarte, R. G.; Ilharco, L. M.; Botelho, A. M.; Ferraria, A. M.; Ferreira, M. G. S. Applied Catalysis B : Environmental Effect of Functionalized Carbon as Pt Electrocatalyst Support on the Methanol Oxidation Reaction. *"Applied Catal. B, Environ.* **2011**, *102* (3–4), 496–504. https://doi.org/10.1016/j.apcatb.2010.12.031.

(75) Chung, D. Y.; Kim, H.; Chung, Y.; Lee, M. J.; Yoo, S. J.; Bokare, A. D.; Choi, W.; Sung, Y. Inhibition of CO Poisoning on Pt Catalyst Coupled with the Reduction of Toxic Hexavalent Chromium in a Dual-Functional Fuel Cell. **2014**, No. Iii, 1–5. https://doi.org/10.1038/srep07450.

(76) Kim, K. S.; Tiwari, R. N.; Singh, G. Recent Progress in the Development of Anode and Cathode Catalysts for Direct Methanol Fuel Cells. *Nano Energy* **2013**. https://doi.org/10.1016/j.nanoen.2013.06.009.

(77) Serov, A.; Kwak, C. Applied Catalysis B : Environmental Review of Non-Platinum Anode Catalysts for DMFC and PEMFC Application. **2009**, *90*, 313–320. https://doi.org/10.1016/j.apcatb.2009.03.030.

(78) Manuscript, A. Rsc.Li/Pccp. **2019**, *19*. https://doi.org/10.1039/C9CP03600H.

(79) Braunchweig, B.; Hibbitts, D.; Neurock, M.; Wieckowski, A. Electrocatalysis : A Direct Alcohol Fuel Cell and Surface Science Perspective. *Catal. Today* **2013**, *202*, 197–209. https://doi.org/10.1016/j.cattod.2012.08.013.

(80) Wei, L. *Electrocatalyst Preparation by Electrodeposition*; Elsevier, 2018. https://doi.org/10.1016/B978-0-12-409547-2.13386-4.

(81) Acresa, G. J. K.; Frosta, J. C.; Hards, G. A.; Pottera, R. J.; Ralph, T. R.; Thompsetta, D.; Bursteinb, G. T.; Hutchings, G. J. Electrocatalysts for Fuel Cells. **1997**, *38*.

(82) Ren, X.; Lv, Q.; Liu, L. Sustainable Energy & Fuels Current Progress of Pt and Pt-Based Electrocatalysts Used for Fuel Cells. **2020**, 15–30. https://doi.org/10.1039/c9se00460b.

(83) Karim, N. A.; Kamarudin, S. K. An Overview on Non-Platinum Cathode Catalysts for Direct Methanol Fuel Cell. *Appl. Energy* **2012**. https://doi.org/10.1016/j.apenergy.2012.09.031.

(84) Mansor, M.; Najiha, S.; Long, K. ScienceDirect Recent Progress of Anode Catalysts and Their Support Materials for Methanol Electrooxidation Reaction. *Int. J. Hydrogen Energy* **2019**, No. xxxx. https://doi.org/10.1016/j.ijhydene.2019.04.100.

(85) Antolini, E. Palladium in Fuel Cell Catalysis. **2009**, 915–931.

https://doi.org/10.1039/b820837a.

(86) Wang, L.; Li, Q.; Zhan, T.; Xu, Q. A Review of Pd-Based Electrocatalyst for the Ethanol Oxidation Reaction in Alkaline Medium. **2014**, *863*, 826–830. https://doi.org/10.4028/www.scientific.net/AMR.860-863.826.

(87) Carlos, J.; Gómez, C.; Moliner, R.; Lázaro, M. J. Palladium-Based Catalysts as Electrodes for Direct Methanol Fuel Cells : A Last Ten Years Review. **2016**. https://doi.org/10.3390/catal6090130.

(88) Bianchini, C.; Shen, P. K. Palladium-Based Electrocatalysts for Alcohol Oxidation in Half Cells and in Direct Alcohol Fuel Cells. **2009**, 4183–4206.

(89) Luo, M.; Sun, Y.; Qin, Y.; Li, Y.; Li, C.; Yang, Y. SC. *Mater. Today Nano* **2018**. https://doi.org/10.1016/j.mtnano.2018.04.008.

(90) Yang, F.; Zhang, Y.; Liu, P.; Cui, Y.; Ge, X. ScienceDirect Pd e Cu Alloy with Hierarchical Network Structure as Enhanced Electrocatalysts for Formic Acid Oxidation. *Int. J. Hydrogen Energy* **2016**, *41* (16), 6773–6780. https://doi.org/10.1016/j.ijhydene.2016.02.145.

(91) Online, V. A.; Duan, B.; Yan, B.; Feng, Y.; Zhang, K.; Wang, J.; Wang, C.; Shiraishi, Y.; Yang, P.; Du, Y. RSC Advances. **2016**. https://doi.org/10.1039/C6RA14321K.

(92) Carvalho, L. L.; Colmati, F.; Tanaka, A. A. ScienceDirect Nickel e Palladium Electrocatalysts for Methanol , Ethanol , and Glycerol Oxidation Reactions. *Int. J. Hydrogen Energy* **2017**, 1–9. https://doi.org/10.1016/j.ijhydene.2017.05.124.

(93) Sui, S.; Wang, X.; Zhou, X.; Su, Y.; Riffat, S.; Liu, C. jun. A Comprehensive Review of Pt Electrocatalysts for the Oxygen Reduction Reaction: Nanostructure, Activity, Mechanism and Carbon Support in PEM Fuel Cells. *J. Mater. Chem. A* **2017**, *5* (5), 1808–1825. https://doi.org/10.1039/C6TA08580F.

(94) Basri, S.; Kamarudin, S. K.; Daud, W. R. W.; Yaakub, Z. Nanocatalyst for Direct Methanol Fuel Cell (DMFC). *Int. J. Hydrogen Energy* **2010**, *35* (15), 7957–7970. https://doi.org/10.1016/j.ijhydene.2010.05.111.

(95) Sharma, S.; Pollet, B. G. Support Materials for PEMFC and DMFC Electrocatalysts - A Review. *J. Power Sources* **2012**, *208*, 96–119. https://doi.org/10.1016/j.jpowsour.2012.02.011.

(96) Monyoncho, E. A.; Ntais, S.; Brazeau, N.; Wu, J. J.; Sun, C. L.; Baranova, E. A. Role of

the Metal-Oxide Support in the Catalytic Activity of Pd Nanoparticles for Ethanol Electrooxidation in Alkaline Media. *ChemElectroChem* **2016**, *3* (2), 218–227. https://doi.org/10.1002/celc.201500432.

(97) Amin, R. S.; Abdel Hameed, R. M.; El-Khatib, K. M.; Elsayed Youssef, M. Electrocatalytic Activity of Nanostructured Ni and Pd-Ni on Vulcan XC-72R Carbon Black for Methanol Oxidation in Alkaline Medium. *Int. J. Hydrogen Energy* **2014**, *39* (5), 2026–2041. https://doi.org/10.1016/j.ijhydene.2013.11.033.

(98) Zhao, Y.; Yang, X.; Tian, J.; Wang, F.; Zhan, L. Methanol Electro-Oxidation on Ni @ Pd Core-Shell Nanoparticles Supported on Multi-Walled Carbon Nanotubes in Alkaline Media. *Int. J. Hydrogen Energy* **2010**, *35* (8), 3249–3257. https://doi.org/10.1016/j.ijhydene.2010.01.112.

(99) Fathirad, F.; Mostafavi, A.; Afzali, D. ScienceDirect Bimetallic Pd e Mo Nanoalloys Supported on Vulcan XC-72R Carbon as Anode Catalysts for Direct Alcohol Fuel Cell. *Int. J. Hydrogen Energy* **2016**, 1–7. https://doi.org/10.1016/j.ijhydene.2016.09.138.

(100) Shen, S. Y.; Zhao, T. S.; Xu, J. B. Electrochimica Acta Carbon-Supported Bimetallic PdIr Catalysts for Ethanol Oxidation in Alkaline Media. **2010**, *55*, 9179–9184. https://doi.org/10.1016/j.electacta.2010.09.018.

(101) Mahendiran, C.; Rajesh, D.; Maiyalagan, T. Pd Nanoparticles-Supported Carbon Nanotube-Encapsulated NiO / MgO Composite as an Enhanced Electrocatalyst for Ethanol Electrooxidation in Alkaline Medium. **2017**, 11438–11444. https://doi.org/10.1002/slct.201702357.

(102) An, H.; Pan, L.; Cui, H.; Zhou, D.; Wang, B.; Zhai, J.; Li, Q.; Pan, Y. Electrocatalytic Performance of Pd Nanoparticles Supported on TiO 2 -MWCNTs for Methanol , Ethanol , and Isopropanol in Alkaline Media. *J. Electroanal. Chem.* **2015**, *741*, 56–63. https://doi.org/10.1016/j.jelechem.2015.01.015.

(103) Caglar, A.; Kivrak, H. ScienceDirect Highly Active Carbon Nanotube Supported PdAu Alloy Catalysts for Ethanol Electrooxidation in Alkaline Environment. *Int. J. Hydrogen Energy* **2019**, No. xxxx. https://doi.org/10.1016/j.ijhydene.2019.03.118.

(104) Hameed, R. M. A.; Fahim, A. E.; Allam, N. K. Tin Oxide as a Promoter for Copper@palladium Nanoparticles on Graphene Sheets during Ethanol Electro-Oxidation in NaOH Solution. *J. Mol. Liq.* **2019**, 111816.

https://doi.org/10.1016/j.molliq.2019.111816.

(105) Awasthi, R.; Singh, R. N. Graphene-Supported Pd – Ru Nanoparticles with Superior Methanol Electrooxidation Activity. *Carbon N. Y.* **2012**, *51*, 282–289. https://doi.org/10.1016/j.carbon.2012.08.055.

(106) Li, L.; Chen, M.; Huang, G.; Yang, N.; Zhang, L.; Wang, H.; Liu, Y.; Wang, W.; Gao, J. A Green Method to Prepare Pd e Ag Nanoparticles Supported on Reduced Graphene Oxide and Their Electrochemical Catalysis of Methanol and Ethanol Oxidation. *J. Power Sources* **2014**, *263*, 13–21. https://doi.org/10.1016/j.jpowsour.2014.04.021.

(107) Na, H.; Zhang, L.; Qiu, H.; Wu, T.; Chen, M.; Yang, N.; Li, L.; Xing, F.; Gao, J. A Two Step Method to Synthesize Palladium e Copper Nanoparticles on Reduced Graphene Oxide and Their Extremely High Electrocatalytic Activity for the Electrooxidation of Methanol and Ethanol. *J. Power Sources* **2015**, *288*, 160–167. https://doi.org/10.1016/j.jpowsour.2015.04.116.

(108) Rostami, H.; Rostami, A. A.; Omrani, A. ScienceDirect Investigation on Ethanol Electrooxidation via Electrodeposited Pd e Co Nanostructures Supported on Graphene Oxide. *Int. J. Hydrogen Energy* **2015**, *40* (33), 10596–10604. https://doi.org/10.1016/j.ijhydene.2015.06.151.

(109) Tan, J. L.; Jesus, A. M. De; Chua, S. L.; Sanetuntikul, J.; Shanmugam, S.; John, B.; Tongol, V.; Kim, H. Applied Catalysis A : General Preparation and Characterization of Palladium-Nickel on Graphene Oxide Support as Anode Catalyst for Alkaline Direct Ethanol Fuel Cell. *"Applied Catal. A, Gen.* **2017**, *531*, 29–35. https://doi.org/10.1016/j.apcata.2016.11.034.

(110) Mao, H.; Wang, L.; Zhu, P.; Xu, Q.; Li, Q. ScienceDirect Carbon-Supported PdSn e SnO 2 Catalyst for Ethanol Electro-Oxidation in Alkaline Media. *Int. J. Hydrogen Energy* **2014**, *39* (31), 17583–17588. https://doi.org/10.1016/j.ijhydene.2014.08.079.

(111) Wen, Z.; Yang, S.; Liang, Y.; He, W.; Tong, H.; Hao, L. Electrochimica Acta The Improved Electrocatalytic Activity of Palladium / Graphene Nanosheets towards Ethanol Oxidation by Tin Oxide. *Electrochim. Acta* **2010**, *56* (1), 139–144. https://doi.org/10.1016/j.electacta.2010.09.032.

(112) Kiyani, R.; Javad, M.; Rowshanzamir, S. ScienceDirect Investigation of the Effect of Carbonaceous Supports on the Activity and Stability of Supported Palladium Catalysts for

Methanol Electro-Oxidation Reaction. *Int. J. Hydrogen Energy* **2017**, 1–15. https://doi.org/10.1016/j.ijhydene.2017.07.113.

(113) Wang, Y.; He, Q.; Ding, K.; Wei, H.; Guo, J.; Wang, Q.; O'Connor, R.; Huang, X.; Luo, Z.; Shen, T. D.; Wei, S.; Guo, Z. Multiwalled Carbon Nanotubes Composited with Palladium Nanocatalysts for Highly Efficient Ethanol Oxidation. *J. Electrochem. Soc.* **2015**, *162* (7), F755–F763. https://doi.org/10.1149/2.0751507jes.

(114) Wang, Y.; He, Q.; Guo, J.; Wang, J.; Luo, Z.; Shen, T. D.; Ding, K.; Khasanov, A.; Wei, S.; Guo, Z. Ultrafine FePd Nanoalloys Decorated Multiwalled Cabon Nanotubes toward Enhanced Ethanol Oxidation Reaction. *ACS Appl. Mater. Interfaces* **2015**, *7* (43), 23920–23931. https://doi.org/10.1021/acsami.5b06194.

(115) Chen, A.; Ostrom, C. Palladium-Based Nanomaterials : Synthesis and Electrochemical Applications. **2020**. https://doi.org/10.1021/acs.chemrev.5b00324.

(116) Meng, H.; Zeng, D.; Xie, F. Recent Development of Pd-Based Electrocatalysts for Proton Exchange Membrane Fuel Cells. **2015**, 1221–1274. https://doi.org/10.3390/catal5031221.

(117) Sheng, J.; Kang, J.; Hu, Z.; Yu, Y.; Fu, X. Z.; Sun, R.; Wong, C. P. Octahedral Pd Nanocages with Porous Shells Converted from Co(OH)2 Nanocages with Nanosheet Surfaces as Robust Electrocatalysts for Ethanol Oxidation. *J. Mater. Chem. A* **2018**, *6* (32), 15789–15796. https://doi.org/10.1039/c8ta04181d.

(118) Xiong, Y.; McLellan, J. M.; Chen, J.; Yin, Y.; Li, Z. Y.; Xia, Y. Kinetically Controlled Synthesis of Triangular and Hexagonal Nanoplates of Palladium and Their SPR/SERS Properties. *J. Am. Chem. Soc.* **2005**, *127* (48), 17118–17127. https://doi.org/10.1021/ja056498s.

(119) Liu, M.; Zheng, Y.; Zhang, L.; Guo, L.; Xia, Y. Transformation of Pd Nanocubes into Octahedra with Controlled Sizes by Maneuvering the Rates of Etching and Regrowth. *J. Am. Chem. Soc.* **2013**, *135* (32), 11752–11755. https://doi.org/10.1021/ja406344j.

(120) You, H.; Gao, F.; Song, T.; Zhang, Y.; Wang, H.; Liu, X.; Yuan, M.; Wang, Y.; Du, Y. Tunable Long-Chains of Core@shell PdAg@Pd as High-Performance Catalysts for Ethanol Oxidation. *J. Colloid Interface Sci.* **2020**, *574*, 182–189. https://doi.org/10.1016/j.jcis.2020.04.051.

(121) Sheng, J.; Kang, J.; Ye, H.; Xie, J.; Zhao, B.; Fu, X. Z.; Yu, Y.; Sun, R.; Wong, C. P. Porous Octahedral PdCu Nanocages as Highly Efficient Electrocatalysts for the Methanol

Oxidation Reaction. *J. Mater. Chem. A* **2018**, *6* (9), 3906–3912. https://doi.org/10.1039/c7ta07879j.

(122) Chen, Z.; He, Y. C.; Chen, J. H.; Fu, X. Z.; Sun, R.; Chen, Y. X.; Wong, C. P. PdCu Alloy Flower-like Nanocages with High Electrocatalytic Performance for Methanol Oxidation. *J. Phys. Chem. C* **2018**, *122* (16), 8976–8983. https://doi.org/10.1021/acs.jpcc.8b01095.

(123) Hasan, M.; Newcomb, S. B.; Rohan, J. F.; Razeeb, K. M. Ni Nanowire Supported 3D Flower-like Pd Nanostructures as an Efficient Electrocatalyst for Electrooxidation of Ethanol in Alkaline Media. *J. Power Sources* **2012**, *218*, 148–156. https://doi.org/10.1016/j.jpowsour.2012.06.017.

(124) Ding, L. X.; Wang, A. L.; Ou, Y. N.; Li, Q.; Guo, R.; Zhao, W. X.; Tong, Y. X.; Li, G. R. Hierarchical Pd-Sn Alloy Nanosheet Dendrites: An Economical and Highly Active Catalyst for Ethanol Electrooxidation. *Sci. Rep.* **2013**, *3*, 1–7. https://doi.org/10.1038/srep01181.

(125) Xie, X.; Gao, G.; Pan, Z.; Wang, T.; Meng, X.; Cai, L. Large-Scale Synthesis of Palladium Concave Nanocubes with High-Index Facets for Sustainable Enhanced Catalytic Performance. *Sci. Rep.* **2014**, *5*, 1–5. https://doi.org/10.1038/srep08515.

(126) Ma, N.; Liu, X.; Yang, Z.; Tai, G.; Yin, Y.; Liu, S.; Li, H.; Guo, P.; Zhao, X. S. Carrageenan Asissted Synthesis of Palladium Nanoflowers and Their Electrocatalytic Activity toward Ethanol. *ACS Sustain. Chem. Eng.* **2018**, *6* (1), 1133–1140. https://doi.org/10.1021/acssuschemeng.7b03425.

(127) Tang, J. X.; Chen, Q. S.; You, L. X.; Liao, H. G.; Sun, S. G.; Zhou, S. G.; Xu, Z. N.; Chen, Y. M.; Guo, G. C. Screw-like PdPt Nanowires as Highly Efficient Electrocatalysts for Methanol and Ethylene Glycol Oxidation. *J. Mater. Chem. A* **2018**, *6* (5), 2327–2336. https://doi.org/10.1039/c7ta09595c.

(128) Zhao, M.; Kang, Z.; Chen, Q.; Yu, X.; Wu, Y.; Fan, X.; Yan, X.; Lin, Y.; Xia, T.; Cai, W. Self-Assembled Growth of Pd-Ni Sub-Microcages as a Highly Active and Durable Electrocatalyst. *J. Mater. Chem. A* **2019**, *7* (10), 5179–5184. https://doi.org/10.1039/c8ta10331c.

(129) Guo, T.; Xiang, H.; Li, W.; Li, H.; Chen, H.; Liu, S.; Yu, G. Synthesis of Ultrathin and Composition-Tunable PdPt Porous Nanowires with Enhanced Electrocatalytic Performance. *ACS Sustain. Chem. Eng.* **2020**, *8* (7), 2901–2909.

https://doi.org/10.1021/acssuschemeng.9b07189.

(130) Hong, W.; Wang, J.; Wang, E. Dendritic Au/Pt and Au/PtCu Nanowires with Enhanced Electrocatalytic Activity for Methanol Electrooxidation. *Small* **2014**, *10* (16), 3262–3265. https://doi.org/10.1002/smll.201400059.

(131) Lu, Y.; Du, S.; Steinberger-Wilckens, R. *One-Dimensional Nanostructured Electrocatalysts for Polymer Electrolyte Membrane Fuel Cells—A Review*; Elsevier B.V., 2016; Vol. 199. https://doi.org/10.1016/j.apcatb.2016.06.022.

(132) Xu, H.; Wei, J.; Zhang, M.; Wang, C.; Shiraishi, Y.; Guo, J.; Du, Y. Solvent-Mediated Length Tuning of Ultrathin Platinum-Cobalt Nanowires for Efficient Electrocatalysis. *J. Mater. Chem. A* **2018**, *6* (47), 24418–24424. https://doi.org/10.1039/c8ta08251k.

(133) Feng, Y.; Bu, L.; Guo, S.; Guo, J.; Huang, X. 3D Platinum–Lead Nanowire Networks as Highly Efficient Ethylene Glycol Oxidation Electrocatalysts. *Small* **2016**, 4464–4470. https://doi.org/10.1002/smll.201601620.

(134) Yin, Y.; Lu, Y.; Sun, Y.; Xia, Y. Silver Nanowires Can Be Directly Coated with Amorphous Silica to Generate Well-Controlled Coaxial Nanocables of Silver/Silica. *Nano Lett.* **2002**, *2* (4), 427–430. https://doi.org/10.1021/nl025508+.

Chapter 2

Nickel Phosphate Modified Carbon Supported Pd Catalyst for Enhanced Alcohol Electro Oxidation

2.1 Abstract

Transition metal phosphates are emerging as a novel class of material for many potential electrochemical applications owing to its several advantages like abundance, environmental friendliness and low cost. The present chapter explored the excellent electro chemical property of monometallic nickel phosphate, $Ni_3(PO_4)_2$ (NP) modified carbon supported Pd for alcohol oxidation. Novel Pd@NP modified VC was synthesized through a very simple method at room temperature. In the presence of NP well dispersed homogeneous Pd particles having reduced size was observed. Approximately, seven-fold increments in the catalytic efficiency towards methanol oxidation and three fold increments towards ethanol oxidation than VC supported pure Pd were achieved. The improved electrochemical property and increased surface area by combining Pd with nickel phosphorous compound and supporting carbon material imparted an excellent catalytic efficiency to the synthesized catalyst.

2.2 Introduction

Urge for an alternative energy source demands the development of cost effective highly efficient catalyst for fuel cell applications. Ni metal, Ni alloy and Ni complexes were found to perform very good electro chemical activity.[1-3] Nickel-phosphorous compounds such as Ni_2P, $Ni_2P_2O_7$ and $Ni_xCo_{3-x}(PO_4)_2$ were gained considerable attention as new electrode materials.[4] The Ni-P alloy acts as an excellent catalyst in decomposing water, lithium-ion battery and super capacitor applications.[5] Ni_2P, Ni_5P_4, solvothermal derived amorphous Ni-P powders, and nickel phosphates are reported as wonderful candidates for supercapacitor electrodes.[5] $Ni(PO_3)_2$ nano sheet and $Ni_3(PO_4)_2$@GO exhibit superior capacitance behavior.[6,7] NP is considered as a promising electrode material due to its significant faradaic pseudo capacitance, low cost and easy fabrication.[4, 7] But the low intrinsic electrical conductivity and relatively low rate capability are the key challenges associated with NP as an electrode material for capacitor application. Combining Ni-P compounds with carbon materials can enhance the electro chemical performance.[4] $Ni_3(PO_4)_2.8H_2O$ modified electrode was used for electrocatalytic oxidation of glucose, formaldehyde and it also act as a supercapattery electrode material.[8-10] Ultra-long nanowires of NP were used for the oxidation of glucose and $Ni_{12}P_5/Ni_3(PO_4)_2$ hollow sphere was employed for H_2O electrolysis.[11, 12] Similarly, Fe doped NP and $Ni_2P_2O_7$ were reported for water oxidation and H_2 production respectively.[13, 14]

Although NP is used in the field of supercapacitor, sensor, and as electrocatalysts for various application, it is not much explored for fuel cell applications.[15, 16] The properties of NP make it a fascinating material for fuel cell applications. The oxophilic nature of nickel and phosphorus increases CO tolerance and there by improves electrocatalytic activity.[8] Thus, combining NP with Pd will reduce CO poisoning and enhance the catalytic activity of Pd towards alcohol oxidation. Even though the catalytic performance of mesoporous, porous chain like network and Si-incorporated mesoporous NP were studied, the surface modification of VC with NP and Pd for alcohol oxidation was not yet explored.[1, 2, 15, 16]

This chapter focuses on facilitating the electrocatalytic activity of Pd particles towards alcohol oxidation by incorporating it with monometallic NP modified VC. The synergism of the components plays a crucial role in the catalyst's performance. The metal provides the active sites for alcohol oxidation, where Ni and P help to oxidize the carbonaceous poisons and thereby

release the active sites. The presence of VC imparts good electrical conductivity and high surface area, thus improves the catalysis. Hence, the collective action of the components contributes towards enhanced alcohol oxidation.

2.3 Experimental section

2.3.1 Materials and reagents

Nickel (II) chloride (99.99%), $PdCl_2$ (99.99%), KOH (99.99%), $NaBH_4$ (99.99%), methanol (99.9%), and ethanol (99.9%) were purchased from Merck. Vulcan XC 72 R was obtained from Cabot Corp. $NH_4H_2PO_4$ (99.9%) was obtained from Fisher Scientific. All chemicals were used without any further purification.

2.3.2 Preparation of NP/VC catalyst

Required amount of $NiCl_2$ and $NH_4H_2PO_4$ were dissolved in 50 ml VC dispersion and stirred well using magnetic stirrer. Further, 0.5 M KOH solution added drop wise as a precipitating agent, and the obtained mixture was stirred for 2 h.[15]

$$NiCl_2 + 2\ KOH \rightarrow Ni(OH)_2 + 2KCl \quad (1)$$

$$NH_4H_2PO_4 \rightarrow NH_4^+ + H_2PO_4^- \quad (2)$$

$$Ni(OH)_2 + NH_4^+ + H_2PO_4^- \rightarrow NH_4NiPO_4 + 2H_2O \quad (3)$$

The resulting precipitate was collected and washed well with distilled water. The obtained powder dried at 60 ˚C over-night. Similarly, Nickel hydroxide/VC was also synthesized without employing $NH_4H_2PO_4$ in the same procedure.

2.3.3 Preparation of Pd@NP/VC catalyst

As prepared powder was annealed at 200 ºC and dispersed in distilled water. H_2PdCl_4 introduced drop wise to the above dispersion and allowed to stir. To the above solution 0.2 M $NaBH_4$ solution was added. After 2 h stirring the sample was collected and washed well with distilled water. Different Pd@NP/VC catalyst (Pd@NP/VC) was prepared by varying the amount of NP to 2, 5 and 10 wt% and designated as Pd@2% NP/VC, Pd@5% NP/VC, and Pd@10% NP/VC, respectively (**Scheme 2.1**). The amount of Pd is 20% in each catalyst. Pd

@Nickel hydroxide/VC (Pd@5% NH/VC) and Pd on VC in the absence of NP (Pd@VC) were synthesized via the same procedure.

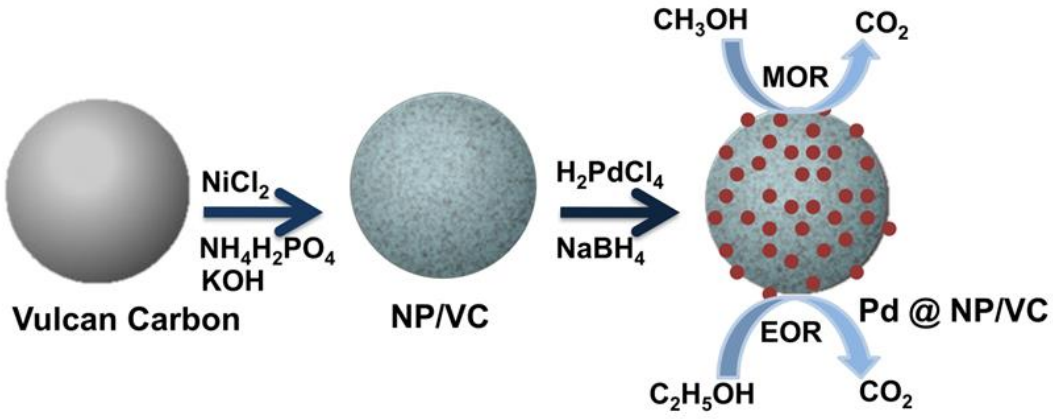

Scheme 2.1 Schematic illustration of the synthesis of Pd@NP/VC.

2.4 Material Characterization

2.4.1 Powder X-ray Diffraction (PXRD) measurement

Phase purity of the prepared catalysts were examined by PXRD using Philips X'pert Pro diffractometer, Ni-filtered Cu-Kα radiation (λ = 1.541 Å) over 2θ ranging from 10 to 90˚ with a step size of 0.08˚. The crystallite size (d) was calculated using Debye-Scherrer equation,

$$d = \frac{0.9\lambda}{\beta\cos\theta}$$

where, λ is the wavelength of incident X-ray radiation, β is the breadth of a diffraction peak at half-height (FWHM) and θ is the position of the peak maximum.[17] The lattice parameter for Pd was obtained by the equation,

$$a = d_{hkl} \sqrt{h^2 + k^2 + l^2}$$

where, 'a' is the lattice constant and d_{hkl} is the inter planar spacing between parallel planes with Miller indices h, k and l.[18]

2.4.2 Scanning Electron Microscopic (SEM) analysis

The morphology and microstructure of the samples were examined using SEM JEOL JSM- 5600 model. Energy Dispersive Analysis by X-rays (EDAX) were utilized to obtain the chemical composition of the catalysts.

2.4.3 Transmission Electron Microscopic (TEM) analysis

Morphology of the catalysts and elemental mapping were analyzed using TEM on a JEOL JEM F-200 microscope operated at 200 kV.

2.4.4 X-ray Photoelectron Spectroscopic (XPS) analysis

PHI 5000 Versa Probe II XPS was employed to investigate the surface composition and valence states of the elements in the catalysts.

2.4.5 Inductively Coupled Plasma Mass Spectrometry (ICP-MS) analysis

Compositions of the elements in the catalysts were estimated by ICP-MS analysis. The calibration curves for the known standards were used to obtain the actual compositions.

2.5 Electrochemical characterization

Electrochemical characterization of the catalysts was performed using the techniques cyclic voltammetry, chronoamperometry and electrochemical impedance spectroscopy.

2.5.1 Cyclic Voltammetry (CV)

CV is an electrochemical technique employed to investigate the reduction and oxidation of molecular species. CV is carried out using three electrode system consisting of working electrode, reference electrode and counter electrode. The potential of the working electrode is controlled with respect to the reference electrode. The controlling potential which is applied across these two electrodes can be considered an excitation signal. A linear potential scan with a triangular wave shape serves as the excitation signal for CV. CV, studies the potential of the working electrode sweeps at a specific sweep rate and the current at the working electrode during the potential scan (**Figure 2.1**). The potential is ramped in the opposite direction to return to the initial potential after attaining the set potential. As many times as necessary, these cycles can be

repeated. Cyclic votammogram displays current at the working electrode versus the applied potential (**Figure 2.2**).[19-21]

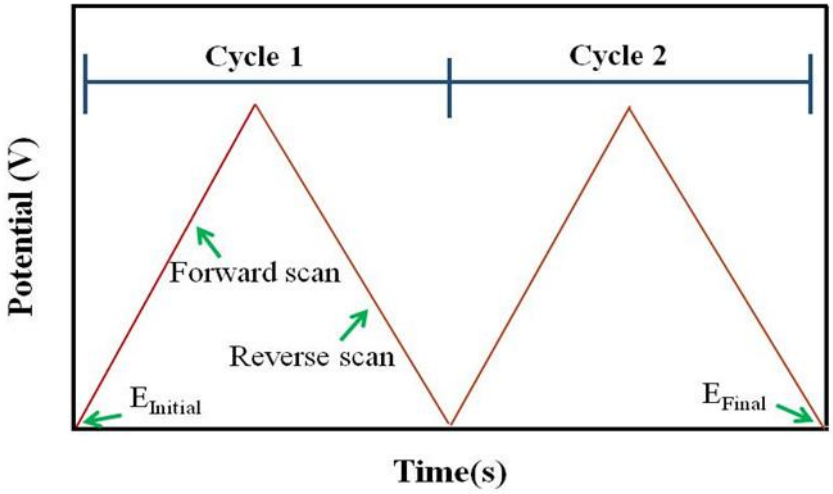

Figure 2.1 CV wave form.

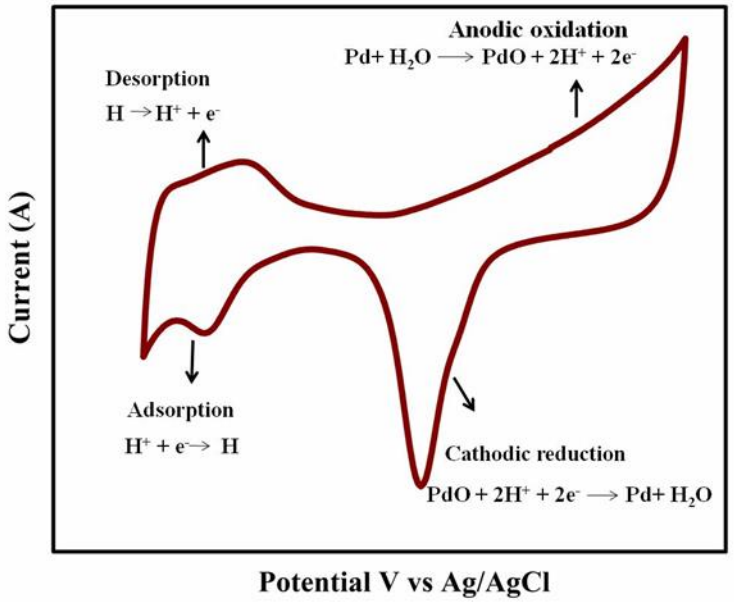

Figure 2.2 CV of Pd in N_2 saturated 0.5 M KOH solution.

The reduction peak of PdO during the backward scan was used to calculate the Electro chemical Surface Area (ECSA). The ECSA indicates the electrochemically active surface area and it provides insights into catalyst performance. The ECSA was estimated based on the following formula.

$$\text{ECSA} = \frac{\text{Q}}{0.405 \times \text{l}}$$

Where, Q stands for the charge associated with the PdO reduction. A charge value of 0.405 mC/cm^2 was needed to reduce the PdO monolayer. The Pd loading is represented by 'l'.[22]

2.5.2 Chronoamperometry

Chronoamperometry is a time dependent technique with a square wave potential applied to the working electrode. Chronoamperometry consists of applying a single voltage step at time t_0 and measuring the current that results from the applied potential (**Figure 2.3**). Electrochemical activity and stability of the electrocatalysts were examined by performing the chronoamperometry.[23]

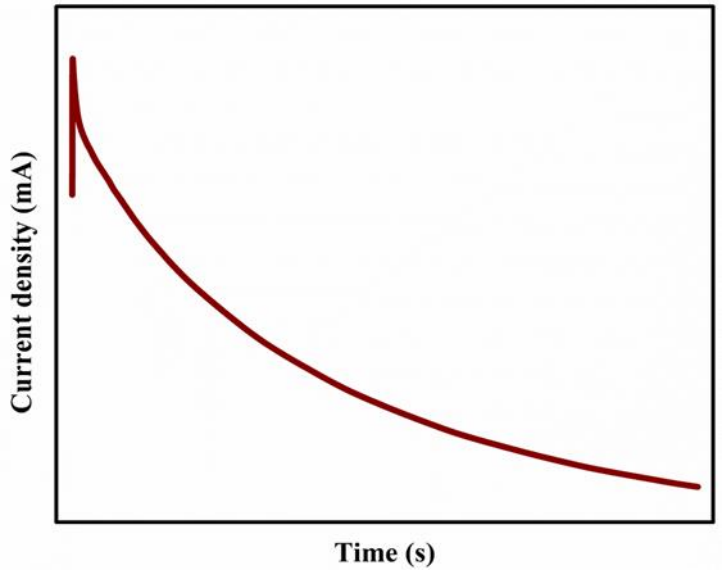

Figure 2.3 Chronoamperometric curve of Pd in N_2 saturated 0.5 M KOH + 0.5 M CH_3OH solution.

2.5.3 Electrochemical Impedance Spectroscopy (EIS)

EIS is one of the most effective electrochemical techniques, which is based on applying an alternating current signal to the working electrode and identifying the corresponding response. EIS could be used to investigate diffusion, charge transfer, and mass transfer processes. An electrochemical system's conductance, resistance, or capacitance can also be studied using EIS. The difference between impedance and resistance is that the resistance in DC circuits directly follows Ohm's Law. Impedance data is expressed as a Nyquist plot containing a real portion and

an imaginary part (**Figure 2.4**). The Y-axis is used to map the imaginary part (Z_{img}), while the X-axis is used to depict the real part (Z_{real}).[24, 25]

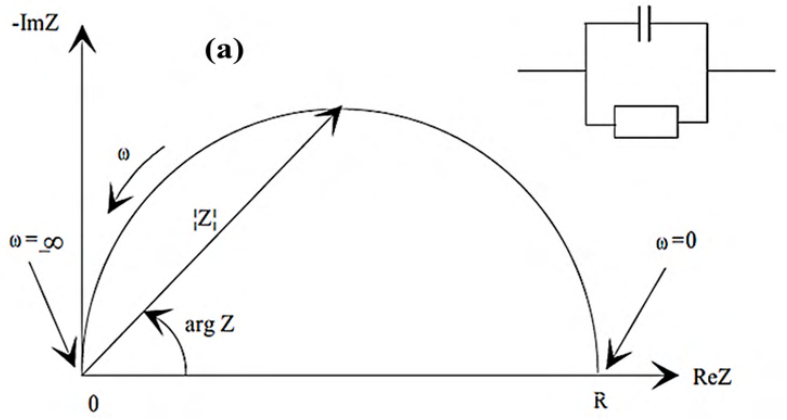

Figure 2.4 Nyquist plot from EIS.

2.6 Results and discussion

2.6.1 PXRD analysis

The crystallinity and phase purity of the prepared Pd@2% NP/VC, Pd@5% NP/VC, Pd@10% NP/VC and Pd@VC were confirmed using XRD measurements, diffraction patterns shown in **Figure 2.5.** The broad peak appeared at 24.29º ascribed to the amorphous Vulcan XC 72R carbon.[26] The sharp peaks obtained at 2θ angle 39.59º, 45.87º, 66.36º and 79.92º corresponds to the (111), (200), (220) and (311) planes of the face centered Pd.[27] However, peaks attributed to NP were missing in the XRD, illustrated the amorphous nature of NP. It was associated with the low reaction temperature (200 ºC) as well as the relatively low weight percentage of NP in the composition. Further, the presence of NP was ensured from XPS analysis. Annealing temperature influence the crystallinity of nickel phosphate, where the increase in temperature transforms the amorphous NP to crystalline.[15, 28] The lattice parameter calculated for Pd in both Pd@10% NP/VC and Pd@VC the catalysts was 0.39 nm.

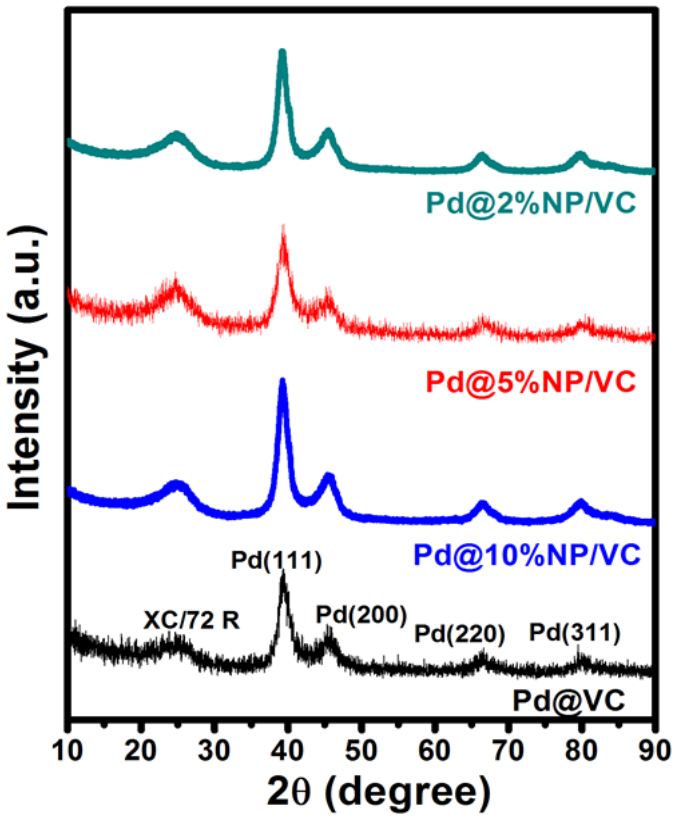

Figure 2.5 PXRD patterns of Pd@2% NP/VC, Pd@5% NP/VC, Pd@10% NP/VC and Pd@VC.

2.6.2 Chemical composition analysis

Surface chemical composition and status of the Pd@5% NP/VC catalyst was analyzed through XPS analysis. The survey spectrum (**Figure 2.6**a) indicates the presence of C, Pd, Ni, P and O. As shown in **Figure 2.6**b, the deconvoluted spectra of Ni 2p consists of peaks at 856.75 and 880.34 eV corresponds to Ni $2p_{3/2}$ and Ni $2p_{1/2}$, respectively, indicating the presence of Ni^{2+}. Additionally, satellite peaks associated with the major peaks were also observed at 862.1 and 874.1 eV. The peak centered at 133.67 eV ascribed to the characteristic peak of phosphate species (**Figure 2.6**c).[29] The peaks at binding energy 335.84 and 341.25 eV in **Figure 2.6**d attributed to Pd $3d_{5/2}$ and $3d_{3/2}$, indicates the presence of Pd (0).[30] The peaks at 337.1 and 342.7 eV were assigned to Pd^{2+}.[31] Analysis of the XPS spectra revealed a shift in Pd binding energy. It suggests that the incorporation of Pd particles has developed a strong electronic modification due to the strain effect. Hence, the presence of NP and Pd particle were confirmed from the XPS

data. The weight percentage of Pd and Ni were obtained as 19.7 and 1.8 from ICP MS analysis for Pd@5% NP/VC. The results were found to be the same as the stoichiometric value.

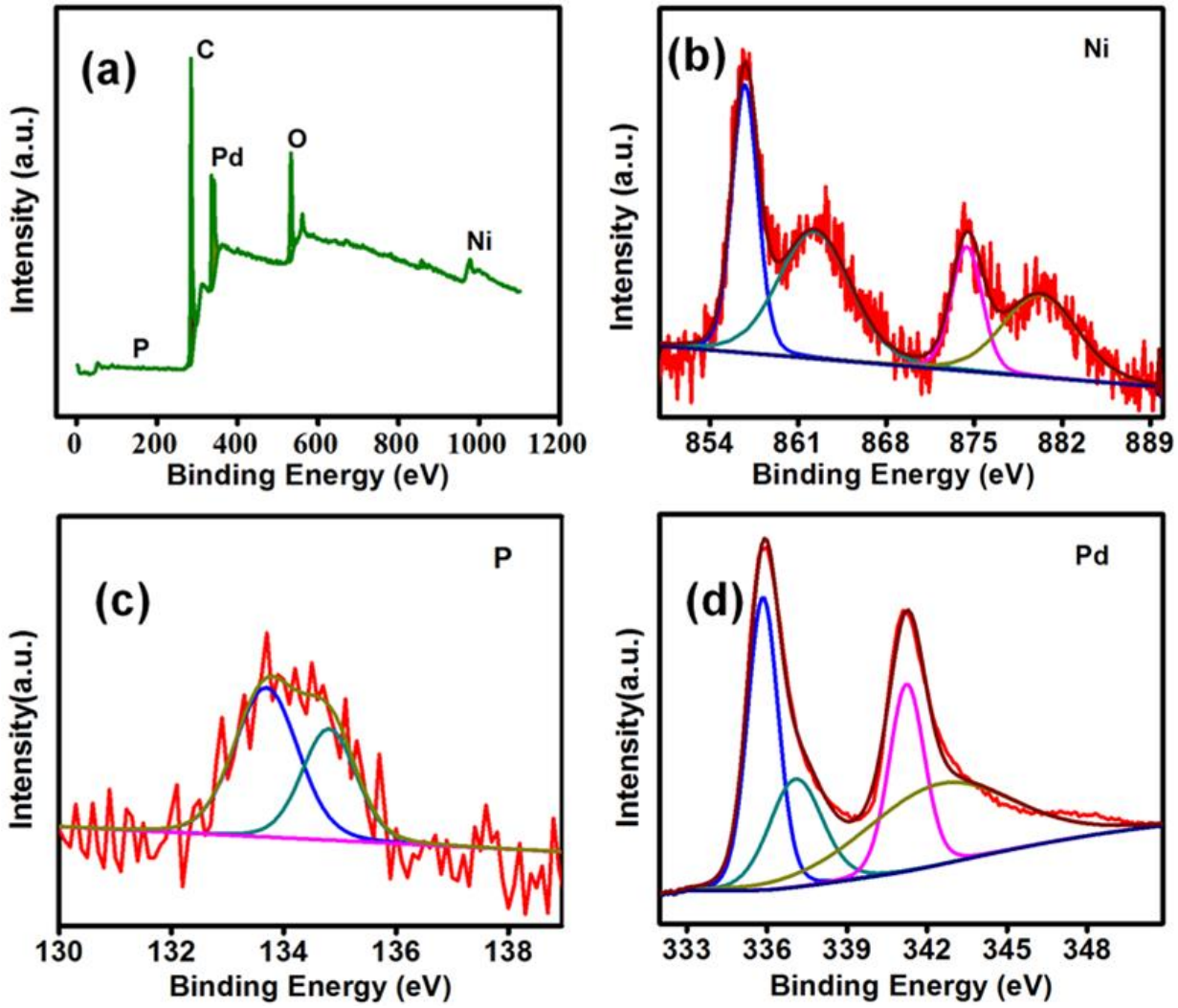

Figure 2.6 (a) Survey spectrum, deconvoluted XPS spectra of (b) Ni 2p, (c) P 2p and (d) Pd 3d of Pd@5% NP/VC.

2.6.3 Morphological analysis

Figure 2.7 shows HRTEM images of all the prepared catalysts and their corresponding histograms. Well dispersed Pd nanoparticles on spherical carbon support were clearly identified from the TEM images. However, the NP modification on carbon surface (**Figure 2.7**a, c, e**)** was not distinguishable with that of the unmodified catalyst (**Figure 2.7**g**).**

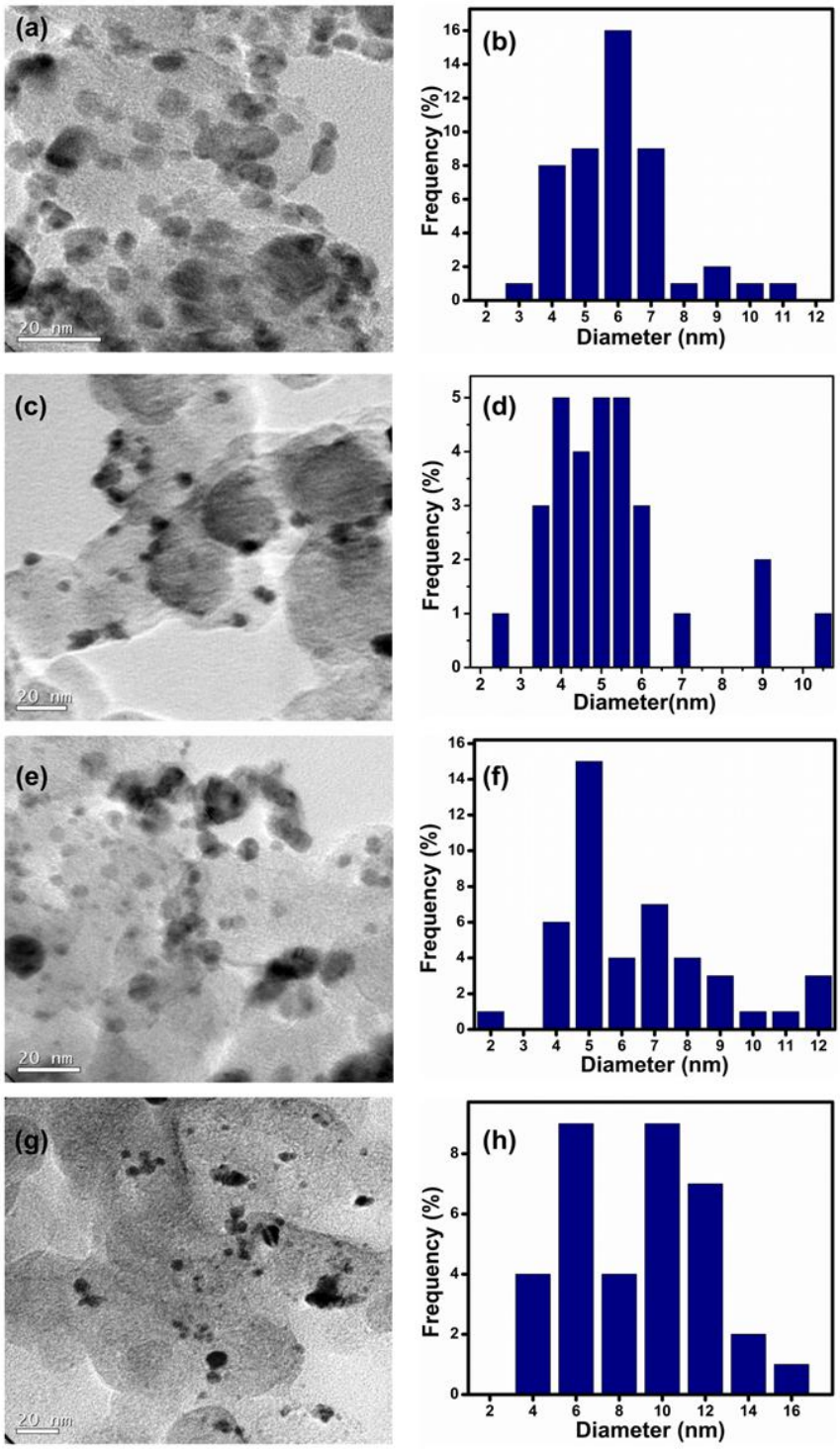

Figure 2.7 TEM images of (a) Pd@2% NP/VC, (c) Pd@5% NP/VC, (e) Pd@10% NP/VC, (g) Pd@VC, histograms of (b) Pd@2% NP/VC, (d) Pd@5% NP/VC, (f) Pd@10% NP/VC and (h) Pd@VC.

From the histograms (**Figure 2.7**b**,** d, f**)** the average particle size of modified catalysts were calculated to be in the range of 5 to 6 nm and that of Pd @VC was 8 nm. The size of Pd particles present in Pd @VC was larger than that of Pd@5% NP/VC (5.03 nm). The presence of NP over the VC helps to prevent the Pd agglomeration and thus reduces the Pd particle size in Pd@5% NP/VC. The Pd particle size reduction plays a crucial role on the catalytic activity.

2.6.4 Electrochemical analysis

2.6.4 (a) Methanol electro-oxidation

Electrochemical properties of the prepared samples were evaluated by cyclic voltammetry technique. **Figure 2.8**a displays the cyclic voltammograms of synthesized catalysts performed in N_2 saturated 0.5 M KOH solution at a scan rate of 50 mV/s to measure the ECSA. The ECSA calculated to be 14.25, 78.12, 23.31, 12.56 m^2/g for Pd@2% NP/VC, Pd@5% NP/VC, Pd@10% NP/VC and Pd@VC, respectively. The highest surface area of Pd@5%NP/VC among the prepared catalysts indicates that the particular composition possesses the maximum available active sites on Pd. ECSA and catalytic efficiency are directly proportional, that reveals the capability of the developed catalyst.

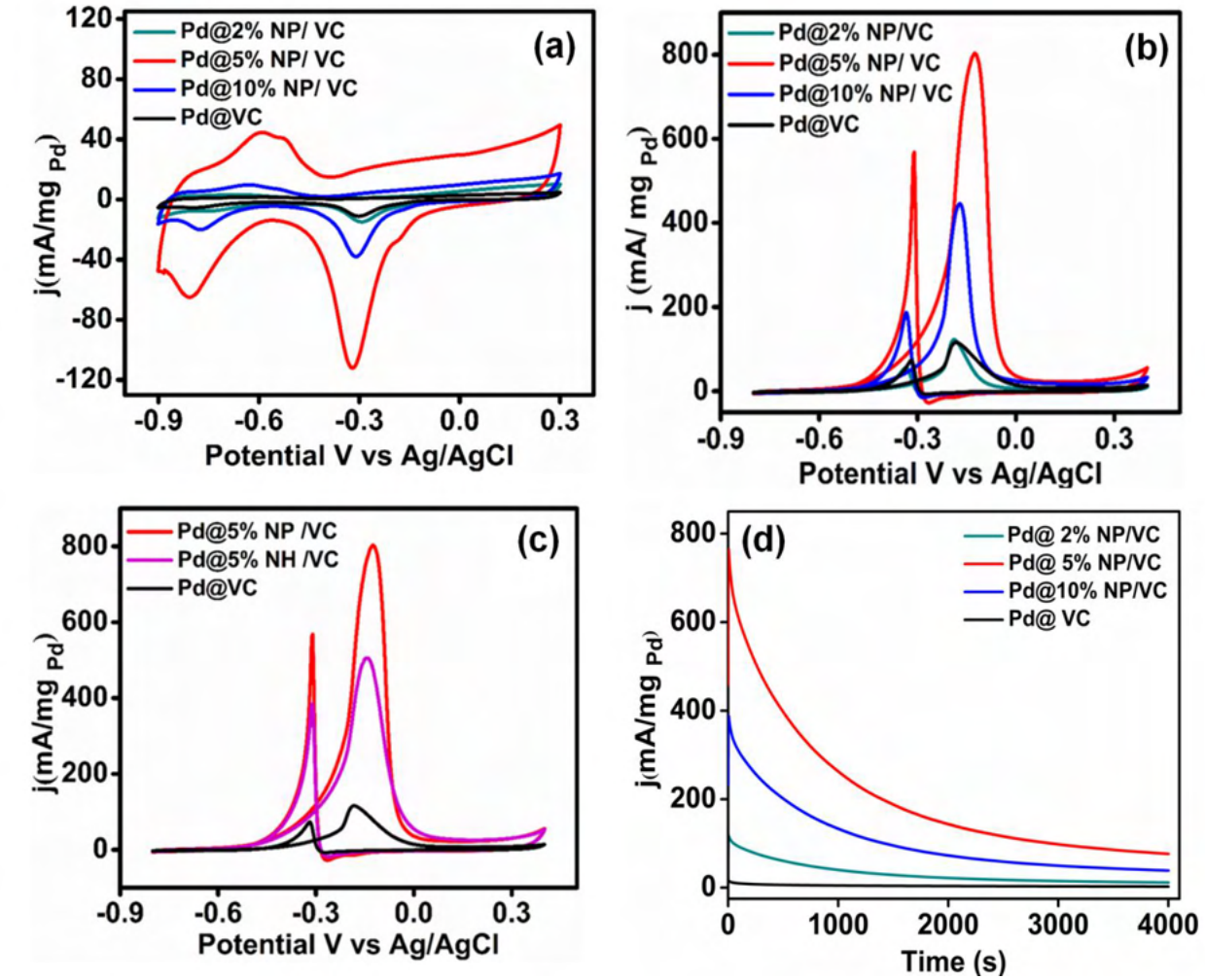

Figure 2.8 CV curves of the prepared catalysts in N_2 saturated (a) 0.5 M KOH, (b) and (c) 0.5 M KOH + 0.5 M CH_3OH solution at a scan rate of 50 mV/s, (d) Chronoamperometric curves of prepared catalysts in N_2 saturated 0.5 M KOH + 0.5 M CH_3OH solution.

Catalytic activity of the prepared samples towards methanol oxidation was carried out in N_2 saturated 0.5 M KOH solution containing 0.5 M methanol at a scan rate of 50 mV/s. **Figure 2.8**b shows the obtained cyclic voltammograms. The anodic peak in the forward scan is attributed to methanol oxidation and the peak observed in the backward scan is due to the oxidation of carbonaceous intermediates.[32, 33] As shown in the CV curves mass activities obtained for the catalysts Pd@2% NP/VC, Pd@5% NP/VC, Pd@10% NP/VC and Pd@VC were 122.67, 804.67, 448.75 and 115.49 mA/mg_{Pd}, respectively. Even though the prepared catalysts impart better activity towards MOR the mass activity exhibited by the Pd@5% NP/VC reveals its supreme catalytic activity. The Pd@5% NP/VC exhibited better catalytic activity in terms of

onset potential and mass activity (**Table 2.1**). Low onset potential and high mass activity are the criteria for a good catalyst. The prepared Pd@5%NP/VC showed low onset potential and high mass activity compared to Pd@2% NP/VC, Pd@10% NP/VC and Pd@ VC. Approximately, a seven-fold increase in mass activity than that of pure Pd@ VC was observed.

Table 2.1 Onset potential and mass activity values of the prepared catalysts

Catalyst	Onset potential (V)	Mass Activity (mA/mg $_{Pd}$)
Pd@2% NP/VC	-0.402	122.67
Pd@5% NP/VC	-0.485	804.67
Pd@10% NP/VC	-0.452	448.75
Pd@ VC	-0.395	115.49

The mechanism of methanol oxidation on Pd catalyst reactions exhibited as follows and the step (10) corresponds to the rate determining step.[34]

$$Pd + CH_3OH \rightarrow Pd\text{-}(CH_3OH)_{ads} \quad (5)$$

$$Pd\text{-}(CH_3OH)_{ads} + OH^- \rightarrow Pd\text{-}(CH_3O)_{ads} + H_2O + e^- \quad (6)$$

$$Pd\text{-}(CH_3O)_{ads} + OH^- \rightarrow Pd\text{-}(CH_2O)_{ads} + H_2O + e^- \quad (7)$$

$$Pd\text{-}(CH_2O)_{ads} + OH^- \rightarrow Pd\text{-}(CHO)_{ads} + H_2O + e^- \quad (8)$$

$$Pd\text{-}(CHO)_{ads} + OH^- \rightarrow Pd\text{-}(CO)_{ads} + 4H_2O + e^- \quad (9)$$

$$Pd\text{-}(CO)_{ads} + 2OH^- \rightarrow Pd + CO_2 + H_2O + 2e^- \quad (10)$$

The activity of Pd@5% NH/VC towards methanol oxidation was compared with Pd@5% NP/VC to know the role of phosphate and shown in **Figure 2.8**c. A mass activity of 508.41 mA/mg$_{Pd}$ was obtained for Pd@5% NH/VC, that confirmed Pd@5% NP/VC catalyst exhibits a significantly better performance than NH/VC. Because, electrical resistivity of Ni-P is lower than that of $Ni(OH)_2$, in addition the oxophilic nature of nickel and phosphorous in NP may also help to remove the intermediate CO species generated during the alcohol oxidation.[5, 8, 35] Carbon based materials are usually employed as supporting materials to provide high surface area and good electrical conductivity.[36] Thus, the presence of both Ni and P along with carbon support increases the active sites of the catalyst and boosts the catalytic activity.

Chronoamperometric measurements were employed to study the stability of the catalysts.[37, 38] **Figure 2.8**d imparts the chronoamperometric curves of all the catalysts recorded at a potential of -0.4 V for 4000 s in N_2 saturated 0.5 M KOH solution containing 0.5 M methanol. Even though the current decays after some time the Pd@5% NP/VC shows better stability than the Pd@VC catalyst. Kinetic properties of the prepared samples were further explicated with electrochemical impedance spectroscopy. The recorded Nyquist plots of methanol electro oxidation on Pd@2% NP/VC, Pd@5% NP/ VC, Pd@10% NP/VC and Pd@VC are depicted in **Figure 2.9**. Simple Randle's circuit was utilized to fit the impedance data. The diameter of the semicircle indicates the charge transfer resistance (R_{ct}) at the electrode-electrolyte interface.[39] The R_{ct} values of Pd@2% NP/VC, Pd@5% NP/ VC, Pd@10% NP/VC and Pd@VC were 22.7, 15.2, 16.9, and 24.5 k , respectively. The results illustrates that the catalysts are suitable for methanol electro-oxidation and the superior performance of the Pd@5% NP/ VC catalyst.

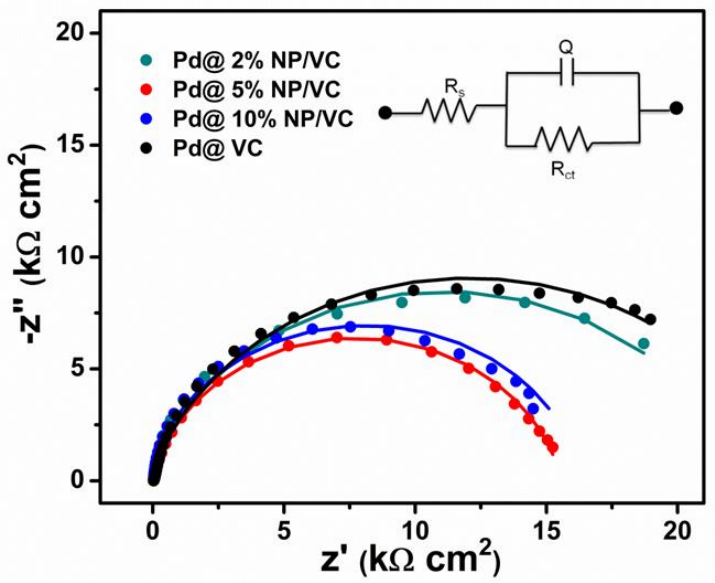

Figure 2.9 Nyquist plots of the prepared catalysts in 0.5 M KOH + 0.5 M CH_3OH solution.

2.6.4 (b) Ethanol electro-oxidation

Similar results were observed in the case of performance towards ethanol oxidation. The activity was evaluated by CV in N_2 saturated 0.5 M KOH solution containing 0.5 M ethanol at a scan rate of 50 mV/s. As shown in **Figure 2.10**a the Pd@2% NP/VC, Pd@5% NP/VC Pd@10% NP/VC, catalysts exhibited a mass activity of 268.20, 772.96, 501.91 mA/mg_{Pd} and that of pure Pd@VC 230.63 mA/mg_{Pd}. The corresponding chronoamperometric measurements were also carried out in N_2 saturated 0.5 M KOH solution containing 0.5 M ethanol at a potential of -0.2 V for 4000 s (**Figure 2.10**b). The Pd@5% NP/VC catalyst displayed better stability.

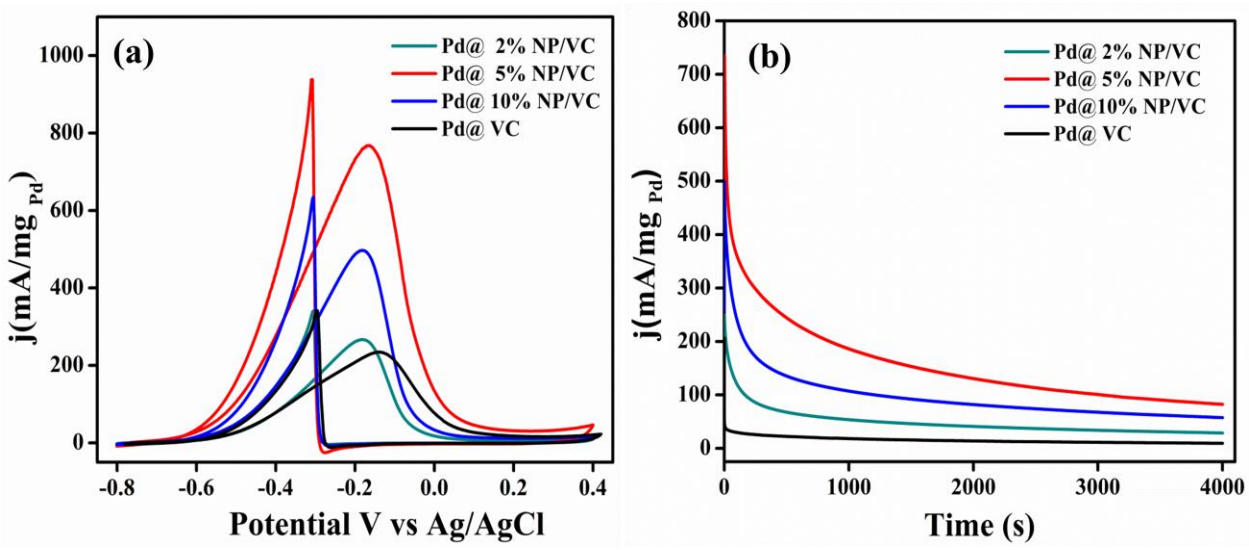

Figure 2.10 (a) CV and (b) Chronoamperometric curves of prepared catalysts in N_2 saturated 0.5 M KOH + 0.5 M C_2H_5OH solution.

2.6.5 Stability studies

The stability study was also done by performing the CV for 500 cycles. The corresponding voltamograms were depicted in **Figure 2.11**.[40] After 500 cycles the Pd@5% NP/VC exhibited better stability in methanol and ethanol than that of Pd@ VC. As depicted in **Figure 2.11** in the case of Pd@5% NP/VC after performing CV for 500 cycles the current is not that much reduced and the onset potential also remained same whereas the mass activity of Pd@ VC was reduced almost to half that of the initial value and onset potential also deviated to higher value.

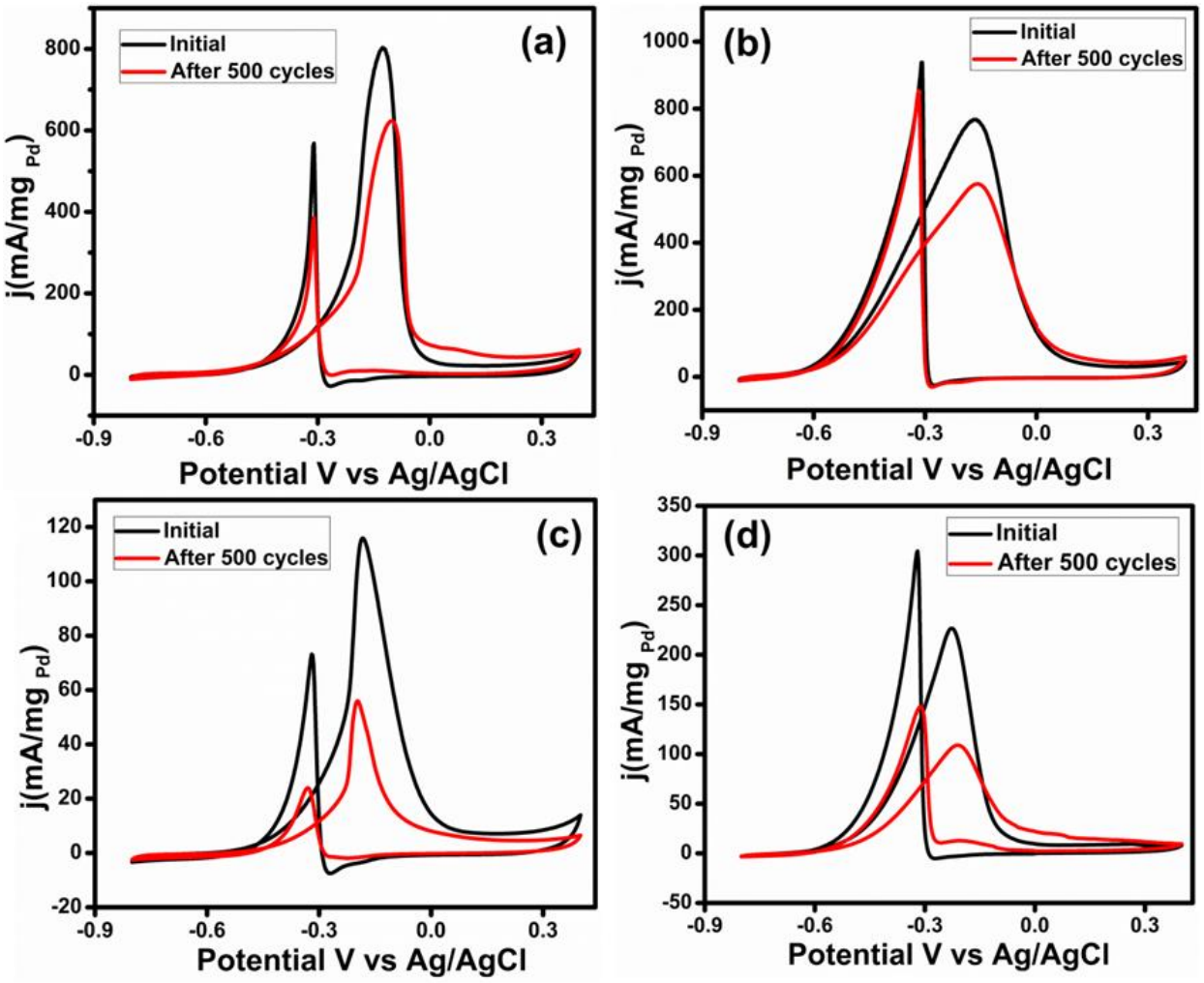

Figure 2.11 CV curves of Pd@5% NP/VC after 500 cycles in N_2 saturated solution of (a) 0.5 M KOH + 0.5 M CH_3OH, (b) 0.5 M KOH + 0.5 M C_2H_5OH and Pd@VC in (c) 0.5 M KOH + 0.5 M CH_3OH, (d) 0.5 M KOH + 0.5 M C_2H_5OH solution.

2.6.6 Comparison study

A comparison of the activity of different carbon supported catalyst towards alcohol oxidation was given in **Table 2.2**

The presence NP enhances the efficiency of the catalysts. The intermediate CO generates during the alcohol oxidation remains as a major hindrance for the activity of the catalysts. The active sites of the catalysts available were occupied by the CO molecule and thereby decelerating the reaction rate. The oxophilic nature of the Ni as well as P helps to improve the performance of the Pd by oxidizing the CO molecules.

Table 2.2 Comparison of activity of catalysts towards alcohol oxidation

Catalysts	Electrolyte	Mass activity ($mA/mg_{Pd/Pt}$)	Reference
Pd/PPY/graphene	0.5M NaOH + 1M Methanol	359.8	41
PdMo/CNT	1M KOH + 1 M Methanol	395.6	42
Pd/MnO_2/CNT	0.5M NaOH + 1M Methanol	431.02	43
Pd_3Mo/VC	1M KOH + 1 M Methanol	647.27	44
$Pd_{10}Ag_{10}$/CNT	1M KOH + 0.5 M Methanol	731.20	45
Commercial Pd/C	0.5 M KOH + 0.5 M Methanol	180.00	46
Pd@5% NP/VC	**0.5 M KOH + 0.5 M Methanol**	**804.67**	**Present work**
Pd@5% NP/VC	**0.5 M KOH + 0.5 M Ethanol**	**772.96**	**Present work**

The low electrical resistance of Ni-P along with the carbon support imparts electrical conductivity that facilitates the kinetics of catalysis. The increment in catalytic activity could be attributed to the enhanced CO tolerance of the catalyst and improved conductivity emerged due to the synergistic effect between Pd, Ni, P and VC.

2.7 Conclusions

Carbon supported Pd@NP catalyst was synthesized through a simple method. Transition metal phosphate modified carbon support is first time introduced for the alcohol electro oxidation application and excellent results were obtained. Unlike the agglomeration observed in the absence of NP, homogeneous Pd particles with reduced particle size were resulted in the presence of NP. Approximately seven-fold enhancement in activity towards methanol oxidation was achieved (804.67 mA/mg_{Pd}). Mass activity of 772.96 mA/mg_{Pd} was exhibited for ethanol oxidation by Pd@5% NP/VC and 230.63 mA/mg_{Pd} by Pd@VC. The synergistic effect of NP modified carbon support with Pd leads to better activity. The collective action of the improved CO tolerance induced by NP and high surface area and conductivity imparted by VC to Pd enhanced the activity of the catalyst towards alcohol oxidation.

2.8 References

(1) Yang, J., Tan, J., Yang, F., Li, X., Liu, X., Ma, D. (2012). Electro-oxidation of methanol on mesoporous nickel phosphate modified GCE. *Electrochem. commun.*, **2012**; *23*, 13–16. https://doi.org/10.1016/j.elecom.2012.06.006.

(2) Tan, J., Yang, J.-H., Liu, X., Yang, F., Li, X., Ma, D Electrochemical oxidation of methanol on mesoporous nickel phosphates and Si-incorporated mesoporous nickel phosphates. *Electrochem. commun.*, **2013**; *27*, 141–143. https://doi.org/10.1016/j.elecom.2012.11.019

(3) Spinner, N., and Mustain, W. E. Effect of nickel oxide synthesis conditions on its physical properties and electro catalytic oxidation of methanol. , *Electrochim. Acta*, **2011**; *56*(16), 5656–5666. https://doi.org/10.1016/j.electacta.2011.04.023.

(4) Yuan, J., Zheng, X., Yao, C. D., Jiang, L., Li, Y., Che, J., Chen, H. Amorphous mesoporous nickel phosphate/reduced graphene oxide with superior performance for electrochemical capacitors. *Dalton Transactions*, **2018**; *47*, 13052. https://doi.org/10.1039/C8DT02304B.

(5) Lin, J.-D., Chou, C.-T. The influence of acid etching on the electrochemical supercapacitive properties of Ni P coatings. *Surface and Coatings Technology*, **2017**; *325*, 360–369. https://doi.org/10.1016/j.surfcoat.2017.06.056.

(6) Liu, Q., Chen, C., Zheng, J., Wang, L., Yang, Z., Yang, W., 3D hierarchical $Ni(PO_3)_2$ nanosheet arrays with superior electrochemical capacitance behavior. *J. Mater. Chem. A*, **2017**; *5*(4), 1421–1427. https://doi.org/10.1039/C6TA09528C.

(7) Li, J.-J., Liu, M.-C., Kong, L.-B., Wang, D., Hu, Y.-M., Han, W., Kang, L. Advanced asymmetric supercapacitors based on $Ni_3 (PO_4)_2$@GO and Fe_2O_3@GO electrodes with high specific capacitance and high energy density. *RSC Adv.*, **2015**; *5*(52), 41721–41728. https://doi.org/10.1039/C5RA06050H.

(8) Al-Omair, M. A., Touny, A. H., Al-Odail, F. A., Saleh, M. M. Electro catalytic Oxidation of Glucose at Nickel Phosphate Nano/Micro Particles Modified Electrode. *Electrocatalysis*, **2017**; *8*(4), 340–350. https://doi.org/10.1007/s12678-017-0376-8.

(9) Touny, A. H., Tammam, R. H., Saleh, M. M. Electrocatalytic oxidation of formaldehyde on nano porous nickel phosphate modified electrode. *Appl. Catal. B Environ.*, **2018**; *224*, 1017–1026. https://doi.org/10.1016/j.apcatb.2017.11.031.

(10) Peng, X., Chai, H., Cao, Y., Wang, Y., Dong, H., Jia, D., Zhou, W. Facile synthesis of cost-effective $Ni_3(PO_4)_2 \cdot 8H_2O$ microstructures as a supercapattery electrode material. *Materials Today Energy*, **2018**; *7*, 129–135. https://doi.org/10.1016/j.mtener.2017.12.004.

(11) Fa, D., Yu, B., Miao, Y. Synthesis of ultra-long nanowires of nickel phosphate by a template-free hydrothermal method for electro catalytic oxidation of glucose. *Colloids and Surfaces A: Physicochemical and Engineering Aspects*, **2019**; *564*, 31–38. https://doi.org/10.1016/j.colsurfa.2018.12.035.

(12) Chang, J., Lv, Q., Li, G., Ge, J., Liu, C., Xing, W. Core-shell structured $Ni_{12}P_5/Ni_3(PO_4)_2$ hollow spheres as difunctional and efficient electrocatalysts for overall water electrolysis. *Appl. Catal. B Environ*, **2017**; *204*, 486–49. https://doi.org/10.1016/j.apcatb.2016.11.050.

(13) Li, Y., Zhao, C. Iron-Doped Nickel Phosphate as Synergistic Electrocatalyst for Water Oxidation. *Chemistry of Materials*, **2016**; *28*(16), 5659–5666. https://doi.org/10.1021/acs.chemmater.6b01522.

(14) Theerthagiri, J., Cardoso, E. S. F., Fortunato, G. V., Casagrande, G. A., Senthilkumar, B., Madhavan, J.,Maia, G,Highly electroactive Ni pyrophosphate/Pt catalyst towards hydrogen evolution reaction. *ACS Appl. Mater. Interfaces*, **2019**; *11*, 4969-4982. https://doi.org/10.1021/acsami.8b18153.

(15) Sharma, P., Radhakrishnan, S., Khil, M.-S., Kim, H.-Y., Kim, B.-S. Simple room temperature synthesis of porous nickel phosphate foams for electro catalytic ethanol oxidation. *Journal of Electroanalytical Chemistry*, **2018**; *808*, 236–244. https://doi.org/10.1016/j.jelechem.2017.12.025.

(16) Song, X., Sun, Q., Gao, L., Chen, W., Wu, Y., Li, Y., Yang, J.-H. Nickel phosphate as advanced promising electrochemical catalyst for the electro-oxidation of methanol. *Int. J. Hydrogen Energy*, **2018**; *43*(27), 12091–12102. https://doi.org/10.1016/j.ijhydene.2018.04.165.

(17) Fu, Shaofang; Zhu, Chengzhou; Du, Dan; Lin, Yuehe Facile One-Step Synthesis of Three-Dimensional Pd–Ag Bimetallic Alloy Networks and Their Electrocatalytic Activity toward Ethanol Oxidation. ACS Appl. Mater. Interfaces., **2015**; 7 13842–13848. https://doi.org/10.1021/acsami.5b01963.

(18) Amado Velázquez; Francesc Centellas; José Antonio Garrido; Conchita Arias; Rosa María Rodríguez; Enric Brillas; Pere-Lluís Cabot. Structure of carbon-supported Pt–Ru

nanoparticles and their electrocatalytic behavior for hydrogen oxidation reaction. , **2010**, *195(3), 710–719*. https://doi.org/10.1016/j.jpowsour.2009.08.039.

(19) Elgrishi, N.; Rountree, K. J.; McCarthy, B. D.; Rountree, E. S.; Eisenhart, T. T.; Dempsey, J. L. A Practical Beginner's Guide to Cyclic Voltammetry. *J. Chem. Educ.* **2018**, *95* (2), 197–206.

(20) Wu, J.; Yuan, X. Z.; Wang, H. Cyclic Voltammetry. *PEM Fuel Cell Diagnostic Tools* **2011**, No. d, 71–85.

(21) Rusling, J. F.; Suib, S. L. Characterizing Materials with Cyclic Voltammetry. *Adv. Mater.* **1994**, *6* (12), 922–930. https://doi.org/10.1021/acs.jchemed.7b00361.

(22) Shih, Zih-Yu; Wang, Chia-Wei; Xu, Guobao; Chang, Huan-Tsung Porous palladium copper nanoparticles for the electrocatalytic oxidation of methanol in direct methanol fuel cells. J. Mater. Chem. A, 1 (2013) 4773. https://doi.org/10.1039/C3TA01664A

(23) Franklin, R. K.; Microsystems, B.; City, S. L. *Chemical and Biological Systems : Chemical Sensing Systems for Liquids $*; Elsevier Ltd., 2016. https://doi.org/10.1016/B978-0-12-803581-8.00549-X.

(24) Chang, B.; Park, S. Electrochemical Impedance Spectroscopy. **1936**. https://doi.org/10.1146/annurev.anchem.012809.102211.

(25) Electrochemistry, P.; Elements, C.; Equivalent, C.; Models, C. Basics of Electrochemical Impedance Spectroscopy.

(26) Wang, F., Yang, L., Tang, Q., Guo, Y., Hao, G. Synthesis of Pd/XC-72 catalysts by a facile glutamate-mediated method for solvent-free selective oxidation of dl-sec-phenethyl alcohol. *Catalysis Science & Technology*, **2013**; *3*(5), 1246. https://doi.org/10.1039/C3CY20803F.

(27) Zhao, Y., Yang, X., Tian, J., Wang, F., Zhan, L. Methanol electro-oxidation on Ni@Pd core-shell nanoparticles supported on multi-walled carbon nanotubes in alkaline media. *Int. J. Hydrogen Energy*, **2010**; *35*(8), 3249–3257. https://doi.org/10.1016/j.ijhydene.2010.01.112.

(28) Omar, F. S., Numan, A., Duraisamy, N., Bashir, S., Ramesh, K., Ramesh, S., Ultrahigh capacitance of amorphous nickel phosphate for asymmetric supercapacitor applications. *RSC Adv.*, **2016**; *6*(80), 76298–76306. https://doi.org/10.1039/C6RA15111F.

(29) Sheng, J., Kang, J., Ye, H., Xie, J., Zhao, B., Fu, X.-Z., Wong, C.-P. Porous octahedral PdCu nano cages as highly efficient electrocatalysts for the methanol oxidation reaction. *J. Mater. Chem. A*, **2018**; *6*(9), 3906–3912. https://doi.org/10.1039/C7TA07879J.

(30) Wang, J., Zhang, P., Xiahou, Y., Wang, D., Xia, H., Möhwald, H. Simple Synthesis of Au–Pd Alloy Nanowire Networks as Macroscopic, Flexible Electrocatalysts with Excellent Performance. *ACS Appl. Mater. Interfaces*, **2017**; *10*(1), 602–613. https://doi.org/10.1021/acsami.7b14955.

(31) Wang, F., Yu, H., Tian, Z., Xue, H., & Feng, L. Active sites contribution from nanostructured interface of palladium and cerium oxide with enhanced catalytic performance for alcohols oxidation in alkaline solution. *Journal of Energy Chemistry*, **2018**, *27(2)*, 395–403. https://doi.org/10.1016/j.jechem.2017.12.011.

(32) Bora, A., Mohan, K., Doley, S., Goswami, P., Dolui, S. K Broadening the sunlight response region with carbon dot sensitized TiO_2 as a support for a Pt catalyst in the methanol oxidation reaction. *Catalysis Science & Technology*, **2018**; *8*(16), 4180–4192. https://doi.org/10.1039/C8CY01040D.

(33) Wang, S., Yang, G., Yang, S, Pt-Frame @Ni quasi Core–Shell Concave Octahedral $PtNi_3$ Bimetallic Nanocrystals for Electro catalytic Methanol Oxidation and Hydrogen Evolution. *J. Phys. Chem. C*, **2015**; *119*(50), 27938–27945. https://doi.org/10.1021/acs.jpcc.5b10083.

(34) Soleimani-Lashkenari, M., Rezaei, S., Fallah, J., Rostami, H. Electro catalytic performance of Pd/PANI/TiO_2 nano composites for methanol electro oxidation in alkaline media. *Synthetic Metals*, **2018**; *235*, 71–79. https://doi.org/10.1016/j.synthmet.2017.12.001.

(35) Chung, D. Y., Kim, H., Chung, Y.-H., Lee, M. J., Yoo, S. J., Bokare, A. D., Sung, Y.E. Inhibition of CO poisoning on Pt catalyst coupled with the reduction of toxic hexavalent chromium in a dual-functional fuel cell. *Sci. Rep.*, **2014**; *4(*1). https://doi.org/10.1038/srep07450.

(36) Liu, Y., Li, S., Zhang, Y., Liu, W., Wang, J., Zhai, C. Electro catalytic oxidation of methanol on Pt-Pd nanoparticles supported on honeycomb-like porous carbons in alkaline media. *Journal of Solid State Electrochemistry*, **2017**; *22*(3), 817–824. https://doi.org/10.1007/s10008-017-3810-1.

(37) Xu, G., Liu, J., Liu, B., Zhang, J. Self-assembly of Pt Nanocrystals into Three-Dimensional Super lattices Results in Enhanced Electro catalytic Performance for Methanol Oxidation. *Cryst Eng Comm*, **2019**; *21*, 411. https://doi.org/10.1039/C8CE01382A.

(38) Douk, A. S., Saravani, H., Yazdan Abad, M. Z., & Noroozifar, M. Controlled organization of building blocks to prepare three-dimensional architecture of Pd–Ag aerogel as a high

active electrocatalyst toward formic acid oxidation. *Composites Part B: Engineering,* **2019**; *172*, 309-315. https://doi.org/10.1016/j.compositesb.2019.05.021.

(39) Wang, Wei; Chu, Qingxin; Zhang, Yingnan; Zhu, Wei; Wang, Xiaofeng; Liu, Xiaoyang (2015). Nickel foam supported mesoporous $NiCo_2O_4$ arrays with excellent methanol electro-oxidation performance. New J. Chem., 39(8), 6491–6497. doi:10.1039/c5nj00766f.

(40) He, Q., Shen, Y., Xiao, K., Xi, J., & Qiu, X. Alcohol electro-oxidation on platinum–ceria/graphene nanosheet in alkaline solutions, **2016**, *Int. J. Hydrogen Energy, 41(45),* 20709–20719. https://doi.org/10.1016/j.ijhydene.2016.07.205.

(41) Yanchun Zhao, Lu Zhan, Jianniao Tian, Sulian Nie, Zhen Ning, Enhanced electro catalytic oxidation of methanol on Pd/polypyrrole–grapheme in alkaline medium, *Electrochim. Acta*, **2011**; 56, 1967- 1972. https://doi.org/10.1016/j.electacta.2010.12.005.

(42) Kakati, N., Maiti, J., Lee, S. H., Yoon, Y. S.Core shell like behavior of PdMo nanoparticles on multiwall carbon nanotubes and their methanol oxidation activity in alkaline medium, *Int. J. Hydrogen Energy* , **2012**; *37(24),* 19055–19064. https://doi.org/10.1016/j.ijhydene.2012.09.083

(43) Y. Zhao, L. Zhan, J. Tian, S. Nie , Z. Ning, , MnO_2 modified multi-walled carbon nanotubes supported Pd nanoparticles for methanol electro-oxidation in alkaline media, *Int. J. Hydrogen Energy*, **2010**; 35, 10522–10526. https://doi.org/10.1016/j.ijhydene.2010.07.048.

(44) Fathirad, F., Mostafavi, A., Afzali, D. Bimetallic Pd–Mo nanoalloys supported on Vulcan XC-72R carbon as anode catalysts for direct alcohol fuel cell. *Int. J. Hydrogen Energy*, **2017**; *42*(5), 3215–3221. https://doi.org/10.1016/j.ijhydene.2016.09.138.

(45) M. Satyanarayana, G. Rajeshkhanna, Malaya K. Sahoo, G. Ranga Rao, Electrocatalytic Activity of Pd20−xAgx Nanoparticles Embedded in Carbon Nanotubes for Methanol Oxidation in Alkaline Media, *ACS. Appl. Energy Mater.,* **2018**; *1*, 3763−3770. https://doi.org/10.1021/acsaem.8b00544.

(46) Shih, Z.-Y., Wang, C.-W., Xu, G., & Chang, H.T. Porous palladium copper nanoparticles for the electrocatalytic oxidation of methanol in direct methanol fuel cells. *Journal of Materials Chemistry A,* **2013**; *1(15),* 4773. https://doi.org/10.1039/C3TA01664A.

Chapter 3

Bimetallic $NiWO_4$ as an efficient interface modulator for Pd towards enhanced electrocatalytic alcohol oxidation

3.1 Abstract

The electronic coupling effect by interfacial engineering between noble metal and transition metal tungstates is considered as an effective strategy for improving electrocatalytic activity. The present chapter introduced a new hybrid electrocatalyst of Pd nanoparticle supported on $NiWO_4$ nanocrystals modified carbon for efficient alcohol electro-oxidation reaction. Bimetallic oxide became as an efficient interface modulator for Pd over mono metallic oxides. The synthesised catalyst, Pd over nickel tungstate modified VC exhibited well dispersed homogeneous Pd particles. Approximately ten times (1202.48 mA/mg_{Pd}) and six times (1508.24 mA/mg_{Pd}) catalytic effectiveness towards methanol and ethanol electro-oxidation were obtained. The enhanced electrochemical property owing to electronic modification and improved surface area, by the strong coupling of Pd with nickel tungstate and carbon support conferred excellent catalytic performance for the synthesised catalyst.

3.2 Introduction

Metal tungstates with general formula MWO_4, emerged as a new class of inorganic material with excellent optical, electrical and sensor properties. They employed as electrode materials in various fields like photo anode, supercapacitors, memory devices, sensors etc.[1,2] Among tungstates $NiWO_4$ have gained considerable attention due to its peculiar electronic structure and has been exploited as heterogeneous catalyst in photovoltaic electrochemical cells etc.[3] Huang *et al* synthesized 2D porous bimetallic cobalt nickel tungstate through hydrothermal method and studied the supercapattery application.[4] The presence of tungsten significantly enhances the conductivity of $NiWO_4$ compared to NiO. Niu *et al* reported $NiWO_4$ nanoparticles prepared by co-precipitation method exhibited enhanced electrical conductivity in the order of 10^{-7} to 10^{-3} Scm^{-1} at different temperatures compared to NiO.[5] Wang *et al* reported nickel tungstate composite supported on reduced graphene oxide for urea oxidation in alkaline medium for direct urea fuel cell applications. Tungsten oxide was found to resolve the CO poisoning of noble metal catalysts.[6] The improved conductivity and CO tolerance of tungstate makes bimetallic $NiWO_4$ a promising supporting material. Strong metal support interaction and the electronic coupling between the metal and supporting material can significantly enhance the catalytic activity of the incorporated noble metal. The electronic modification of Pd nanoparticles due to the synergistic action between Pd metal and $NiWO_4$ support can boost the catalytic performance. Compared to monometallic compounds, bimetallic compounds help to maximize the catalytic activity because of their intensive interaction of two types of metals. In addition, the oxophilic nature of Ni and W can also contribute towards catalytic activity of Pd particles by reducing CO poisoning. The integration of $NiWO_4$ with VC improves the electrical conductivity and further it elevates the catalytic activity of Pd particles.[7-10] Considering these characteristics we have been motivated to investigate Pd over nickel tungstate modified carbon towards electro-catalytic alcohol reaction. Chapter 3 explored nickel tungstate modified carbon as supporting substrate for Pd towards alcohol electro-oxidation reaction and excellent activity with stability was achieved.

3.3 Experimental Section

3.3.1 Materials and methods

$Na_2WO_4.2H_2O$ (99.99%), $NiCl_2.6H_2O$ (99.99%), $PdCl_2$ (99.99%), KOH (99.9%), $NaBH_4$ (99.9%), HCl (99.9%), methanol (99.9%) and ethanol (99.9%) procured from Sigma Aldrich, VC obtained from Cabot corp. and used without purification.

3.3.2 Synthesis of Nickel tungstate/VC catalyst

Nickel tungstate modified carbon (NW/VC) was developed by a simple hydrothermal reaction as per the reported method with some modifications. Six mM Na_2WO_4 was dissolved in 20 ml water and poured into calculated amount of carbon. The mixture was sonicated well and subsequently added 6 mM of $NiCl_2.6H_2O$ dropwise under continuous stirring. The reaction mixture was transferred to 50 ml capacitive Teflon lined stain less steel autoclave and treated at 180 ˚C for 24 h. The obtained precipitate washed with distilled water, ethanol several times and dried. The sample was further calcined at 600 ˚C in N_2 atmosphere.[4]

3.3.3 Preparation of Pd@NW/VC catalysts

As obtained NW/VC powder dispersed in distilled water and allowed to stir. Further, H_2PdCl_4 solution introduced into NW/VC dispersion drop wise while stirring and heated to 80 ˚C. At 80 ˚C, 0.2 M $NaBH_4$ solution was added as reducing agent and stirred for 2 h. The sample filtered out and washed with distilled water. In the same way, different compositions of catalysts were synthesised by varying the amount of nickel tungstate (NW) as 5, 10, 15 wt% and named as Pd@5%NW/VC, Pd@10%NW/VC, Pd@15%NW/VC, respectively (**Scheme 3.1**). The amount of Pd was 20% in all the prepared catalysts. Pd deposited carbon (Pd@VC) was synthesised without NW by following the same procedure.

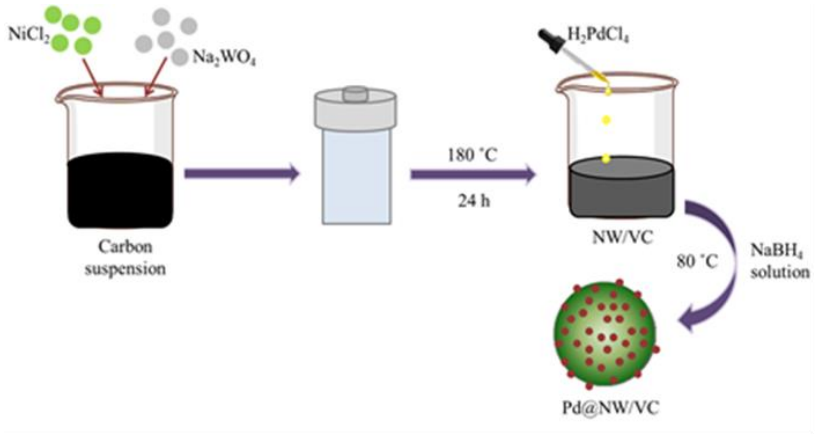

Scheme 3.1 Preparation of Pd@NW/VC catalyst.

3.3.4 Preparation of Pd@Tungsten oxide/VC catalyst

Sodium tungstate solution ultrasonicated with calculated amount of carbon and HCl solution was added drop wise to the solution under stirring. The precipitate filtered out and washed with distilled water, which was dried and calcined at 400˚C.[11] Pd@10%WO_3/VC synthesised by adding H_2PdCl_4 solution to the dispersion of WO_3/VC powder under stirring and allowed to heat. At 80 ˚C, 0.2 M $NaBH_4$ solution added drop wise and stirred for 2 h. Sample was collected and washed using distilled water. The sample was designated as Pd@10% WO/VC.

3.3.5 Preparation of Pd@Nickel oxide/VC catalyst

Requisite quantity of $NiCl_2$ added at 20 ml ultrasonicated carbon dispersion and stirred well. KOH solution added drop wise to the mixture under stirring and continued for 2 h. The precipitate washed well and calcined at 600 ˚C at N_2 atmosphere.[12] Pd@10%NO/VC prepared using the same procedure as explained earlier. The sample was designated as Pd@10% NO/VC.

3.4 Results and discussion

3.4.1 PXRD analysis

The catalysts formation and phase purity was examined using PXRD analysis. **Figure 3.1** shows the obtained PXRD patterns of the as synthesized Pd@5%NW/VC, Pd@10%NW/VC, Pd@15%NW/VC and Pd@VC catalysts. Peaks correspond to NW observed for all the 5, 10, 15

wt% NW/VC (JCPDS 00-015-7055). Peaks at 2θ angle 39.59, 45.87, 66.36 and 79.92º correspond to the (111), (200), (220) and (311) planes of Pd (JCPDS 00-005-0681). The broad peak at 2θ, 24.66˚ indicates the presence of Vulcan XC 72 carbon. The obtained crystallite sizes of Pd@5%NW/VC, Pd@10%NW/VC, Pd@15%NW/VC and Pd@VC are, 3.6, 4.2, 5.8 and 7.6 nm, respectively.

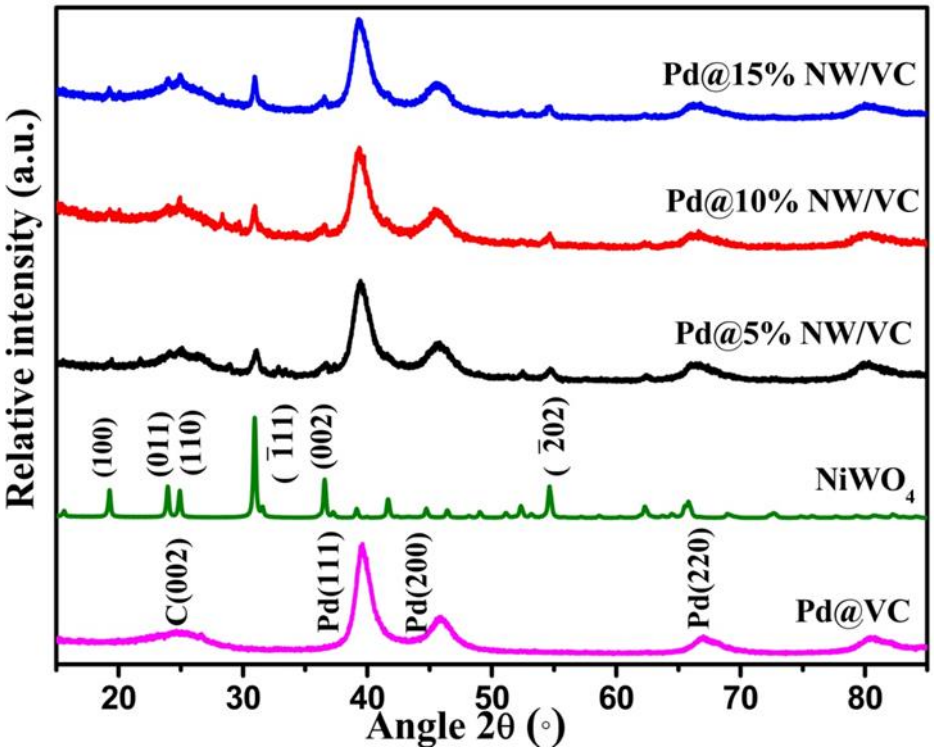

Figure 3.1. PXRD patterns of Pd@15% NW/VC, Pd@10% NW/VC, Pd@5% NW/VC, $NiWO_4$ and Pd@VC.

3.4.2 Morphological analysis

Morphology of the prepared samples were monitored using TEM analysis. **Figure 3.2** represents the TEM images of Pd@5%NW/VC, Pd@10%NW/VC, Pd@15%NW/VC and Pd@VC. Agglomerated Pd particles were observed in the case of pure Pd@VC catalyst, whereas well dispersed Pd nanoparticles were obtained in presence of NW support. The high-resolution TEM image of Pd@10%NW/VC in **Figure 3.2a** depicts fringes with spacing 0.232 and 0.241 nm corresponding to (111) plane of Pd and (002) planes of NW, respectively. Further, the presence of constituent elements Pd, Ni, W and O were identified from TEM elemental mapping

displayed in **Figure 3.3(b, c, d, e, f)**. The calculated value of the prepared catalyst composition was in agreement with the experimental value from TEM-EDX (**Figure 3.4**).

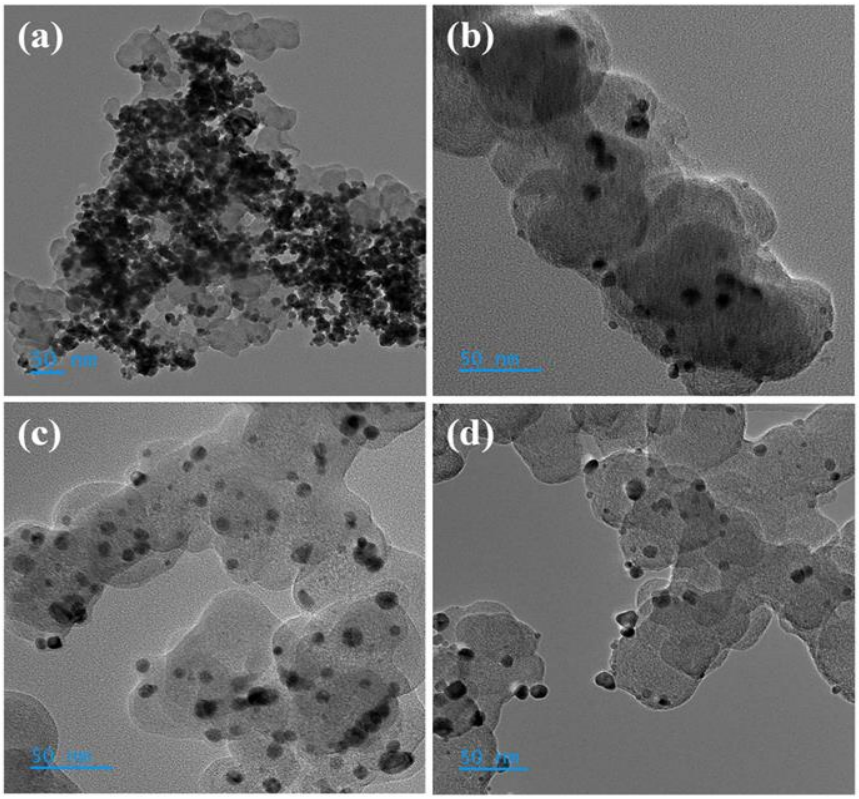

Figure 3.2 TEM images of (a) Pd@VC, (b) Pd@5% NW/VC, (c) Pd@10% NW/VC and (d) Pd@15% NW/VC.

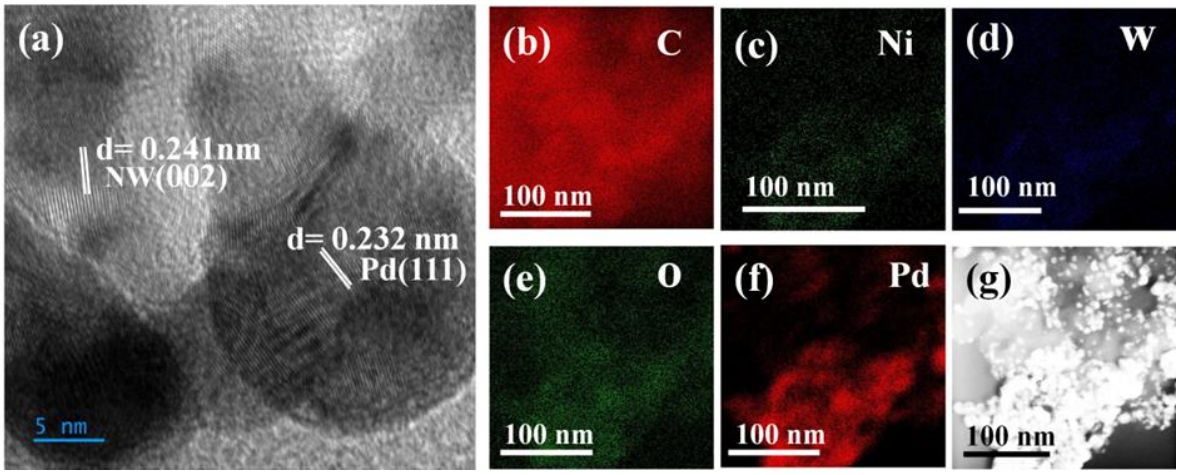

Figure 3.3 HRTEM image of (a) Pd@10% NW/VC, TEM elemental mapping of (b) C, (c) Ni, (d) W, (e) O, (f) Pd and (g) STEM image of Pd@10% NW/VC.

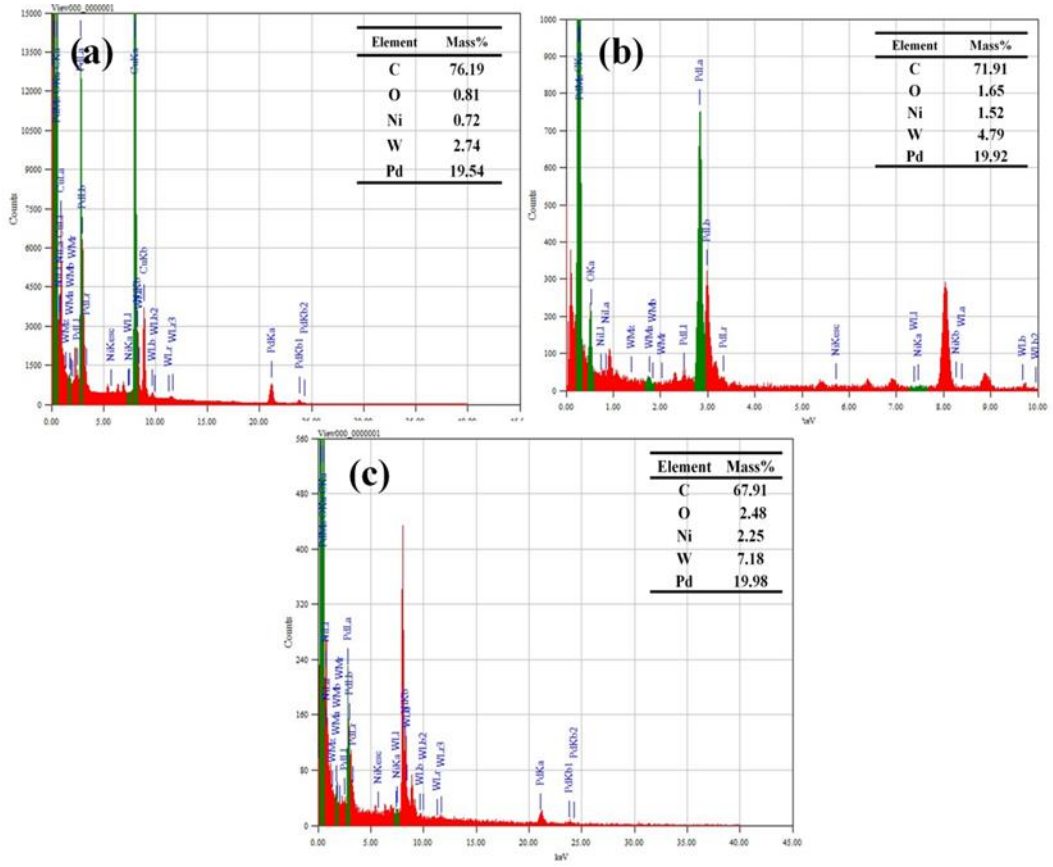

Figure 3.4 TEM-EDX spectrum of (a) Pd@5% NW/VC, (b) Pd@10% NW/VC and (c) Pd@15% NW/VC.

3.4.3 XPS analysis

The oxidation state of the elements in Pd@10%NW/VC was examined through XPS analysis. Survey spectrum (**Figure 3.5a**) indicates the presence of elements Pd, Ni, W, O and C. The deconvoluted high resolution spectra of Ni (**Figure 3.5b**) shows peaks at binding energy 856.7 and 874.5 eV corresponding to the $2p_{3/2}$ and $2p_{1/2}$ energy levels and indicates the presence of Ni^{2+}. The peaks centered at 862.2 and 880.3 eV correspond to the satellite peaks associated with Ni^{2+}. The high-resolution spectra of W 4f in **Figure 3.5c** illustrated the spin orbit doublets $4f_{7/2}$ and $4f_{5/2}$ at binding energy 35.8 and 38.01 eV, respectively, that confirms the +6 oxidation state of W.[10] Binding energies at 532.9 eV in the deconvoluted high resolution O 1s spectra (**Figure 3.5d**) implies the oxygen bond with Ni and W in $NiWO_4$.[9] Thus, confirmed the $NiWO_4$ formation from XPS analysis.

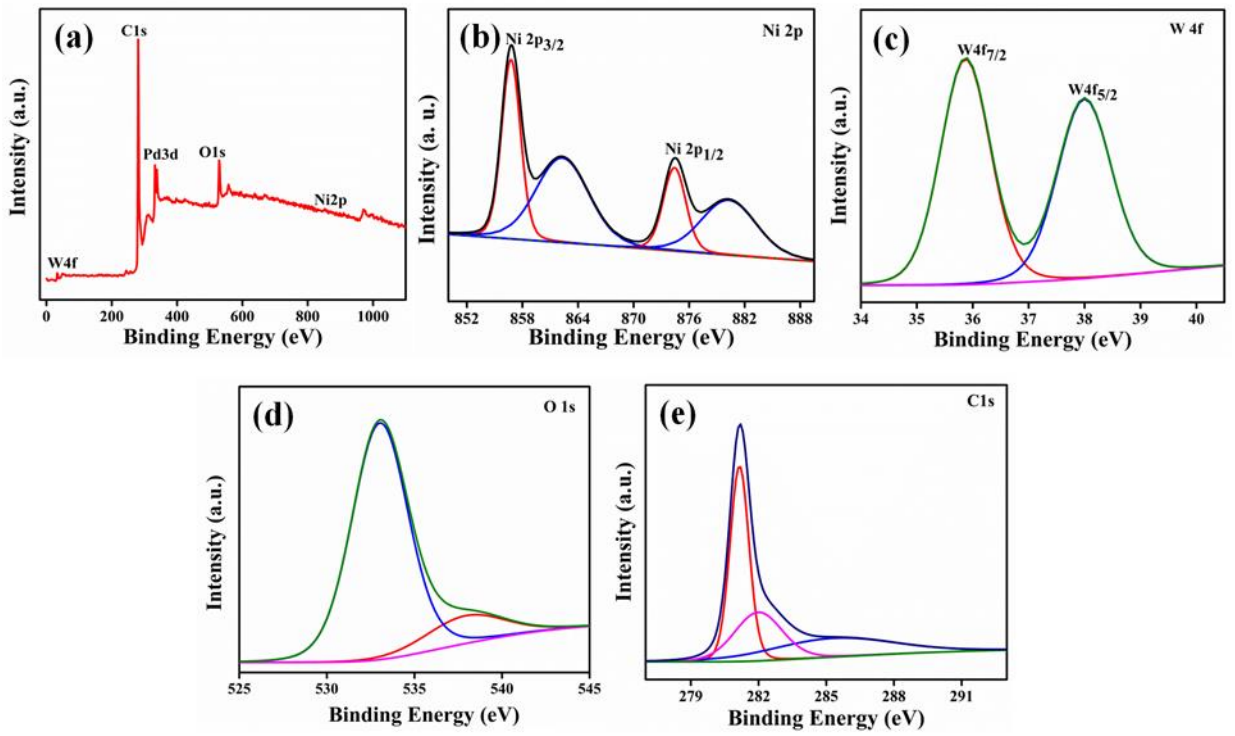

Figure 3. 5 (a) Survey spectrum of Pd@10% NW/VC, deconvoluted high resolution spectra of (b) Ni 2p, (c) W 4f, (d) O 1s and (e) C 1s of Pd@10% NW/VC.

Deconvoluted high resolution spectra of Pd 3d in Pd@10% NW/VC, Pd@10%WO/VC and Pd@10%NO/VC were compared in **Figure 3.6**. All the spectra were deconvoluted into two pairs of doublets, in which, sharp high intense peaks correspond to Pd^0 and broad low intense peaks correspond to Pd^{2+}. In the case of Pd@VC sample, Pd^0 binding energy peaks were observed at 335.40, 340.92 eV and Pd^{2+} peaks at 336.52 and 342.11 eV. However, the respective peaks are slightly shifted to higher energy, after modifying C with NO, WO and NW. The extent of binding energy shift observed is in the order NO < WO < NW. The shift in Pd 3d binding energy peaks indicates an electronic modification on Pd. Since, the shift was towards higher binding energy it confirms a decrease in electron density on Pd and a downshift of the d band center.[13] When C is modified with NO or WO, Pd interacts with Ni or W, such that it develops an electron density movement on Pd, evident by the binding energy change. Whereas, when it comes to NW modification, a hypo-hyper d electronic mechanism was developed in between supporting substrate $NiWO_4$ and Pd. The hypo d tungstate builds a strong interaction with hyper d electrons in Pd, at the interphase between Pd and nickel tungstate.[14] Due to this strong bimetal

interaction of Ni and W with Pd, the extent of binding energy shift is comparably higher than that of NO/VC and WO/VC, where there is only a monometallic interaction is possible. Eventually, the greater electronic modification of Pd in Pd@10% NW/VC compared to Pd@10%WO/VC and Pd@10%NO/VC helped to improve the catalytic activity towards alcohol electro-oxidation.

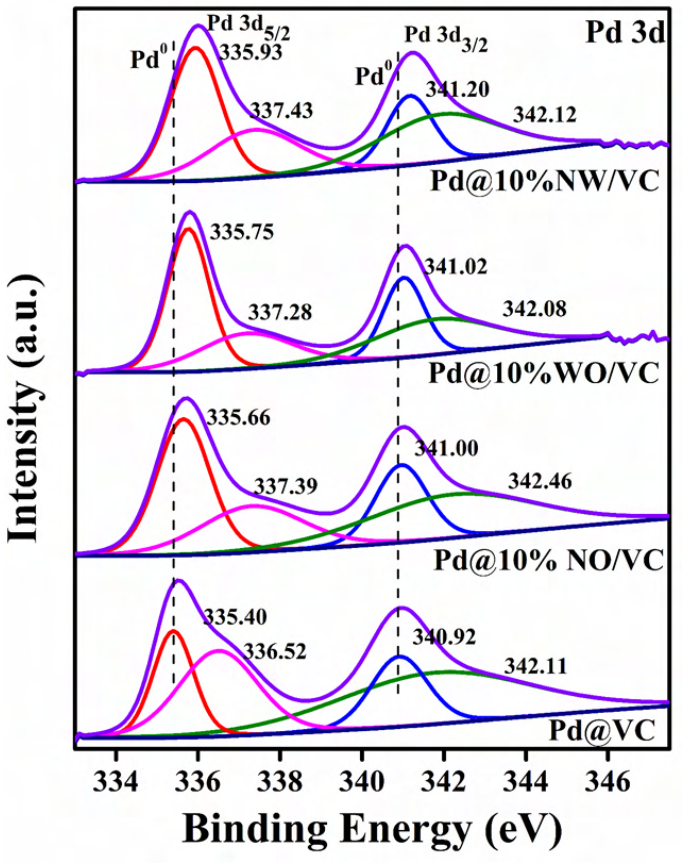

Figure 3.6 Deconvoluted high-resolution XPS spectra of Pd 3d of Pd@10% NW/VC, Pd@10% WO/VC, Pd@10% NO/VC and Pd@VC.

3.4.4 Electrochemical analysis

3.4.4 (a) Methanol electro-oxidation

Electrocatalytic property of the catalysts were carried out in N_2 saturated 0.5 M KOH solution at a scan rate of 50 mV/s. The cyclic voltammograms of the catalysts were depicted in **Figure 3.7a** and the ECSA was calculated. The ECSA indicates the electrochemically active surface area and it provides insights into catalyst performance. The ECSA calculated to be 36.83,

99.67, 50.96 and 12.56 m^2/g for Pd@5%NW/VC, Pd@10%NW/VC, Pd@15%NW/VC and Pd@VC, respectively. The improved surface area in the case of Pd@10%NW/VC enhances the catalytic activity. The ECSA gives an indication about the potential of the catalyst.

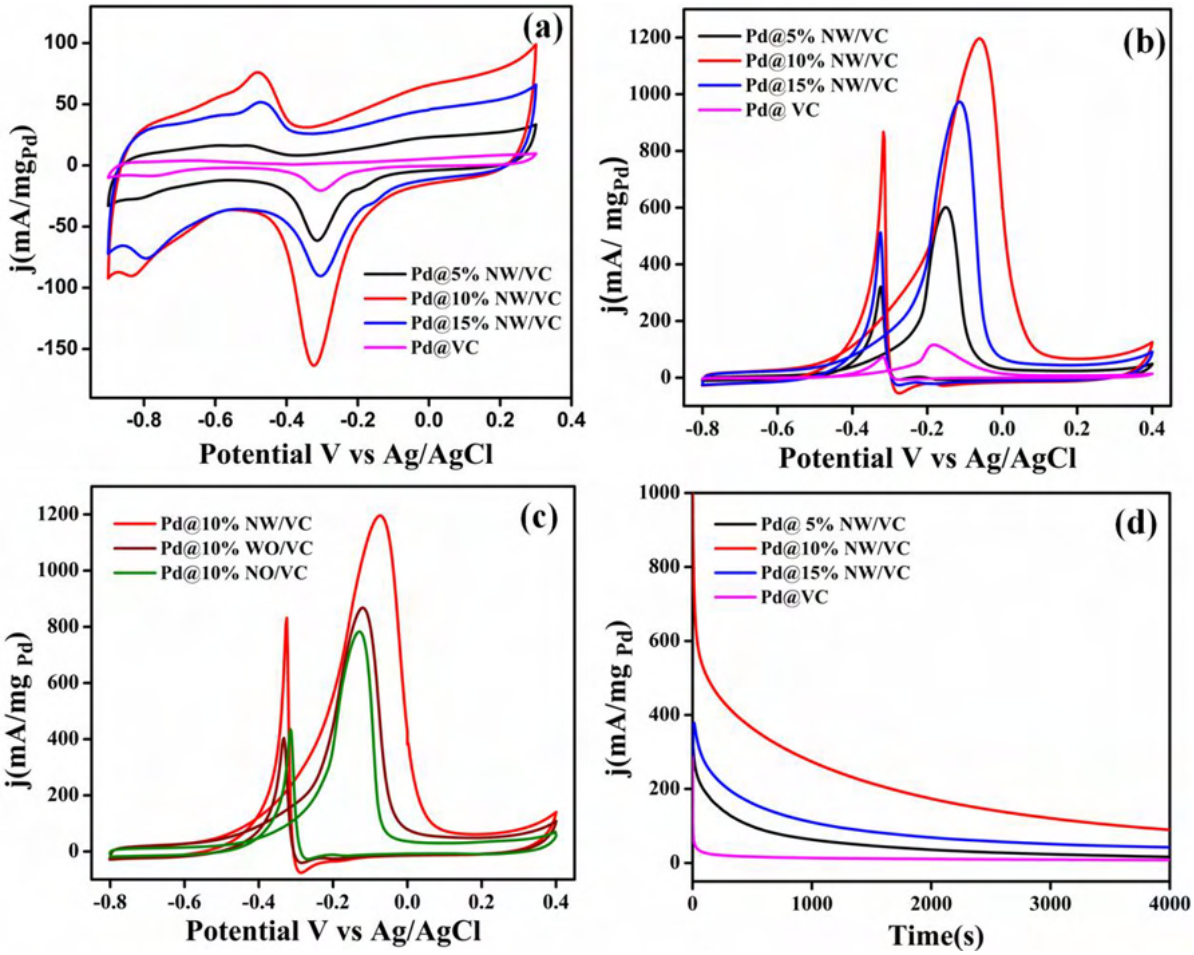

Figure 3.7 (a) CV curves of prepared catalysts in 0.5 M KOH, (b, c) in 0.5 M KOH + 0.5 M CH_3OH solution at a scan rate of 50 mV/s and (d) Chronoamperometric studies of the catalysts in 0.5 M KOH + 0.5 M CH_3OH solution.

Performance of the catalysts towards MOR were investigated by carrying out the CV in N_2 saturated 0.5 M KOH and 0.5 M methanol solution at a scan rate of 50 mV/s. The corresponding CV curves were displayed in **Figure 3.7b** Pd@5%NW/VC, Pd@10%NW/VC, Pd@15%NW/VC and Pd@VC catalysts exhibited mass activity 606.69, 1202.48, 982.21, 117.04 mA/mg_{Pd}, respectively. Pd particles over NW/VC catalysts possess better activity than that of Pd deposited carbon catalyst. Incorporation of NW helps to enhance the catalytic activity of the Pd

particles. The low onset potential, peak potential and high mass activity depicted by Pd@10%NW/VC catalyst indicates its superior activity towards MOR than the other prepared catalysts (**Table 3.1**).

Table 3.1. Onset potential and mass activity values of the prepared catalysts**.**

Catalyst	Onset potential (V)	Mass Activity (mA/mg_{Pd})
Pd@5%NW/VC	-0.408	606.69
Pd@10%NW/VC	-0.486	1202.48
Pd@15%NW/VC	-0.456	982.21
Pd@VC	-0.354	117.04

The methanol oxidation on Pd surface follows the mechanism (eq. 5-10) in which step (10) was the rate determining step.[15]

$$Pd + CH_3OH \rightarrow Pd\text{-}(CH_3OH)_{ads} \quad (5)$$

$$Pd\text{-}(CH_3OH)_{ads} + OH^- \rightarrow Pd\text{-}(CH_3O)_{ads} + H_2O + e^- \quad (6)$$

$$Pd\text{-}(CH_3O)_{ads} + OH^- \rightarrow Pd\text{-}(CH_2O)_{ads} + H_2O + e^- \quad (7)$$

$$Pd\text{-}(CH_2O)_{ads} + OH^- \rightarrow Pd\text{-}(CHO)_{ads} + H_2O + e^- \quad (8)$$

$$Pd\text{-}(CHO)_{ads} + OH^- \rightarrow Pd\text{-}(CO)_{ads} + H_2O + e^- \quad (9)$$

$$Pd\text{-}(CO)_{ads} + 2OH^- \rightarrow Pd + CO_2 + H_2O + 2e^- \quad (10)$$

The activity of Pd@10%NW/VC catalyst was compared with Pd@WO/VC and Pd@NO/VC. The obtained cyclic voltammograms were shown in **Figure 3.7c**. A mass activity of 872.46 mA/mg_{Pd} was obtained for Pd@10%WO/VC and an activity of 782.60 mA/mg_{Pd} was obtained for Pd@10%NO/VC catalyst. Comparing these results, Pd@10%NW/VC catalyst exhibited better performance than that of Pd@10%WO/VC and Pd on10%NO/VC catalysts. The extended electronic modification of Pd in Pd@10%NW/VC than that in Pd@10%WO/VC and Pd@10%NO/VC due to the metal support interaction between Pd and NW boosts the efficiency of Pd. The down shift in d band center leads to the weakening of CO adsorption.[16] The presence of both Ni and W also contribute towards the enhanced catalytic activity. The oxophilic nature of both Ni and W helps to get rid of the attached CO molecules on Pd surface formed during the

MOR.[17-19] The CO molecules get oxidized faster and thereby increase the reaction rate of methanol oxidation. The combined action of NW, carbon, and Pd promoted the catalytic activity of catalyst.

The electrocatalytic stability of the catalysts were investigated using chronoamperometric measurements. **Figure 3.7d** shows the Chronoamperometric measurements of catalysts recorded at a potential of -0.1 V for 4000 s in 0.5 M KOH solution containing 0.5 M methanol. Even if the current disintegrates after a while, the Pd@10%NW/VC imparts lowest rate of disintegration among all the recorded catalysts, indicating its better durability.

EIS was employed to explore the kinetic properties of the catalysts. EIS characterizations of catalysts were consistent with CV measurements which are depicted in the **Figure 3.8**. A large diameter in the Nyquist plot indicates a large Faradaic resistance, which corresponds to a low methanol oxidation current density.[20] Charge transfer resistance of synthesized catalysts Pd@5%NW/VC, Pd@10%NW/VC, Pd@15%NW/VC and Pd@VC were 16.9, 12.2, 15.2 and 24.2 $k\Omega cm^{-2}$, respectively. Lower resistance of Pd@10%NW/VC supports its better catalytic activity.

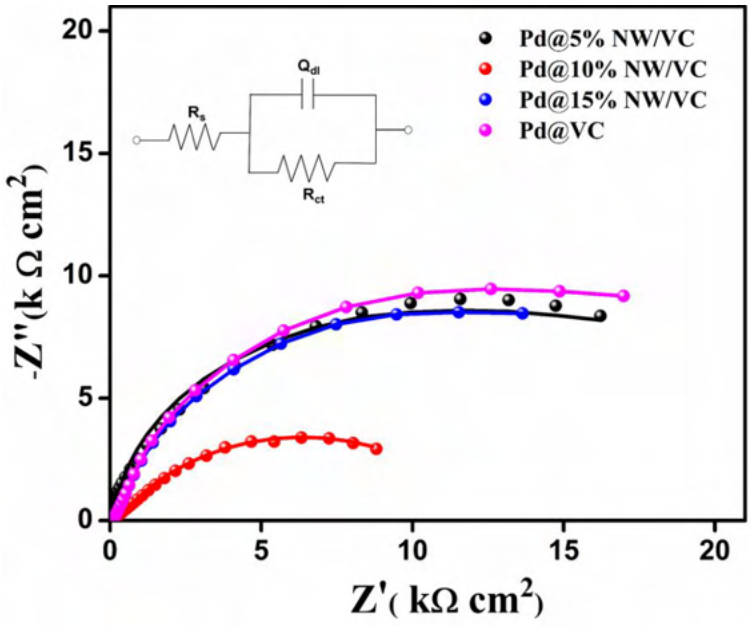

Figure 3.8 Nyquist plots of the catalysts in 0.5 M KOH + 0.5 M CH_3OH solution.

3.4.4 (b) Ethanol electro-oxidation

Efficiency of the catalysts towards EOR was illustrated by carrying out the CV in 0.5 M KOH containing 0.5 M ethanol. **Figure 3.9** depicts the cyclic voltammograms of the catalysts for EOR. The CV curves exhibited a similar result for EOR as that of MOR.

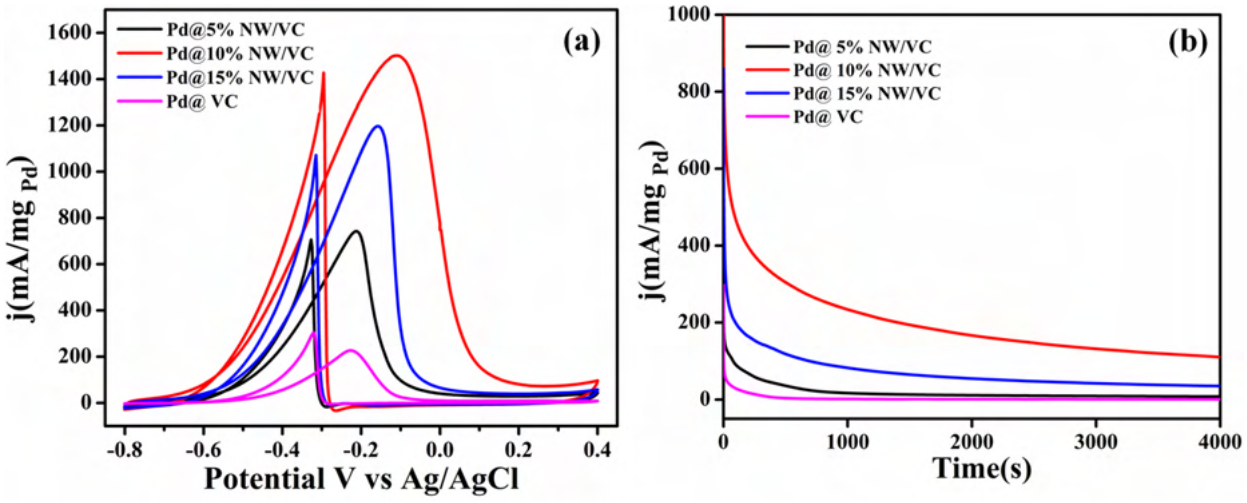

Figure 3.9 (a) CV curves of prepared catalysts in 0.5 M KOH + 0.5 M C_2H_5OH solution and (b) Chronoamperometric curves of the catalysts in 0.5 M KOH + 0.5 M C_2H_5OH solution.

As shown in **Figure 3.9a**, Pd@10%NW/VC exhibited highest mass activity than that of other catalysts and pure Pd@VC catalyst. A mass activity of 746.16, 1508.24, 1201.93 mA/mg_{Pd} were obtained for Pd@5%NW/VC, Pd@10%NW/VC, Pd@15%NW/VC catalyst whereas an activity of 234.33 mA/mg_{Pd} was observed for pure Pd@VC catalyst. Furthermore, the electrocatalytic stability of the catalysts was assessed by making the chronoamperometric measurements at -0.1 V for 4000 s (**Figure 3.9b**). In comparison with Pd@5%NW/VC, Pd@15%NW/VC and pure Pd@VC catalyst, Pd@10%NW/VC possesses excellent stability.

3.4.5 Stability studies

Stability of the synthesized catalysts were analyzed by performing the CV for 500 cycles. **Figure 3.10** displays the CV curves of the catalysts conducted for MOR and EOR.

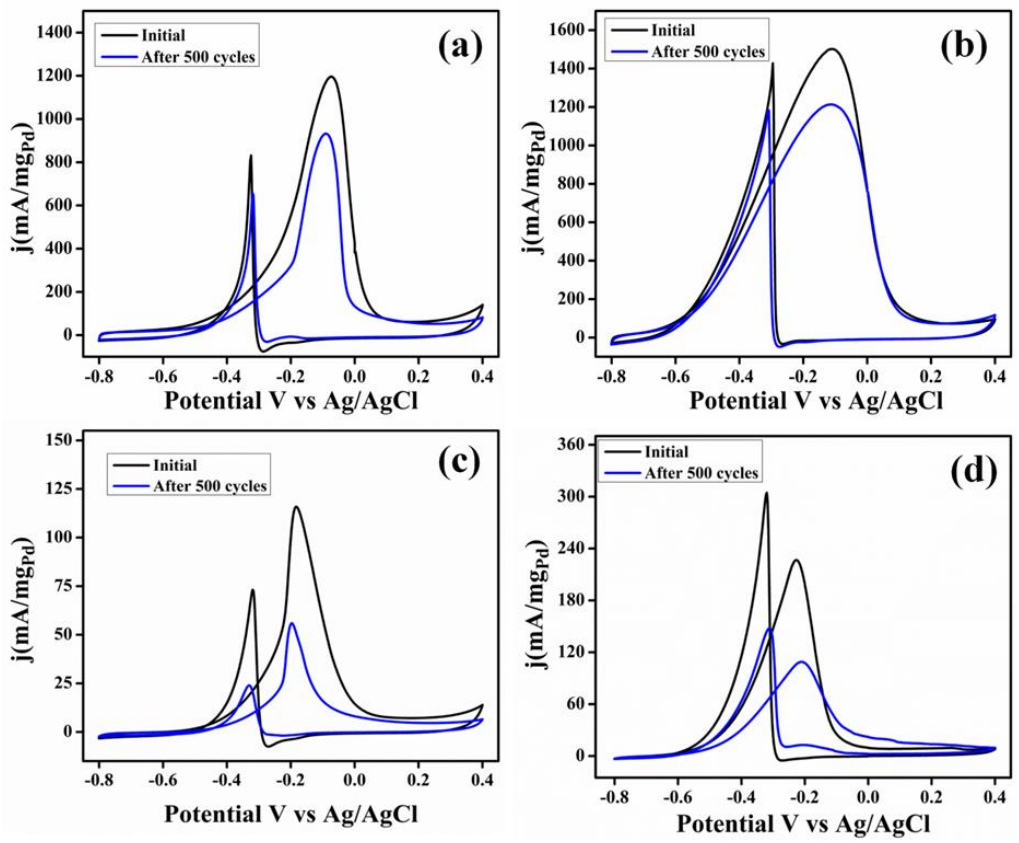

Figure 3.10 Stability studies after 500 cycles in N_2 saturated solution of Pd@10% NW/VC (a) 0.5 M KOH + 0.5 M CH_3OH, (b) 0.5 M KOH + 0.5 M C_2H_5OH and Pd@VC (c) 0.5 M KOH + 0.5 M CH_3OH and (d) 0.5 M KOH + 0.5 M C_2H_5OH.

Pd@10%NW/VC catalyst exhibited comparably better stability even after completing the CV for 500 cycles. The obtained current value maintained without much reduction for both MOR and EOR in the case of Pd@10%NW/VC catalyst, instead a drastic current decay was noted for pure Pd@VC catalyst.

3.4.6 Comparative study

Activity of different carbon supported catalysts was compared with the present work and tabulated (**Table 3.2**). NW plays an important role in enhancing the efficiency of the synthesized catalyst.

Table 3.2 Catalytic activity comparison towards alcohol oxidation

Catalysts	Electrolyte	Mass activity (mA/mg_{Pd})	Reference
Pd/PPY/graphene	0.5M NaOH + 1M Methanol	359.8	21
PdMo/VCNT	1M KOH + 1 M Methanol	395.6	22
Pd/MnO_2/VCNT	0.5M NaOH + 1M Methanol	431.02	23
Pd_3Mo/VC	1M KOH + 1 M Methanol	647.27	24
$Pd_{10}Ag_{10}$/VCNT	1M KOH + 0.5 M Methanol	731.20	25
Cu_1Pd_2/VC	0.5 M KOH + 0.5 M Methanol	220.00	26
Cu_1Pd_2/VC	0.5 M KOH + 0.5 M Ethanol	520.00	26
$Pd_{90}Au_{10}$/VCNT	1M KOH + 1 M Ethanol	1050.00	27
Commercial Pd/VC	0.5 M KOH + 0.5 M Methanol	180.00	28
Pd@5% NP/VC	0.5 M KOH + 0.5 M Methanol	804.67	19
Pd@5% NP/VC	0.5 M KOH + 0.5 M Ethanol	772.96	19
Pd@10% NW/VC	**0.5 M KOH + 0.5 M Methanol**	**1202.48**	**Present work**
Pd@10% NW/VC	**0.5 M KOH + 0.5 M Ethanol**	**1508.24**	**Present work**

3.5 Conclusion

NW modified carbon supported Pd catalyst was employed for the alcohol electro-oxidation in alkaline medium. The synthesised catalysts showcased excellent catalytic activity towards MOR and EOR. A ten-fold and six-fold increment in catalytic activity towards MOR and EOR, respectively, were achieved for Pd@10%NW/VC catalyst compared to that of Pd deposited carbon catalyst. A mass activity of 1202.48 mA/mg_{Pd} and 1508.24 mA/mg_{Pd} were obtained for MOR and EOR, respectively. The incorporation of NW substantially enhanced the catalytic activity through electronic modification due to metal support interaction and improved CO tolerance. The synergistic effect of nickel tungstate and Pd along with the conductive carbon led to impressive activity and durability of Pd@10%NW/VC catalyst towards both MOR and EOR.

3.6 References

(1) El-Sheikh, S.M., Rashad, M.M. Novel Synthesis of Cobalt Nickel Tungstate Nanopowders and its Photocatalytic Application. *J Clust Sci*. **2015**; *26*, 743–757. https://doi.org/10.1007/s10876-014-0735-z.

(2) Yang, M., Zheng, C., Wang, Q. *et al.* Improvement of specific capacitance and rate performance of $NiWO_4$ synthesized through modified chemical precipitation. *J Mater Sci: Mater Electron*. **2021**; *32*, 12232–12240. https://doi.org/10.1007/s10854-021-05852-3.

(3) S.M.M. Zawawi, R. Yahya, A. Hassan, H.N.M.E. Mahmud, M.N. Daud, Structural and optical characterization of metal tungstates (MWO4; M = Ni, Ba, Bi) synthesized by a sucrose-templated method. *Chem. Central J.* **2013**; *7*, 80−90. https://doi.org/10.1186/1752-153X-7-80.

(4) Huang Biao, Wang Huayu, Liang Shunfei, Qin Huizhen, Li Yang, Luo Ziyang, Zhao Chenglan, Xie Li, Chen Lingyun. Two-dimensional porous cobaltâ€“nickel tungstate thin sheets for high performance supercapattery. *Energy Storage Mater*. **2020**; *32*, 105-114. https://doi.org/10.1016/j.ensm.2020.07.014.

(5) Mani, S., Vediyappan, V., Chen, SM. *et al.* Hydrothermal synthesis of $NiWO_4$ crystals for high performance non-enzymatic glucose biosensors. *Sci Rep*. **2016**; *6*, 24128. https://doi.org/10.1038/srep24128.

(6) Wang Ya, Liu Gang. Reduced graphene oxide supported nickel tungstate nano-composite electrocatalyst for anodic urea oxidation reaction in direct urea fuel cell. *Int. J. Hydrogen Energy.* **2020**; *45*, 33500-33511. https://doi.org/10.1016/j.ijhydene.2020.09.095.

(7) Suwen Li , Yu Zhang , Yuanxia Han , Fangfei Lv , Baocang Liu , Lili Huo. Bimetallic molybdenum-tungsten carbide/reduced graphene oxide hybrid promoted Pt catalyst with enhanced electrocatalytic activity and stability for direct methanol fuel cell, *Appl.Surf.Sci*, **2022**; *600,*154134, https://doi.org/10.1016/j.apsusc.2022.154134.

(8) Liang Huang;Xiliang Zheng;Ge Gao;He Zhang;Kai Rong;Jinxing Chen;Yongqin Liu;Xinyang Zhu;Weiwei Wu;Ying Wang;Jin Wang;Shaojun Dong. Interfacial Electron Engineering of Palladium and Molybdenum Carbide for Highly Efficient Oxygen

Reduction. *J. Am. Chem. Soc.* **2021**; *143*, 6933–6941. https://doi.org/10.1021/jacs.1c00656.

(9) Wang, Yanhui; Su, Jing; Dong, Liang; Zhao, Pengjuan; Wang, Weiping; Zhang, Yan; Jia, Shaopei; Zang, Jianbing. A novel hybrid of Ni and WC on new-diamond supported Pt electrocatalyst for methanol oxidation and oxygen reduction reactions. *ChemCatChem*, **2017**; *9*, 3982-3988,http://dx.doi.org/10.1002/VCctc.201700866.

(10) Mohamed, Mohamed Mokhtar, Khairy, M. Eid, Salah. Polyethylene glycol assisted one-pot hydrothermal synthesis of $NiWO_4$ /WO_3 heterojunction for direct Methanol fuel cells. *Electrochimica Acta*, **2018**; *26*3, 286-298. doi.org/10.1016/j.electacta.2018.01.063.

(11) Sitthisuntorn Supothina; Panpailin Seeharaj; Sorachon Yoriya; Mana Sriyudthsak Synthesis of tungsten oxide nanoparticles by acid precipitation method. *Ceram.Int*. **2007**; *33*,931–936. doi:10.1016/j.ceramint.2006.02.007.

(12) El-Kemary, M.; Nagy, N.; El-Mehasseb, I. Nickel oxide nanoparticles: Synthesis and spectral studies of interactions with glucose. *Mater. Sci. in Semicond. Process*. **2013**; *16*, 1747–1752. https://doi.org/10.1016/j.mssp.2013.05.018.

(13) Lu, Yizhong; Jiang, Yuanyuan; Gao, Xiaohui; Wang, Xiaodan; Chen, Wei. Strongly Coupled Pd Nanotetrahedron/Tungsten Oxide Nanosheet Hybrids with Enhanced Catalytic Activity and Stability as Oxygen Reduction Electrocatalysts. *J. Am. Chem. Soc.*, **2014**; *136*, 11687–11697. https://doi.org/10.1021/ja5041094.

(14) Ermete Antolini Composite materials: An emerging class of fuel cell catalyst supports. *Appl. Catal. B Environ.* , **2010**; *100*, 413–426. doi:10.1016/j.apcatb.2010.08.025.

(15) Soleimani-Lashkenari, Mohammad; Rezaei, Sajjad; Fallah, Jaber; Rostami, Hussein Electrocatalytic performance of Pd/PANI/TiO_2 nanocomposites for methanol electrooxidation in alkaline media. *Synth. Met*. **2018**; *23*, 571–79. http://dx.doi.org/10.1016/j.synthmet.2017.12.001.

(16) Kyung Rok Lee; Danim Yun; Dae Sung Park; Yang Sik Yun; Chyan Kyung Song; Younhwa Kim; Jungwon Park; Jongheop Yi. In situ manipulation of the d-band center in metals for catalytic activity in CO oxidation. *Chem. Commun*., **2021**; *57*, 3403.

(17) Shibli, S.M.A.; Anupama, V.R.; Arun, P.S.; Jineesh, P.; Suji, L. Synthesis and development of nano WO_3 catalyst incorporated Ni–P coating for electrocatalytic

hydrogen evolution reaction. *Int. J. Hydrogen Energy*., **2016**; *41*, 10090-10102. https://doi.org/10.1016/j.ijhydene.2016.04.156.

(18) Kepp, Kasper P. A Quantitative Scale of Oxophilicity and Thiophilicity. *Inorg. Chem*. **2016**; *55*, 9461–9470. https://doi.org/10.1021/acs.inorgchem.6b01702.

(19) Kottayintavida, R., Gopalan, N. K. Nickel phosphate modified carbon supported Pd catalyst for enhanced alcohol electro oxidation, *Int. J. Hydrogen Energy*.**, 2020**; *45*, 11116-11126. https://doi.org/10.1016/j.ijhydene.2020.02.050.

(20) Wang, Wei; Chu, Qingxin; Zhang, Yingnan; Zhu, Wei; Wang, Xiaofeng; Liu, Xiaoyang. Nickel foam supported mesoporous $NiCo_2O_4$ arrays with excellent methanol electro-oxidation performance, *NewJ.Chem*., **2015**; 39(8),6491–6497. doi:10.1039/c5nj00766f.

(21) Yanchun Zhao, Lu Zhan, Jianniao Tian, Sulian Nie, Zhen Ning. Enhanced electro catalytic oxidation of methanol on Pd/polypyrrole–grapheme in alkaline medium, *Electrochim. Acta*, **2011**; *56*,1967- 1972. https://doi.org/10.1016/j.electacta.2010.12.005.

(22) Kakati, N., Maiti, J., Lee, S. H., Yoon, Y. S. Core shell like behavior of PdMo nanoparticles on multiwall carbon nanotubes and their methanol oxidation activity in alkaline medium, *Int. J. Hydrogen Energy*., **2012**; *37* 19055–19064. https://doi.org/10.1016/j.ijhydene.2012.09.083.

(23) Y. Zhao, L. Zhan, J. Tian, S. Nie , Z. Ning. MnO_2 modified multi-walled carbon nanotubes supported Pd nanoparticles for methanol electro-oxidation in alkaline media, *Int. J. Hydrogen Energy.*, **2010**; *35*,10522–1052.doi.org/10.1016/j.ijhydene.2010.07.048

(24) Fathirad, F., Mostafavi, A., Afzali, D. Bimetallic Pd–Mo nanoalloys supported on Vulcan XC-72R carbon as anode catalysts for direct alcohol fuel cell. *Int. J. Hydrogen Energy*.; **2017**; *42*, 3215–3221. https://doi.org/10.1016/j.ijhydene.2016.09.138.

(25) M. Satyanarayana, G. Rajeshkhanna, Malaya K. Sahoo, G. Ranga Rao. Electrocatalytic Activity of Pd20−xAgx Nanoparticles Embedded in Carbon Nanotubes for Methanol Oxidation in Alkaline Media, *ACS. Appl. Energy Mater*., **2018**; *1*, 3763−3770. https://doi.org/10.1021/acsaem.8b00544.

(26) Mao, Han; Huang, Tao; Yu, Aishui. Surface Palladium rich CuxPdy/VCarbon catalysts for methanol and ethanol oxidation in alkaline media. *Electrochim. Acta*., **2015**; *174* ,1–7. https://doi.org/10.1016/j.electacta.2015.05.160.

(27) Caglar, Aykut; Kivrak, Hilal. Highly active carbon nanotube supported PdAu alloy catalysts for ethanol electrooxidation in alkaline environment. *Int. J. Hydrogen Energy*., **2019**; *44*,11734-11743. https://doi.org/10.1016/j.ijhydene.2019.03.118.

(28) Shih, Z.-Y., Wang, C.-W., Xu, G., & Chang, H.T. Porous palladium copper nanoparticles for the electrocatalytic oxidation of methanol in direct methanol fuel cells. *J. Mater. Chem. A*, **2013**; *1*, 4773. doi.org/10.1039/VC3TA01664A.

Chapter 4

Pd modified Ni nanowire as an efficient electro-catalyst for alcohol oxidation reaction

4.1 Abstract

Nano-structural architecture plays a crucial role in the catalytic activity. The present chapter reports a cost effective one-dimensional (1D) nano structured electro-catalyst for improved alcohol oxidation reaction rate. Pd modified Ni nanowire catalyst for methanol electro oxidation was prepared by a simple galvanic replacement reaction. Exclusive nanowire morphology achieved through a wet chemical reduction method without employing any capping agents or surfactants. Pd modified Ni nanowires exhibited a supreme catalytic activity and durability towards methanol electro-oxidation. The distinctive 1D morphology and strong metal support interaction (SMSI) between Pd and Ni along with the bifunctional effects of Pd and Ni attributed to the enhanced catalytic activity. The amount of precious Pd metal was reduced by 90 wt% with enhanced catalytic efficiency. Ethanol electro-oxidation study showed an improved catalytic activity with mass activity of 1479.79 $mA/mg_{Pd.}$

4.2 Introduction

The catalytic activity of Pd can be enhanced by alloying it with other metals such as Au, Rh, Cu, Ag, Sn, Co, Ni etc.[1-4] Variety of Pd based nano materials such as Pd nanosphere, PdNi nanosphere, PdCu nanoparticles and PdCu aerogel are also reported.[5] Among which PdNi electro-catalyst has gained great attention. Zhang *et al*. found negatively shifted onset potential and high peak current for core shell Ni-Pd/C compared to Pd/C.[6] Wang *et al*. reported the high activity and excellent stability for Pd supported Ni foam.[7] By chemical reduction method Liu *et al*. synthesized Pd Ni nanoparticles, Pd Ni film and its alloy obtained by electro deposition exhibited enhanced catalytic activity compared with pure Pd.[8] The presence of Ni promotes the CO tolerance capability of Pd and thereby increases the catalytic efficiency.[9-11] However, development of a facile method for synthesizing highly active Pd electro-catalysts with well-defined nano-structures still remains a great challenge.

The galvanic replacement is one of the interesting technique employed for the manufacture of metal nanoparticles for catalytic applications. It allows the rapid synthesis of bimetallic nano materials in a single step reaction utilizing water as the solvent.[12] The galvanic replacement reaction involves a redox process between metal ions in solution and a metal which is used as a sacrificial template. The reaction is driven by the difference in electrical reduction potential between the sacrificial template and the metal ions in solution. Upon contact in solution phase, oxidation and dissolution of the template along with reduction of metal ions in solution takes place and the metal ions get plated on to the surface of the template. This strategy leads to wide variety of metal nanostructures displaying a high surface to volume ratio.[13-14] The present study focused to reduce the Pd loading in the catalyst composition without compromising catalytic efficiency. 1D Ni nanowires (Ni NW) were prepared by a wet chemical reduction method without the involvement of surfactants and templates; through self-oriented attachment of nano particles. [15] Pd modified Ni NW catalyst synthesized by galvanic replacement reaction. Ni NW was selected as the supporting material where the oxophilic nature of Ni particles can also contribute to the catalytic activity of the incorporated Pd.[16-19] The unique morphology and metal support interaction of the catalyst along with the bifunctional mechanism between Pd and Ni enhanced the activity of the catalyst towards alcohol oxidation.

4.3 Experimental Section

4.3.1 Materials and methods

All chemicals were of analytical grade and used without any further purification. Nickel (II) chloride (99.99%), Ethylene glycol (99.99%), Palladium (II) chloride (99.99%) and Potassium hydroxide (99.99%) were purchased from Aldrich. Hydrazine hydrate (99.99%), hydrochloric acid (99.99%), methanol (99.9%) and ethanol (99.9%) were purchased from Merck.

4.3.2 Synthesis of Ni NW catalyst

Ni NW were prepared by the reduction of Nickel chloride using ethylene glycol as solvent and hydrazine hydrate as the reducing agent.[15] Required volume of 1 M aqueous nickel chloride was added to 7.5 ml of ethylene glycol to obtain a 10 mM solution of Ni^{2+}. Then the mixture was heated to 120 ˚C followed by the addition of 0.5 ml of hydrazine hydrate solution. The solution turned black and the formed nickel wires were found floating on the surface of the solution. In order to remove the excess solvent and hydrazine hydrate, the recovered nano-wires were washed first with deionized water and then with ethanol followed by storing in isopropanol solution.

Scheme 4.1 Synthesis of Ni NW.

4.3.3 Synthesis of Pd modified Ni NW catalyst

The Pd modified Ni NW (5, 10 and 15 wt% Pd on Ni NW) were prepared by a spontaneous displacement reaction. Required amount of as prepared Ni NW were ultrasonically

dispersed in water, followed by the addition of required amount of 10 mM H_2PdCl_4 solution. Then, the solution was continuously stirred for 3 h and left for one day to complete the reaction. The solid product that remained at the end of the reaction was filtered and washed with DI water and dried. The 5, 10 and 15 wt% Pd on Ni NW were designated as 5% Pd on Ni NW, 10% Pd on Ni NW and 15% Pd on Ni NW, respectively.

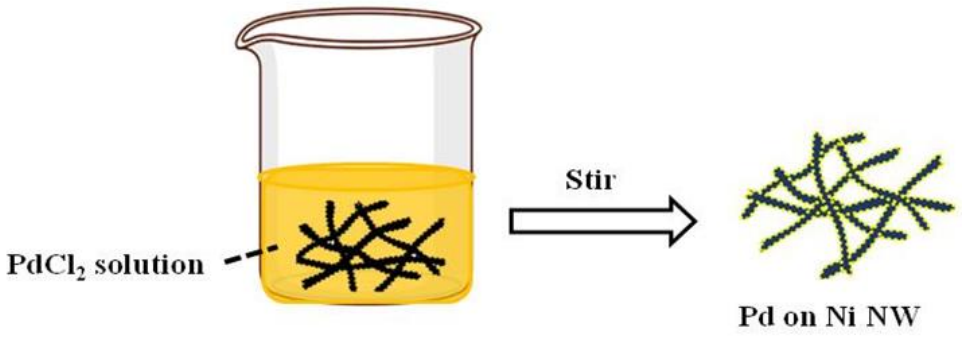

Scheme 4.2 Synthesis of Pd modified Ni NW catalyst.

4.4 Results and discussion

4.4.1 Morphological analysis

The SEM images in **Figure 4.1a,** illustrated the wire morphology of the Ni nanomaterial obtained through a simple wet chemical reduction method. The attractive wire morphology was prepared by the reduction of nickel chloride using hydrazine hydrate reducing agent in ethylene glycol at 120 ˚C. **Figure 4.1b** shows the SEM images of the Pd modified Ni NW prepared through the galvanic replacement reaction. The Ni^{2+} species have (Ni^{2+}/Ni = -0.25 V vs. SHE) lower reduction potential than that of $PdCl_4^{2-}$/Pd redox pair (0.62 V vs. SHE). Retention of the wire morphology even after the modification was understood from these images. The obtained SEM images of 5, 10 and 15% Pd on Ni NW were depicted in **Figure 4.2(a, b, c)**. The compositions of the prepared catalysts were understood from the corresponding SEM-EDS spectrum shown in **Figure 4.2(d, e, f)**.

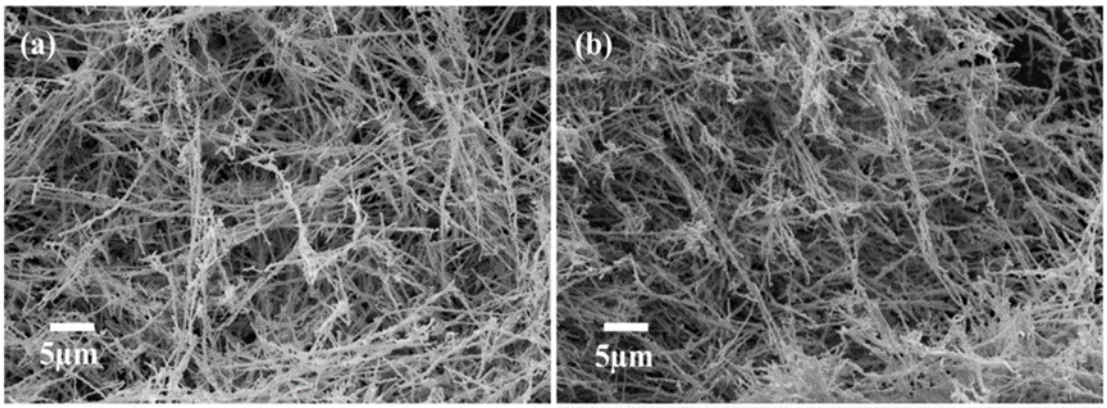

Figure 4.1 SEM images of (a) Ni NW and (b) Pd modified Ni NW.

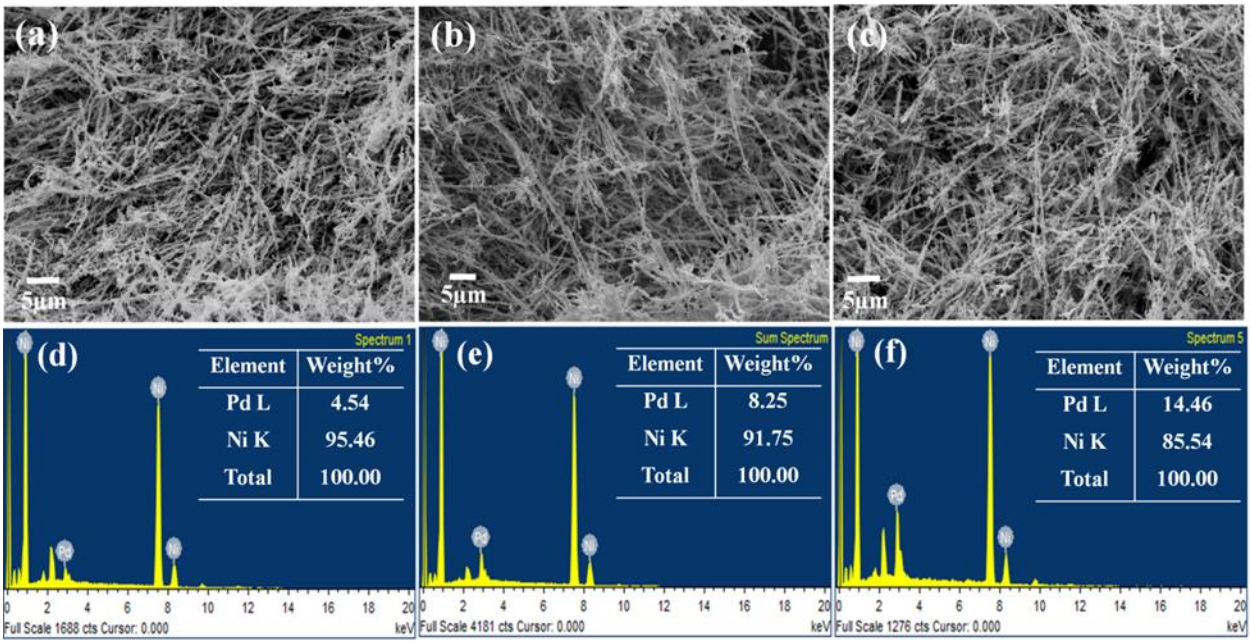

Figure 4.2 SEM images of (a) 5% Pd on Ni NW, (b) 10% Pd on Ni NW, (c) 15% Pd on Ni NW, SEM-EDS of (d) 5% Pd on Ni NW, (e) 10% Pd on Ni NW and (f) 15% Pd on Ni NW.

Further investigation on the morphological features was done by high resolution TEM images. The wire morphology of the Ni nanomaterial was well understood from the TEM images depicted in **Figure 4.3(a, b)**. The incorporation of Pd on Ni NW were further analyzed by TEM elemental mapping (**Figure 4.4**). The presence of well dispersed Pd particles on Ni NW was clear from the TEM images of 5 and 10% Pd on Ni NW catalyst whereas, an agglomeration of Pd particles were observed in the case of 15% Pd modified Ni NW.

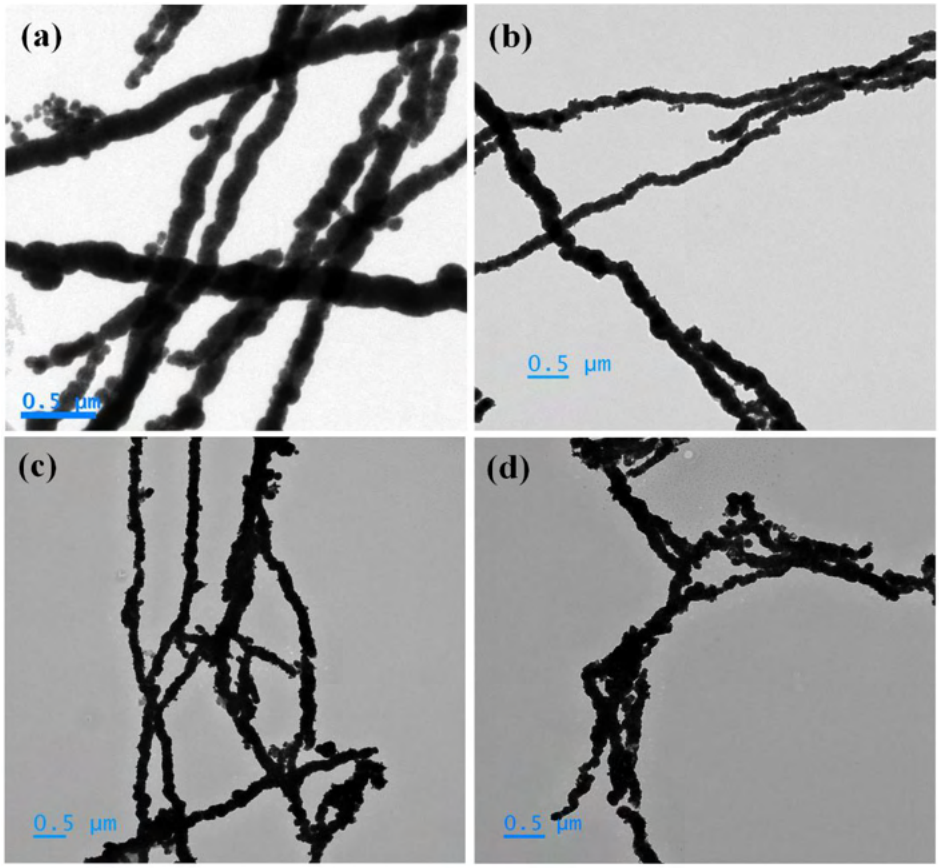

Figure 4.3 TEM images of (a) Ni NW, (b) 5% Pd on Ni NW, (c) 10% Pd on Ni NW and (d) 15% Pd on Ni NW.

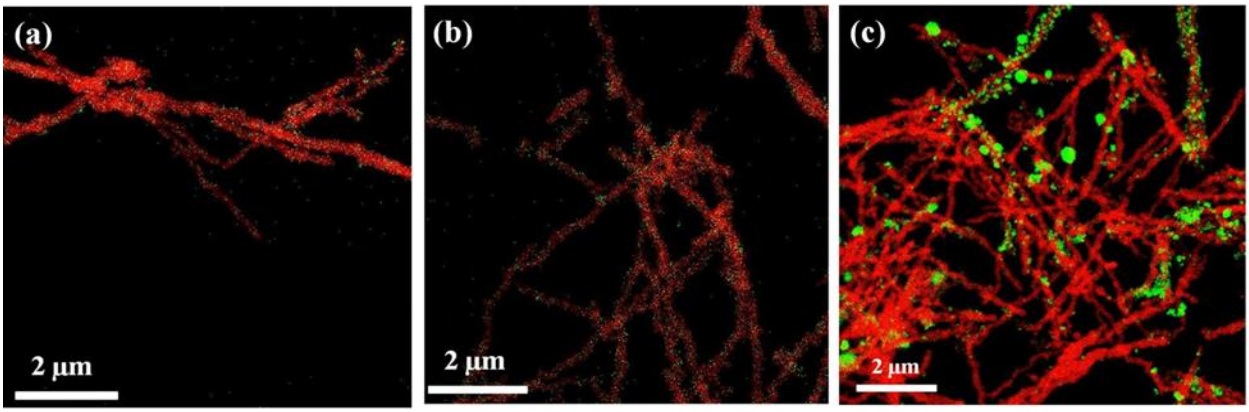

Figure 4.4 TEM elemental mapping of (a) 5% Pd on Ni NW, (b) 10% Pd on Ni NW and (c) 15% Pd on Ni NW.

4.4.2 PXRD analysis

The crystallographic studies of the catalysts were done by PXRD analysis. **Figure 4.5a** represents the PXRD patterns of pure Ni NW, Pd, 5, 10 and 15% Pd modified Ni NW. The diffraction pattern of Ni NW showed peaks at 2θ values 44.58, 51.72 and 76.49º corresponds to the (111), (200), (220) Miller planes and that of Pd showed peaks at 2θ, 40.33, 46.93, 68.29, 82.27 and 86.92º attributed to the Pd (111), (200), (220), (311), (222) planes, respectively. Synthesized Ni NW and Pd were confirmed by indexing the PXRD patterns with JCPDS files 04-0850 and 46-1043, respectively. The results were in good agreement with the characteristic FCC structure of both Ni and Pd.[20, 21] The catalyst, 10% Pd modified Ni NW consists the peaks of Ni and Pd. However, a slight shift in all the peaks towards the low 2 theta value indicated the replacement of Pd atoms on the Ni NW.[22] The lattice parameter obtained for Pd is 0.3912 nm and that of 5, 10, 15% Pd modified Ni NW is 0.3889, 0.3526, 0.3890 nm, respectively. The replacement of Ni atoms by Pd atoms on Ni NW surface induced a contraction in the crystal lattice resulting in a decrease in the lattice parameter. That means the formation of Pd-Ni alloy developed a shrinkage in crystal lattice.

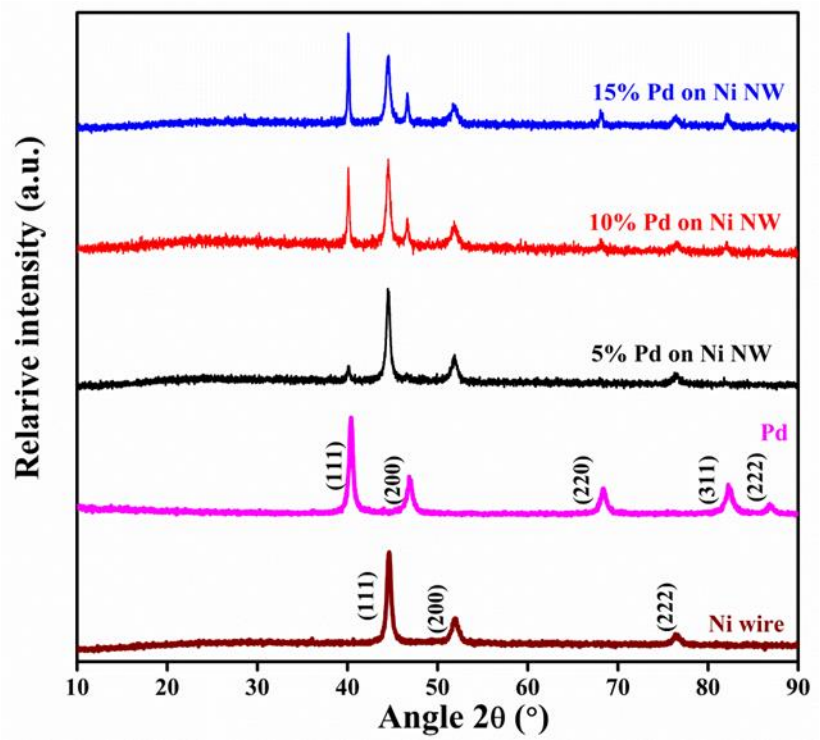

Figure 4.5 PXRD patterns of the synthesized Ni NW, Pd and 5, 10, 15% Pd on Ni NW.

4.4.3 XPS analysis

The existence of Pd and Ni were further unveiled by the XPS analysis. **Figure 4.6** depicts the deconvoluted high-resolution spectra of Pd 3d and Ni 2p. The Pd spectrum was fitted into two sets of spin-orbit doublets Pd ($3d_{5/2}$, $_{3/2}$). The deconvoluted peaks at binding energies 335.6, 340.7 eV assigned to Pd $3d_{5/2}$, $3d_{3/2,}$ respectively, of Pd(0) whereas 337.7, 342.81 eV corresponded to PdO.[23] The peaks located at 852.5, 854.3 and 856.15 eV in Ni 2p spectrum was resulted from the Ni $2P_{3/2}$, ascribed to the Ni (0) and NiO, respectively. Apart from which binding energy peak at 861 eV corresponded to the satellite peak of Ni^{2+}.[24] It is important to note that there is a shift in the Pd ($3d_{5/2}$, $_{3/2}$) binding energy as compared to the reported value 333.0 and 340.3 eV.[25] The shift could be due to the strong electronic modification of Pd occurred by the strain induced within the Pd-Ni alloy crystal lattice because of the substrate effect. It was reported that the lattice mismatch between the surface and substrate can be used to modify the electronic properties of the surface atoms.[12,26,27] The XPS result are consistent with the PXRD analysis.

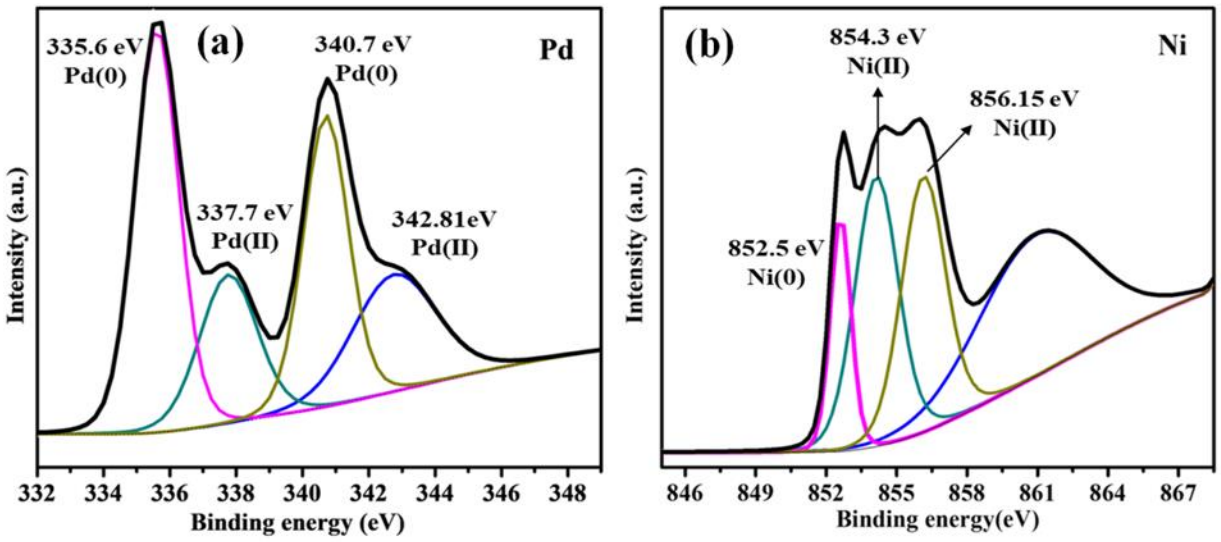

Figure 4.6 Deconvoluted XPS spectra of (a) Pd 3d and (b) Ni 2p of 10% Pd on Ni NW.

4.4.4 Electrochemical analysis

4.4.4(a) Methanol electro-oxidation

The electrochemical activities of the prepared samples were characterized using cyclic voltammetry technique. **Figure 4.7a** shows the CV of 5, 10 and 15 wt% Pd modified Ni NW and pure Pd catalysts in 0.5 M KOH at a scan rate of 50 mV/s. Redox peaks associated with the oxidation and reduction of Pd was clear from the CV curves. Forward scan indicates the adsorption of hydrogen and oxidation of Pd to PdO. The hydrogen adsorption occurs around -0.8 to -0.4 V and PdO formation take place at positive potentials. The reduction of PdO to Pd was represented by the backward sweep of the CV and it occurs around -0.2 to -0.6 V. ECSA were calculated from the CV curves of the catalysts in 0.5 M KOH at a scan rate of 50 mV/s. The ECSA were estimated to be 12.70, 58.92, 13.76 and 11.45 m^2/g for 5, 10, 15% Pd modified Ni NW and pure Pd catalyst, respectively. A significant enhancement in the surface area was observed in the case of 10% Pd modified Ni NW. It must be due to the unique 1D structure of the synthesized catalyst. At the same time, due to the agglomeration of Pd particles, surface area of 15 wt% Pd modified Ni NW got decreased.

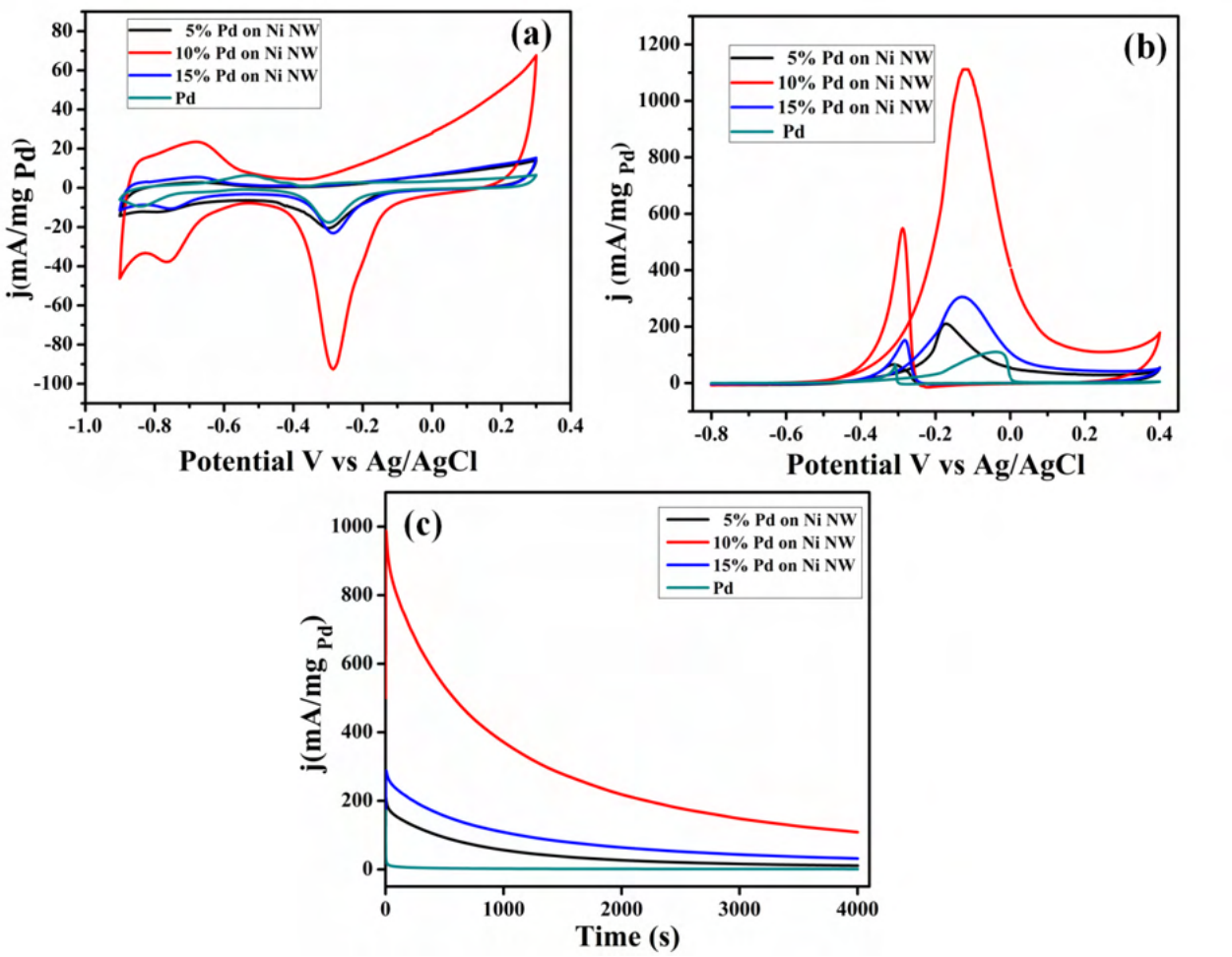

Figure 4.7 CV curves of Pd modified Ni NW and Pd catalysts in N_2 saturated solution of (a) 0.5 M KOH and (b) 0.5 M KOH + 0.5 M CH_3OH, (c) Chronoamperometric curves of Pd modified Ni NW and Pd catalysts in N_2 saturated solutions of 0.5 M KOH + 0.5 M CH_3OH.

The activity of Pd modified Ni NW catalysts towards methanol oxidation were studied in 0.5 M KOH and 0.5 M CH_3OH solution at a scan rate of 50 mV/s. The mass activities of the catalysts are shown in **Figure 4.7b**. The peak in the potential range of -0.4 to 0.4 V in the forward scan was attributed to the oxidation of methanol and in the backward scan at potential range of -0.2 to -0.6 V was due to the oxidation of intermediates. It is clear from the CV curves that all the Pd modified Ni NW catalysts possess a better onset potential and mass activities than the pure Pd, in which 10% Pd modified Ni NW showed significantly improved activity in terms of onset potential, peak potential and mass activity compared to other catalysts. Mass activities obtained for 5, 10 and 15% Pd modified Ni NW were 213.19, 1118.35 and 304.2 mA/mg_{Pd},

respectively and the attained mass activity for pure Pd is 110.09 $mA/mg_{Pd.}$ Even after reducing the amount of precious Pd metal by 90 wt% the catalyst was able to perform a mass activity five times greater than that of pure Pd metal. The strong coupling of Pd particles over Ni NW is responsible for the drastic increase in the catalytic performance of the prepared compositions. Chronoamperometric measurements performed further to study the stability of the catalysts at a potential of -0.4 V for 4000 s in a solution of 0.5 M methanol in 0.5 M KOH (**Figure 4.7c**).[28] The current decay of 10% Pd modified NW observed to be slower indicating its better durability over the other catalysts. Because of the presence of intermediate CO species, the current value was decreased over time. Among the various Pd modified Ni NW and pure Pd catalysts the 10% Pd modified Ni NW showed better durability. The experimental results thus revealed the better activity and durability of 10% Pd on Ni NW catalyst towards methanol oxidation. Pd particles agglomeration in 15% Pd modified Ni NW decreased the active Pd sites that resulted in reduced catalytic activity. EIS were carried out to study the kinetic properties of the prepared samples. **Figure 4.8** displays the recorded Nyquist plots of methanol electro oxidation of 5, 10, 15% Pd on Ni NW and pure Pd catalysts. R_{ct} formed between electrode and electrolyte represented by the diameter of the semicircle.[29] The R_{ct} values of 5, 10, 15% Pd on Ni NW and pure Pd were 13.15, 7.32, 10.56 and 20.10 k cm^2, respectively. Lower R_{ct} of 10% Pd modified Ni NW indicates its better activity.[30]

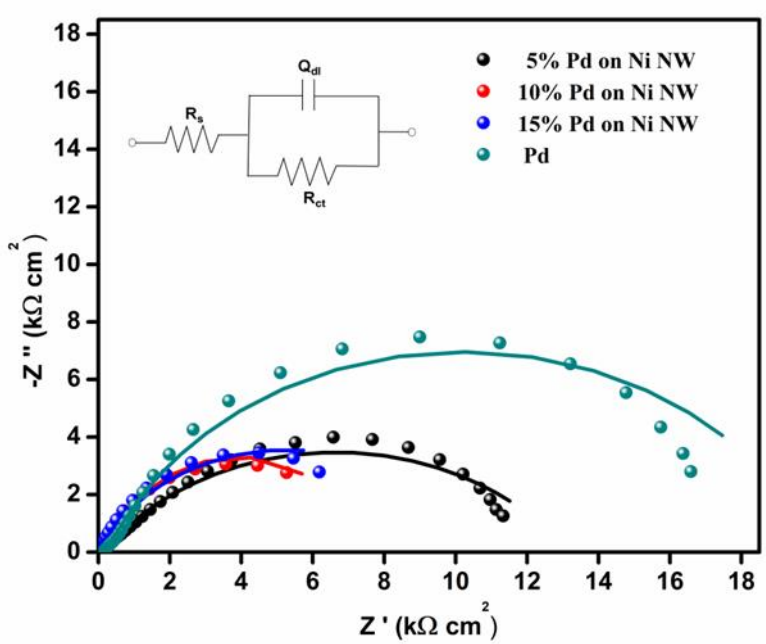

Figure 4.8 Nyquist plots of Pd modified Ni NW and Pd catalysts in 0.5 M KOH + 0.5 M CH_3OH solution.

4.4.4 (b) Ethanol electro-oxidation

Ethanol oxidation also carried out using the highly active 10% Pd modified Ni NW catalyst in N_2 saturated solution containing 0.5 M KOH and 0.5 M C_2H_5OH. In this case also Pd modified Ni NW showed a better onset and peak potential than the pure Pd. The corresponding mass activities obtained for 5, 10, 15% Pd modified Ni NW and pure Pd catalysts were 635.53, 1479.79, 857.4 and 206.15 mA/mg_{Pd}, respectively. **Figure 4.9a** represents the corresponding CV curve. The superior catalytic activity of the 10% Pd modified Ni NW catalyst over pure Pd is clear from the observed data. Stability of the prepared catalysts were tested using chronoamperometric measurements and 10% Pd on Ni NW exhibited a better stability (**Figure 4.9b**).

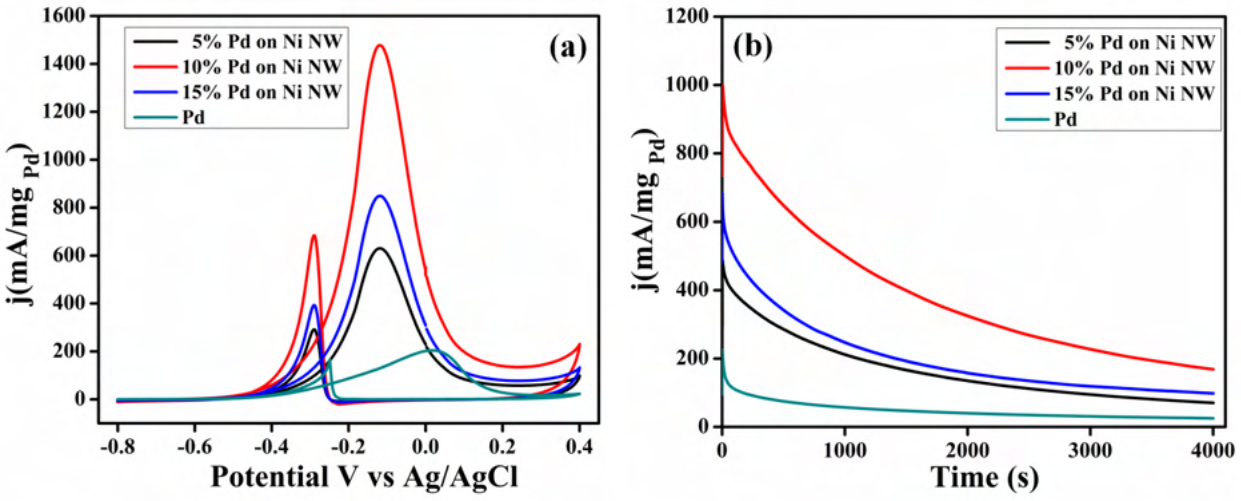

Figure 4.9 (a) CV and (b) Chronoamperometric curves of Pd modified Ni NW and Pd catalysts in N_2 saturated 0.5 M KOH + 0.5 M C_2H_5OH solution.

4.4.5 Comparative study

Comparison in the performance of Pd modified Ni NW with other literature studies were tabulated (**Table 4.1**). Electro catalytic activities of Pd modified Ni NW exhibited superior performance over the other reported PdNi electrocatalysts towards alcohol oxidation.

Table 4.1 Comparison of catalytic activity towards alcohol oxidation

Catalysts	Electrolyte	Mass activity (mA /mg $_{Pd}$)	Reference
Ni@Pd/MWCNTs	0.5 M NaOH + 1 M Methanol	770.7	31
Pd Ni catalyst	0.1 M NaOH + 1 M Methanol	63	9
PdNi/ EGO	0.1 M NaOH + 1 M Ethanol	770.6	23
NiNWA/PdNF	0.5 M KOH + 0.1 M Ethanol	765	32
Pd Ni catalyst	1 M KOH + 1 M Methanol	677.08	33
$Pd_{59}Ni_{41}/C$	0.1 M KOH + 0.5 M Ethanol	450	34
Pd modified Ni NW	**0.5 M KOH + 0.5 M Methanol**	**1118.35**	**Present work**
Pd modified Ni NW	**0.5 M KOH + 0.5 M Ethanol**	**1479.79**	**Present work**

4.4.6 Stability studies

The durability of 10% Pd modified Ni NW catalyst was substantiated by performing the CV analysis for 500 cycles. In the case of 10% Pd modified Ni NW catalyst there is no significant reduction in current value and change in onset potential for both MOR and EOR. Whereas for pure Pd, the current value reached half of the initial value and onset potential shifted to higher value.

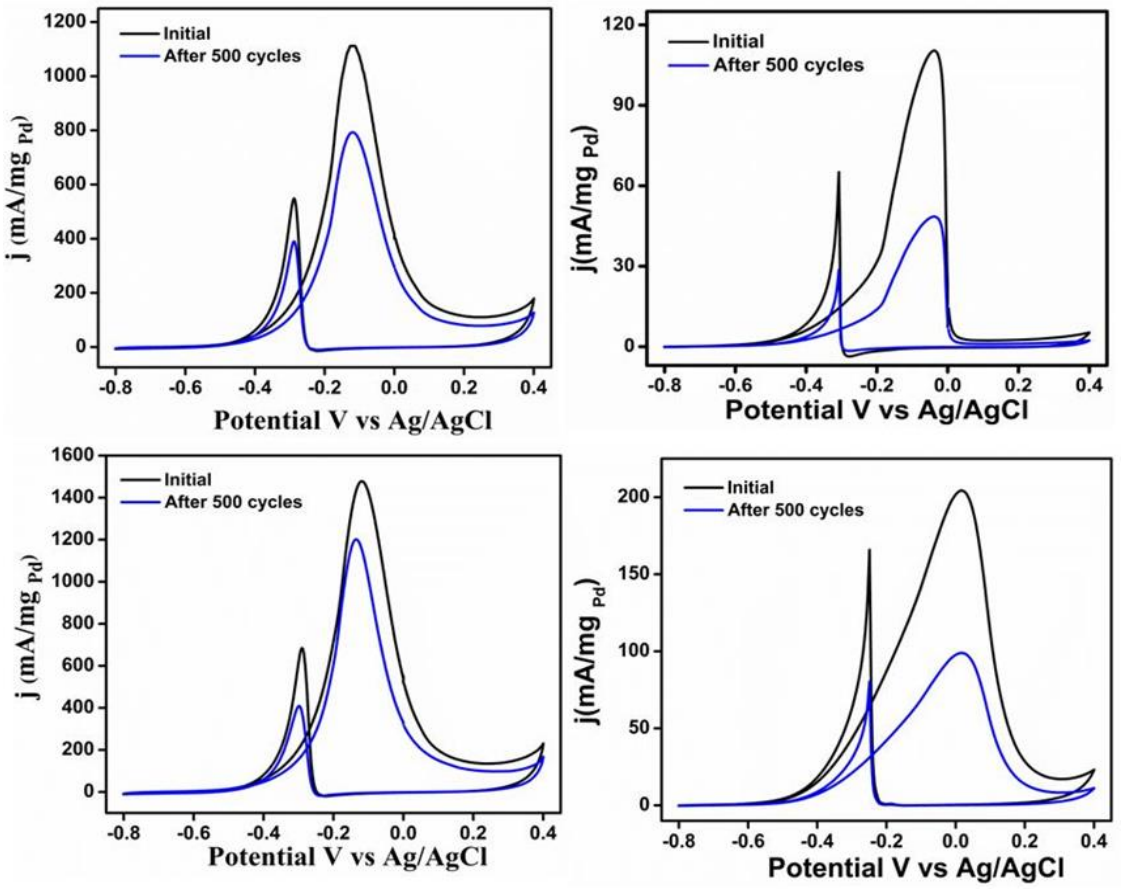

Figure 4.10 CV curves of (a) 10% Pd on Ni NW, (b) Pd catalysts after 500 cycles in N_2 saturated 0.5 M KOH + 0.5 M CH_3OH solution and CV curves of (c) 10% Pd on Ni NW, (d) Pd catalysts after 500 cycles in N_2 saturated 0.5 M KOH + 0.5 M C_2H_5OH solution.

The enhancement in efficiency of the Pd modified Ni NW was attributed to the unique morphology, electronic modifications, SMSI and the bifunctional mechanism between Pd and Ni. The effective surface area of alloys that took part in the catalytic reaction in this case was remarkably higher than that in the Pd particles. The increased surface area can be utilized for the

catalytic applications. The structural features of the unique morphology promote the electron conduction through the system. The electronic structure of Pd deposited on the Ni NW surface is different from that of bulk Pd because of the strain effect of the substrate. Electronically modified surface of Pd could be attributed to the improved activity. The XPS data provided the evidence for the electronic effects originating from Pd atoms withdrawing electrons from the neighbouring Ni in Pd modified Ni NW catalyst. The oxophilic nature of Ni helps to reduce the CO poisoning of the Pd particles and thereby increase the catalytic rate. The high electrochemical surface area, lowest onset, peak potential and high mass activity for methanol and ethanol oxidation of 10% Pd modified Ni NW over all the prepared catalysts disclosed its supreme catalytic activity

4.5 Conclusions

Herein, Ni NW were synthesized using hydrazine hydrate as the reducing agent through a wet chemical reduction method without employing any surfactants and capping agents. The as prepared Ni NW were modified by varying the amount of Pd precursor through a simple galvanic replacement reaction. TEM, PXRD and XPS analysis confirmed the incorporation of Pd atoms on Ni NW surface. The electrochemical measurements revealed that the composition 10% Pd modified Ni NW showed a supreme catalytic activity for methanol oxidation over all the other Pd modified Ni NW and pure Pd catalysts, in terms of ECSA, onset potential, peak potential and mass activity. The better stability of the catalyst also demonstrated. The combination of increased surface area due to NW morphology, electronic modifications due to SMSI and Pd-Ni bifunctional mechanism resulted in improved catalytic efficiency for Pd modified Ni NW. The results established a potential Pd based electrocatalyst for methanol oxidation having low Pd wt% and inexpensive Ni material.

4.6 References

(1) Yang H, Wang H, Li H, Ji S, Davids MW and Wang R, Effect of stabilizers on the synthesis of palladium–nickel nanoparticles supported on carbon for ethanol oxidation in alkaline medium, *J. Power Sources*, **2014**; *260*: 12–18. https://doi.org/10.1016/j.jpowsour.2014.02.110

(2) Gao Y, Wang G, Wu B, Deng C and Ying G, Highly active carbon-supported PdNi catalyst for formic acid electrooxidation, *J. Appl. Electrochem*., **2011**; *41*: 1–6. https://doi.org/10.1007/s10800-010-0201-z.

(3) Kübler M, Jurzinsky T, Ziegenbalg D and Cremers C, Methanol oxidation reaction on core-shell structured Ruthenium-Palladium nanoparticles: Relationship between structure and electrochemical behavior, *J. Power Sources*, **2018**; *375*: 320–334. https://doi.org/10.1016/j.jpowsour.2017.07.114.

(4) Hu, Q.-Y., Zhang, R.-H., Chen, D., Guo, Y.-F., Zhan, W., Luo, L.-M., & Zhou, X.-W.Facile aqueous phase synthesis of 3D-netlike Pd–Rh nanocatalysts for methanol oxidation, *Int. J. Hydrogen Energy*, **2019**; *44*: 16287-16296. https://doi.org/10.1016/j.ijhydene.2019.05.048

(5) Sheng J, Kang J, Hu Z, Yu Y, Fu XZ, Sun R and Wong CP, Octahedral Pd nanocages with porous shells converted from $Co(OH)_2$ nanocages with nanosheet surfaces as robust electrocatalysts for ethanol oxidation, *J. Mater. Chem. A*, **2018**; *6*: 15789–15796. https://doi.org/10.1039/C8TA04181D.

(6) Zhang M, Yan Z andXie J, Core/shell Ni@Pd nanoparticles supported on MWCNTs at improved electrocatalytic performance for alcohol oxidation in alkaline media, *Electrochim. Acta*, **2012**; *77*: 237–243. https://doi.org/10.1016/j.electacta.2012.05.098

(7) Obradovic MD, Stancic ZM, Lacnjevac U, Radmilovic VV, Gavrilovic-Wohlmuther A, Radmilovic VR and Gojkovic SL, Electrochemical oxidation of ethanol on palladium-nickel nanocatalyst in alkaline media, *Appl. Catal. B Environ*., **2016**; *189*: 110–118. https://doi.org/10.1016/j.apcatb.2016.02.039.

(8) Hosseini MG, Abdolmaleki M and Ashrafpoor S, Methanol electro-oxidation on a porous nanostructured Ni/Pd-Ni electrode in alkaline media, *Chinese J. Catal*., **2013**; *34*: 1712–1719. https://doi.org/10.1016/S1872-2067(12)60643-3.

(9) Calderon JC, Nieto-Monge MJ, Perez-Rodriguez S, Pardo JI, Moliner R and Lazaro MJ, Palladium–nickel catalysts supported on different chemically-treated carbon blacks for methanol oxidation in alkaline media, *Int. J. Hydrogen Energy*, **2016**; *41*: 19556–19569. https://doi.org/10.1016/j.ijhydene.2016.07.121.

(10) Moraes LPR, Matos BR, Radtke C, Santiago EI, Fonseca FC, Amico SC and Malfatti CF, Synthesis and performance of palladium-based electrocatalysts in alkaline direct ethanol fuel cell, *Int. J. Hydrogen Energy*., **2016**; *41*: 6457–6468. https://doi.org/10.1016/j.ijhydene.2016.02.150.

(11) Del Rosario JAD, Ocon JD, Jeon H, Yi Y, Lee KJ and Lee J, Enhancing Role of Nickel in the Nickel–Palladium Bilayer for Electrocatalytic Oxidation of Ethanol in Alkaline Media, *J. Phys. Chem. C*, **2014**; *118*: 22473–22478. https://doi.org/10.1021/jp411601c.

(12) da Silva, Anderson; Rodrigues, Thenner; Haigh, Sarah J; Camargo, Pedro.Galvanic Replacement Reaction: Recent Developments for Engineering Metal Nanostructures towards Catalytic Applications**.** *Chem. Commun***.**, **2017**, *53*, 7135-7148. https://doi.org/10.1039/C7CC02352A.

(13) Xia, Xiaohu; Wang, Yi; Ruditskiy, Aleksey; Xia, Younan 25th Anniversary Article: Galvanic Replacement: A Simple and Versatile Route to Hollow Nanostructures with Tunable and Well-Controlled Properties. *Advanced Materials*, **2013**; *25*, 6313–6333. https://doi.org/10.1002/adma.201302820.

(14) Lei, Hao; Li, Xiaotong; Sun, Changbin; Zeng, Junrong; Siwal, Samarjeet Singh; Zhang, Qibo. Galvanic Replacement-Mediated Synthesis of Ni-Supported Pd Nanoparticles with Strong Metal-Support Interaction for Methanol Electro-oxidation. *Small*, **2019**; *15*, 1804722. https://doi.org/10.1002/smll.201804722.

(15) Kong YY, Pang SC and Chin SF, Facile synthesis of nickel nanowires with controllable morphology, *Mater. Lett.*, **2015**; *142*: 1–3. https://doi.org/10.1016/j.matlet.2014.11.140.

(16) Qi Z, Geng H, Wang X, Zhao C, Ji H, Zhang C, Xu J and Zhang Z, Novel nanocrystalline PdNi alloy catalyst for methanol and ethanol electro-oxidation in alkaline media, *J. Power Sources*, **2011**; *196*: 5823–5828. https://doi.org/10.1016/j.jpowsour.2011.02.083.

(17) Gopalsamy K, Balamurugan J, Thanh TD, Kim NH, Hui D and Lee JH, Surfactant-free synthesis of NiPd nanoalloy/graphene bifunctional nanocomposite for fuel cell, *Compos. Part B Eng.*, **2017**; *114*: 319–327. https://doi.org/10.1016/j.compositesb.2017.01.061.

(18) Chung DY, Kim H, Chung Y, Lee MJ, Yoo SJ, Bokare AD, Choi W and Sung YE, Inhibition of CO poisoning on Pt catalyst coupled with the reduction of toxic hexavalent chromium in a dual-functional fuel cell, *Sci. Rep*., **2014**; *4*, 7450. https://doi.org/10.1038/srep07450.

(19) Miao B, Wu ZP, Zhang M, Chen Y and Wang L, Role of Ni in Bimetallic PdNi Catalysts for Ethanol Oxidation Reaction, *J. Phys. Chem. C*, **2018**; *122*, 22448–22459. https://doi.org/10.1021/acs.jpcc.8b05812.

(20) Krishnadas KR, Sajanlal PR and Pradeep T, Pristine and Hybrid Nickel Nanowires: Template-, Magnetic Field, and Surfactant-Free Wet Chemical Synthesis and Raman Studies, *J. Phys. Chem. C*, **2011**; 115, 4483–4490. https://doi.org/10.1021/jp110498x.

(21) Zhao Y, Yang X, Tian J, Wang F and Zhan L, Methanol electro-oxidation on Ni@Pd core-shell nanoparticles supported on multi-walled carbon nanotubes in alkaline media, *Int. J. Hydrogen Energy*, **2010**; 35, 3249–3257. https://doi.org/10.1016/j.ijhydene.2010.01.112

(22) Amin RS, Abdel Hameed RM, El-Khatib KM and Elsayed Youssef M, Electro catalytic activity of nano structured Ni and Pd–Ni on Vulcan XC-72R carbon black for methanol oxidation in alkaline medium, *Int. J. Hydrogen Energy*, **2014**; *39*, 2026–2041. https://doi.org/10.1016/j.ijhydene.2013.11.033.

(23) Tan JL, De Jesus AM, Chua SL, Sanetuntikul J, Shanmugam S, Tongol BJV and Kim H, Preparation and characterization of palladium-nickel on graphene oxide support as anode catalyst for alkaline direct ethanol fuel cell, *Appl. Catal. A Gen*., **2017**; *531*, 29–35. https://doi.org/10.1016/j.apcata.2016.11.034.

(24) Saric I, Peter R, Kavre I, Badovinac IJ and Petravic M, Oxidation of nickel surfaces by low energy ion bombardment, *Nucl. Instruments Methods Phys. Res. Sect. B Beam Interact. with Mater. Atoms*, **2016**; *371*, 286–289. https://doi.org/10.1016/j.nimb.2015.08.090.

(25) Wang J, Zhang P, Xiahou Y, Wang D, Xia H and Mohwald H, Simple Synthesis of Au–Pd Alloy Nanowire Networks as Macroscopic, Flexible Electrocatalysts with Excellent Performance, *ACS Appl. Mater. Interfaces*, **2018**; *10*, 602–613. https://doi.org/10.1021/acsami.7b14955.

(26) Meng Q, Liu J, Weng X, Sun P, Darr JA and Wu Z, In situ valence modification of Pd/NiO nano-catalysts in supercritical water towards toluene oxidation, *Catal. Sci. Technol*., **2018**; *8*, 1858–1866. https://doi.org/10.1039/C7CY02366A.

(27) Nishanth KG, Sridhar P and Pitchumani S, Carbon-supported Pt encapsulated Pd nanostructure as methanol-tolerant oxygen reduction electro-catalyst, *Int. J. Hydrogen Energy*, **2012**; *38*, 612–619. https://doi.org/10.1016/j.ijhydene.2012.06.116.

(28) Feng, Y.-Y., Song, G.-H., Zhang, Q., Lv, J.-N., Hu, X.-Y., He, Y.L., & Shen, X., Morphology effect of MnO_2 promoter to the catalytic performance of Pt toward methanol electro oxidation reaction. *Int. J. Hydrogen Energy*, **2019**; *44*, 3744-3750. https://doi.org/10.1016/j.ijhydene.2018.12.108.

(29) Wang, Wei; Chu, Qingxin; Zhang, Yingnan; Zhu, Wei; Wang, Xiaofeng; Liu, Xiaoyang. Nickel foam supported mesoporous $NiCo_2O_4$ arrays with excellent methanol electrooxidationperformance,*NewJ.Chem*.,**2015**;39(8),64916497. doi:10.1039/c5nj00766f .

(30) Song, X., Sun, Q., Gao, L., Chen, W., Wu, Y., Li, Y., Yang, J.-H. Nickel phosphate as advanced promising electrochemical catalyst for the electro-oxidation of methanol. *Int. J. Hydrogen Energy*, 2018; *43*(27), 12091–12102.

(31) Zhao Y, Yang X, Tian J, Wang F, and Zhan L, Methanol electro-oxidation on Ni @ Pd core-shell nanoparticles supported on multi-walled carbon nano tubes in alkaline media, *Int. J. Hydrogen Energy*, **2010**; *35*, 3249–3257. https://doi.org/10.1016/j.ijhydene.2018.04.165.

(32) Hasan M, Newcomb SB, Rohan JF, and Razeeb M, Ni nanowire supported 3D fl ower-like Pd nanostructures as an efficient electrocatalyst for electro oxidation of ethanol in alkaline media, *J. Power Sources*, **2012**; *218*, 148–156. https://doi.org/10.1016/j.ijhydene.2020.01.006.

(33) Gu Z, Xu H, Bin D, Yan B, Li S, Xiong Z, Zhang K, and Du Y, Preparation of PdNi nanospheres with enhanced catalytic performance for methanol electrooxidation in alkaline medium, *Colloids Surfaces A*, **2017**; *529*, 651–658. https://doi.org/10.1016/j.colsurfa.2017.06.044

(34) Lee K, Kang SW, Lee SU, Park KH, Lee YW and Han SW, One-Pot Synthesis of Monodisperse 5 nm Pd–Ni Nanoalloys for Electrocatalytic Ethanol Oxidation, *ACS Appl. Mater. Interfaces*, **2012**; *4*, 4208–4214. https://doi.org/10.1021/am300923s.

Chapter 5

PdAu alloy nanowires for the elevated alcohol electro-oxidation reaction

5.1 Abstract

Searching for a satisfactory electrocatalyst for fuel cells, herein, we are reporting Au rich PdAu nanowires with excellent electro-catalytic activity towards methanol and ethanol oxidation. Ultrathin one-dimensional PdAu nanowires were prepared rapidly through a simple one-step process. Among the prepared catalysts, the 10% Pd incorporated PdAu nanowire catalyst imparted more significant catalytic activity, which exhibited twenty times enhancement in activity towards methanol and fourteen times higher activity towards ethanol than that of the pure Pd catalyst. Eventually, the amount of Pd metal was reduced to 90 wt% without compromising its catalytic efficiency. Distinctive properties of one-dimensional Au were attributed to the improved catalytic activity.

5.2 Introduction

Gold is known as an amazing element owing to its unique properties including its inert nature. Interestingly, the tremendous change in physical properties due to the size reduction from bulk to nano regime brought significant enhancement in its catalytic activity[1-5]. Hence it was extensively used in catalysis and sensing.[5,6] Additionally, the gold nanoparticles are very active towards CO oxidation which encouraged its application in CO oxidation at ambient temperatures.[7-12] Therefore, by accelerating CO oxidation on Pd, the combination of Au and Pd can effectively minimize CO poisoning in an AOR. Several studies have been reported in the field of electrochemistry using Au and Pd. Luo *et al.,* developed PdAu nanocatalyst with variable atom ratio for methanol oxidation.[13]AykutCaglar and Hilal Kivrak reported carbon nanotube supported PdAu alloy catalyst for ethanol oxidation.[14]Au@PdAg core-shell nanotubes were used for the oxidation of methanol and Au@PdAg NSs decorated rGO was used for ethanol oxidation.[15,16] Liu *et al.,* synthesized AuPd alloy on graphene for ethanol oxidation.[17] AuPtPd nano dendrites performed as an excellent catalyst towards hydrogen evolution and oxygen reduction and AuPd nano alloys were reported as a good catalyst for hydrogen peroxide oxidation.[18,19] Similarly, the nano-porous AuPd showed better activity for alcohol oxidation. Lu *et al*., reported porous Pd Au films for methanol oxidation.[20] Au decorated Pd cubes were also reported for methanol oxidation.[21]

Meanwhile, very few reports are available on AuPd alloy nanowire for electrocatalytic application. Zhu *et al.,* prepared PdAu alloy nanowire through a template assisted method for sensing non-enzymatic glucose. But the synthetic protocol is complicated and relatively time-consuming.[22] Wang *et al.,* synthesized PdAu nanowire for methanol oxidation through a simple procedure, yet the consumption of hazardous aminopyridine makes it non-reliable.[23] Moreover, no attempts have been made to reduce the amount of Pd. Herein the chapter demonstrates a highly rapid synthesis (~5 min) of ultrathin PdAu nanowire of diameter ~ 5 nm, with high aspect ratio without utilizing any complicated synthetic strategy. As prepared catalyst exhibited excellent catalytic activity towards alcohol oxidation. The Pd incorporated Au nanowire (PdAu NW) was obtained through a simple reduction method and the catalyst eliminate the carbon corrosion problem associated with carbon-supporting materials.

5.3 Experimental section

5.3.1 Materials and methods

Chloroauric acid (99.99%), Palladium (II) chloride (99.99%), ά-naphthol (99.99%), Sodium borohydride (99.99%), Potassium hydroxide (99.99%), Methanol (99.9%) and Ethanol (99.9%) were purchased from Merck chemicals and utilized as obtained.

5.3.2 Preparation of PdAu NW catalysts

A mixture of 4.5 ml 0.05 M $HAuCl_4$ and a required amount of 10 mM H_2PdCl_4 were heated to 60 ˚C under a water bath. Subsequently, 0.5 M α-naphthol, ethanol and 0.2 M $NaBH_4$ were added to the solution. The pale yellow colour of the solution immediately changed to black. The obtained product collected by centrifugation and washed well using ethanol.[24] Different compositions of PdAu NW was synthesized by varying the stoichiometry of precursors. Schematic representation of the synthesis procedure was shown in **Scheme 5.1**. The required amount of gold and palladium precursors were mixed with α-naphthol-ethanol solution and sodium borohydride at moderate temperature followed by aging for a very short span. The oxygen ligand in α-naphthol coordinates with Au (III) to form metal complex. The π-π interactions between the rings in the α naphthol may lead to self-assembly of complexes into one dimensional Au NW.[24] Therefore, α-naphthol functioned as a coordination agent, reducing agent and structural directing agent simultaneously. By varying the quantity of precursors, 5, 10 and 15 wt% Pd containing Au rich PdAu NW were prepared, which are designated as 5% PdAu NW, 10% PdAu NW and 15% PdAu NW, respectively. Pure Pd nanoparticle catalyst was prepared by the reduction of Pd precursor using $NaBH_4$ reducing agent, for the activity comparison with the prepared PdAu NW catalyst.

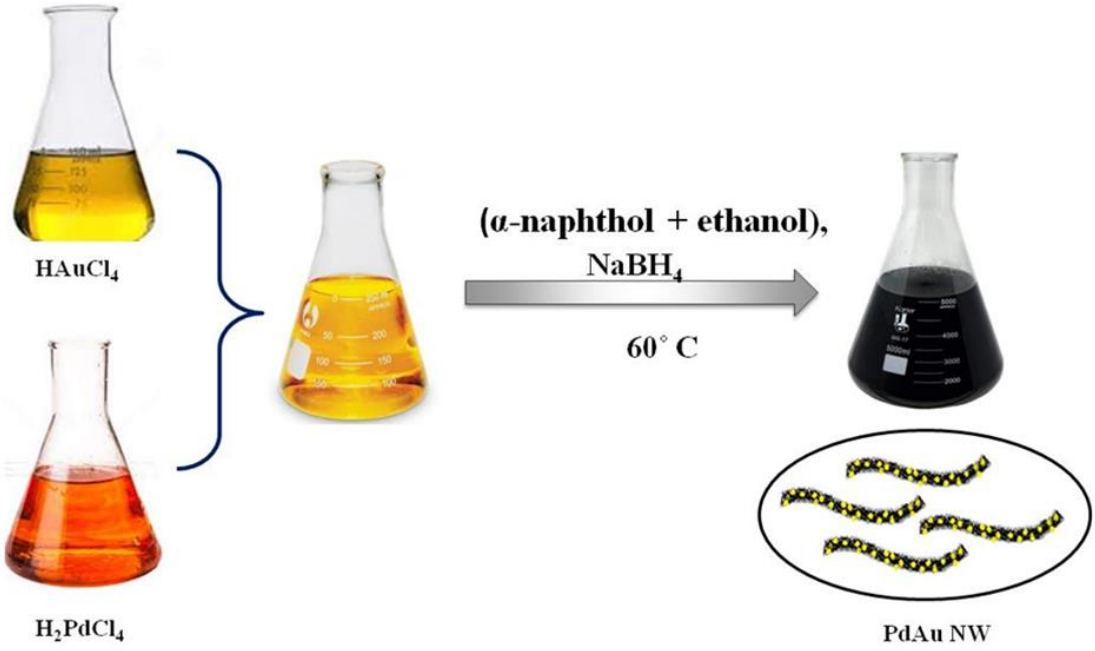

Scheme 5.1 Schematic representation of the formation of PdAu NW.

5.4 Results and discussion

5.4.1 Morphological analysis

Morphology of the prepared catalysts monitored by TEM and depicted in **Figure 5.1**(**a-d**). It shows well defined uniform wire morphology having a diameter of ~ 5 nm and length up to several hundreds of nanometers. Thus, the as synthesized nanowires possess a high aspect ratio. The high-resolution images of 10% PdAu NW in **Figure 5.2**, exhibited crystalline lattice fringes, where the interplanar spacing was calculated and indexed (**Figure 5.2f**). The lattice spacing calculated for the prepared PdAu nanowires is 0.232 nm, which lies in between the Pd (111) lattice spacing (0.225 nm) and Au (111) lattice spacing (0.236 nm). The result indicates the PdAu alloy formation.[15, 16, 25] The lattice plane indexed high resolution TEM images of 5% PdAu NW and 15% PdAu NW are depicted in **Figure 5.2** (**a, b, c**) and **5.2** (**g, h, i**), respectively. **Figure 5.3** shows the TEM images of highly interconnected Pd nano particles with an average particle size ~20 nm.

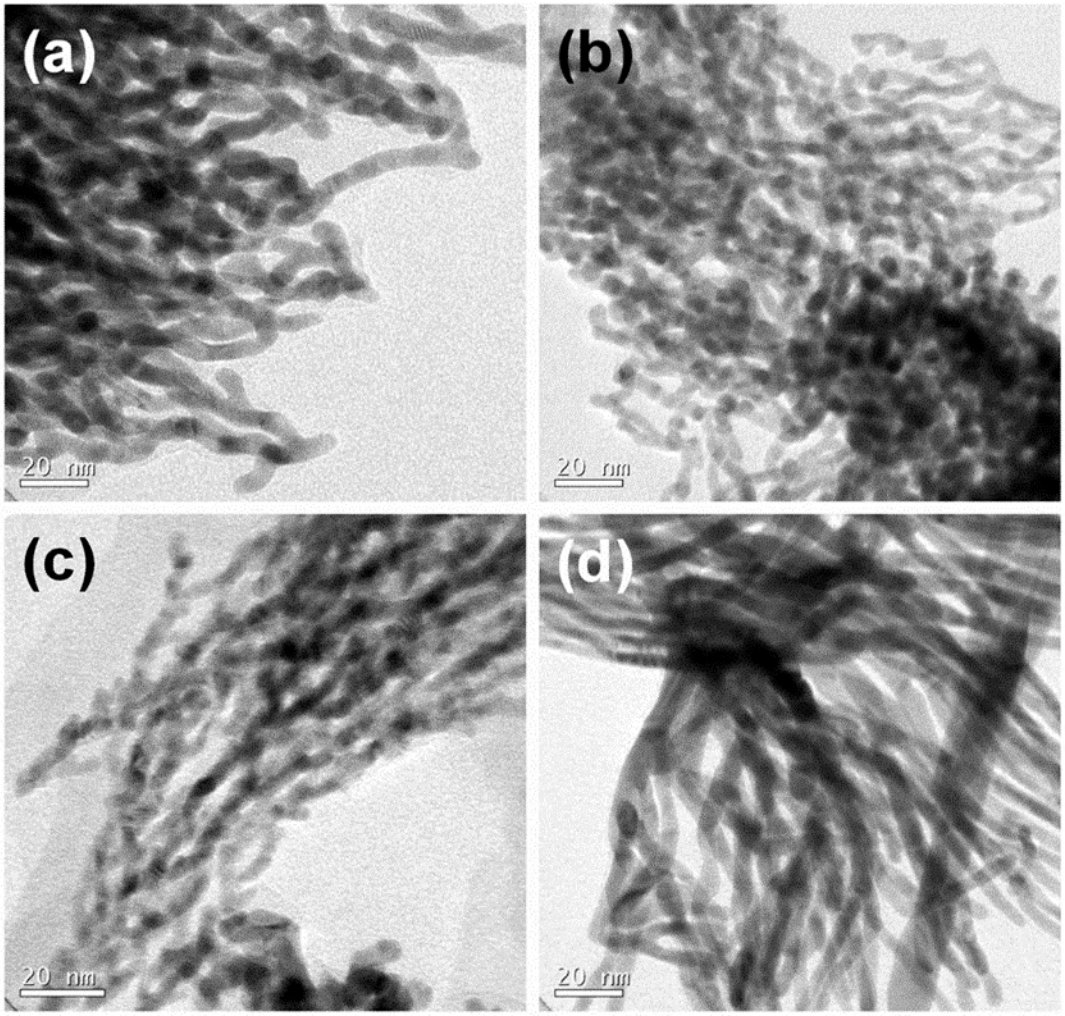

Figure 5.1 TEM images of (a) 5% PdAu NW, (b) 10% PdAu NW, (c) 15% PdAu NW and (d) Au NW.

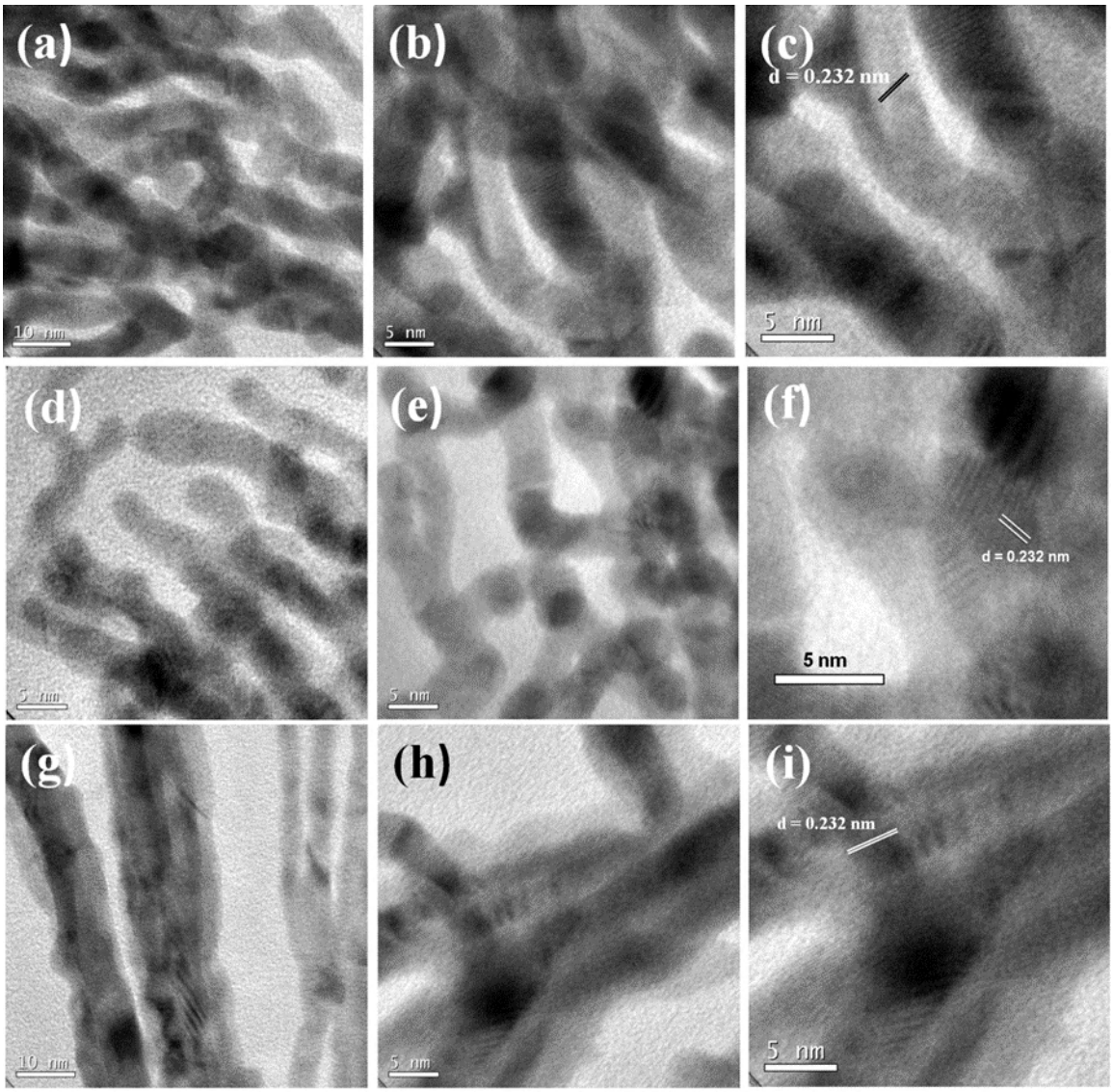

Figure 5.2 HRTEM images of (a, b, c) 5% PdAu NW, (d, e, f) 10% PdAu NW and (g, h, i) 15% PdAu NW.

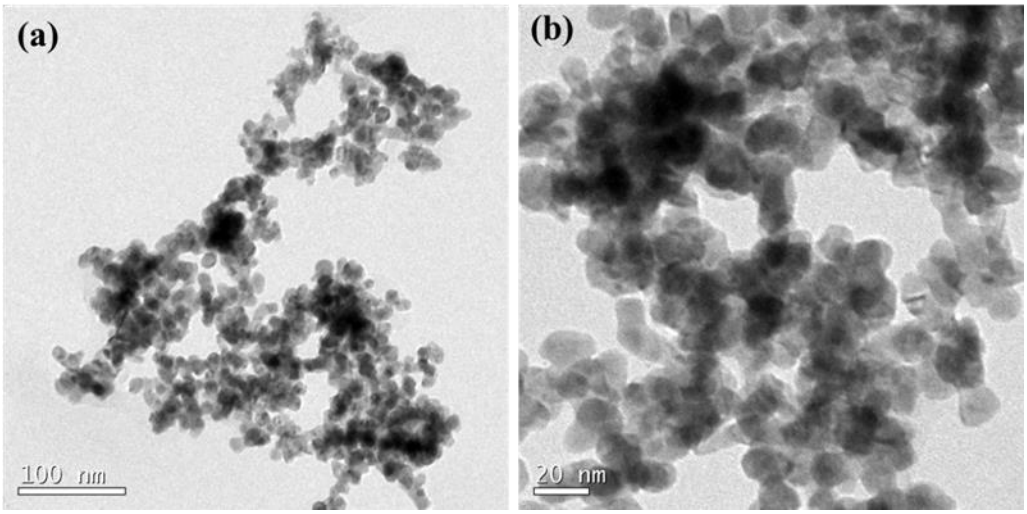

Figure 5.3 HRTEM images of pure Pd nanoparticles.

5.4.2 Composition analysis

The composition of the prepared catalysts samples was analyzed using SEM-EDS analysis (**Figure 5.4**). The prepared 5, 10 and 15% PdAu NW contain 5.37, 10.08, 13.60 wt% Pd and 94.63, 89.92, 86.40 wt% Au, respectively. Thus the compositions of the synthesized samples were confirmed.

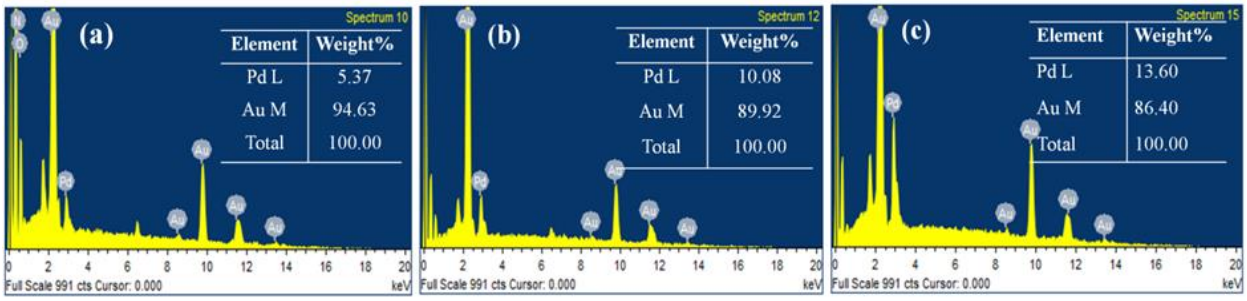

Figure 5.4 SEM-EDS of (a) 5% PdAu NW, (b) 10% PdAu NW and (c) 15% PdAu NW.

5.4.3 PXRD analysis

The phase purity of the prepared catalysts was examined using PXRD, and the obtained pattern were depicted in **Figure 5.5**. The obtained pure Pd PXRD pattern is well matched with the standard cubic structure of Pd (JCPDS 46-1043). The diffraction peaks at 2θ, 40.33, 46.93, 68.29, 82.27 and 86.92˚ correspond to (111), (200), (220), (311), (222) planes of Pd. Similarly, Au exhibited peaks at 38.56, 44.76, 64.92, 77.87 and 82.06˚ which are ascribed to the (111),

(200), (220), (311), (222) Miller planes of cubic Au structure (04-0784).[17] As shown in **Figure 5.5a**, PdAu NW exhibited a shift in PXRD peaks to lower diffraction angles from that of Au and Pd. The observation designates the successful formation of PdAu NW and suggests an expansion in the lattice parameters. However, the extent of lattice expansion tends to decrease on varying the alloy composition from 5, 10 and 15 wt%, since the diffraction peaks have shifted to a higher 2θ angle, **Figure 5.5b**. Moreover, the crystallinity of the prepared NW catalysts was found to decrease from that of pure Pd and Au, understood from the decrease in diffraction peak intensity and increase in FWHM. The calculated crystallite size using the Scherrer formula of each alloy compound are 16.64, 14.49 and 11.97 nm for 5, 10 and 15 wt% PdAu NWs, respectively.

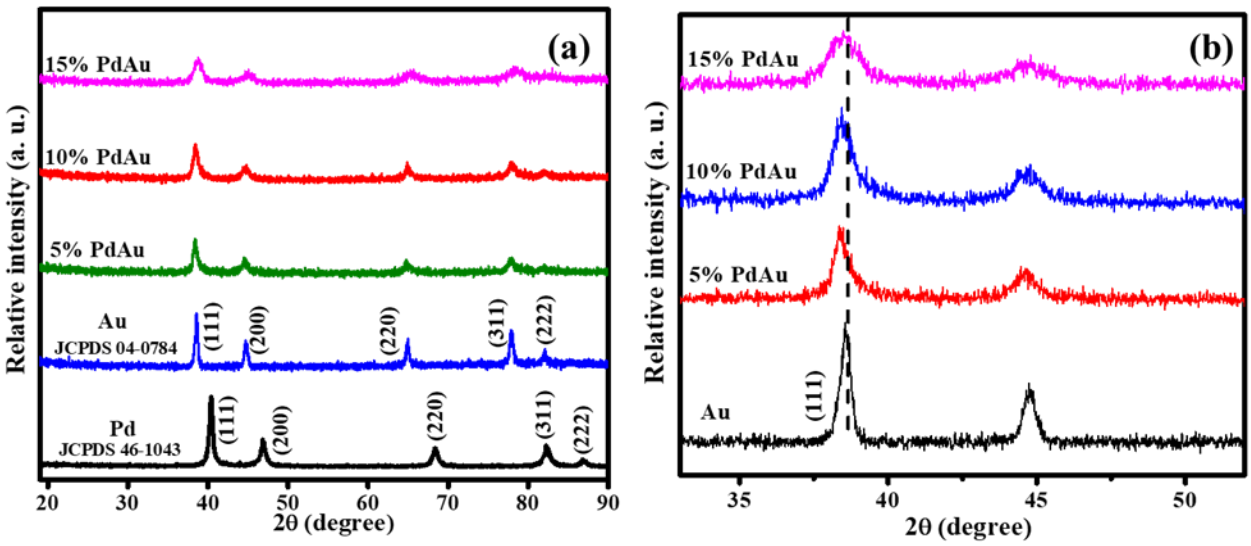

Figure 5.5 PXRD patterns of (a) PdAu NW catalysts, pure Pd and Au, (b) shift in (111) lattice plane.

5.4.4 XPS analysis

The surface chemical composition and oxidation states of the elements present in the developed PdAu NW catalyst are determined by conducting XPS measurements, which also helped to understand the existence of Pd and Au. **Figures 5.6** (**a, b**) display the deconvoluted spectra of Au and Pd, respectively. The binding energy values at 84.0 and 87.7 eV, as illustrated in **Figure 5.6a,** are assigned to Au $4f_{7/2}$ and $4f_{5/2}$ states, indicative of Au(0). As exposed in **Figure 5.6b**, Pd deconvoluted spectra have been fitted to four peaks. The peaks located at binding energies 335.6, 340.9 eV attributed to Pd $3d_{5/2}$, $3d_{3/2}$ corresponds to Pd(0). The small

peaks at 337.8 and 343.1 eV assigned to Pd^{2+}.[26] A slight shift in the binding energy values from the reported values of pure Pd (335.0 and 340.3eV) and Au (83.8 and 87.4 eV) implies a strong electronic modification between the Pd and Au metals.[13,27] Thus the alloy formation is confirmed from the XPS technique.

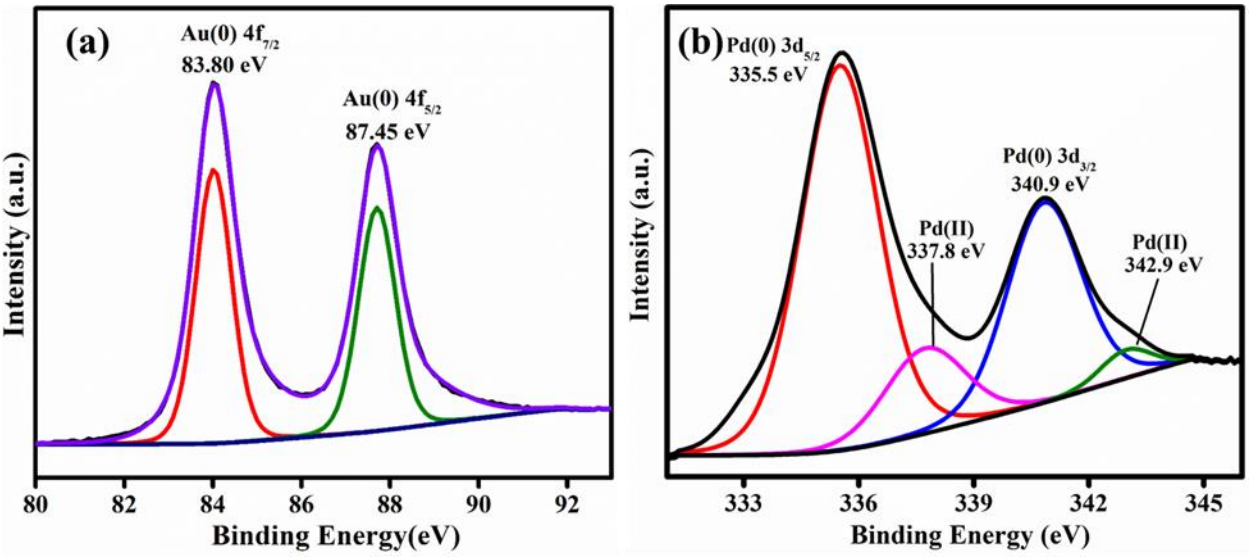

Figure 5.6 Deconvoluted high resolution XPS spectra of (a) Au 4f and (b) Pd 3d in 10% PdAu NW.

5.4.5 Electrochemical analysis

5.4.5 (a) Methanol electro-oxidation

The electrochemical properties of the samples are studied using cyclic voltammetry**.** **Figure 5.7a** represents the respective CV curves recorded in N_2 saturated 0.5 M KOH solution at a scan rate of 50 mV/s. The ECSA for the catalysts 5, 10, 15% PdAu NW and pure Pd are calculated to be 74.8, 115.7, 96.8 and 11.2 m^2/g, respectively. The unique morphology is attributed to the improved ECSA. The 1D wire-type morphologies usually provide more active sites to take part. The remarkably higher activity of 10% PdAu NW is evident from the ECSA.

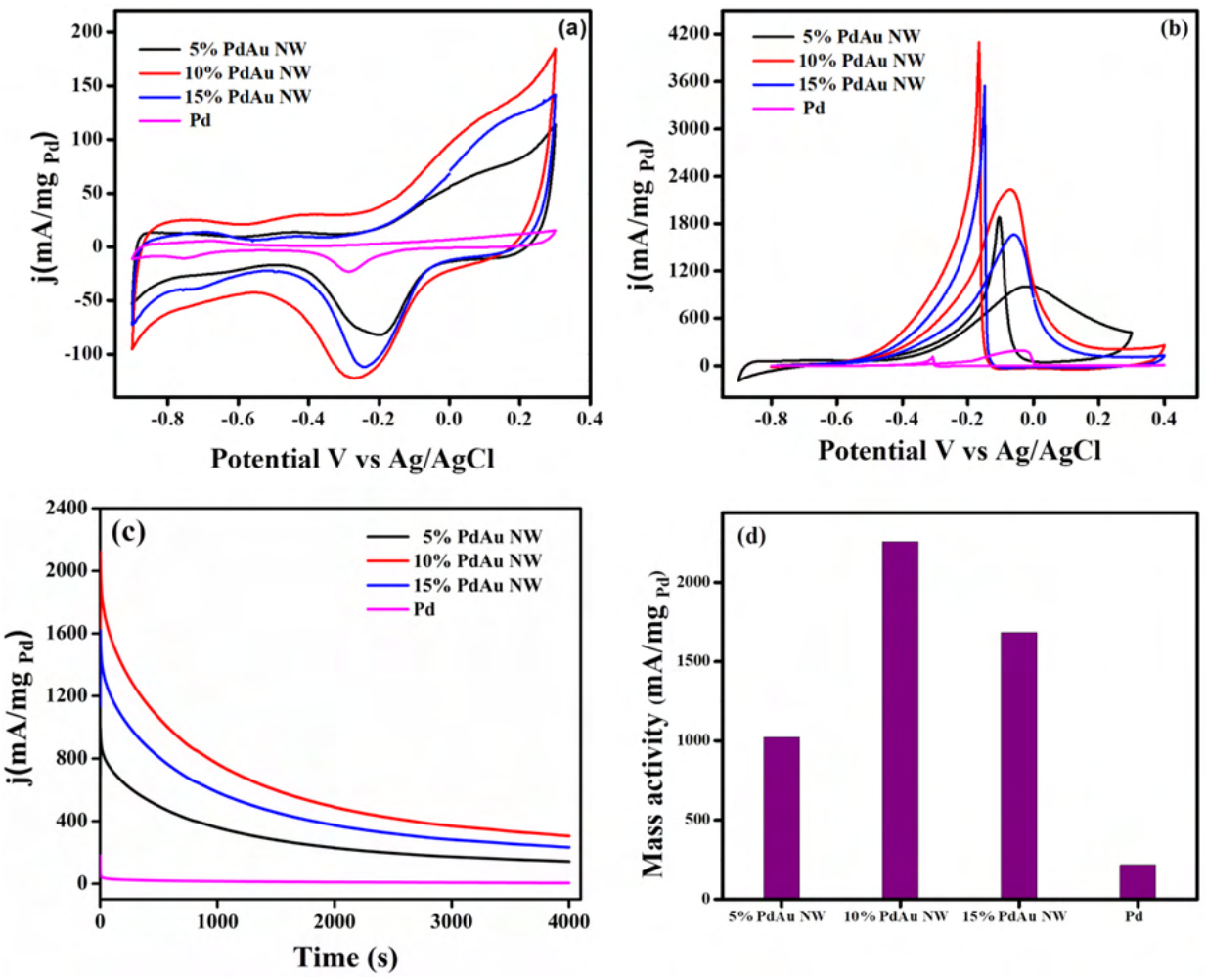

Figure 5.7 CV curves of PdAu NW, pure Pd catalysts in N_2 saturated (a) 0.5 M KOH, (b) 0.5 M KOH + 0.5 M CH_3OH solution at a scan rate of 50 mV/s and (c) Chronoamperometric curves of PdAu NW, pure Pd catalysts in N_2 saturated 0.5 M KOH + 0.5 M CH_3OH solution and (d) mass activities of PdAu NW, pure Pd catalysts.

The electrocatalytic activity of the prepared catalysts towards methanol oxidation is evaluated by performing the CV in N_2 saturated solution containing 0.5 M KOH and 0.5 M methanol at a scan rate of 50 mV/s. Typical CV curves of different PdAu NW catalysts were depicted in **Figure 5.7b**. Mass activities obtained for the catalysts are tabulated in **Table 5.1**. Even though all the prepared catalysts imparted improved activity than the pure Pd, 10% PdAu NW showed superior catalytic activity than others in terms of onset peak potential and mass activity. Ten times increment in the mass activity was observed even after reducing the Pd content to 90 wt% (**Figure 5.7d)**. The bifunctional effects of Pd and Au along with the 1D

morphology of the catalyst could be attributed to the considerable enhancement in the activity of the catalyst. In addition, the problem of carbon corrosion can be eliminated. The 1D morphology reduces the aggregation, dissolution and Ostwald ripening of Pd particles and improves the activity of Pd. The anisotropic morphology also imparts better electronic transportation which in turn increases the performance.

Table 5.1 Onset potential and mass activity data of the synthesized catalysts.

Catalyst	Onset potential (V)	Mass Activity (mA/mg_{Pd})
5% PdAu NW	-0.41	1021.4
10% PdAu NW	-0.44	2253.3
15% PdAu NW	-0.42	1681.2
Pd	-0.38	110.09

The mechanism of methanol oxidation is given below.[28,29] The outstanding catalytic property of gold towards CO oxidation significantly helped to remove the CO molecules adsorbed on the Pd surface by facilitating the reaction kinetics. The CO tolerance of Pd gets enhanced by the presence of Au. The released active sites have proceeded further via the following reactions.

$$Pd + CH_3OH \rightarrow Pd\text{-}(CH_3OH)_{ads} \quad (1)$$

$$Pd\text{-}(CH_3OH)_{ads} + OH^- \rightarrow Pd\text{-}(CH_3O)_{ads} + H_2O + e^- \quad (2)$$

$$Pd\text{-}(CH_3O)_{ads} + OH^- \rightarrow Pd\text{-}(CH_2O)_{ads} + H_2O + e^- \quad (3)$$

$$Pd\text{-}(CH_2O)_{ads} + OH^- \rightarrow Pd\text{-}(CHO)_{ads} + H_2O + e^- \quad (4)$$

$$Pd\text{-}(CHO)_{ads} + OH^- \rightarrow Pd\text{-}(CO)_{ads} + 4H_2O + e^- \quad (5)$$

$$Au + H_2O \rightarrow Au\text{-}OH_{ads} + H^+ + e^- \quad (6)$$

$$Pd\text{-}(CO)_{ads} + Au\text{-}OH_{ads} \rightarrow Pd + Au + CO_2 + H^+ + e^- \quad (7)$$

Stability studies of the prepared catalyst were done by Chronoamperometric measurements at a potential of -0.4 V for 4000 s in an N_2 saturated solution containing 0.5 M KOH and 0.5 M methanol. Due to the formation of the intermediate CO, the current value decreases after some time. As shown in **Figure 5.7c** the slow decay value indicates the 10 wt% PdAu NW possesses a better stability than the other catalysts for methanol oxidation.

EIS is used to study the kinetic properties of the prepared catalysts. A large diameter in the Nyquist plot indicates a large Faradaic resistance, attributed to a low methanol oxidation current density.[30] The synthesized catalysts 5, 10, 15% PdAu NW and pure Pd exhibited a charge transfer resistance value of 8.61, 5.62, 6.10 and 20.10 $k\Omega cm^{-2}$, respectively (**Figure 5.8**). The lower resistance of 10% PdAu NW indicates its better catalytic activity.[31]

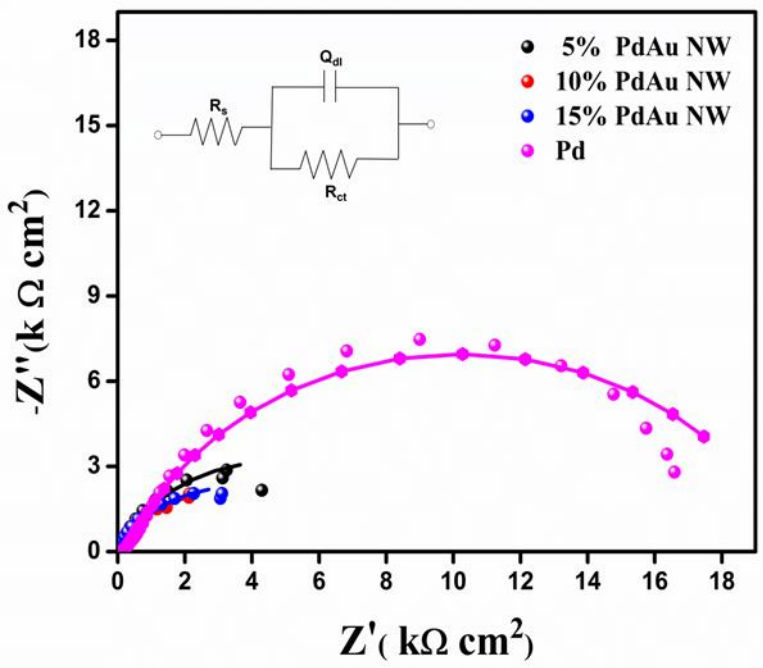

Figure 5.8 Nyquist plots of PdAu NW, pure Pd catalysts in 0.5 M KOH + 0.5 M CH_3OH solution.

5.4.5 (b) Ethanol electro-oxidation

The catalytic activity towards ethanol electro-oxidation was carried out in N_2 saturated solution containing 0.5 M KOH and 0.5 M ethanol at a scan rate of 50 mV/s. Similar results were observed in EOR. Developed PdAu NW catalysts exhibited relatively better activity than that of the pure Pd catalyst. Among them, 10% PdAu NW showed supreme catalytic activity than others. A mass activity of 2137.9, 2960.40, 2724.4 mA/mg_{Pd} are obtained for 5, 10 and 15% PdAu NWs, respectively, and the activity for pure Pd is calculated to be 206.15 mA/mg. The respective CV curves are depicted in **Figure 5.9a** Chronoamperometric measurements performed

at a potential of -0.4 V for 4000 s in a N_2 saturated solution containing 0.5 M KOH and 0.5 M ethanol (**Figure 5.9b)** revealed the stability of 10% PdAu NW catalyst.

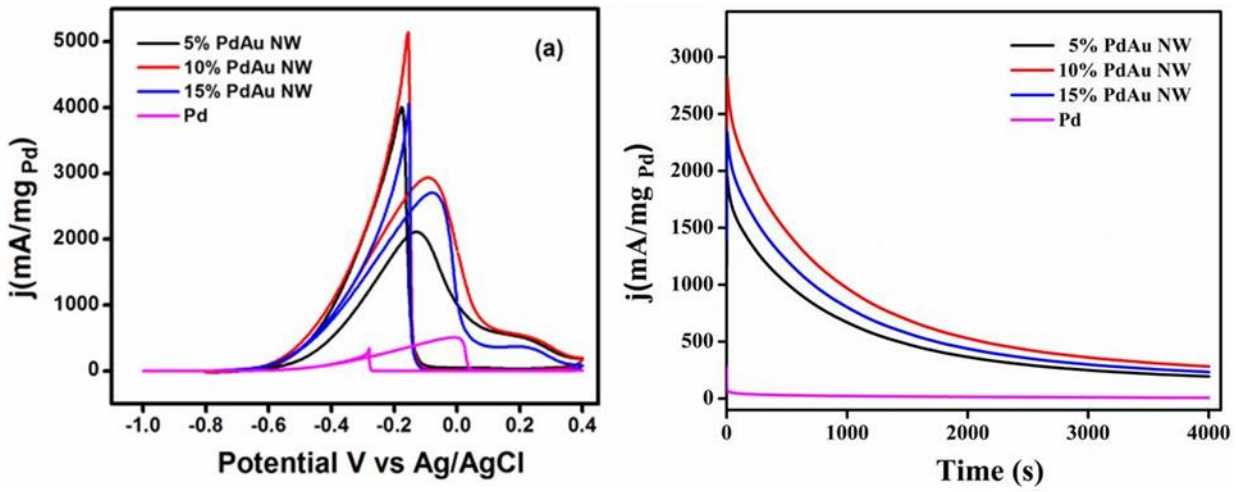

Figure 5.9 (a) CV and (b) Chronoamperometric curves of prepared catalysts in N_2 saturated 0.5 M KOH + 0.5 M C_2H_5OH solution.

5.4.6 Stability studies

Stability studies were conducted by performing the cyclic voltammetry analysis for 500 cycles. **Figure 5.10** depicts the corresponding CV curves. The current decay rate for 10% PdAu NW catalyst was better than that of pure Pd. In the case of MOR for 10% PdAu NW, the initial current value 2253.34 mA/mg_{Pd} reached 1753.48 mA/mg_{Pd}, whereas for pure Pd the current value 193.4 mA/mg_{Pd} reduced at 99.86 mA/mg_{Pd}, almost half of the initial value. The onset potential for 10% PdAu NW slightly deviated from -0.39 to -0.37 V. At the same time, the onset potential was shifted from -0.38 to -0.31 V for pure Pd. The catalyst 10% PdAu NW exhibited a similar trend towards EOR, where only a slight reduction in current value and change in onset potential was recorded. The current value 2960.40 mA/mg_{Pd} was reduced to 2548.88 mA/mg_{Pd} and the onset potential remained at 0.51 V. But for Pd the current value reached almost half of the initial value and the onset potential shifted to higher value. The initial current value from 522.8 mA/mg_{pd} reduced to 274.74 mA/mg_{Pd} and onset potential deviated from -0.52 to -0.45 V. Eventually, stability of 10% PdAu NW catalyst was confirmed.

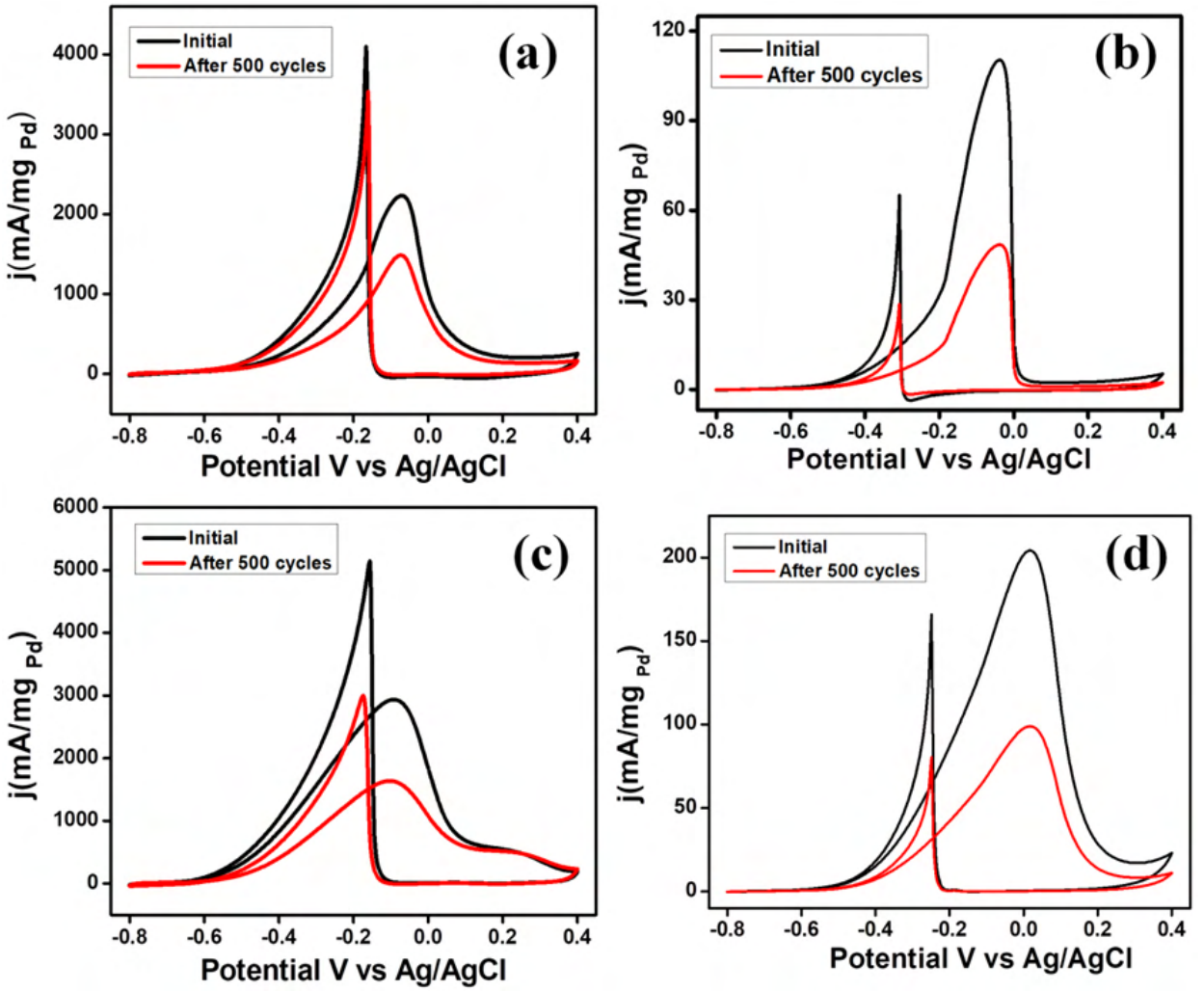

Figure 5.10 CV curves of (a) 10% PdAu NW and (b) Pd catalyst after 500 cycles in N_2 saturated 0.5 M KOH + 0.5 M CH_3OH solution, CV curves of (c) 10% PdAu NW (d) Pd catalyst after 500 cycles in N_2 saturated 0.5 M KOH + 0.5 M C_2H_5OH solution.

5.4.7 Comparative study

Table 5.2 displayed the catalytic activity of various Pt and PdAu catalysts towards alcohol oxidation. The synthesized NW catalyst exhibited a better activity than that of different PdAu catalysts listed in the table. The results indicated that the combination of Pd and Au metals having NW morphology substantially improved the catalytic activity of Pd due to the superior CO tolerance introduced by Au.

Table 5.2 Mass activity values of different PdAu catalysts.

Catalysts	Electrolyte	Mass activity ($mA /mg_{Pd/Pt}$)	Reference
Pd_2Au-180	1M NaOH + 1M Methanol	491.84	13
$Pd_{90}Au_{10}$	1M KOH + 1M Ethanol	1050.00	14
PdAu/C	0.5 M KOH + 0.5M Ethanol	1700.00	32
Pd_5Au_1	1M KOH + 1M Ethanol	1739.93	21
Au@Pd/fuv-MWCNTs	0.5M KOH + 2M Methanol	785.70	33
NP- PdAu	0.5M KOH + 1 M Methanol	866.5	34
$Pd_{30}Au_{70}$/C	1M KOH + 1M Methanol	950.6	35
10%PdAu NW	**0.5 M KOH + 0.5M Methanol**	**2256.9**	**Present work**
10%PdAu NW	**0.5 M KOH + 0.5M Ethanol**	**2932.5**	**Present work**

1D NW with ultrathin diameter and high aspect ratio greatly influenced the catalytic activity. Because, the NW morphology reduces the particle agglomeration and dissolution, in addition provides a large surface area. Moreover, it can also improve the electron transport characteristics due to structural anisotropy. Therefore, the prepared PdAu NW have exhibited superior activity than that of pure Pd. The presence of Au facilitated the catalytic activity of Pd by releasing the intermediate CO from the active sites of Pd, thus enhancing the kinetics of methanol oxidation. Experiments revealed the superior catalytic performance of 10% PdAu NW towards methanol and ethanol electro-oxidation. The catalyst delivered ten times better activity towards methanol and six times higher activity towards ethanol when compared to pure Pd, even after reducing the amount of Pd by 90 wt%. Bifunctional effects of Pd and Au along with the one-dimensional morphology attributed to the increased catalytic activity towards alcohol oxidation.

5.5 Conclusions

Au rich PdAu NW with different compositions were prepared by a simple method. Well-defined ultrathin NW morphology of the catalyst was observed in TEM images. The XRD and XPS results confirmed the successful incorporation of Pd on Au NW. The synthesized catalysts exhibited excellent catalytic activity and stability toward methanol and ethanol oxidation. The catalytic performance shown by 10% PdAu NW was superior to other catalysts and pure Pd catalyst. The efficiency of the catalyst enhanced significantly even after reducing the amount of Pd by 90 wt%. The unique structural features and bifunctional effects of Au and Pd hold the key to this. The estimated mass activity towards methanol and ethanol oxidation was approximately ten and six times, respectively, and higher than that of the pure Pd catalyst.

5.6 References

1. Falsig, H., Hvolbæk, B., Kristensen, I. S., Jiang, T., Bligaard, T., Christensen, C. H., Nørskov, J. K. Trends in the Catalytic CO Oxidation Activity of Nanoparticles. *Angew. Chem. Int. Ed.*, **2008**, *47(26),* 4835–4839,https://doi.org/10.1002/anie.200801479.
2. Xu, C., Su, J., Xu, X., Liu, P., Zhao, H., Tian, F., Ding, Y.Low Temperature CO Oxidation over Unsupported NanoporousGold.*J. Am. Chem. Soc.* **2007**, 129, 1, 42-43,https://doi.org/10.1021/ja0675503.
3. Song, P., Li, S.-S., He, L.-L., Feng, J.-J., Wu, L., Zhong, S.-X., Wang, A.-J. Facile large-scale synthesis of Au–Pt alloyed nanowire networks as efficient electrocatalysts for methanol oxidation and oxygen reduction reactions. *RSC Adv.***2015**, *5*, 87061-87068,https://doi.org/10.1039/C5RA18133J.
4. Luo, J., Njoki, P. N., Lin, Y., Mott, D., Wang, Zhong, C.-J. Characterization of Carbon-Supported AuPt Nanoparticles for Electrocatalytic Methanol Oxidation Reaction. *Langmuir*, **2006**, *22, 6*, 2892-2898,https://doi.org/10.1021/la0529557.
5. Vega, A. A., Newman, R. C, Methanol electro-oxidation on nanoporous metals formed by dealloying of Ag–Au–Pt alloys.,*J.Appl. Electrochem.*,**2016**, *46(9),* 995–1010,https://doi.org/10.1007/s10800-016-0978-5.
6. Graf, M., Haensch, M., Carstens, J., Wittstock, G., Weissmüller, J. Electrocatalytic methanol oxidation with nanoporous gold: microstructure and selectivity. *Nanoscale,* **2017**, ***9***, 17839-17848,https://doi.org/10.1039/C7NR05124G.
7. Rodriguez, P., Kwon, Y., Koper, M. T. M. The promoting effect of adsorbed carbon monoxide on the oxidation of alcohols on a gold catalyst. *Nat. Chem.*, **2011**, *4(3),* 177–182,https://doi.org/10.1038/nchem.1221.
8. Blizanac, B. B., Arenz, M., Ross, P. N., Marković, N. M. *Surface* Electrochemistry of CO on Reconstructed Gold Single Crystal Surfaces Studied by Infrared Reflection Absorption Spectroscopy and Rotating Disk Electrode. *J. Am. Chem. Soc.* **2004**, *126, 32,* 10130-10141,https://doi.org/10.1021/ja049038s.
9. Lu, Y., Tu, J., Gu, C., Xia, X., Wang, X., Mao, S. X. (2011). Growth of and methanol electro-oxidation by gold nanowires with high density stacking faults. *J. Mater. Chem.*, **2011**, *21*, 4843-4849,https://doi.org/10.1039/C0JM04083E.

10. Rodríguez, P., Koverga, A. A., Koper, M. T. M. Carbon Monoxide as a Promoter for its own Oxidation on a Gold Electrode. *Angew. Chem. Int. Ed.*,**2010**, *49(7),* 1241–1243,https://doi.org/10.1002/ange.200905387.
11. Zanganeh, N., Guda, V. K., Toghiani, H.,Keith, J. M. Sinter-Resistant and Highly Active Sub-5 nm Bimetallic Au–Cu Nanoparticle Catalysts Encapsulated in Silica for High-Temperature Carbon Monoxide Oxidation. *ACS Appl. Mater. Interfaces*, **2018**, *10, 5*, 4776-4785,https://doi.org/10.1021/acsami.7b19299.
12. Wang, Caiqin; Zhang, Ke; Xu, Hui; Du, Yukou; Cynthia Goh, M., Anchoring Gold Nanoparticles on Poly(3,4-ethylenedioxythiophene) (PEDOT) Nanonet as Three-dimensional Electrocatalysts toward Ethanol and 2-propanol Oxidation,*J. Colloid Interface Sci.*, **2019**, 541, 258-268, https://doi:10.1016/j.jcis.2019.01.055.
13. Luo, L.-M., Zhang, R.-H., Chen, D., Hu, Q.-Y., Zhang, X., Yang, C.-Y., Zhou, X.-W. Hydrothermal synthesis of PdAunanocatalysts with variable atom ratio for methanol oxidation. *Electrochim. Acta*, **2018**, *259*, 284–292,https://doi.org/10.1016/j.electacta.2017.10.177.
14. Caglar, A., Kivrak, H. Highly active carbon nanotube supported PdAu alloy catalysts for ethanol electrooxidation in alkaline environment. *Int. J. Hydrogen Energy***2019**,*44*, 11734-11743,https://doi.org/10.1016/j.ijhydene.2019.03.118.
15. Yang, W., Zhang, Q., Peng, C., Wu, E., Chen, S., Ma, Y., Deng, L. Au@PdAg core–shell nanotubes as advanced electrocatalysts for methanol electrooxidation in alkaline media. *RSC Adv.*, **2019**, *9*, 931-939,,https://doi.org/10.1039/C8RA08781D.
16. Wu, E., Zhang, Q., Xie, A., Yang, W., Peng, C., Hou, J.,Deng, L. Synthesis of hollow echinus-like Au@PdAgNSs decorated reduced graphene oxide as an excellent electrocatalyst for enhanced ethanol electrooxidation. *J. Alloys Compd.*,**2019**, *789*, 174–182,https://doi.org/10.1016/j.jallcom.2019.03.086.
17. Liu, C., Cai, X., Wang, J., Liu, J., Riese, A., Chen, Z., Wang, S.-D. One-step synthesis of AuPd alloy nanoparticles on graphene as a stable catalyst for ethanol electro-oxidation.*Int. J. Hydrogen Energy,* **2016**, *41(31),* 13476–13484,https://doi.org/10.1016/j.ijhydene.2016.05.194.
18. Chen, H.-Y., Wang, A.-J., Zhang, L., Yuan, J., Zhang, Q.-L., Feng, J.-J. One-pot wet-chemical synthesis of uniform AuPtPdnanodendrites as efficient electrocatalyst for

boosting hydrogen evolution and oxygen reduction reactions., *Int. J. Hydrogen Energy*, **2018,***43*, 22187-22194,https://doi.org/10.1016/j.ijhydene.2018.10.120.

19. Jirkovský, J. S., Panas, I., Ahlberg, E., Halasa, M., Romani, S., Schiffrin, D. J. Single Atom Hot-Spots at Au–Pd Nanoalloys for Electrocatalytic H2O2Production, *J. Am. Chem. Soc.*, **2011**, *133, 48*, 19432-19441,https://doi.org/10.1021/ja206477z.
20. Liu, J., Wang, J., Kong, F., Huang, T.,Yu, A. Facile preparation of three-dimensional porous Pd–Au films and their electrocatalytic activity for methanol oxidation.*Catal. Commun.*, **2016**, *73*, 22–26,https://doi.org/10.1016/j.catcom.2015.09.033.
21. Zhong, J., Bin, D., Feng, Y., Zhang, K., Wang, J., Wang, C., Du, Y. Synthesis and high electrocatalytic activity of Au-decorated Pd heterogeneous nanocube catalysts for ethanol electro-oxidation in alkaline media**.***Catal. Sci. Technol.*, **2016**, *6*, 5397-5404,https://doi.org/10.1039/C6CY00140H.
22. ChengzhouZhu; Shaojun Guo; Shaojun Dong. PdM (M = Pt, Au) Bimetallic Alloy Nanowires with Enhanced Electrocatalytic Activity for Electro-oxidation of Small Molecules.,*J.Adv.Mater.*,**2012**,*24(17),2326–2331*,https://doi.org/10.1002/adma.201104951.
23. Wang, Q.-L., Fang, R., He, L.-L., Feng, J.-J., Yuan, J., Wang, A.-J. Bimetallic PdAu alloyed nanowires: Rapid synthesis via oriented attachment growth and their high electrocatalytic activity for methanol oxidation reaction., *J. Alloys Compd.*, **2016**, *684*, 379–388,https://doi.org/10.1016/j.jallcom.2016.05.188.
24. Jiang, X., Qiu, X., Fu, G., Sun, J., Huang, Z., Sun, D., Tang, Y. Highly simple and rapid synthesis of ultrathin gold nanowires with (111)-dominant facets and enhanced electrocatalytic properties, *J. Mater. Chem. A***,2018**, *6*, 17682-17687,https://doi.org/10.1039/C8TA06676K.
25. Cao, R., Xia, T., Zhu, R., Liu, Z., Guo, J., Chang, G., He, Y. Novel synthesis of core-shell Au-Pt dendritic nanoparticles supported on carbon black for enhanced methanol electro-oxidation. *Appl. Surf. Sci.*,**2018**, *433*, 840–846,https://doi.org/10.1016/j.apsusc.2017.10.104.
26. Wang,Z.L., Yan,J.M., Wang, H.L., Ping,Y., Jiang,Q.Au@Pd core–shell nanoclusters growing on nitrogendoped mildly reduced graphene oxide with enhancedcatalytic

performance for hydrogen generation fromformic acid. *J. Mater. Chem. A,* **2013**, *1*, 12721-12725.

27. Wang, J., Zhang, P., Xiahou, Y., Wang, D., Xia, H., Möhwald, H. Simple Synthesis of Au–Pd Alloy Nanowire Networks as Macroscopic, Flexible Electrocatalysts with Excellent Performance. *ACS Appl. Mater. Interfaces*, **2018**, *10, 1*, 602-613,https://doi.org/10.1021/acsami.7b14955.
28. Thota, A., Boga, K., Narayan, R., Bojja, S., & Rao, C. R. K. Synthesis of star shaped electroactive, LEB state aniline oligomer and its high performing Pt and Pt-Au nanocatalyst for MOR.*Int. J. Hydrogen Energy*.**2019,***44,* 11066-11078,https://doi.org/10.1016/j.ijhydene.2019.02.207.
29. Magal, R. T., Selvaraj, V. A comparative study for the electrocatalytic oxidation of alcohol on Pt-Au nanoparticle-supported copolymer-grafted graphene oxide composite for fuel cell application. *Ionics,* **2017**, *24(5),* 1439–1450,https://doi.org/10.1007/s11581-017-2295-3.
30. Wang, Wei; Chu, Qingxin; Zhang, Yingnan; Zhu, Wei; Wang, Xiaofeng; Liu, Xiaoyang. Nickel foam supported mesoporous $NiCo_2O_4$ arrays with excellent methanol electro-oxidation performance, *NewJ.Chem.*, **2015**; 39(8),6491–6497. doi:10.1039/c5nj00766f.
31. Qian, L.,Gu, L.,Yang,L., Yuan,H., Xiao, D. Direct growth of $NiCo_2O_4$ nanostructures on conductive substrates with enhanced electrocatalytic activity and stability for methanoloxidation.*Nanoscale*2013, 5(16), 7388, doi:10.1039/C3NR01104F.
32. Mao, H., Huang, T., Yu, A. Surface noble metal modified PdM/C (M = Ru, Pt, Au) as anode catalysts for direct ethanol fuel cells.*J. Alloys Compd.,* **2016**, *676,* 390–396,https://doi.org/10.1016/j.jallcom.2016.03.200.
33. Xu, M.-L., Yang, X.-K., Zhang, Y.-J., Xia, S.-B., Dong, P.Yang, G.-T. Enhanced methanol oxidation activity of Au@Pd nanoparticles supported on MWCNTs functionalized by MB under ultraviolet irradiation. *Rare Metals,* **2014**, *34(1),* 12–16,https://doi.org/10.1007/s12598-014-0400-6.
34. Wang, X., Tang, B., Huang, X., Ma, Y., Zhang, Z. High activity of novel nanoporous Pd–Au catalyst for methanol electro-oxidation in alkaline media.*J. Alloys Compd.*,**2013**, *565*, 120–126, https://doi.org/10.1016/j.jallcom.2013.02.170.

35. Yin, Z., Chi, M., Zhu, Q., Ma, D., Sun, J., Bao, X. Supported bimetallic PdAu nanoparticles with superior electrocatalytic activity towards methanol oxidation. *J. Mater. Chem. A*, **2013**, *1*, 9157-9163,https://doi.org/10.1039/C3TA11592E.

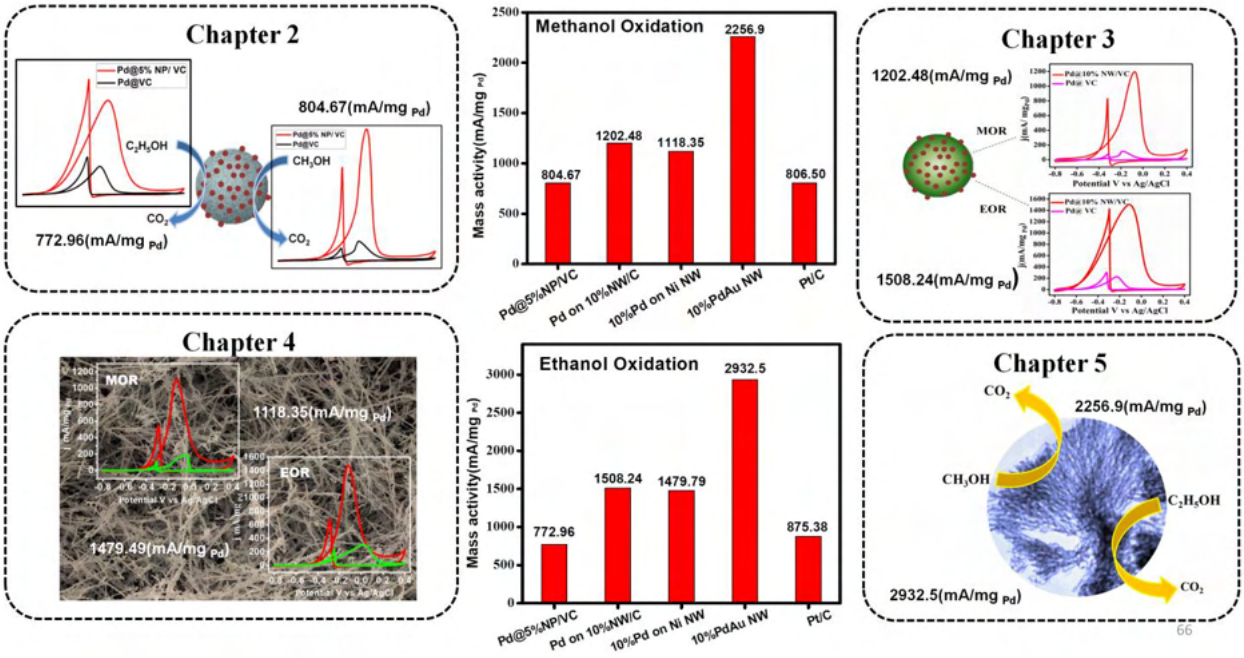

The development of an efficient electrocatalyst for fuel cell is essential due to the sluggish kinetics of alcohol oxidation and the extensive use of Pt based catalysts. Pd was recommended as a potential alternative for Pt-based catalysts since it is less expensive and more abundant than Pt. The present thesis focused to develop surface modified carbon supported Pd and Pd modified 1D nano-architecture catalysts for alcohol electro-oxidation without employing any tedious procedure. Pd decorated over nickel phosphate modified carbon and Pd deposited on nickel tungstate modified carbon catalysts were synthesized through the hydrothermal method. Pd modified Ni NW catalyst obtained through a galvanic replacement reaction and the PdAu NW catalyst was prepared through a one-step reduction method. The amount of Pd metal employed in all the synthesized catalysts was reduced by a significant amount without compromising its catalytic efficiency. Pd@5% NP/VC, Pd@10% NW/VC, 10% Pd on NW and 10% PdAu NW catalysts are the best compositions that exhibited the mass activity of 804.67, 1202.48, 1118.35 and 2256.9 mA/mg_{Pd}, respectively, towards methanol oxidation. Furthermore, in ethanol oxidation, the catalysts Pd@5% NP/VC, Pd@10% NW/VC, 10% Pd on NW and 10% PdAu NW

showcased a mass activity of 772.96, 1508.24, 1479.79 and 2932.5 mA/mg_{Pd}, respectively. Nickel phosphate and nickel tungstate modification in Pd@5% NP/VC, Pd@10% NW/VC catalysts played a crucial role in enhancing the efficiency by providing a better CO tolerance. At the same time the benefit of unique 1D morphology became significant in the case of 10% Pd on NW and 10% PdAu NW catalysts.

Catalyst	***Mass activity (mA/mg $_{Pd/Pt}$)***	
	Methanol	**Ethanol**
Pd@5%NP/VC	804.67	772.96
10% Pd on Ni NW	1118.35	1479.79
Pd@ 10% NW/VC	1202.48	1508.24
10% PdAu NW	2256.90	2932.5
Commercial Pt/C	806.50	875.38

Further, the obtained results were compared with the catalytic activity of commercial Pt/C towards methanol and ethanol oxidation. A mass activity of 806.50 mA/mg_{Pt} was obtained for methanol oxidation and an activity of 875.38 mA/mg_{Pt} was observed for ethanol oxidation. While comparing the results, the synthesized catalysts Pd@10% NW/VC, 10% Pd on NW and 10% PdAu NW exhibited superior catalytic performance than commercial Pt/C. Among the synthesised catalysts 10% PdAu NW catalyst exhibited supreme catalytic activity towards methanol and ethanol electro-oxidation. The catalyst 10% PdAu NW can be considered as a suitable replacement for commercial Pt/C in DAFC application.

Future scope

- Scale up of the synthesised catalysts and electrode fabrication.
- Fabrication of DAFC using the synthesized catalysts.
- Durability study of the fabricated DAFC.

ABSTRACT

Name of the student: Roshima K	**Registration No:10CC17A39002**
Faculty of study: Chemical sciences	**Year of submission: 2023**
CSIR Lab: National Institute for Interdisciplinary Science & Technology (CSIR-NIIST), Thiruvananthapuram, Kerala	**Name of the Supervisor: Dr K G Nishanth**

Title of the thesis: ***Studies on Pd based catalysts for the electro-oxidation of alcohols*****.**

The thesis primarily aims to develop an efficient cost effective Pd based catalyst for alcohol electro oxidation reaction. The thesis consists of five chapters. Chapter 1 provides an introduction to fuel cells, its working principle and classification. Chapter mainly attentive on classification of direct alcohol fuel cells (DAFC) and its mechanism. Further it provides a brief idea on the present challenges in DAFC and the role of Pd based electrocatalysts as a potential replacement for Pt metal anode catalyst in DAFC. In this regard the subsequent chapters are constructed. Chapter 2 demonstrates the development of Pd supported nickel phosphate modified carbon catalyst. The monometallic modification of carbon using nickel phosphate enhanced the catalytic activity of Pd particles. To further improve the performance of Pd nanoparticles, a bimetallic modification was done on the carbon substrate using nickel tungstate, in chapter 3. Chapter 4 reports one dimensional Pd modified Ni nano wire catalyst obtained through a galvanic replacement reaction and chapter 5 discusses PdAu nano wire catalyst synthesised by a rapid one step procedure. The unique one-dimensional morphology and bifunctional effects of Pd-Ni and Pd-Au combinations, enhanced the catalytic efficiency of PdNi NW catalyst and PdAu NW catalyst, respectively. The amount of Pd used in all of the designed catalysts was substantially reduced without affecting its catalytic efficiency. The performance of the synthesized Pd-based catalysts was compared to the catalytic activity of commercial Pt/C and found to be superior.

Thesis Output

List of publications emanating from the thesis work

1. **Roshima K.**, Nishanth K. G. Nickel phosphate modified carbon supported Pd catalyst for enhanced alcohol oxidation reaction. *Int. J. Hydrogen Energy*. **2020**, 45, 11116−11126.
2. **Roshima K.** , Nishanth K. G. Pd modified Ni nano wire as an efficient electro-catalyst for alcohol oxidation reaction. *Int. J. Hydrogen Energy*. **2020**, 45, 8396-8404.
3. **Roshima K.** , Nishanth K. G. PdAu alloy nano wire for the elevated alcohol oxidation reaction. *Electrochim. Acta*. **2021,** 369, 138405.
4. **Roshima K**, Nishanth K G. Transition metal tungstate modified carbon supported Pd catalyst for alcohol electro-oxidation reaction. (Communicated).

List of conference presentations

1. **Roshima K**, K G Nishanth*. Oral presentation entitled "Pd modified Ni nanowire as an efficient electro catalyst for methanol oxidation reaction" in twelfth International Symposium on Advances in Electrochemical Science and Technology, January 8 to 10, 2019 at Hotel Trident/ Chennai, Tamilnadu, India.
2. **Roshima K**, K G Nishanth*. Oral presentation entitled "Pd decorated Modified Vulcan Carbon Catalyst for Enhanced Alcohol Electro-Oxidation" in Third International Conference on Advanced Functional Materials (ICAFM), CSIR-NIIST, Thiruvananthapuram, Kerala (December 9-10, 2019).

INTERNATIONAL JOURNAL OF HYDROGEN ENERGY 45 (2020) 8396–8404

Available online at www.sciencedirect.com

ScienceDirect

journal homepage: www.elsevier.com/locate/he

Pd modified Ni nanowire as an efficient electro-catalyst for alcohol oxidation reaction

Roshima Kottayintavida [a,b], *Nishanth Karimbintherikkal Gopalan* [a,b,*]

[a] *Materials Science and Technology Division, CSIR-National Institute for Interdisciplinary Science and Technology (NIIST), Thiruvananthapuram, 695019, India*

[b] *Academy of Scientific and Innovative Research (AcSIR), Ghaziabad, 201002, India*

HIGHLIGHTS

- Pd Modified Ni NW catalyst prepared by galvanic replacement reaction.
- 10 wt% Pd on Ni NW found to be a better catalyst for alcohol oxidation.
- Mass activity enhanced five times than the pure Pd for methanol oxidation.
- Durability of the catalysts was revealed by chronoamperometry.
- Reduced the amount of Pd to 90 wt % without compromising its activity.

GRAPHICAL ABSTRACT

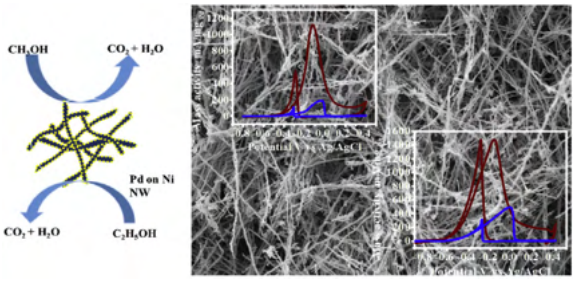

ARTICLE INFO

Article history:
Received 25 October 2019
Received in revised form
30 December 2019
Accepted 2 January 2020
Available online 22 January 2020

Keywords:
Electrocatalyst
Nickel nanowire

ABSTRACT

Developing highly efficient and economically viable electro-catalyst is very crucial research topic nowadays for achieving affordable direct alcohol fuel cells. Nano-structural architecture plays a crucial role in the catalytic activity. Herein we are reporting, a cost effective one-dimensional (1D) nano structured electro-catalyst for improved methanol oxidation reaction. Pd modified Ni nanowire catalyst towards methanol electro oxidation were prepared by a simple galvanic replacement reaction. Exclusive nano-wire morphology achieved through a wet chemical reduction method without employing any capping agents or surfactants. Pd modified Ni nano-wires exhibited a supreme catalytic activity and durability towards methanol electro-oxidation. The distinctive 1D morphology and strong metal support interaction (SMSI) between Pd and NiO along with the bifunctional effects of Pd

* *Corresponding author*. Materials Science and Technology Division, CSIR-National Institute for Interdisciplinary Science and Technology (NIIST), Thiruvananthapuram, 695019, India.
E-mail address: nishanthkg@niist.res.in (N.K. Gopalan).

https://doi.org/10.1016/j.ijhydene.2020.01.006

Palladium
Alcohol electro-oxidation
Bifunctional effect
SMSI

and Ni attributed to the enhanced catalytic activity. The amount of precious Pd metal was reduced by 90 wt% with enhanced catalytic efficiency. Ethanol electro-oxidation study showed an improved catalytic activity with mass activity of 1479.79 mA/mg $_{Pd.}$

Introduction

Everlasting need for global energy demands alternative energy resources. Fuel cell technology has emerged as a promising alternative power source as they can directly convert the chemical energy in the fuels to electrical energy [1–3]. The high energy conversion efficiency and ambient operation temperature of Direct Alcohol Fuel Cells (DAFCs) have made them most attractive among the fuel cell family [4–8]. Pt has proved to be the excellent catalyst for Methanol Oxidation Reaction (MOR) so far, the expense and scarcity of the metal remains as an obstacle for the wide usage of the metal as the catalyst [9–12]. In recent years Pd metal was found to be a better alternative by considering the similar properties of these two metals. Relatively low cost and availability of Pd metal motivated the development of different Pd based catalysts [13–15]. Unlike Pt based catalysts, the catalyst based on Pd are highly active in the alkaline medium. Non-noble metals are stable and the incorporation of these metals with Pd is also possible in alkaline medium [16].

The catalytic activity of Pd can be further enhanced by alloying it with other metals such as Au, Rh, Cu, Ag, Sn, Co, Ni etc. [17–20] Variety of Pd based nano materials such as Pd nanosphere, PdNi nanosphere, PdCu nanoparticles and PdCu aerogel are also reported [21]. Among which PdNi electrocatalyst has gained great attention. Zhang et al. found negatively shifted onset potential and high peak current for core shell Ni–Pd/C compared to Pd/C [22]. Wang et al. reported the high activity and excellent stability for Pd supported Ni foam [23]. By chemical reduction method Liu et al. synthesized Pd Ni nanoparticles, Pd Ni film and alloy obtained by electro deposition exhibited enhanced catalytic activity compared with pure Pd [24]. The presence of Ni promotes the CO tolerance capability of Pd and thereby increases the catalytic efficiency [25–27]. Development of a facile method for synthesizing highly active Pd electro-catalysts with well-defined nanostructures are still remains as a great challenge.

Morphologies play a crucial role in the performance of the catalysts [28–30]. There are different types of nano-structured materials have been reported [31–39]. Among them, one dimensional nano materials got great attraction because of its several advantages over commonly used 0D nanoparticles. Due to reduced surface energy, 1D nano-materials are able to control agglomeration, dissolution and Ostwald ripening; the problems usually associated with nanoparticles and also help to promote the electron transport characteristics [40–42]. The present study we focused to reduce the Pd loading in the catalyst composition without compromising catalytic efficiency. The 1D Ni nano-wires (Ni NWs) were prepared by a wet chemical reduction method without the involvement of surfactants and templates; through nano particles self oriented attachment [43]. Ni wire was selected as the supporting material as the oxophilic nature of Ni particles can also contribute to the catalytic activity of the incorporated Pd [44–47]. The unique morphology and metal support interaction of the catalyst along with the bifunctional mechanism between Pd and Ni enhanced the activity of the catalyst towards methanol oxidation.

Experimental section

Materials

All chemicals were of analytical grade and used without any further purification. Nickel (II) chloride, Ethylene glycol, Palladium (II) chloride and Potassium hydroxide were purchased from Aldrich. Hydrazine hydrate, Hydrochloric acid, Methanol and Ethanol were purchased from Merck.

Synthesis of nickel nano wire

Nickel nano-wires were prepared by the reduction of nickel chloride using ethylene glycol as solvent and hydrazine hydrate as the reducing agent [43]. Required volume of 1 M aqueous nickel chloride was added to 7.5 ml of ethylene glycol to obtain a 10 mM solution of Ni^{2+}. Then the mixture was heated to 120 °C followed by the addition of 0.5 ml of hydrazine hydrate solution. The solution turned black and the formed nickel wires were found floating on the surface of the solution. In order to remove the excess solvent and hydrazine hydrate, the recovered nanowires were washed with deionized water followed by ethanol and stored in isopropanol solution.

Synthesis of Pd modified nickel wire catalyst

The Pd modified Ni NWs (5, 10 and 15 wt% Pd on Ni NWs) were prepared by a spontaneous displacement reaction. Required amount of as-prepared Ni NWs were ultrasonically dispersed in water, followed by the addition of required amount of 10 mM H_2PdCl_4 solution. Then, the solution was continuously stirred for about 3 h and left for one day for completing the reaction. The solid product that remained at the end of the reaction was filtered and washed with DI water and dried.

Characterization

The morphology and microstructure of the samples were examined using scanning electron microscopy (SEM) JEOL JSM- 5600 model. Transmission electron microscopy (TEM) FEI (Tecnai 30 G2 S- TWIN microscope), The Netherlands was

used to characterize the transmission electron microscopy images and elemental analysis. The crystallographic structures of the samples were analyzed from X-ray diffractometer (XRD), (Philips X'pert Pro) with Cu K ά (λ = 0.154060 nm) radiation over 2θ ranging from 10 to 90° with a step size of 0.08°. From X-ray photoelectron spectrometer (XPS), (PHI 5000 Versa Probe II) the electronic state and the elemental composition of the samples were obtained. The electrochemical tests were conducted on an electrochemical workstation (Autolab M204).

Electrochemical measurements

Electrochemical measurements were performed using Auto lab (M204). A classical three electrode system with catalyst coated glassy carbon electrode as a working electrode, a double junction Ag/AgCl electrode as a reference electrode and a Pt wire as a counter electrode were employed. The glassy carbon electrode (GCE) was first polished with Al_2O_3 powder and then washed well with distilled water. The catalyst ink was obtained by dispersing the synthesized catalyst in distilled water by ultrasonication. To prepare the working electrode 4 μl of the ink was mounted onto the GCE followed by 3 μl of 0.5 wt% nafion solution using a micropipette. It was then allowed to dry at room temperature. Catalyst loading was 0.225 mg/cm^2. The cyclic voltammograms of the catalysts were recorded in the potential range between −0.8 and 0.4 V at a scan rate of 50 mV/s in N_2 saturated 0.5 M KOH with and without 0.5 M methanol and the chrono amperometric measurements performed at a potential of −0.4 V for 4000 s in a solution of 0.5 M methanol in 0.5 M KOH.

Results and discussions

The SEM images presented in Fig. 1a, illustrated the wire morphology of the Ni material obtained through a simple wet chemical reduction method. The attractive wire morphology was prepared by the reduction of nickel chloride in ethylene glycol with hydrazine hydrate reducing agent at 120 °C. Fig. 1b shows the SEM images of the Pd modified Ni NWs prepared through the galvanic replacement reaction. The Ni^{2+}species have (Ni^{2+}/Ni = −0.25V vs. SHE) lower reduction potential than that of $PdCl_4^{2-}$/Pd redox pair (0.62V vs. SHE). Retention of the wire morphology even after the modification could be understood from the images. The incorporation of Pd on Ni NW was confirmed by the elemental mapping and it was shown in Fig. 1c, d. The detailed investigation of the structural features was done by High resolution TEM images. The wire morphology of the Ni nano material was well understood from the TEM images depicted in Fig. 2 (a, b). Fig. 2c illustrates the Pd modified Ni wire and the dark field image shown in Fig. 2 (d) indicates the presence of Pd on Ni nano wire. Pd metal observed as white spots on the surface of Ni wire [48].

The crystallographic studies of the catalysts done by XRD technique are presented in Fig. 3. Fig. 3 (a) represents the XRD pattern of Ni NW, Pd, and 10 wt% Pd modified Ni NW. The diffraction pattern of Ni wire showed peaks at 2θ values 44.58, 51.72 and 76.49 corresponds to the (111), (200), (220) miller planes and that of Pd showed peaks at 2θ, 40.33, 46.93, 68.29, 82.27, and 86.92 attributed to the Pd(111), (200), (220), (311), (222) planes respectively. Synthesized Ni wire and Pd were confirmed by indexing respective XRD pattern with JCPDS files 04–0850 and 46–1043. The results were in good agreement with the characteristic FCC structure of both Ni and Pd [49,50]. The catalyst, 10 wt% Pd modified Ni wire consisted with the peaks of Ni and Pd. However, a slight shift in all the peaks towards the low 2 theta value indicated the replacement of Pd atoms on the Ni wires [51]. The magnified image of (111) plane is given in inset. The lattice parameters of Pd and 10 wt% Pd modified Ni NW were estimated using the equation,

$$a = d\sqrt{h^2} + 1^2 + K^2$$

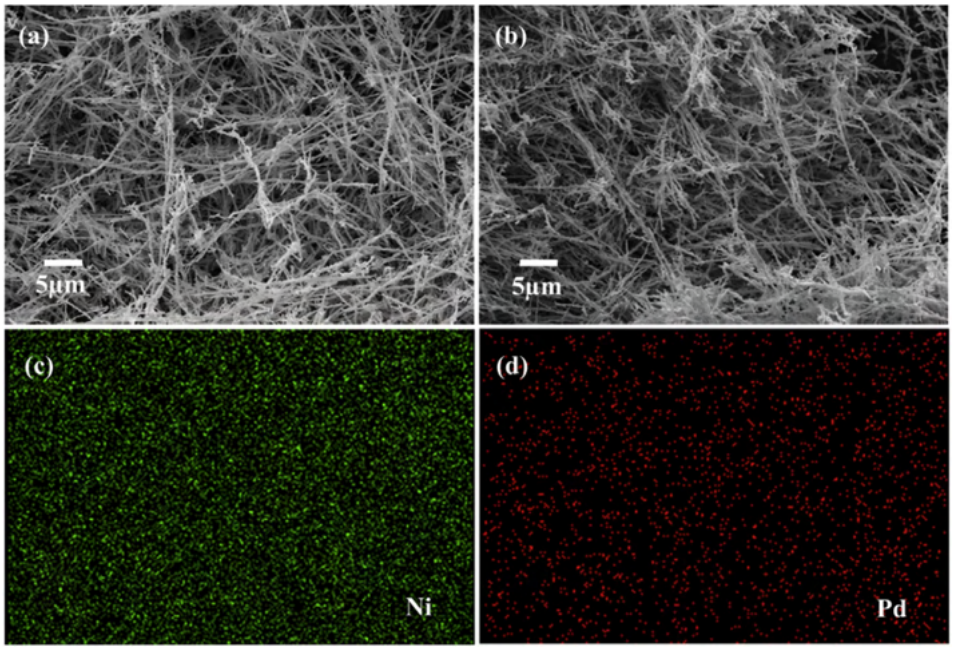

Fig. 1 – SEM images of (a) Ni wire (b) 10 wt% Pd on Ni wire, (c) & (d) Elemental mapping of Ni and Pd.

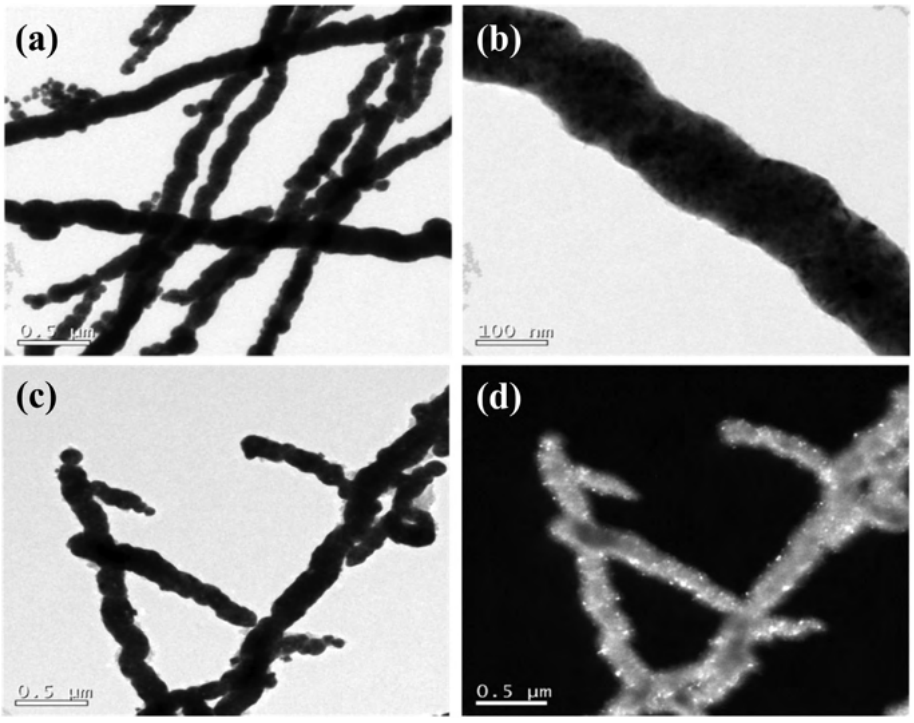

Fig. 2 – (a), (b), TEM images of Ni wire, (c), 10 wt% Pd on Ni wire, (d) Dark field image of 10 wt% Pd on Ni wire.

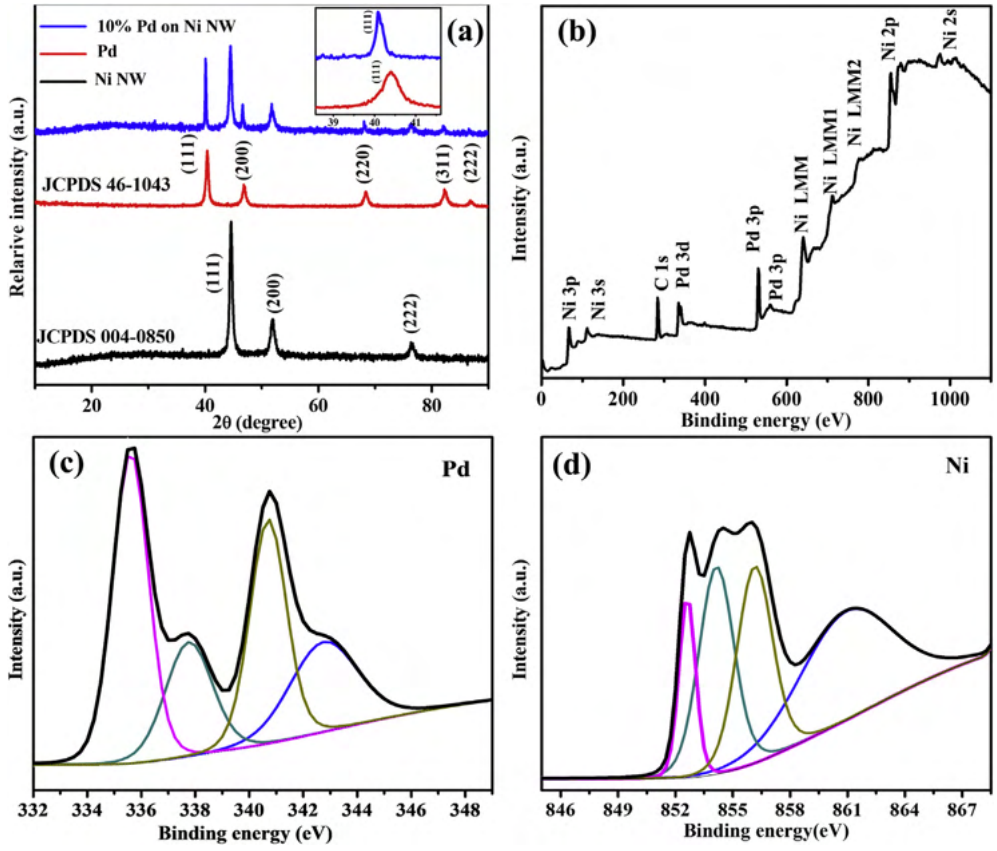

Fig. 3 – (a) XRD pattern of the synthesized Ni wire, Pd and 10 wt% Pd on Ni wire, XPS spectra of 10 wt% Pd on Ni wire (b) survey spectrum, (c) High resolution Pd 3d spectrum (d) High resolution Ni 2p spectrum.

where'a' is the lattice parameter,'d' is the interplanar distance and h, k, l are the Miller indices. The lattice parameter obtained for Pd is 0.39 nm and that of 10 wt% Pd modified Ni NW is 0.35 nm. The replacement of Ni atoms on the surface of Ni wire by Pd atoms lead to a contraction in the lattice and caused a decrease in the lattice parameter. The incorporation of Pd on Ni nano wire generates a strain in the Pd–Ni alloy and that creates shrinkage in the lattice parameters.

The existence of Pd and Ni were further unveiled by the XPS. Fig. 3 (b, c, d) depicts the data obtained from the spectrum. The spectrum of Pd can be fitted into two sets of spin-orbit doublets Pd ($3d_{5/2}$, $_{3/2}$). The deconvoluted peaks with binding energies 335.6, 340.7 eV assigned to Pd $3d_{5/2}$,$3d_{3/2}$, respectively indicate of Pd(0) and that of 337.7, 342.81eV corresponded to PdO [52]. The peaks located at 852.5, 854.3 and 856.15 eV resulted from the deconvolution of Ni $2P_{3/2}$, ascribed to the Ni (0) and NiO respectively. Apart from this 861 eV corresponded to the satellite peak associated with Ni^{2+} [53]. It is important to note that there is shift in the Pd ($3d_{5/2}$, $_{3/2}$) binding energy as compared to the reported value 333.0 and 340.3 eV [38]. The shift could be due to the strong electronic modification of Pd occurred due to the strain induced within the Pd–Ni alloy because of the substrate effect. It has reported that the lattice mismatch between the surface and substrate may be used to modify the electronic properties of the surface atoms [28,54,55]. The XPS result furtherer corroborate with the XRD analysis.

Electrochemical analysis

The electrochemical activities of the prepared samples were characterized using cyclic voltammetry technique. Fig. 4a shows the Cyclic Voltammograms of 5, 10, 15 wt% Pd modified Ni NW and pure Pd catalysts in 0.5 M KOH at a scan rate of 50 mV/s. Redox peaks associated with the oxidation and reduction of Pd was clear from the CV curves. Forward scan indicates the adsorption of hydrogen and oxidation of Pd to PdO. The hydrogen adsorption occurred around −0.8 to −0.4V and PdO formation took place at positive potentials. The reduction of PdO to Pd was represented by the backward sweep of the CV and it occurs around −0.2to −0.6V. This cathodic peak was used for the calculation of the electrochemically active surface area of the catalysts.

The electrochemical active surface area (ECSA) is an important parameter which determines the active sites of the catalyst. ECSAs were calculated from the CV curves of the catalysts in 0.5 M KOH at a scan rate of 50 mV/s. Cathodic peaks can be used to determine the ECSA of the Pd catalysts. It was measured by determining the coulombic charge for the reduction of PdO [56,57].

$$\text{ECSA} = \frac{Q}{0.405 * l}$$

where, Q is the charge for the reduction of PdO. Area under the CV curve of PdO reduction peak when divided by the scan rate

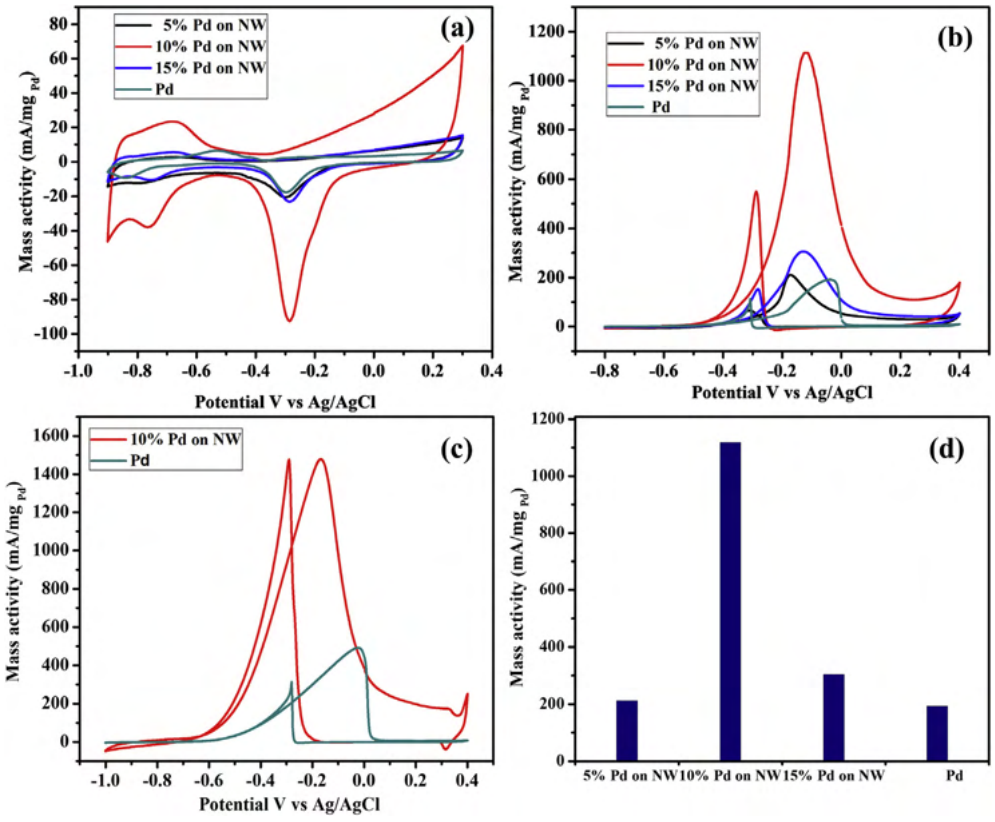

Fig. 4 – CV curves of (a) prepared samples and Pd catalyst in N_2 saturated 0.5 M KOH at a scan rate of 50 mV/s (b) prepared samples and Pd catalyst in N_2 saturated 0.5 M KOH and 0.5 M CH_3OH solution at a scan rate of 50 mV/s (c) 10 wt% Pd on NW and Pd catalyst in N_2 saturated 0.5 M KOH+0.5 M C_2H_5OH solution at a scan rate of 50 mV/s(d) MAs of as prepared samples and Pd catalyst.

Table 1 – Comparison of the electro catalytic activity of different electrocatalysts toward alcohol.

Catalysts	Electrolyte	Mass activity (mA/mg Pd)	Reference
Ni@Pd/MWCNTs	0.5 M NaOH + 1 M Methanol	770.7	[60]
Pd Ni catalyst	0.1 M NaOH + 1 M Methanol	63	[25]
PdNi/EGO	0.1 M NaOH + 1 M Ethanol	770.6	[52]
NiNWA/PdNF	0.5 M KOH + 0.1 M Ethanol	765	[61]
Pd Ni catalyst	1 M KOH + 1 M Methanol	677.08	[62]
$Pd_{59}Ni_{41}/C$	0.1 M KOH + 0.5 M Ethanol	450	[14]
Pd modified Ni NW	0.5 M KOH + 0.5 M Methanol	1118.35	This work
Pd modified Ni NW	0.5 M KOH + 0.5 M Ethanol	1479.79	This work

indicates the charge for the reduction of PdO. 'l' is the catalyst loading and a charge value of 0.405 mC/cm^2 was assumed for the reduction of PdO monolayer [9,50,58,59]. The ECSAs were estimated to be 12.70, 58.92, 13.76 and 11.45 m^2/g for 5, 10, 15 wt% Pd modified NW and pure Pd catalyst. A significant enhancement in the surface area was observed in the case of 10 wt% Pd modified Ni NW. The better surface area might be due to the unique 1D structure of the synthesized catalyst.

The activity of the Pd modified Ni NW catalysts towards methanol oxidation were studied in 0.5 M KOH and 0.5 M CH_3OH solution at a scan rate of 50 mV/s. The mass activities of the catalysts are shown in Fig. 4b. The peak in the a potential range of −0.4 to 0.4 V for the forward scan was attributed to the oxidation of methanol and that in the backward scan at potential range of −0.2 to −0.6 V was due to the oxidation of intermediates. It can be clear from the CV curves that all the Pd modified Ni NW catalysts possess a better onset potential and mass activities than the pure Pd and the 10 wt% Pd modified Ni NW showed significantly improved activity in terms of onset potential, peak potential and mass activity compared to other catalysts. Mass activities (MAs) obtained for 5, 10, 15 wt% Pd modified Ni NW were 213.19, 1118.35, 304.2 mA/mg$_{Pd}$ respectively and the attained mass activity for pure Pd is 193.69 mA/mg$_{Pd,}$ which is shown in histogram Fig. 4d. Even after reducing the amount of precious Pd metal by 90 wt% the catalyst was able to perform a mass activity five times greater than that of pure Pd metal. Drastic increase in the performance of the prepared catalyst could be attributed to the modification occurred due the strong coupling of the Pd particles over Ni NW. Ethanol oxidation also carried out using the highly active 10 wt% Pd modified NW catalyst in N_2 saturated solution containing 0.5 M KOH and 0.5 M C_2H_5OH since ethanol also used as a fuel in DAFCs. In this case also Pd modified NW showed a better onset and peak potential than the pure Pd. The corresponding mass activities obtained for 10 wt% Pd modified NW and pure Pd catalysts were 1479.79 and 506.55 mA/mg $_{Pd}$ respectively. Fig. 4c represents the corresponding CV curve. The superior catalytic activity of the 10 wt% Pd modified Ni catalyst over pure Pd is clear from the observed data. Comparison of the electro catalytic activities of different electrocatalysts toward alcohol was given in Table 1.

Chronoamperometric measurements performed further to study the stability of the catalysts at a potential of −0.4 V for 4000 s in a solution of 0.5 M methanol in 0.5 M KOH (Fig. 5a) [63]. The current decay of 10 wt% Pd modified NW observed to be slower indicating its better durability over the other catalysts. As time increase, the decrement, in the current value had been observed due to the presence of intermediate CO species. Among the various Pd modified NW, and pure Pd catalysts the 10 wt% Pd modified NW showed better durability. The experimental results thus revealed the better activity and durability of 10 wt% Pd on NW catalyst towards methanol oxidation. Further, the durability of the 10 wt% Pd modified NW catalyst was substantiated by performing the CV analysis for 200 cycles in N_2 saturated 0.5 M KOH and 0.5 M CH_3OH at a scan rate of 50 mV/s (Fig. 5b). It is clear that even after 200 cycles methanol oxidation study catalyst activity remained very close to the initial cycle, both in terms of onset potential and peak current.

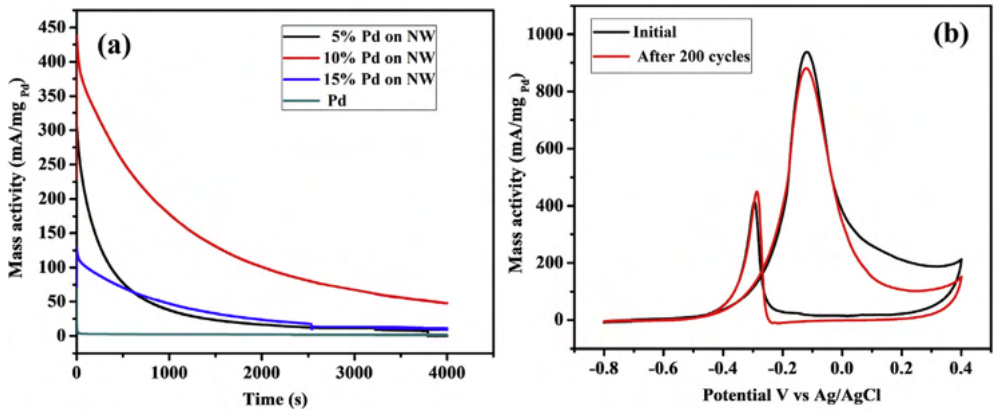

Fig. 5 – (a) Chronoamperometric curves of Pd modified Ni NW catalysts and Pd catalyst in N_2 saturated 0.5 M KOH and 0.5 M CH_3OH solution (b) CV curves of 10 wt% Pd on NW after 200 cycles in N_2 saturated 0.5 M KOH + 0.5 M CH_3OH solution.

The high electrochemical surface area, lowest onset and peak potential and high mass activity for methanol and ethanol oxidation of 10 wt% Pd modified Ni NW over all other prepared catalysts disclosed its supreme catalytic activity. The enhancement in efficiency of the Pd modified Ni NW was attributed to the unique morphology, electronic modifications and the bifunctional mechanism between Pd and Ni. The effective surface area of Pd particles that took part in the catalytic reaction in this case was remarkably higher than that in the alloys. The increased surface area can be utilized for the catalytic applications. The structural features of the unique morphology promote the electron conduction through the system. The electronic structure of Pd deposited on the Ni NWs surface is different from that of bulk Pd because of the so-called strain and ligand effects of the substrate. Electronically modified surface of Pd could be attributed to the improved activity. The XPS data provided the evidence for the electronic effects originating from Pd atoms withdrawing electrons from the neighbouring Ni in Pd modified Ni NW catalyst. The SMSI between the Pd and NiO facilitated the incorporation of the Pd and Ni and the synergetic behaviour of these two also contribute to the enhanced catalytic activity [64]. The oxophilic nature of Ni helps to reduce the CO poisoning of the Pd particles and thereby increase the catalytic rate.

Conclusions

Herein, Ni NWs were synthesized by a wet chemical reduction method without employing any surfactants and capping agents and using hydrazine hydrate as the reducing agent. The as prepared Ni wires were modified by varying the amount of Pd precursor through a simple galvanic replacement reaction. TEM, XRD and XPS analysis confirmed the incorporation of Pd atoms on Ni NW. Electrochemical measurements were carried out and the 10 wt% Pd modified Ni NW showed a supreme catalytic activity for methanol oxidation in terms of ECSA, onset potential, peak potential and mass activity over all other Pd modified Ni NW and pure Pd catalysts. The better stability of the catalyst also demonstrated. The increased surface area due to NW morphology, electronic modifications due to strong metal support interaction and Pd–Ni bifunctional mechanism combinedly led to the better catalytic efficiency for Pd modified Ni NW. The results established an excellent Pd based electrocatalyst for methanol oxidation with reduced Pd wt% utilizing a cheap Ni material.

Acknowledgment

The financial support from the DST- Science & Engineering Research Board (SERB), Government of India (Grant No: EEQ//2016/000342) is gratefully acknowledged. Roshima K acknowledges CSIR, New Delhi for the award of Junior Research Fellowship. We thank Mr. Kiran Mohan and Mr. Hareesh Raj V for microscopic analysis.

Appendix A. Supplementary data

Supplementary data to this article can be found online at https://doi.org/10.1016/j.ijhydene.2020.01.006.

REFERENCES

[1] Castegnaro MV, Gorgeski A, Balke B, Alves MC M, Morais J. Charge transfer effects on the chemical reactivity of Pd_xCu_{1-x} nanoalloys. Nanoscale 2016;8:641–7.
[2] Pan ZF, An L, Zhao TS, Tang ZK. Advances and challenges in alkaline anion exchange membrane fuel cells. Prog Energy Combust Sci 2018;66:141–75.
[3] Chen D, Zhao Y, Fan Y, Peng X, Wang X. Synthesis of Ni@PbPt supported on graphene by galvanic displacement reaction for improving ethanol electro-oxidation. J Mater Chem A 2013;1:13227–32.
[4] Zhao L, Wang ZB, Li JL, Zhang JJ, Sui XL, Zhang LM. One-pot synthesis of a three-dimensional graphene aerogel supported Pt catalyst for methanol electrooxidation. RSC Adv 2015;5:98160–5.
[5] Liu X, Xu G, Chen Y, Lu T, Tang Y, Xing W. A strategy for fabricating porous PdNi@ Pt core-shell nanostructures and their enhanced activity and durability for the methanol electrooxidation. Sci Rep 2015;5:6–11.
[6] Hu GZ, Nitze F, Jia X, Sharifi T, Barzegar HR, Gracia-Espino E, Wågberg T. Reduction free room temperature synthesis of a durable and efficient Pd/ordered mesoporous carbon composite electrocatalyst for alkaline direct alcohols fuel cell. RSC Adv 2014;4:676–82.
[7] Ruiz-Camacho B, Medina-Ramirez A, Villicana Aguilera M, Minchaca-Mojica JI. Pt supported on mesoporous material for methanol and ethanol oxidation in alkaline medium. Int J Hydrogen Energy 2019;44:12365–73.
[8] Bhavani KS, Anusha T, Brahman PK. Fabrication and characterization of gold nanoparticles and fullerene-C60 nanocomposite film at glassy carbon electrode as potential electro-catalyst towards the methanol oxidation. Int J Hydrogen Energy 2019:25863–73.
[9] Soleimani-Lashkenari M, Rezaei S, Fallah J, Rostami H. Electrocatalytic performance of Pd/PANI/TiO2nanocomposites for methanol electrooxidation in alkaline media. Synth Met 2018;235:71–9.
[10] Amin RS, Hameed RMA, El-Khatib KM. Microwave heated synthesis of carbon supported Pd, Ni and Pd–Ni nanoparticles for methanol oxidation in KOH solution. Appl Catal B Environ 2014;148–149:557–67.
[11] Tsang CHA, Leung DYC. Use of Pd-Pt loaded graphene aerogel on nickel foam in direct ethanol fuel cell. Solid State Sci 2018;75:21–6.
[12] Themsirimongkon S, Sarakonsri T, Lapanantnoppakhun S, Jakmunee J, Saipanya S. Carbon nanotube-supported Pt-Alloyed metal anode catalysts for methanol and ethanol oxidation. Int J Hydrogen Energy 2018:30719–31.
[13] Zhong J, Bin D, Yan B, Feng Y, Zhang K, Wang J, Wang C, Shiraishi Y, Yang P, Du Y. Highly active and durable flowerlike Pd/Ni(OH)2 catalyst for the electrooxidation of ethanol in alkaline medium. RSC Adv 2016;6:72722–7.
[14] Lee K, Kang SW, Lee SU, Park KH, Lee YW, Han SW. One-Pot synthesis of monodisperse 5 nm Pd–Ni nanoalloys for electrocatalytic ethanol oxidation. ACS Appl Mater Interfaces 2012;4:4208–14.

[15] Karuppasamy L, Chen C-Y, Anandan S, Wu JJ. Sonochemical reduction method for synthesis of TiO_2Pd nanocomposites and investigation of anode and cathode catalyst for ethanol oxidation and oxygen reduction reaction in alkaline medium. Int J Hydrogen Energy 2018:1–14.
[16] Lv X, Xu Z, Yan Z, Li X. Bimetallic nickel–iron-supported Pd electrocatalyst for ethanol electrooxidation in alkaline solution. Electrocatalysis 2011;2:82–8.
[17] Yang H, Wang H, Li H, Ji S, Davids MW, Wang R. Effect of stabilizers on the synthesis of palladium–nickel nanoparticles supported on carbon for ethanol oxidation in alkaline medium. J Power Sources 2014;260:12–8.
[18] Gao Y, Wang G, Wu B, Deng C, Ying G. Highly active carbon-supported PdNi catalyst for formic acid electrooxidation. J Appl Electrochem 2011;41:1–6.
[19] Kübler M, Jurzinsky T, Ziegenbalg D, Cremers C. Methanol oxidation reaction on core-shell structured Ruthenium-Palladium nanoparticles: relationship between structure and electrochemical behavior. J Power Sources 2018;375:320–34.
[20] Hu QY, Zhang RH, Chen D, Guo YF, Zhan W, Luo LM, Zhou XW. Facile aqueous phase synthesis of 3D-netlike Pd–Rh nanocatalysts for methanol oxidation. Int J Hydrogen Energy 2019;44:16287–96.
[21] Sheng J, Kang J, Hu Z, Yu Y, Fu XZ, Sun R, Wong CP. Octahedral Pd nanocages with porous shells converted from $Co(OH)_2$ nanocages with nanosheet surfaces as robust electrocatalysts for ethanol oxidation. J Mater Chem A 2018;6:15789–96.
[22] Zhang M, Yan Z, Xie J. Core/shell Ni@Pd nanoparticles supported on MWCNTs at improved electrocatalytic performance for alcohol oxidation in alkaline media. Electrochim Acta 2012;77:237–43.
[23] Obradovic MD, Stancic ZM, Lacnjevac U, Radmilovic VV, Gavrilovic-Wohlmuther A, Radmilovic VR, Gojkovic SL. Electrochemical oxidation of ethanol on palladium-nickel nanocatalyst in alkaline media. Appl Catal B Environ 2016;189:110–8.
[24] Hosseini MG, Abdolmaleki M, Ashrafpoor S. Methanol electro-oxidation on a porous nanostructured Ni/Pd-Ni electrode in alkaline media. Chin J Catal 2013;34:1712–9.
[25] Calderon JC, Nieto-Monge MJ, Perez-Rodriguez S, Pardo JI, Moliner R, Lazaro MJ. Palladium–nickel catalysts supported on different chemically-treated carbon blacks for methanol oxidation in alkaline media. Int J Hydrogen Energy 2016;41:19556–69.
[26] Moraes LPR, Matos BR, Radtke C, Santiago EI, Fonseca FC, Amico SC, Malfatti CF. Synthesis and performance of palladium-based electrocatalysts in alkaline direct ethanol fuel cell. Int J Hydrogen Energy 2016;41:6457–68.
[27] Del Rosario JAD, Ocon JD, Jeon H, Yi Y, Lee KJ, Lee J. Enhancing role of nickel in the nickel–palladium bilayer for electrocatalytic oxidation of ethanol in alkaline media. J Phys Chem C 2014;118:22473–8.
[28] Sheng J, Kang J, Ye H, Xie J, Zhao B, Fu XZ, Yu Y, Sun R, Wong CP. Porous octahedral PdCu nano cages as highly efficient electrocatalysts for the methanol oxidation reaction. J Mater Chem A 2018;6:3906–12.
[29] Shang C, Hong W, Wang J, Wang E. Carbon supported trimetallic nickel palladium–gold hollow nanoparticles with superior catalytic activity for methanol electro oxidation. J Power Sources 2015;285:12–5.
[30] Bi Y, Lu G. Control growth of uniform platinum nano tubes and their catalytic properties for methanol electro oxidation. Electrochem commun 2009;11:45–9.
[31] Du C, Chen M, Wang W, Yin G. Nano porous PdNi alloy nanowires as highly active catalysts for the electro-oxidation of formic acid. ACS Appl Mater Interfaces 2011;3:105–9.
[32] Li S, Wang N, Yue Y, Wang G, Zu Z, Zhang Y. Copper doped ceria porous nanostructures towards a highly efficient bifunctional catalyst for carbon monoxide and nitric oxide elimination. Chem Sci 2015;6:2495–500.
[33] Yu L, Bin Wu H, Lou XWD. Self- templated formation of hollow structures for electrochemical energy applications. Acc Chem Res 2017;50:293–301.
[34] Zhang J, Li CM. Nanoporous metals: fabrication strategies and advanced electrochemical applications in catalysis, sensing and energy systems. Chem Soc Rev 2012;41:7016–31.
[35] Jin R, Yang Y, Xing Y, Chen L, Song S, Jin R. Facile synthesis and properties of hierarchical double-walled copper silicate hollow nano fibers assembled by nano tubes. ACS Nano 2014;8:3664–70.
[36] Zhang G, Yu L, Bin Wu H, Hoster HE, Lou XW. Formation of $ZnMn_2O_4$ ball-in-ball hollow microspheres as a high-performance anode for lithium-ion batteries. Adv Mater 2012;24:4609–13.
[37] Fu G, Gong M, Tang Y, Xu L, Sun D, Lee JM. Hollow and porous palladium nanocrystals: synthesis and electro catalytic application. J Mater Chem A 2015;3:21995–9.
[38] Wang J, Zhang P, Xiahou Y, Wang D, Xia H, Mohwald H. Simple synthesis of Au–Pd alloy nanowire networks as macroscopic, flexible electrocatalysts with excellent performance. ACS Appl Mater Interfaces 2018;10:602–13.
[39] Zhang L, Xie Z, Gong J. Shape-controlled synthesis of Au–Pd bimetallic nanocrystals for catalytic applications. Chem Soc Rev 2016;45:3916–34.
[40] Lu Y, Du S, Steinberger-Wilckens R. One-dimensional nanostructured electrocatalysts for polymer electrolyte membrane fuel cells—a review. Appl Catal B Environ 2016;199:292–314.
[41] Zheng J, Cullen DA, Forest RV, Wittkopf JA, Zhuang Z, Sheng W, Chen JG, Yan Y. Platinum–ruthenium nanotubes and platinum–ruthenium coated copper nanowires as efficient catalysts for electro-oxidation of methanol. ACS Catal 2015;5:1468–74.
[42] Zheng Y, Qiao J, Hu J, Song F, Huo D, Yuan J, Wang A. PtIr alloy nanowire assembly on carbon cloth as advanced anode catalysts for methanol oxidation. Int J Hydrogen Energy 2019;44:20336–44.
[43] Kong YY, Pang SC, Chin SF. Facile synthesis of nickel nanowires with controllable morphology. Mater Lett 2015;142:1–3.
[44] Qi Z, Geng H, Wang X, Zhao C, Ji H, Zhang C, Xu J, Zhang Z. Novel nanocrystalline PdNi alloy catalyst for methanol and ethanol electro-oxidation in alkaline media. J Power Sources 2011;196:5823–8.
[45] Gopalsamy K, Balamurugan J, Thanh TD, Kim NH, Hui D, Lee JH. Surfactant-free synthesis of NiPd nanoalloy/graphene bifunctional nanocomposite for fuel cell. Compos B Eng 2017;114:319–27.
[46] Chung DY, Kim H, Chung Y, Lee MJ, Yoo SJ, Bokare AD, Choi W, Sung YE. Inhibition of CO poisoning on Pt catalyst coupled with the reduction of toxic hexavalent chromium in a dual-functional fuel cell. Sci Rep 2014;4:7450.
[47] Miao B, Wu ZP, Zhang M, Chen Y, Wang L. Role of Ni in bimetallic PdNi catalysts for ethanol oxidation reaction. J Phys Chem C 2018;122:22448–59.
[48] Chen AN, Mcclain SM, House SD, Yang JC, Skrabalak SE. Mechanistic study of galvanic replacement of chemically heterogeneous templates. Chem Mater 2019;31:1344–51.
[49] Krishnadas KR, Sajanlal PR, Pradeep T. Pristine and hybrid nickel nanowires: template-, magnetic field, and surfactant-free wet chemical synthesis and Raman studies. J Phys Chem C 2011:4483–90.
[50] Zhao Y, Yang X, Tian J, Wang F, Zhan L. Methanol electro-oxidation on Ni@Pd core-shell nanoparticles supported on

multi-walled carbon nanotubes in alkaline media. Int J Hydrogen Energy 2010;35:3249–57.
[51] Amin RS, Abdel Hameed RM, El-Khatib KM, Elsayed Youssef M. Electro catalytic activity of nano structured Ni and Pd–Ni on Vulcan XC-72R carbon black for methanol oxidation in alkaline medium. Int J Hydrogen Energy 2014;39:2026–41.
[52] Tan JL, De Jesus AM, Chua SL, Sanetuntikul J, Shanmugam S, Tongol BJV, Kim H. Preparation and characterization of palladium-nickel on graphene oxide support as anode catalyst for alkaline direct ethanol fuel cell. Appl Catal A Gen 2017;531:29–35.
[53] Saric I, Peter R, Kavre I, Badovinac IJ, Petravic M. Oxidation of nickel surfaces by low energy ion bombardment. Nucl Instrum Methods Phys Res Sect B Beam Interact Mater Atoms 2016;371:286–9.
[54] Meng Q, Liu J, Weng X, Sun P, Darr JA, Wu Z. In situ valence modification of Pd/NiO nano-catalysts in supercritical water towards toluene oxidation. Catal. Sci. Technol. 2018;8:1858–66.
[55] Nishanth KG, Sridhar P, Pitchumani S. Carbon-supported Pt encapsulated Pd nanostructure as methanol-tolerant oxygen reduction electro-catalyst. Int J Hydrogen Energy 2012;38:612–9.
[56] Liang X, Liu B, Zhang J, Lu S, Zhuang Z. Ternary Pd–Ni–P hybrid electrocatalysts derived from Pd–Ni core–shell nanoparticles with enhanced formic acid oxidation activity. Chem Commun 2016;52:11143–6.
[57] Chen W, Zhang Y, Wei X. Catalytic performances of PdNi/MWCNT for electrooxidations of methanol and ethanol in alkaline media. Int J Hydrogen Energy 2015;40:1154–62.
[58] Roy Chowdhury S, Ghosh S, Bhattachrya SK. Enhanced and synergistic catalysis of one-pot synthesized palladium-nickel alloy nanoparticles for anodic oxidation of methanol in alkali. Electrochim Acta 2017;250:124–34.
[59] Shih ZY, Wang CW, Xu G, Chang HT. Porous palladium copper nanoparticles for the electro catalytic oxidation of methanol in direct methanol fuel cells. J Mater Chem A 2013;1:4773–8.
[60] Zhao Y, Yang X, Tian J, Wang F, Zhan L. Methanol electro-oxidation on Ni @ Pd core-shell nanoparticles supported on multi-walled carbon nano tubes in alkaline media. Int J Hydrogen Energy 2010;35:3249–57.
[61] Hasan M, Newcomb SB, Rohan JF, Razeeb M. Ni nanowire supported 3D fl ower-like Pd nanostructures as an efficient electrocatalyst for electro oxidation of ethanol in alkaline media. J Power Sources 2012;218:148–56.
[62] Gu Z, Xu H, Bin D, Yan B, Li S, Xiong Z, Zhang K, Du Y. Preparation of PdNi nanospheres with enhanced catalytic performance for methanol electrooxidation in alkaline medium. Colloids Surf, A 2017;529:651–8.
[63] Feng YY, Song GH, Zhang Q, Lv JN, Hu XY, He YL, Shen X. Morphology effect of MnO_2 promoter to the catalytic performance of Pt toward methanol electro oxidation reaction. Int J Hydrogen Energy 2019;44:3744–50.
[64] Murphin Kumar PSM, Ponnusamy VK, Ramakrishnan DK, Kumar G, Pugazhendhi A, Abe H, Krishnan SK. Controlled synthesis of Pt nano particle supported TiO2 nano rods as efficient and stable electrocatalyst for oxygen reduction reaction. J Mater Chem A 2018;6:23435.

Available online at www.sciencedirect.com

ScienceDirect

journal homepage: www.elsevier.com/locate/he

Nickel phosphate modified carbon supported Pd catalyst for enhanced alcohol electro oxidation

Roshima Kottayintavida [a,b], *Nishanth Karimbintherikkal Gopalan* [a,b,*]

[a] *Materials Science and Technology Division, CSIR-National Institute for Interdisciplinary Science and Technology (NIIST), Thiruvananthapuram-695019, India*

[b] *Academy of Scientific and Innovative Research (AcSIR), Ghaziabad- 201002, India*

HIGHLIGHTS

- Ni_3 $(PO_4)_2$ modified carbon supported Pd catalyst was synthesized through a simple method.
- Transition metal phosphate modified carbon support is first time introduced for the alcohol electro oxidation application.
- Reduced Pd particles without agglomeration were observed in the presence of nickel phosphate.
- Modified catalyst showed seven-fold increments in the catalytic efficiency towards methanol oxidation.
- Three fold increments towards ethanol oxidation were achieved by the modified catalyst.

GRAPHICAL ABSTRACT

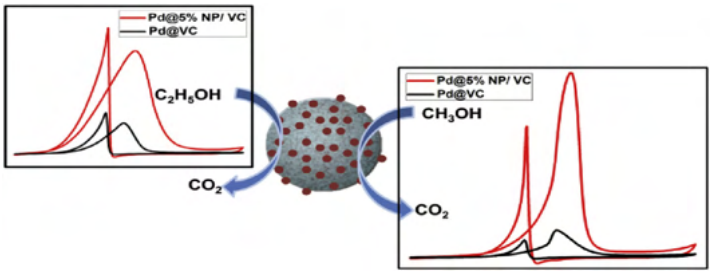

ARTICLE INFO

Article history:
Received 2 October 2019
Received in revised form
21 December 2019
Accepted 10 February 2020
Available online 5 March 2020

Keywords:
Alcohol oxidation
Pd catalyst

ABSTRACT

Urge for an alternative energy source demands the development of cost effective highly efficient catalyst for fuel cell applications. Transition metal phosphates are emerging as a novel class of material for many potential electrochemical applications owing its several advantages like abundance, environmental friendliness and low cost. Herein we explore the excellent electro chemical property of nickel phosphate (NP) as an electrocatalyst for alcohol oxidation. Novel vulcan carbon supported Pd @NP was synthesized through a very simple method at room temperature. In the presence of NP well dispersed homogeneous Pd particles having reduced size was observed. Approximately, seven-fold increments in the catalytic efficiency towards methanol oxidation and three fold increments towards ethanol oxidation than vulcan carbon supported pure Pd were achieved. The improved

* *Corresponding author*. Materials Science and Technology Division, CSIR-National Institute for Interdisciplinary Science and Technology (NIIST), Thiruvananthapuram-695019, India.
E-mail address: nishanthkg@niist.res.in (N.K. Gopalan).

https://doi.org/10.1016/j.ijhydene.2020.02.050

Vulcan carbon
Nickel phosphate
Fuel cell
Electro - oxidation

electrochemical property and increased surface area by the combination of Pd with nickel phosphorous compound and supporting carbon material imparted an excellent catalytic efficiency to the synthesized catalyst.

Introduction

Development of alternative energy sources is necessary for the ever-increasing energy requirements. Direct Methanol Fuel Cells (DMFC) are emerged as an excellent alternative power source for portable electronic devices due to its high efficiency, eco friendliness and simplicity [1–4]. Until now, Pt has proved to be the excellent catalyst for alcohol oxidation [5,6]. The fabrication expense due to the scarcity of Pt hinders the commercialization of DMFC. Search for an alternative catalyst suggested Pd as a suitable substitution owing to its similar properties and relative abundance [7–10]. Apart from this, Pd metal is active in alkaline medium [10]. A number of non-noble metals are also stable in alkaline media and thus enables the incorporation of them with Pd [11]. For the past few years researchers put efforts on further reduction of Pd metal content so that the DMFC can be commercially more viable. It was achieved by alloying Pd with different metals and fine tuning its morphology with better active surface area [12–15]. Morphology, size and distribution of particles, alloying metals play vital role in the electro-catalytic activity of the catalyst [16,17]. In this direction different combinations of Pd with Au, Co, Ni, Cu etc have already explored and more investigations for new efficient combinations are undergoing [18]. It is necessary to have highly efficient and cost effective electrocatalyst for the large-scale production of DMFC, where the search for an appropriate electrocatalyst is still in pursuit.

Recently, Ni metal, Ni alloy and Ni complexes were found to perform very good electro chemical activity [19–21]. Nickel-phosphorous compounds such as Ni_2P, $Ni_2P_2O_7$ and $Ni_xCo_{3-x}(PO_4)_2$were gained considerable attention as new electrode materials [22]. The Ni-P alloy acts as excellent catalyst in the decomposition of water, lithium ion battery, and super capacitor applications [23]. $Ni_3(PO_4)_2{\cdot}8H_2O$ modified electrode was used for electrocatalytic oxidation of glucose, formaldehyde and it also act as a supercapattery electrode material [24–26]. Ultra-long nanowires of $Ni_3(PO_4)_2$were used for the oxidation of glucose and Ni_2P_5/$Ni_3(PO)_4$ hollow sphere was employed for H_2O electrolysis [27,28]. Similarly, Fe doped NP and $Ni_2P_2O_7$ were reported for water oxidation and H_2 production respectively [29,30]. $NiPO_3$ nano sheet and $Ni_3(PO)_4$@GO exhibit superior capacitance behavior [31,32]. Ni_2P, Ni_5P_4, solvothermal derived amorphous Ni-P powders, and nickel phosphates are reported as wonderful candidate for super capacitor electrodes [23]. NP is considered as the promising electrode material due to its significant faradaic pseudo capacitance, low cost and easy fabrication [22,32]. But the low intrinsic electrical conductivity and relatively low rate capability are the key challenges associated with Ni_3PO_4 as an electrode material for capacitor application. The combination of Ni-P compounds with carbon materials can enhance the electro chemical performances [22].

Although NP ($Ni_3(PO_4)_2$) is used in the field of super capacitor, sensor, and as electrocatalysts for various application, it is not much explored for fuel cell applications [33,34]. The properties of NP make it a fascinating material for fuel cell applications. The oxophilic nature of nickel as well as phosphorus increases the CO tolerance and there by improve the electrocatalytic activity [24]. Thus, the combination of NP with Pd will reduce the CO poisoning and enhance the catalytic activity of Pd towards alcohol oxidation. Even though the catalytic performance of mesoporous, porous chain like network and Si-incorporated mesoporous nickel phosphates were studied, the surface modification of vulcan carbon with NP and Pd for alcohol oxidation was not yet explored [19,20,33,34].

In this work we tried to facilitate the electrocatalytic activity of Pd particles towards alcohol oxidation by incorporating it with NP modified Vulcan carbon. The synergism of the components plays a crucial role in the performance of the catalyst. The metal provides the active sites for alcohol oxidation, where Ni and P help to oxidize the carbonaceous poisons and there by release the active sites. The presence of vulcan carbon imparts good electrical conductivity and high surface area which in turn improves the catalysis. Hence, the collective action of the components contributes towards an enhanced alcohol oxidation.

Experimental section

Materials and reagents

Nickel (II) chloride, $PdCl_2$, KOH, $NaBH_4$, Methanol, and Ethanol were purchased from Sigma- Aldrich. Vulcan XC 72R was obtained from Cabot Corp. $NH_4H_2PO_4$ was obtained from Fisher Scientific. All chemicals were used without any further purification.

Preparation of nickel phosphate/vulcan carbon

Required amount of $NiCl_2$ and $NH_4H_2PO_4$ were dissolved in 50 ml vulcan carbon solution and stirred well using magnetic stirrer. Then, 0.5 M KOH solution added dropwise as a precipitating agent. The obtained mixture was then allowed to stir for 2 h [33].

$$NiCl_2 + 2\ KOH \rightarrow Ni(OH)_2 + 2KCl \quad (1)$$

$$NH_4H_2PO_4 \rightarrow NH_4^+ + H_2PO_4^- \quad (2)$$

$$Ni(OH)_2 + NH_4^+ + H_2PO_4^- \rightarrow NH_4NiPO_4 + 2H_2O \quad (3)$$

The resulting precipitate was then collected and washed well with distilled water. The obtained powder dried at 200 °C over-night. Different nickel phosphate/vulcan carbon (NP/VC) was prepared by varying the amount of NP such as 2, 5 and 10 wt% and designated as 2% NP/VC, 5% NP/VC, and 10% NP/VC respectively. Nickel hydroxide/vulcan carbon was synthesized without employing $NH_4H_2PO_4$ in this procedure.

Preparation of Pd @ nickel phosphate/vulcan carbon catalyst

20 wt% of Pd on modified carbon supported (NP/VC) were prepared by wet chemical method. In brief, required amount of modified carbon was dispersed in DI water and adequate amount H_2PdCl_4 solution was introduced dropwise. The mixture was allowed to stirrer for 30 min. Subsequently, the temperature was raised to 60 °C followed by the addition of 0.2 M of $NaBH_4$ solution. After 2 h stirring the sample was collected and washed well with distilled water. Pd on various NP/VC was prepared and designated as Pd@2% NP/VC, Pd@5% NP/VC, and Pd@10% NP/VC respectively (Scheme 1). Pd @Nickel hydroxide/vulcan carbon (Pd@5% NH/VC) and Pd on vulcan carbon in the absence of NP (Pd@VC) was synthesized via the same procedure.

Characterization techniques

X-ray diffraction patterns of the prepared materials were recorded on X-ray diffractometer (XRD), (Philips X'pert Pro) with Cu K ά ($\lambda = 0.154060$ nm) radiation over 2θ ranging from 10 to 90° with a step size of 0.08°. Morphology of the prepared samples and elemental analysis were characterized using High Resolution Transmission electron microscopy (HRTEM) FEI (Tecnai 30 G2 S- TWIN microscope), The Netherlands. X-ray photoelectron spectrometer (XPS), (PHI 5000 Versa Probe II) was employed to analyze the electronic state and the elemental composition of the prepared samples. The electrochemical tests were conducted on an electrochemical workstation (Autolab M204). The composition analysis of the catalyst was done using ICP- MS.

Electrochemical measurements

Electrochemical measurements were conducted using a standard three electrode system with catalyst coated glassy carbon electrode (GCE) as working electrode, a double junction Ag/AgCl as reference electrode and platinum wire as counter electrode. The working electrode having geometrical area 0.071 cm^2 was polished carefully to a mirror finish using alumina slurry and washed well with distilled water. For the preparation of the catalyst ink the as synthesized samples were ultrasonically dispersed in distilled water. Then 4 μL of the ink was transferred onto the GCE using a micropipette and subsequently added 3 μl of 0.5 wt% Nafion solution. The electrode was kept at room temperature and allowed to dry. Cyclic voltammetry measurements were performed over a potential range of 0.8 to −0.4 V in N_2 saturated 0.5 M KOH solution at a scan rate of 50 mV/s with alcohol and without alcohol. Electrochemical impedance spectroscopy (EIS) measurements were performed over a frequency range from 100 kHz to 0.01 Hz and amplitude 5 mV under the open circuit potential. Chronoamperometric measurements were carried out at −0.4 V for 4000 s.

Results and discussion

The crystallinity and phase purity of the prepared Pd@2% NP/VC, Pd@5% NP/VC Pd@10% NP/VC and Pd@VC were confirmed using XRD measurements, diffraction patterns shown in Fig. 1. The broad peak appeared at 24.29° ascribed to the amorphous Vulcan XC 72R carbon [35]. The sharp peaks obtained at 2θ angle 39.59°, 45.87°, 66.36° and 79.92° corresponds to the (111), (200), (220) and (311) planes of the face centered Pd [36]. However, peaks attributed to NP were missing in the XRD, illustrated the amorphous nature of NP. It was associated with the low reaction temperature (200 °C). Moreover, the weight percentage of NP was relatively low. Further the presence of NP was ensured from XPS analysis. Annealing temperature influence the crystallinity of nickel phosphate, where increase in temperature transforms the amorphous NP to crystalline in nature [33,37]. The lattice parameter calculated for Pd in both the catalysts was 0.39 nm.

Surface chemical composition and status of the Pd@5% NP/VC catalyst was analyzed through XPS analysis. Survey spectrum (Fig. 2a) indicates the presence of C, Pd, Ni, P and O. As shown in Fig. 2b, the deconvoluted spectra of Ni 2p consists of peaks at 856.75 and 880.34 eV corresponds to Ni $2p_{3/2}$ and Ni $2p_{1/2}$ respectively, indicating the presence of Ni^{2+}. Apart from which satellite peaks associated with the major peaks were also observed at 862.1 and 874.1 eV. The peak centered at 133.67 eV ascribed to the characteristic peak of phosphate species (Fig. 2c) [14]. The binding energies at 335.84 and 341.25 eV in Fig. 2d attributed to Pd $3d_{5/2}$ and $3d_{3/2}$, indicates

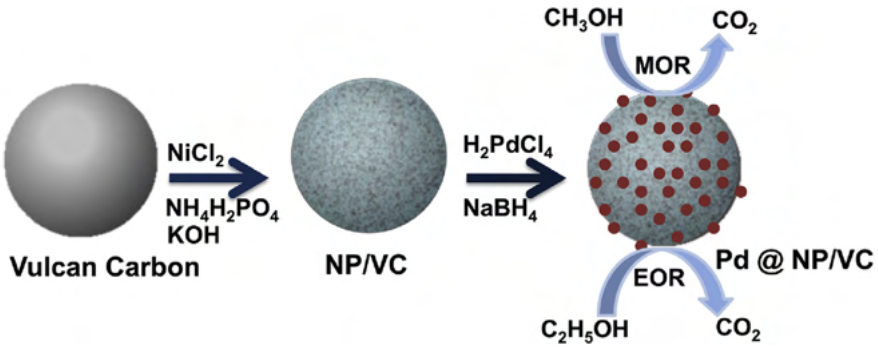

Scheme 1 – Schematic illustration of the synthesis of Pd @ NP/VC.

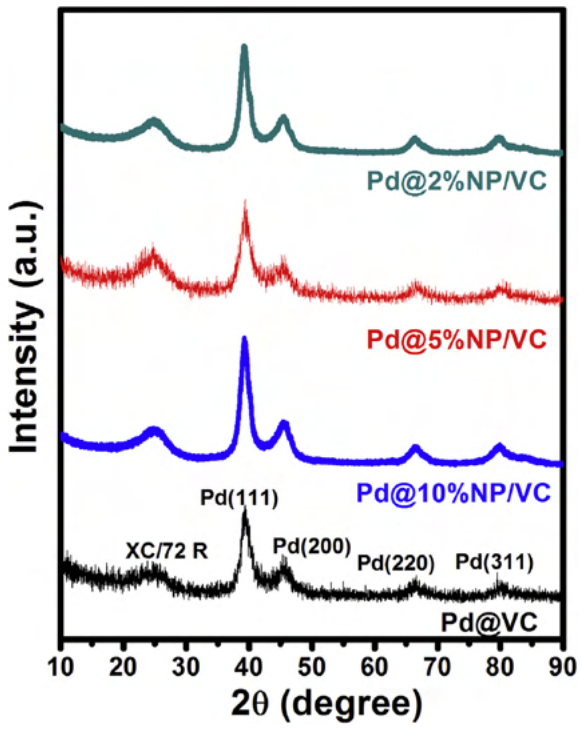

Fig. 1 – XRD pattern of Pd@2% NP/VC, Pd@5% NP/VC Pd@10% NP/VC and Pd@VC.

the presence of Pd (0) [38]. The peaks at 337.1 and 342.7 eV were assigned to Pd^{2+} [39]. Analysis of the XPS spectra revealed a shift in Pd binding energy. It suggests that the incorporation of Pd particles has developed a strong electronic modification due to the strain effect. Hence, the presence of NP and Pd particle were confirmed from the XPS data. The weight percentage of Pd and Ni were obtained as 19.8 and 0.71, 19.7 and 1.8, 19.8 and 3.76 respectively, for Pd@ 2% NP/VC, Pd@ 5% NP/VC and Pd@ 10% NP/VC from ICP MS analysis. The results were found to be the very close to the stoichiometric value.

Fig. 3 shows HRTEM images of all the prepared catalysts and their corresponding histograms. Well dispersed Pd nanoparticles on spherical carbon support were clearly identified from the TEM images. However, the NP modification on carbon surface (Fig. 3a,c,e) was not distinguishable with that of the unmodified catalyst (Fig. 3g). From the histograms (Fig. 3b,d,f) the average particle size of modified catalysts were calculated to be in the range of 5–6 nm and that of Pd@VC was 8 nm. The size of Pd particles present in Pd@VC was larger than that of Pd@5% NP/VC (5.03 nm). The presence of NP over the Vulcan carbon act as an obstacle thus prevent the Pd agglomeration in turn reduce the Pd particle size in Pd@ 5% NP/VC. The Pd particle size reduction plays a crucial role on the catalytic activity.

Electrochemical properties of the prepared samples were evaluated by cyclic voltammetry technique. Fig. 4a displays the cyclic voltammograms of synthesized catalysts performed in N_2 saturated 0.5 M KOH solution at a scan rate of 50 mV/s in order to measure the electrochemical active surface area (ECSA). ECSA was evaluated by integrating the charge associated with the reduction region of PdO with an assumption of a charge value of 0.405 mC/cm^2 was required for the reduction of PdO monolayer [40,41]. The parameter ECSA indicates the

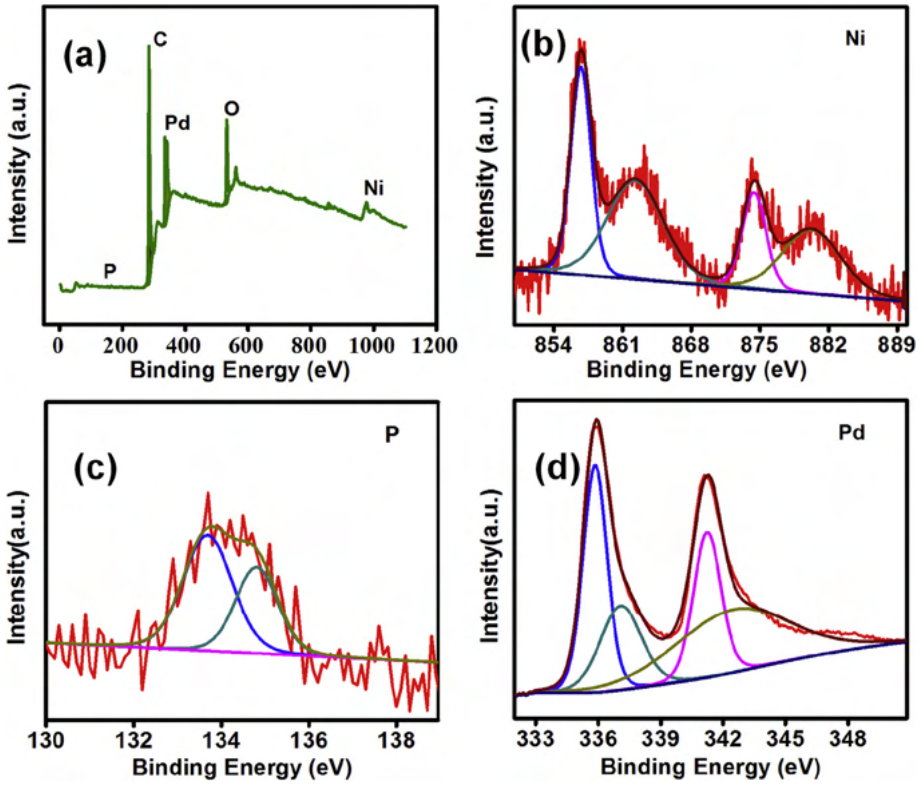

Fig. 2 – (a) Survey spectrum of Pd@ 5% NP/VC, XPS spectra (b), Ni 2p, (c) P 2p and (d) Pd 3d of Pd@5% NP/VC.

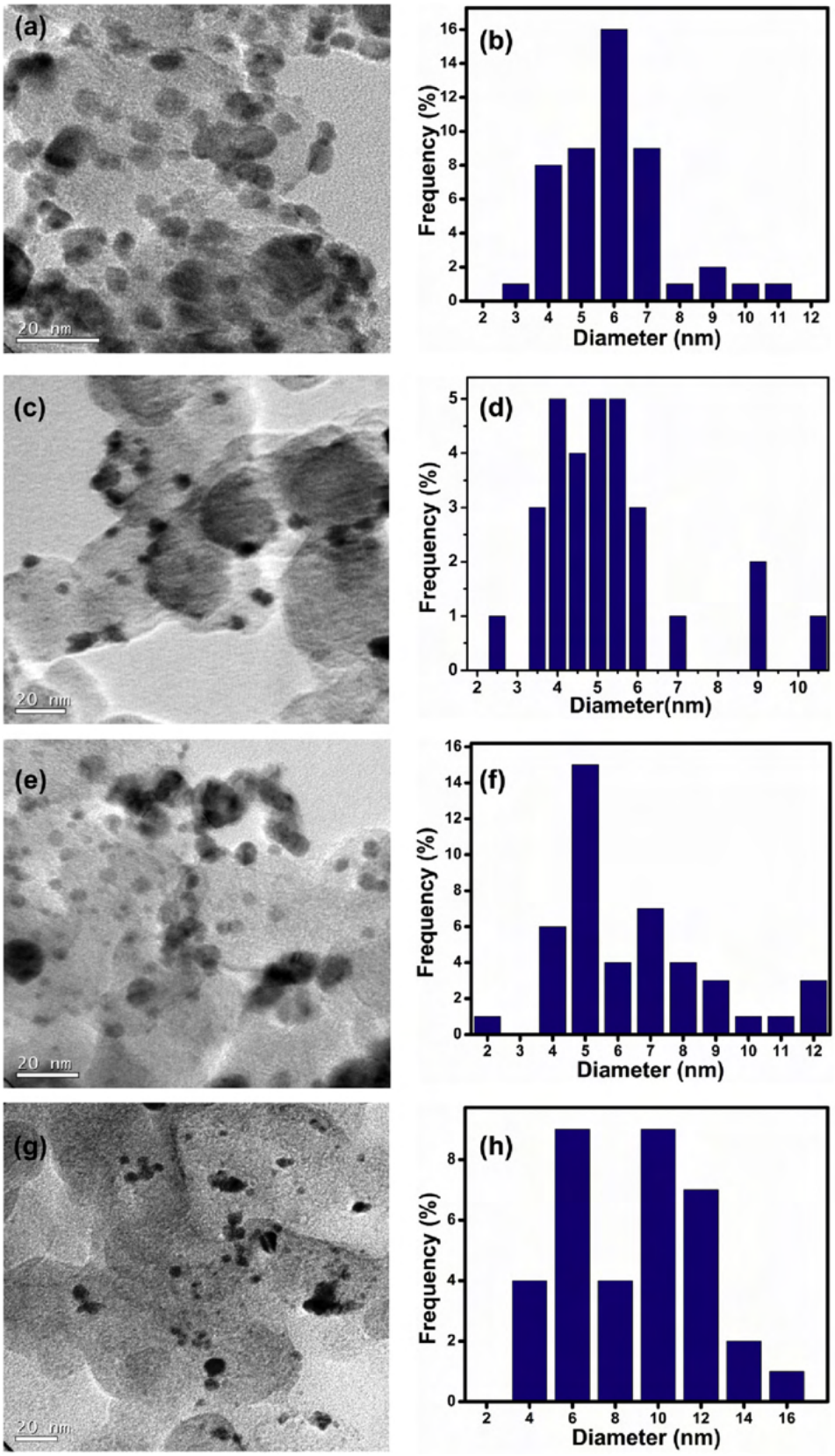

Fig. 3 – TEM images of (a) Pd@ 2% NP/VC, (c) Pd@ 5% NP/VC, (e) Pd@10% NP/VC (g) Pd @VC, Histograms of (b) Pd@ 2% NP/VC, (d) Pd@ 5% NP/VC, (f) Pd@ 10% NP/VC (h) Pd@VC.

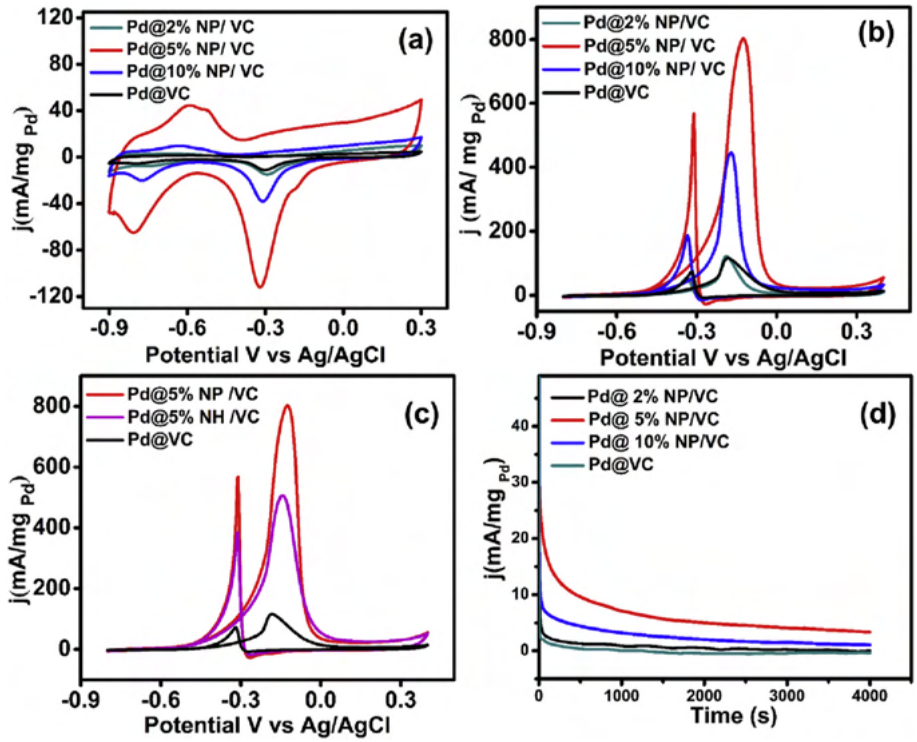

Fig. 4 – CV curves of the prepared samples in N_2 saturated 0.5 M KOH at a scan rate of 50 mV/s, (b) and (c) CV curves of the as prepared samples in N_2 saturated 0.5 M KOH and 0.5 M CH_3OH solution at a scan rate of 50 mV/s, (d) Chronoamperometric curves of prepared samples in N_2 saturated 0.5 M KOH and 0.5 M CH_3OH solution.

number of active sites of the catalyst and thus it estimates the performance of the catalyst. ECSA was calculated using the following equation [42,43].

$$ECSA = \frac{Q}{0.405 \times l} \quad (4)$$

Where Q represents the charge associated with the PdO reduction and 'l' is the amount of Pd loaded. The ECSA calculated to be 8.74, 78.12, 23.31, 7.16 m^2/g for Pd@2% NP/VC, Pd@5% NP/VC, Pd@10% NP/VC and Pd@VC, respectively. The large surface area in the case of Pd@5%NP/VC indicates the available active sites on Pd. This may be generated due to the presence of nickel phosphate. The oxophilic nature of both Ni and P reduce the catalyst poisoning by oxidizing the carbonaceous species and there by provide more active sites to take part in the reaction. The ECSA and the efficiency of the catalyst were directly proportional, thus reveals the capability of the developed catalyst.

Catalytic activity of the prepared samples towards methanol oxidation was carried out in N_2 saturated 0.5 M KOH solution containing 0.5 M methanol at a scan rate of 50 mV/s. Fig. 4b shows the obtained cyclic voltammograms. The anodic peak in the forward scan is attributed to the oxidation of methanol and the peak observed in the backward scan is due to the oxidation of carbonaceous intermediates [44,45]. As shown in the CV curves mass activities obtained for the catalysts Pd@2%NP/VC, Pd@5% NP/VC, Pd@ 10% NP/VC and Pd@VC were 122.67, 804.67, 448.75 and 115.49 mA/mg_{Pd} respectively. Even though the prepared catalysts impart better activity towards methanol oxidation

Table 1 – Onset potential and mass activity values of the prepared catalysts.

Catalyst	Onset potential (V)	Mass Activity (mA/mg_{Pd})
Pd@ 2% NP/VC	−0.402	122.67
Pd@ 5% NP/VC	−0.485	804.67
Pd@ 10% NP/VC	−0.452	448.75
Pd@ VC	−0.395	115.49

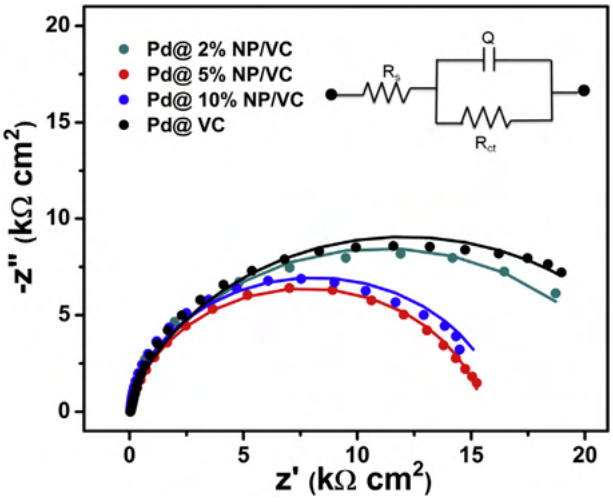

Fig. 5 – EIS Nyquist plots of all the prepared catalysts in 0.5 M KOH containing 0.5 M methanol at 50 mV/s.

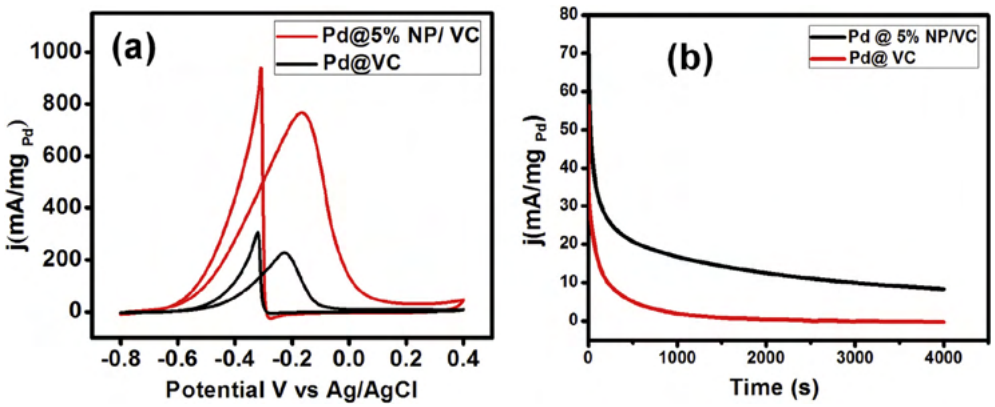

Fig. 6 – (a) CV curves of Pd@ 5% NP/VC and Pd@VC in N_2 saturated 0.5 M KOH + 0.5 M C_2H_5OH solution, (b) Chronoamperometric curves of Pd@ 5% NP/VC and Pd@VC N_2 saturated 0.5 M KOH and 0.5 M C_2H_5OH solution.

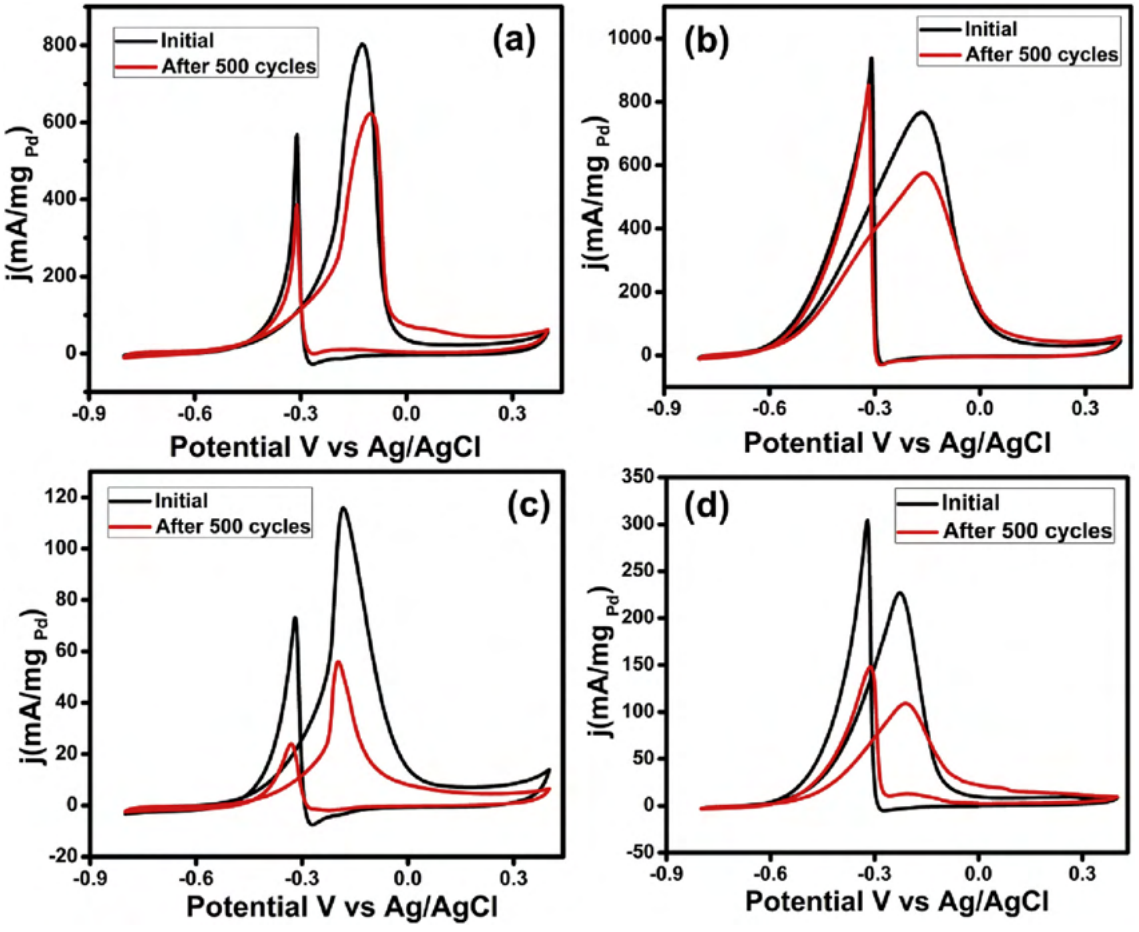

Fig. 7 – CV curves of (a) Pd@ 5% NP/VC after 500 cycles in N_2 saturated 0.5 M KOH + 0.5 M CH_3OH solution (b) Pd@ 5% NP/VC after 500 cycles in N_2 saturated 0.5 M KOH + 0.5 M C_2H_5OH solution (c) Pd@ VC after 500 cycles in N_2 saturated 0.5 M KOH + 0.5 M CH_3OH solution (d) Pd@ VC after 500 cycles in N_2 saturated 0.5 M KOH + 0.5 M C_2H_5OH solution.

reaction (MOR) the mass activity exhibited by the Pd@5%NP/VC reveals its supreme catalytic activity. A better catalytic activity was exhibited by the Pd@5% NP/VC in terms of onset potential and mass activity (Table 1). Low onset potential and high mass activity are the criteria for a good catalyst. Among the various prepared catalyst Pd@5%NP/VC showed much lower onset potential and high mass activity. Approximately, a seven-fold increase in mass activity than that of pure Pd@VC was observed.

The mechanism of methanol oxidation on Pd catalyst reactions exhibited as follows and the step 10 corresponds to the rate determining step [46].

$$Pd + CH_3OH \rightarrow Pd\text{-}(CH_3OH)_{ads} \quad (5)$$

$$Pd\text{-}(CH_3OH)_{ads} + OH^- \rightarrow Pd\text{-}(CH_3O)_{ads} + H_2O + e^- \quad (6)$$

$$Pd\text{-}(CH_3O)_{ads} + OH^- \rightarrow Pd\text{-}(CH_2O)_{ads} + H_2O + e^- \quad (7)$$

$$Pd\text{-}(CH_2O)_{ads} + OH^- \rightarrow Pd\text{-}(CHO)_{ads} + H_2O + e^- \quad (8)$$

$$Pd\text{-}(CHO)_{ads} + OH^- \rightarrow Pd\text{-}(CO)_{ads} + 4H_2O + e^- \quad (9)$$

$$Pd\text{-}(CO)_{ads} + 2OH^- \rightarrow Pd + CO_2 + H_2O + 2e^- \quad (10)$$

To further validate the role of phosphate towards improved methanol electrooxidation reaction, we compared the catalytic activity of Pd on 5% NP/VC and nickel hydroxide modified carbon (Pd@5% NH/VC) and shown in Fig. 4c. From the result it is clear that Pd@5% NP/VC shows better performance than Pd@5% NH/VC. The electrical resistivity of Ni-P is lower than that of $Ni(OH)_2$ and the oxophilic nature of both nickel and phosphorous in NP may help to remove the intermediate CO species generate during the alcohol oxidation [23,24,47]. Carbon based materials are usually employed as supporting materials to provide high surface area and good electrical conductivity [48]. Thus, the presence of both Ni and P along with carbon support increases the active sites of the catalyst and boosts the catalytic activity.

Chronoamperometric measurements were employed to study the stability of the catalysts [49,50]. Fig. 4d imparts the chronoamperometric curves of all the catalysts recorded at a potential of −0.4 V for 4000 s in N_2 saturated 0.5 M KOH solution containing 0.5 M methanol. Even though the current decays after some time the Pd@5% NP/VC shows a better stability than Pd@VC catalyst. Kinetic properties of the prepared samples were further explicated with electrochemical impedance spectroscopy. The recorded Nyquist plots of methanol electro oxidation on Pd@2%NP/VC, Pd@5% NP/VC, Pd@ 10% NP/VC and Pd@VC are depicted in Fig. 5. Simple Randle's circuit was utilized to fit the impedance data. The diameter of the osemicircle indicates the charge transfer resistance (R_{ct}) between electrode and electrolyte [51]. The R_{ct} values of Pd@2%NP/VC, Pd@5% NP/VC, Pd@ 10% NP/VC and Pd@ VC was 22.7, 15.2, 16.9, and 24.5 kΩ, and corresponding, exchange current density values (i_0) were 0.19, 28, 25 and 0.18 μF respectively. The reduced R_{ct} of Pd@5%NP/VC than Pd@ VC indicates the faster electro oxidation reaction [20,34]. The presence of NP in Pd@5% NP/VC facilitates the rate determining step and thereby enhances the catalytic kinetic performance towards oxidation. The obtained impedance data thus supports the mass activity evaluated from the CV analysis.

Similar results were observed in the case of performance towards ethanol oxidation. The activity was evaluated by CV in N_2 saturated 0.5 M KOH solution containing 0.5 M ethanol at a scan rate of 50 mV/s. As shown in Fig. 6a the Pd@5% NP/VC catalyst exhibited a mass activity 772.96 mA/mg_{Pd} and that of pure Pd@VC 230.63 mA/mg_{Pd}. The corresponding chronoamperometric measurements were also carried out in N_2 saturated 0.5 M KOH solution containing 0.5 M ethanol at a potential of −0.4 V for 4000 s (Fig. 6b). The Pd@5% NP/VC catalyst displayed a better stability. The tolerance of the catalyst towards carbonaceous species can be estimated using the ratio of forward anodic peak current (i_f) and backward anodic current (i_b). The i_f/i_b value of Pd@5% NP/VC and Pd@ VC in ethanol was 0.82, 0.75 and that in methanol it was 1.46, 1.41 respectively. The intermediates of methanol oxidation, CO can be oxidized easily than that of the intermediate (CH_3CO) produced during ethanol oxidation. Further, the cleavage of C-C bond is difficult in ethanol oxidation. Thus the activity of catalyst towards methanol oxidation is higher than that of ethanol [52].

The stability study was also done by performing the CV for 500 cycles. The corresponding voltamograms were depicted in Fig. 7 [53]. After 500 cycles the Pd@5% NP/VC exhibited a better stability in methanol and ethanol than that of Pd@ VC. As depicted in Fig. 6 the mass activity of Pd@ VC was reduced almost to half that of the initial value.

A comparison of the activity of different carbon supported catalyst towards alcohol oxidation was given in Table 2.

The presence NP enhances the efficiency of the catalysts. The intermediate CO generates during the alcohol oxidation remains as a major hindrance for the activity of the catalysts. The active sites of the catalysts available were occupied by the CO molecule and there by decelerate the reaction rate. The oxophilic nature of the Ni as well as P may help to improve the performance of the Pd by oxidizing the CO molecules. The low electrical resistance of Ni-P along with the carbon support imparts electrical conductivity that may facilitate the kinetics of catalysis. The increment in catalytic activity could be attributed to the enhanced CO tolerance of the catalyst and improved conductivity emerged due to the synergistic effect between Pd, Ni, P and vulcan carbon.

Table 2 – Comparison of activity of catalysts towards alcohol oxidation.

Catalysts	Electrolyte	Mass activity ($mA/mg_{Pd/Pt}$)	Reference
Pd/PPY/graphene	0.5 M NaOH + 1 M Methanol	359.8	[54]
PdMo/CNT	1 M KOH + 1 M Methanol	395.6	[55]
Pd/MnO_2/CNT	0.5 M NaOH + 1 M Methanol	431.02	[56]
Pd_3Mo/VC	1 M KOH + 1 M Methanol	647.27	[57]
$Pd_{10}Ag_{10}$/CNT	1 M KOH + 0.5 M Methanol	731.20	[58]
Commercial Pd/C	0.5 M KOH + 0.5 M Methanol	180.00	[59]
Pd@5% NP/VC	0.5 M KOH + 0.5 M Methanol	804.67	Present work
Pd@5% NP/VC	0.5 M KOH + 0.5 M Ethanol	772.96	Present work

Conclusions

Carbon supported Pd@NP catalyst was synthesized through a simple method. Transition metal phosphate modified carbon support is first time introduced for the alcohol electro oxidation application and excellent results were obtained. Unlike the agglomeration observed in the absence of NP, homogeneous Pd particles with reduced particle size were resulted in the presence of NP. Approximately seven-fold enhancement in activity towards methanol oxidation was achieved. Mass activity of 772.96 mA/mg_{Pd} was exhibited for ethanol oxidation by Pd@5%NP/VC and 230.63 mA/mg_{Pd} by Pd@VC. Thesynergistic effect of NP modified carbon support with Pd leads to the better activity. Collective action of the improved CO tolerance induced by NP and high surface area and conductivity imparted by vulcan carbon to Pd enhanced the activity of the catalyst towards alcohol oxidation.

Acknowledgment

DST- Science & Engineering Research Board (SERB), Government of India (Grant No: EEQ//2016/000342) is gratefully acknowledged for financial support. Roshima K acknowledges CSIR, New Delhi for the award of Junior Research Fellowship. We thank Mr. Kiran Mohan for microscopic analysis.

REFERENCES

[1] Kim Min Joong, Kwon Cho Rong, Eom Kwang Sup, Kim JiHyun, Cho Eun Ae. Electrospun Nb-doped TiO_2 nano fiber support for Pt nanoparticles with high electro catalytic activity and durability. Sci Rep 2017;7:44411.

[2] Lei M, Wang J, Li JR, Wang YG, Tang HL, Wang WJ. Emerging methanol-tolerant AlN nanowire oxygen reduction electrocatalyst for alkaline direct methanol fuel cell. Sci Rep 2014;4:6013.

[3] Arukula R, Vinothkannan M, Kim AR, Yoo D. J cumulative effect of bimetallic alloy, conductive polymer and graphene toward electro oxidation of methanol: an efficient anode catalyst for direct methanol fuel cells. J Alloys Compd 2019;771:477–88.

[4] Ramakrishnan S, Karuppannan M, Vinothkannan M, Ramachandran K, Kwon OJ, Yoo DJ. Ultrafine Pt nanoparticles stabilized by MoS2/N-doped reduced graphene oxide as durable electrocatalyst for alcohol oxidation and oxygen reduction reactions. ACS Appl Mater Interfaces 2019;11(13):12504–15.

[5] Kannan R, Kim AR, Nahm KS, Yoo DJ. One-pot synthesis and electro catalytic performance of Pd/MnOx/graphene nano composite for electro oxidation of ethylene glycol. Int J Hydrogen Energy 2015;40(35):11960–7.

[6] Kannan R, Kim AR, Nahm KS, Lee H-K, Jin Yoo D. Synchronized synthesis of Pd@C-RGO carbocatalyst for improved anode and cathode performance for direct ethylene glycol fuel cell. Chem Commun 2014;50(93):14623–6.

[7] Rozmanowski T, Krawczyk P. Influence of chemical exfoliation process on the activity of $NiCl_2$ -$FeCl_3$ -$PdCl_2$ -graphite intercalation compound towards methanol electro oxidation. Appl Catal B Environ 2018;224:53–9.

[8] Cui Xuexue, Wang Xiaosong, Xu Xiaowei, Yang Shuguang, Wang Yi. One-step stabilizer-free synthesis of porous bimetallic PdCu nano finger supported on graphene for highly efficient methanol electro-oxidation. Electrochim Acta 2018;260:47–54.

[9] Jiang J, Gao H, Lu S, Zhang X, Wang C-Y, Wang W-K, Yu H-Q. Ni–Pd core–shell nanoparticles with Pt-like oxygen reduction electro catalytic performance in both acidic and alkaline electrolytes. J Mater Chem A 2017;5(19):9233–40.

[10] Lv Xiaoyi, Xu Zhihua, Yan Zhaoxiong, Li Xihong. Bimetallic nickel–iron-supported Pd electrocatalyst for ethanol electro oxidation in alkaline solution. Electrocatalysis 2011;2(2):82–8.

[11] Kazemi R, Kiani A. Deposition of palladium sub monolayer on nanoporous gold film and investigation of its performance for the methanol electro oxidation reaction. Int J Hydrogen Energy 2012;37(5):4098–106.

[12] Calderón JC, Nieto-Monge MJ, Pérez-Rodríguez S, Pardo JI, Moliner R, Lázaro MJ. Palladium–nickel catalysts supported on different chemically-treated carbon blacks for methanol oxidation in alkaline media. Int J Hydrogen Energy 2016;41(43):19556–69.

[13] Chen Z, He Y-C, Chen J-H, Fu X-Z, Sun R, Chen Y-X, Wong C-P. PdCu alloy flower-like nano cages with high electro catalytic performance for methanol oxidation. J Phys Chem C 2018;122(16):8976–83.

[14] Sheng J, Kang J, Ye H, Xie J, Zhao B, Fu X-Z, Wong C-P. Porous octahedral PdCu nano cages as highly efficient electrocatalysts for the methanol oxidation reaction. J Mater Chem A 2018;6(9):3906–12.

[15] Wang LL, Li QX, Zhan TY, Xu QJ. A review of Pd-based electrocatalyst for the ethanol oxidation reaction in alkaline medium. Adv Mater 2013;860–863:826–30.

[16] Douk AS, Saravani H, Farsadrooh M. Three-dimensional inorganic polymer of Pd aerogel as a highly active support-less anode catalyst toward formic acid oxidation. Int J Hydrogen Energy 2019;44(33):18028–37.

[17] Shafaei Douk A, Saravani H, Noroozifar M. One-pot synthesis of ultrasmall Pt Ag nanoparticles decorated on graphene as a high-performance catalyst toward methanol oxidation. Int J Hydrogen Energy 2018;43(16):7946–55.

[18] Douk AS, Saravani H, Farsadrooh M, Noroozifar M. An environmentally friendly one-pot synthesis method by the ultrasound assistance for the decoration of ultra small Pd-Ag NPs on graphene as high active anode catalyst towards ethanol oxidation. Ultrason Sonochem 2019;58:104616.

[19] Yang J, Tan J, Yang F, Li X, Liu X, Ma D. Electro-oxidation of methanol on mesoporous nickel phosphate modified GCE. Electrochem commun 2012;23:13–6. 2012.

[20] Tan J, Yang J-H, Liu X, Yang F, Li X, Ma D. Electrochemical oxidation of methanol on mesoporous nickel phosphates and Si-incorporated mesoporous nickel phosphates. Electrochem Commun 2013;27:141–3.

[21] Spinner N, Mustain WE. Effect of nickel oxide synthesis conditions on its physical properties and electro catalytic oxidation of methanol. Electrochim Acta 2011;56(16):5656–66.

[22] Yuan J, Zheng X, Yao CD, Jiang L, Li Y, Che J, Chen H. Amorphous mesoporous nickel phosphate/reduced graphene oxide with superior performance for electrochemical capacitors. Dalton Trans 2018;47:13052.

[23] Lin J-D, Chou C-T. The influence of acid etching on the electrochemical supercapacitive properties of Ni P coatings. Surf Coating Technol 2017;325:360–9.

[24] Al-Omair MA, Touny AH, Al-Odail FA, Saleh MM. Electro catalytic oxidation of glucose at nickel phosphate nano/

micro particles modified electrode. Electrocatalysis 2017;8(4):340–50.
[25] Touny AH, Tammam RH, Saleh MM. Electrocatalytic oxidation of formaldehyde on nano porous nickel phosphate modified electrode. Appl Catal B Environ 2018;224:1017–26.
[26] Peng X, Chai H, Cao Y, Wang Y, Dong H, Jia D, Zhou W. Facile synthesis of cost-effective $Ni_3(PO_4)_2 \cdot 8H_2O$ microstructures as a supercapattery electrode material. Mater Today Energy 2018;7:129–35.
[27] Fa D, Yu B, Miao Y. Synthesis of ultra-long nanowires of nickel phosphate by a template-free hydrothermal method for electro catalytic oxidation of glucose. Colloid Surface Physicochem Eng Aspect 2019;564:31–8.
[28] Chang J, Lv Q, Li G, Ge J, Liu C, Xing W. Core-shell structured $Ni_{12}P_5/Ni_3(PO_4)_2$ hollow spheres as difunctional and efficient electrocatalysts for overall water electrolysis. Appl Catal B Environ 2017;204:486–549.
[29] Li Y, Zhao C. Iron-doped nickel phosphate as synergistic electrocatalyst for water oxidation. Chem Mater 2016;28(16):5659–66.
[30] Theerthagiri J, Cardoso ESF, Fortunato GV, Casagrande GA, Senthilkumar B, Madhavan J, Maia G. Highly electroactive Ni pyrophosphate/Pt catalyst towards hydrogen evolution reaction. ACS Appl Mater Interfaces 2019;11:4969–82.
[31] Liu Q, Chen C, Zheng J, Wang L, Yang Z, Yang W. 3D hierarchical $Ni(PO_3)_2$ nanosheet arrays with superior electrochemical capacitance behavior. J Mater Chem A 2017;5(4):1421–7.
[32] Li J-J, Liu M-C, Kong L-B, Wang D, Hu Y-M, Han W, Kang L. Advanced asymmetric supercapacitors based on $Ni_3(PO_4)_2$@GO and Fe_2O_3@GO electrodes with high specific capacitance and high energy density. RSC Adv 2015;5(52):41721–8.
[33] Sharma P, Radhakrishnan S, Khil M-S, Kim H-Y, Kim B-S. Simple room temperature synthesis of porous nickel phosphate foams for electro catalytic ethanol oxidation. J Electroanal Chem 2018;808:236–44.
[34] Song X, Sun Q, Gao L, Chen W, Wu Y, Li Y, Yang J-H. Nickel phosphate as advanced promising electrochemical catalyst for the electro-oxidation of methanol. Int J Hydrogen Energy 2018;43(27):12091–102.
[35] Wang F, Yang L, Tang Q, Guo Y, Hao G. Synthesis of Pd/XC-72 catalysts by a facile glutamate-mediated method for solvent-free selective oxidation of dl-sec-phenethyl alcohol. Catal Sci Technol 2013;3(5):1246.
[36] Zhao Y, Yang X, Tian J, Wang F, Zhan L. Methanol electro-oxidation on Ni@Pd core-shell nanoparticles supported on multi-walled carbon nanotubes in alkaline media. Int J Hydrogen Energy 2010;35(8):3249–57.
[37] Omar FS, Numan A, Duraisamy N, Bashir S, Ramesh K, Ramesh S. Ultrahigh capacitance of amorphous nickel phosphate for asymmetric supercapacitor applications. RSC Adv 2016;6(80):76298–306.
[38] Wang J, Zhang P, Xiahou Y, Wang D, Xia H, Möhwald H. Simple synthesis of Au–Pd alloy nanowire networks as macroscopic, flexible electrocatalysts with excellent performance. ACS Appl Mater Interfaces 2017;10(1):602–13.
[39] Wang F, Yu H, Tian Z, Xue H, Feng L. Active sites contribution from nanostructured interface of palladium and cerium oxide with enhanced catalytic performance for alcohols oxidation in alkaline solution. J Energy Chem 2018;27(2):395–403.
[40] Chen Z, He Y-C, Chen J-H, Fu X-Z, Sun R, Chen Y-X, Wong C-P. PdCu alloy flower-like nano cages with high electro catalytic performance for methanol oxidation. J Phys Chem C 2018;122(16):8976–83.
[41] Shih Z-Y, Wang C-W, Xu G, Chang H-T. Porous palladium copper nanoparticles for the electro catalytic oxidation of methanol in direct methanol fuel cells. J Mater Chem A 2013;1(15):4773.
[42] Shafaei Douk A, Saravani H, Noroozifar M. Three-dimensional assembly of building blocks for the fabrication of Pd aerogel as a high performance electrocatalyst toward ethanol oxidation. Electrochim Acta 2018;275:182–91.
[43] Yazdan-Abad Mehdi Zareie, Noroozifar Meissam, Douk Abdollatif Shafaei, Modarresi-Alam Ali Reza, Saravani Hamideh. Shape engineering of palladium aerogels assembled by nanosheets to achieve a high performance electrocatalyst. Appl Catal B Environ 2019;250:242–9.
[44] Bora A, Mohan K, Doley S, Goswami P, Dolui SK. Broadening the sunlight response region with carbon dot sensitized TiO_2 as a support for a Pt catalyst in the methanol oxidation reaction. Catal Sci Technol 2018;8(16):4180–92.
[45] Wang S, Yang G, Yang S. Pt-frame @Ni quasi core–shell concave octahedral $PtNi_3$ bimetallic nanocrystals for electro catalytic methanol oxidation and hydrogen evolution. J Phys Chem C 2015;119(50):27938–45.
[46] Soleimani-Lashkenari M, Rezaei S, Fallah J, Rostami H. Electro catalytic performance of Pd/PANI/TiO_2 nano composites for methanol electro oxidation in alkaline media. Synth Met 2018;235:71–9.
[47] Chung DY, Kim H, Chung Y-H, Lee MJ, Yoo SJ, Bokare AD, Sung YE. Inhibition of CO poisoning on Pt catalyst coupled with the reduction of toxic hexavalent chromium in a dual-functional fuel cell. Sci Rep 2014;4(1).
[48] Liu Y, Li S, Zhang Y, Liu W, Wang J, Zhai C. Electro catalytic oxidation of methanol on Pt-Pd nanoparticles supported on honeycomb-like porous carbons in alkaline media. J Solid State Electrochem 2017;22(3):817–24.
[49] Xu G, Liu J, Liu B, Zhang J. Self-assembly of Pt nanocrystals into three-dimensional super lattices results in enhanced electro catalytic performance for methanol oxidation. CrystEngComm 2019;21:411.
[50] Douk AS, Saravani H, Yazdan Abad MZ, Noroozifar M. Controlled organization of building blocks to prepare three-dimensional architecture of Pd–Ag aerogel as a high active electrocatalyst toward formic acid oxidation. Compos B Eng 2019;172:309–15.
[51] Omar FS, Numan A, Bashir S, Duraisamy N, Vikneswaran R, Loo YL, Ramesh S. Enhancing rate capability of amorphous nickel phosphate supercapattery electrode via composition with crystalline silver phosphate. Electrochim Acta 2018;273:216–28.
[52] Chen W, Zhang Y, Wei X. Catalytic performances of PdNi/MWCNT for electro oxidations of methanol and ethanol in alkaline media. Int J Hydrogen Energy 2015;40(2):1154–62.
[53] He Q, Shen Y, Xiao K, Xi J, Qiu X. Alcohol electro-oxidation on platinum–ceria/graphene nanosheet in alkaline solutions. Int J Hydrogen Energy 2016;41(45):20709–19.
[54] Zhao Yanchun, Lu Zhan, Tian Jianniao, Nie Sulian, Ning Zhen. Enhanced electro catalytic oxidation of methanol on Pd/polypyrrole–grapheme in alkaline medium. Electrochim Acta 2011;56:1967–72.
[55] Kakati N, Maiti J, Lee SH, Yoon YS. Core shell like behavior of PdMo nanoparticles on multiwall carbon nanotubes and their methanol oxidation activity in alkaline medium. Int J Hydrogen Energy 2012;37(24):19055–64.
[56] Zhao Y, Zhan L, Tian J, Nie S, Ning Z. MnO_2 modified multi-walled carbon nanotubes supported Pd nanoparticles for methanol electro-oxidation in alkaline media. Int J Hydrogen Energy 2010;35:10522–6.

[57] Fathirad F, Mostafavi A, Afzali D. Bimetallic Pd–Mo nanoalloys supported on Vulcan XC-72R carbon as anode catalysts for direct alcohol fuel cell. Int J Hydrogen Energy 2017;42(5):3215–21.
[58] Satyanarayana M, Rajeshkhanna G, Sahoo Malaya K, Ranga Rao G. Electrocatalytic activity of Pd20–xAgx nanoparticles embedded in carbon nanotubes for methanol oxidation in alkaline media. ACS Appl Energy Mater 2018;1:3763–70.
[59] Shih Z-Y, Wang C-W, Xu G, Chang HT. Porous palladium copper nanoparticles for the electrocatalytic oxidation of methanol in direct methanol fuel cells. J Mater Chem 2013;1(15):4773.

Electrochimica Acta 384 (2021) 138405

Contents lists available at ScienceDirect

Electrochimica Acta

journal homepage: www.elsevier.com/locate/electacta

PdAu alloy nano wires for the elevated alcohol electro-oxidation reaction

Roshima Kottayintavida[a,b], Nishanth Karimbintherikkal Gopalan, Validation Data curation Writing – review & editing[a,b,*]

[a] Materials Science and Technology Division, CSIR-National Institute for Interdisciplinary Science and Technology (NIIST), Thiruvananthapuram 695019, India
[b] Academy of Scientific and Innovative Research (AcSIR), Ghaziabad 201002, India

ARTICLE INFO

Article history:
Received 15 December 2020
Revised 10 March 2021
Accepted 14 April 2021
Available online 20 April 2021

Keywords:
Ultrathin PdAu nanowire
Palladium catalyst
Alcohol oxidation
Direct alcohol fuel cell
Electro-catalyst
One dimensional morphology

ABSTRACT

In the search of a satisfactory electrocatalyst for fuel cells, herein, we are reporting Au rich PdAu nano wires with excellent electro-catalytic activity towards methanol and ethanol oxidation. Ultrathin one-dimensional PdAu nanowires were prepared rapidly through a simple one step process. Among the prepared catalysts, the 10% Pd incorporated PdAu nano wire catalyst imparted greater catalytic activity, which exhibited ten times enhancement higher activity towards methanol as well as six times higher activity towards ethanol than that of the pure Pd catalyst. Eventually, the amount of Pd metal reduced to 90% without compromising its catalytic efficiency. Distinctive properties of one-dimensional Au were attributed to the improved catalytic activity.

1. Introduction

In the field of fuel cells, the selection and the development of an efficient catalyst is very vital, and therefore, the controllable production of catalysts with variety of size and shape has attracted extensive interest in this area [1,2]. Even though the DAFCs (Direct Alcohol Fuel Cells) are known as the promising energy source for fulfilling the inevitable energy demands especially in portable electronic devices, the efficiency of catalysts is still not satisfactory [3–6]. Until now, Pt has been viewed as the most efficient catalyst for anode reaction [7,8]. But, the expensive and limited supply of Pt extremely interrupted the large scale manufacturing of DAFC [9-11]. As of now, Pd is considered to be the appropriate alternative of Pt owing to exhibiting similar properties with Pt [12,13]. Meanwhile, it is 50 times abundant, and relatively cheaper than Pt [14–16]. Eventually, Pd exhibits an outstanding activity and stability in alkaline medium [17–19]. However, it is indeed necessary to reduce the amount of Pd owing to its very high cost, and simultaneously, the activity also need to be improvised. In this view, one of the highly rated strategies developed is combining the transition metals with Pd to obtain an alloy. Incorporation of Ni, Cu, Ag, Fe, Au, etc. with Pd is observed to influenced the catalytic activity and improved the efficiency through bi-functional mechanism [20–24].

The particle morphology is one of the crucial factors upon which the catalytic active sites are highly dependent [25–28]. Therefore, development of various catalysts with fascinating morphologies having high surface area has become another crucial strategy for enhancing the catalytic efficiency [29,30]. Recently, one dimensional nanostructure is emerged as the new class of material in various fields including catalysis, optoelectronics, nano science, sensing, biological applications, etc. [31,32]. The unique structural features with high aspect ratios hold the key for its fascinating optical and electrical properties. The specific architecture possesses advantages like structural anisotropy, large surface area, high flexibility and high conductance [33,34]. The common issues associated with nano particles include dissolution, aggregation and Ostwald ripening, which can be controlled to an extent. The peculiar structure can able to promote the electron transport characteristic due to the path directing effect of structural anisotropy. The easy transport of electrons associated with the 1D structure also favor the enhancement of catalytic activity [35]. The structural robustness provides more active surface area to take part in the reaction and in turn boost the activity.

Gold is known as an amazing element owing to its unique properties including its inert nature. Most interesting fact is when size

* Corresponding authors at: Materials Science and Technology Division, CSIR-National Institute for Interdisciplinary Science and Technology (NIIST), Thiruvananthapuram 695019, India
E-mail address: nishanthkg@niist.res.in (N.K. Gopalan).

https://doi.org/10.1016/j.electacta.2021.138405
0013-4686/

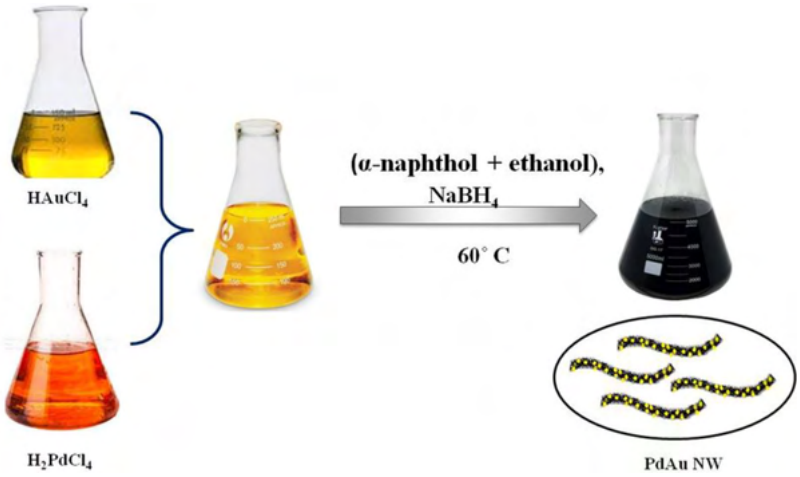

Scheme 1. Schematic representation of the formation of PdAu NW.

is reduced to nano level, gold show tremendous changes in its physical properties, and its activeness enhanced significantly from its bulk state owing to which it is much more reactive in its nanostate [36–40]. This unique feature encouraged the researchers to apply gold in the field of catalysis and sensing [40,41]. The gold nano particles are observed to be very active towards CO oxidation which is highly encouraging factor to apply gold nano particles in CO oxidation at ambient temperatures [42–47]. The combination of Au with Pd can effectively promote the oxidation of the adsorbed intermediate CO species on Pd. Several studies have done in the field of electrochemistry using Au and Pd. Luo et al., developed PdAu nanocatalyst with variable atom ratio for methanol oxidation [48]. Caglar and Kivrak reported carbon nanotube supported PdAu alloy catalyst for ethanol oxidation [49]. Au@PdAg core shell nanotubes were used for the oxidation of methanol and Au@PdAg NSs decorated rGO was used for ethanol oxidation [50,51]. Liu et al., synthesised AuPd alloy on graphene for ethanol oxidation [52]. AuPtPd nano dendrites performed as excellent catalyst towards hydrogen evolution and oxygen reduction and AuPd nano alloys reported as good catalyst for hydrogen peroxide oxidation [53,54]. Meanwhile, the nano porous AuPd showed better activity for alcohol oxidation. Lu et al. reported porous Pd Au films for methanol oxidation [55]. Au decorated Pd cubes were also reported for methanol oxidation [56].

Very few efforts have made in synthesizing AuPd alloy nano wire for electrocatalyst application so far. Zhu et al. prepared PdAu alloy nano wire through a template assisted method for sensing nonenzymatic glucose. The synthetic protocol involves complicated and relatively time-consuming processes [57]. Wang et al. synthesized PdAu nano wire for methanol oxidation, where the adopted method was simple, though the consumption of hazardous aminopyridine makes the preparation non-reliable [58]. In addition, no attempts have done in the direction of reducing the amount of Pd. Here we demonstrate an extremely rapid synthesis (~ 5 min) of ultrathin PdAu nano wire with high aspect ratio without utilizing any complicated synthetic strategy. The as prepared catalyst exhibited an excellent catalytic activity towards alcohol oxidation. In this work bimetallic PdAu nano wires having diameter of 5 nm was synthesized by a simple and rapid method. The Pd incorporated Au wire was obtained through a simple reduction method there by eliminating the carbon corrosion problem. Morphology, chemical composition and purity of the prepared catalysts were analyzed in detail. The electrocatalytic properties of the samples were investigated using cyclic voltammetry (CV) and chronoamperometric measurements.

2. Experimental section

2.1. Materials

Chloroauric acid, Palladium (II) chloride, $\acute{\alpha}$-naphthol, Sodium borohydride, Potassium hydroxide, Methanol and Ethanol. All chemicals were purchased from Merck chemicals and utilized as obtained.

2.2. Preparation of PdAu nano wire

A mixture of 4.5 ml 0.05 M $HAuCl_4$ and required amount of 10 mM H_2PdCl_4 were heated to 60°C under water bath. Subsequently added 0.5 M α-naphthol ethanol and 0.2 M $NaBH_4$ solution. The pale yellow color of the solution immediately changed to black. The obtained product collected by centrifugation and washed well using ethanol solution [59]. Different composition of PdAu nano wire was synthesized by varying the quantity of precursors. The simple and rapid synthetic procedure was elaborated schematically (**Scheme 1**). Required amount of gold and palladium precursors were mixed with α-naphthol ethanol solution and sodium borohydride at moderate temperature followed by aging for a very short span. The oxygen ligand in the α-naphthol coordinates with Au (III) and form metal complex. The π-π interactions between the rings in the α naphthol may lead to self-assembly of complexes in to one dimensional gold wires [59]. Therefore, α-naphthol functioned as coordination agent, reducing agent and structural directing agent simultaneously. By varying the quantity of precursors, 5, 10, 15% Pd containing Au rich PdAu nano wires were prepared, which are designated as 5% PdAu NW, 10% PdAu NW, and 15% PdAu NW, respectively. Pure Pd nanoparticle catalyst was prepared by the reduction of Pd precursor using $NaBH_4$ reducing agent, for the comparative analysis of the catalytic activity of prepared PdAu NW catalyst. The compositions of the prepared samples were analyzed using SEM-EDS (**Fig. S1**).

2.3. Materials characterization

X-ray diffraction pattern was collected using X-ray diffractometer (XRD), (Philips X'pert Pro) equipped with Cu Kα (λ = 0.154060 nm) radiation over 2θ ranging from 10 to 90° with a step size of 0.08°. The microstructures of the prepared samples were examined by Transmission Electron Microscopy (TEM). X-ray photoelectron study was conducted on X- ray photoelectron spectrometer (XPS), (PHI 5000 Versa Probe II). The obtained spectra

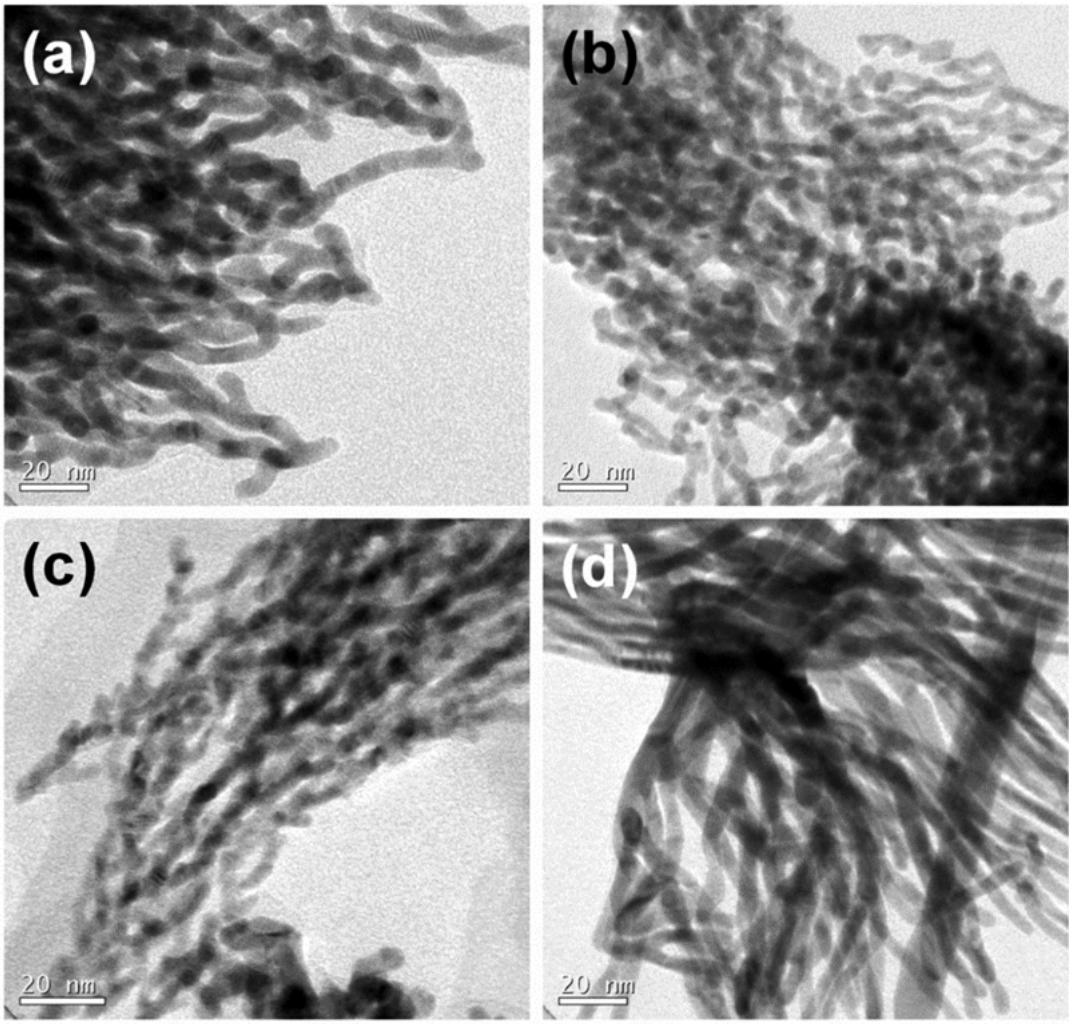

Fig. 1. TEM images of (a) 5%PdAu NW, (b) 10%PdAu NW, (c) 15%PdAu NW, (d) Au NW.

were referenced to the C 1 s binding energy of 284.8 eV. The oxidation states of the metal in the sample were analyzed using XPS.

2.4. Electrochemical measurements

The electrochemical work station Autolab (M204) was utilized to perform the electrochemical measurements. In a standard three electrode system a catalyst modified glassy carbon electrode, a double junction Ag/AgCl electrode and a platinum wire were served as the working, reference and counter electrode respectively. Catalyst ink prepared by dispersing the catalyst in distilled water, were dropped on the cleaned glassy carbon electrode surface. Subsequently added 3 µl 0.5 wt% Nafion solutions using a micropipette. The catalyst loading was 0.225 mg/cm^2. Cyclic voltamograms were recorded in N_2 saturated 0.5 M KOH solution at scan rate of 50 mV/s. CVs of Methanol Oxidation Reaction (MOR) and Ethanol Oxidation Reaction (EOR) were obtained in N_2 saturated 0.5 M KOH solution containing 0.5 M methanol and ethanol respectively at a scan rate of 50 mV/s.

3. Results and discussions

Morphology of the prepared catalysts monitored by TEM and depicted in **Fig. 1**, showing well defined uniform wires having the diameter of ~ 5 nm, and length up to several hundreds of nanometers. Thus, the as synthesized nano wires possess high aspect ratio. Higher resolution images presented in **Fig. S2,** shows crystalline lattice fringes in 10% PdAu NW. The interplanar spacing has also been calculated and indexed (**Fig. S2**c). The lattice spacing calculated for the prepared PdAu nanowires is 0.232 nm, which is observed in between the Pd (111) lattice spacing (0.225 nm) and Au (111) lattice spacing (0.236 nm). The result indicates the PdAu alloy formation [50,51,60]. The higher resolution images of 5% PdAu NW and 15% PdAu NW are depicted in **Fig. S3** and **S4** the values of inter planar spacing are also indexed. **Fig. S5** shows the TEM images of highly interconnected pure Pd nanoparticles with an average particle size ~20 nm.

Phase purity of the prepared catalysts has been examined using X-ray diffractometer, and the obtained pattern is depicted in **Fig. 2**. The peaks observed for pure Pd are well matched with the standard cubic structure of Pd (JCPDS 46–1043). The diffraction peaks at 2θ, 40.33°, 46.93°, 68.29°, 82.27°, and 86.92° are corresponding to (111), (200), (220), (311), (222) planes of Pd. Au shows peaks at 38.56°, 44.76°, 64.92°, 77.87°, and 82.06° which are ascribed to the (111), (200), (220), (311), (222) miller planes of cubic Au structure (04–0784) [52]. As shown in the **Fig. 2a**, Pd incorporated Au nano wires exhibited a shift in XRD peaks to lower diffraction angle from that of Au and Pd. The observation clearly designates the successful formation of PdAu alloy NW and suggests an expansion in the lattice parameters. However, the extent of lattice expansion tend to decrease on varying the alloy composition from 5, 10 and 15 wt%, since the diffraction peaks have shifted to higher 2θ an-

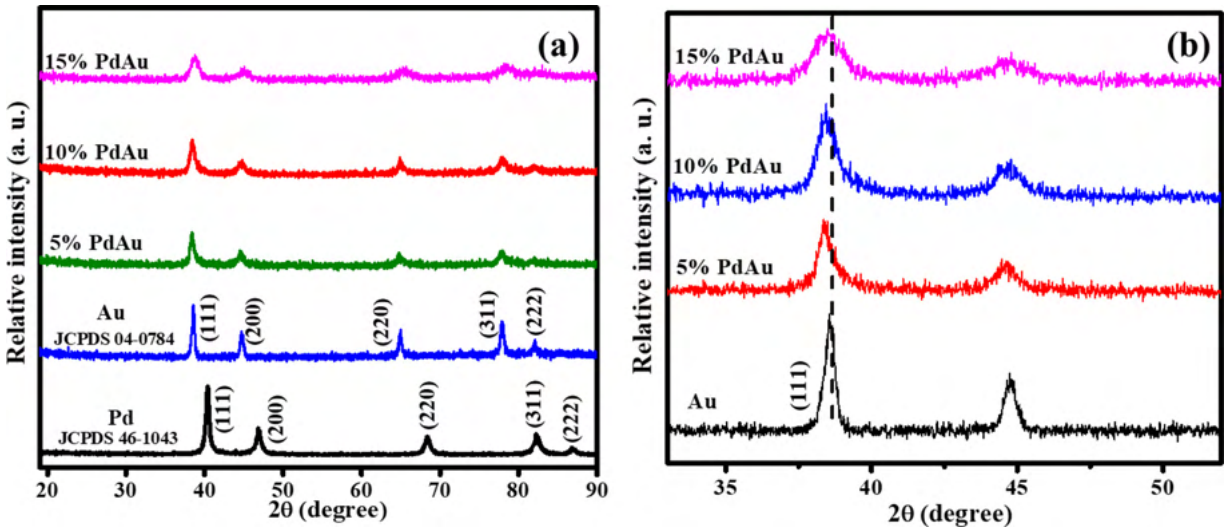

Fig. 2. XRD pattern of (a) PdAu catalysts, Pd and Au, (b) shift in (111) lattice plane of alloys from that of Au.

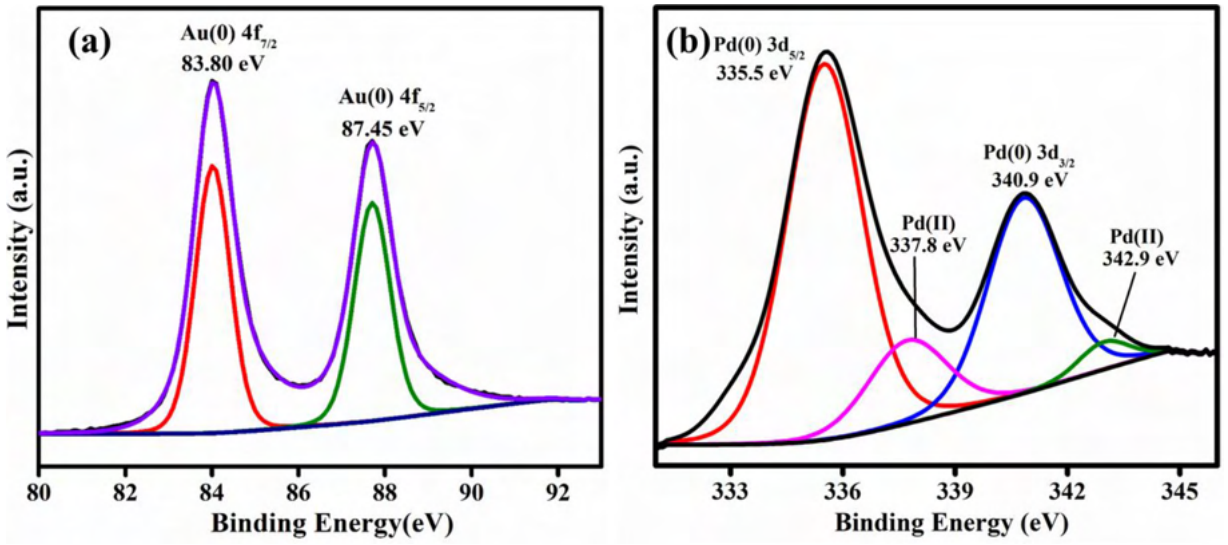

Fig. 3. High resolution XPS spectra of (a) Au 4f and (b) Pd 3d in 10% PdAu NW.

gle, Fig. 2**b**. Moreover, crystallinity of the prepared NW catalysts found to decrease from that of pure Pd and Au, understood from the decrease in diffraction peak intensity and increase in FWHM. The calculated crystallite size using Scherrer formula of each alloy compounds are 16.64, 14.49 and 11.97 nm for 5, 10 and 15 wt% PdAu NWs, respectively. Further, based on Vegard's law alloying degree of the prepared catalysts have calculated to be 6.4, 12.6 and 17.2% for 5, 10 and 15 wt% PdAu NWs, respectively [61,62].

The surface chemical composition and oxidation states of the elements present in the developed PdAu NW catalyst are determined by conducting X- ray photoelectron spectroscopy measurements, which is also helping to understand the existence of Pd and Au. Fig. 3**a** and 3**b** display the deconvoluted spectra of Au and Pd, respectively. The binding energy values at 84.0 and 87.7 eV, as illustrated in Fig. 3**a,** assigned to Au $4f_{7/2}$ and $4f_{5/2}$ states of indicative of Au(0). As exposed in Fig. 3**b**, Pd deconvoluted spectra has been fitted to four peaks. The peaks located at binding energies 335.6, 340.9 eV attributed to Pd $3d_{5/2}$, $3d_{3/2}$ corresponds to Pd(0). The small peaks at 337.8 and 343.1 eV assigned to Pd^{2+} [63]. The small shift in the binding energy values from the reported values of pure Pd (335.0 and 340.3 eV) and Au (83.8 and 87.4 eV) implies a strong electronic modification between the metals Pd and Au [48,64]. Thus the alloy formation is confirmed from the XPS technology.

The electrochemical properties of the samples are studied using cyclic voltammetry**.** Fig. 4**a** represents the respective CV curves recorded in N_2 saturated 0.5 M KOH solution at a scan rate of 50 mV/s. The potential range −0.8 to −0.4 V in the forward scan correspond to hydrogen adsorption and oxidation of Pd to PdO was observed at higher positive potential range. Further, reduction of PdO in the backward scan potential range −0.1 to −0.6 V resulted in the regeneration of Pd. [65,66] The parameter associated with the active sites of the catalysts, electrochemical active surface area (ECSA) is calculated by integrating the charge required for the reduction of PdO. ECSA estimated using the equation,

$$\mathrm{ECSA} = \frac{Q}{0.405 \times l}$$

Where 'Q' represents the PdO reduction charge and 'l' indicates the catalyst loading. The value of charge is assumed to be 0.405 mC /cm^2 for the PdO monolayer reduction [67]. The ECSA for the catalysts 5, 10, 15% PdAu NW and pure Pd are calculated to be 74.8, 115.7, 96.8 and 11.2 m^2/g, respectively. The unique morphology attributed to the improved ECSA. The one-dimensional wire

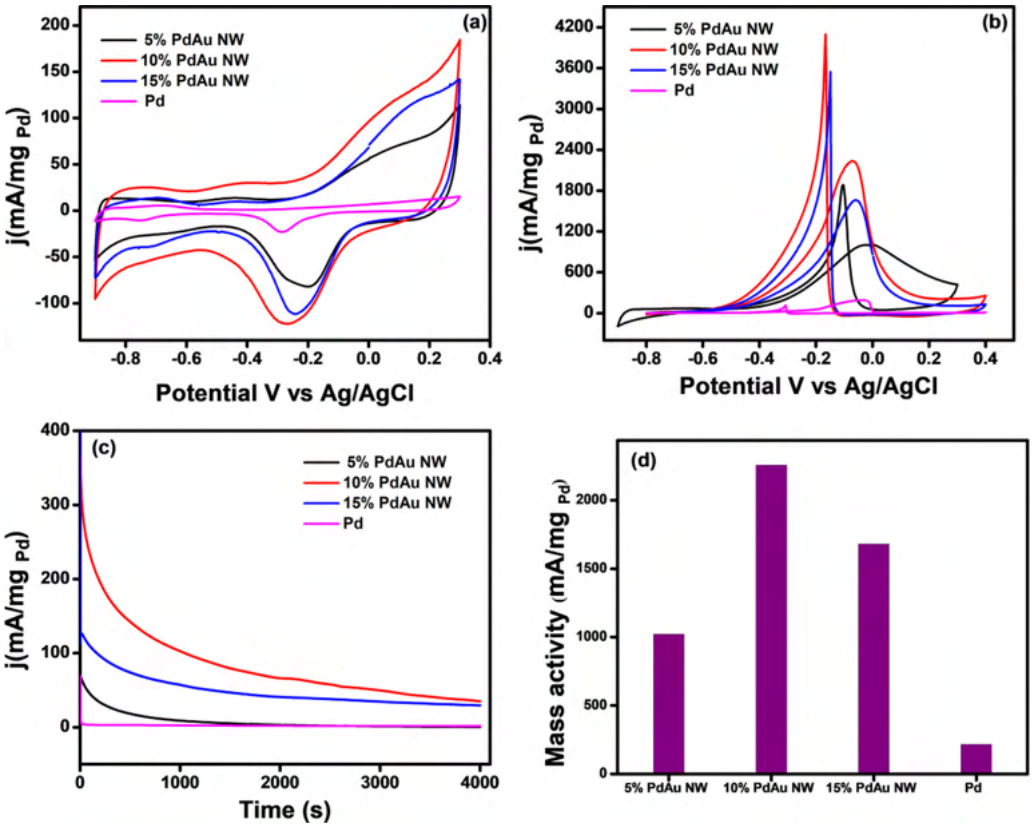

Fig. 4. CV curves of (a) prepared samples and Pd catalyst in N_2 saturated 0.5 M KOH at a scan rate of 50 mV/s. (b) prepared samples and Pd catalyst in N_2 saturated 0.5 M KOH and 0.5 M CH_3OH solution at a scan rate of 50 mV/s. (c) Chronoamperometric curves of prepared samples and Pd catalyst in N_2 saturated 0.5 M KOH + 0.5 M CH_3OH solution. (d) MAs of as prepared samples and Pd catalyst.

Table 1
Onset potential and Mass activity data of the synthesized catalysts.

Catalyst	Onset potential (V)	Mass Activity (mA/mg $_{Pd}$)
5% PdAu NW	−0.41	1021.4
10% PdAu NW	−0.44	2253.3
15% PdAu NW	−0.42	1681.2
Pd	−0.38	193.4

type morphologies usually provide more active sites to take part. The remarkably higher activity of 10%PdAu NW is evident from the ECSA.

Electrocatalytic activity of the prepared catalysts towards methanol oxidation is evaluated by performing the CV in N_2 saturated solution containing 0.5 M KOH and 0.5 M methanol at a scan rate of 50 mV/s. Typical cyclic voltammograms of different Pd Au NW catalysts are depicted in **Fig. 4b**. Mass activities obtained for the catalysts are tabulated in **Table 1**. Even though all the prepared catalysts imparted improved activity than the pure Pd, 10 wt% PdAu NW showed superior catalytic activity than others in terms of onset as well as peak potential and mass activity. Ten times increment in the mass activity is observed even after reducing the amount of Pd to 90% (**Fig. 4d**). Bifunctional effects of Pd and Au along with the one-dimensional morphology of the catalyst could be attributed to the considerable enhancement in the activity of the catalyst. The problem of carbon corrosion can be eliminated. The 1D morphology reduces the aggregation, dissolution and Ostwald ripening of Pd particles and improves the activity of Pd. The anisotropic morphology also imparts better electronic transportation which in turn increases the performance.

The mechanism of methanol oxidation is given below [68,69]. The outstanding catalytic property of gold towards CO oxidation significantly helped to remove the CO molecules adsorbed on the Pd surface there by facilitating the reaction kinetics. The CO tolerance of Pd gets enhanced by the presence of Au. The released active sites have been proceeded further via the following reactions.

$$Pd + CH_3OH \rightarrow Pd\text{-}(CH_3OH)_{ads} \quad (1)$$

$$Pd\text{-}(CH_3OH)_{ads} \rightarrow Pd\text{-}(CO)_{ads} + 4H^+ + 4e \quad (2)$$

$$Au + H_2O \rightarrow Au\text{-}OH_{ads} + H^+ + e^- \quad (3)$$

$$Pd\text{-}(CO)_{ads} + Au\text{-}OH_{ads} \rightarrow Pd + Au + CO_2 + H^+ + e^- \quad (4)$$

Stability studies of the prepared catalyst are done by Chronoamperometric measurements at a potential of −0.4 V for 4000 s in an N_2 saturated solution containing 0.5 M KOH and 0.5 M methanol. Due to the formation of the intermediate CO, current value decreases after some times. As shown in **Fig. 4c** the slow decay value indicates the 10 wt% PdAu NW possesses a better stability than the other catalysts for methanol oxidation. Stability studies are further conducted by performing the cyclic voltammetry analysis for 500 cycles. **Fig. 5** depicts the corresponding cyclic voltammograms. Decay rate of current in the case of 10% PdAu NW catalyst is better than that of pure Pd. In the case of 10% PdAu NW the initial current value 2253.34 mA/mg_{Pd} reached 1753.48 mA/mg_{Pd} whereas for pure Pd the current value 193.4 mA/mg_{Pd} reduced to 99.86 mA/mg_{Pd}, almost half of the initial value. The onset potential for 10% PdAu NW is deviated by less extent −0.39 V to −0.37 V. For pure Pd the onset potential shifted

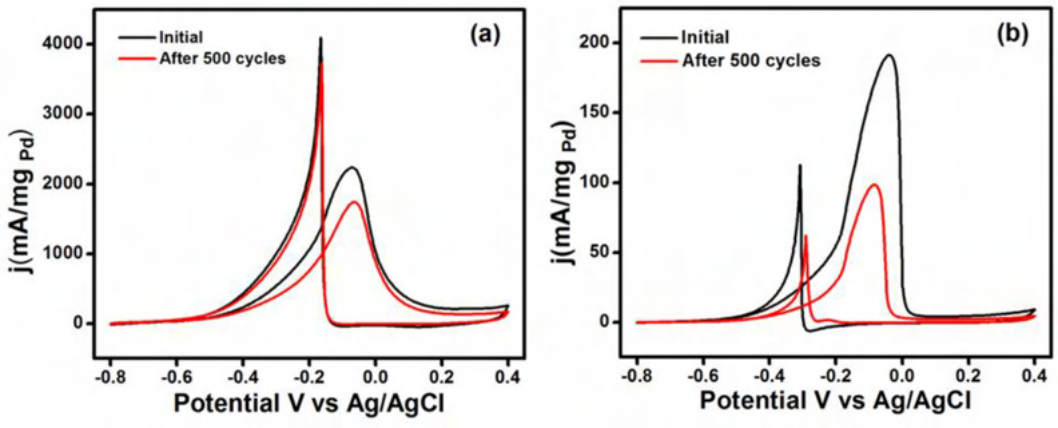

Fig. 5. CV curves of (a) 10%PdAu NW after 500 cycles in N_2 saturated 0.5 M KOH + 0.5 M CH_3OH solution, (b) Pd catalyst after 500 cycles in N_2 saturated 0.5 M KOH + 0.5 M CH_3OH solution.

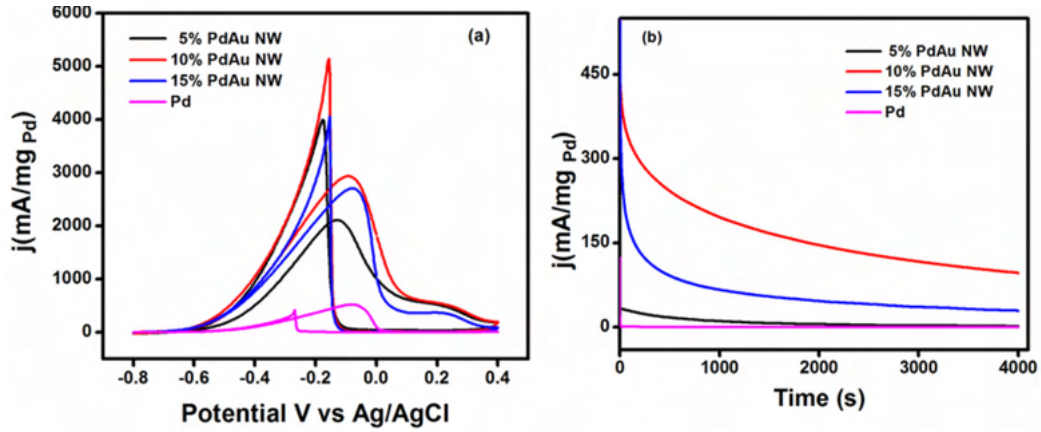

Fig. 6. (a) CV curves of prepared samples and Pd catalyst in N_2 saturated 0.5 M KOH + 0.5 M C_2H_5OH solution, (b) Chronoamperometric curves of prepared samples and Pd catalyst in N_2 saturated 0.5 M KOH + 0.5 M C_2H_5OH solution.

from −0.38 to −0.31 V. A higher deviation has been observed in the case of pure Pd.

The catalytic activity towards electro oxidation of ethanol has also been carried out in an N_2 saturated solution containing 0.5 M KOH and 0.5 M ethanol at a scan rate of 50 mV/s. Similar results are observed in this case also. Developed PdAu NW catalysts exhibited increased activity than that of the pure Pd catalyst. Among them 10 wt% PdAu NW showed supreme catalytic activity than others. A mass activity of 2137.9, 2960.40, 2724.4 mA/mg_{Pd} are obtained for 5, 10, 15% PdAu NWs, respectively, and the activity for pure Pd is calculated to be 522.8 mA/mg. The respective CV curves are depicted in **Fig. 6a**. Chronoamperometric measurements performed at a potential of −0.4 V for 4000 s in an N_2 saturated solution containing 0.5 M KOH and 0.5 M ethanol (**Fig. 6b)** reveals the stability of the catalyst 10% PdAu NWs.

Stability studies are further confirmed by performing the cyclic voltammetry analysis for 500 cycles (**Fig. 7**). There is not that much reduction in current value and change in onset potential in the case of 10% PdAu catalyst. The current value 2960.40 mA/mg_{Pd} reached 2548.88 mA/mg_{Pd} and onset potential remained 0.51 V. But for Pd the current value reached almost half of the initial value and the onset potential also shifted to higher value. The initial current value 522.8 mA/mg_{Pd} reduced to 274.74 mA/mg_{Pd} and onset potential deviated from −0.52 to −0.45 V. Thus, stability of the 10% PdAu NW catalyst has been confirmed.

Table 2 displays the catalytic activity of various Pt and PdAu catalysts towards alcohol oxidation. The as synthesized NW catalyst exhibited better activity than that of other different PdAu catalysts [70–78]. The tabulated results on analysis clearly marks that the combination of Pd and Au metals with NW morphology could substantially improve the catalytic activity of Pd due to the superior CO tolerance of Au.

One dimensional nano wire with ultrathin diameter and high aspect ratio greatly influenced the catalytic activity. The prepared PdAu NWs have exhibited superior activity than that of pure Pd. The properties associated with the characteristic structure helped to enhance the performance. Blending Au with Pd would facilitate the catalytic activity of Pd. Release of the intermediate CO from active sites of Pd due to the presence of Au can enhance the kinetics of methanol oxidation. Experiments performed revealed the superior catalytic performance of 10% PdAu NWs towards methanol as well as ethanol electro-oxidation. The catalyst is able to perform ten times better activity towards methanol and six times higher activity towards ethanol than pure Pd even by reducing the amount of Pd to 90%. Bifunctional effects of Pd and Au along with the one-dimensional morphology of the synthesized catalyst attributed to the increased catalytic activity towards alcohol oxidation. Alloying of Pd with Au may boost up the kinetic reaction towards the intermediate poison, leading to an enhanced poison tolerance. The unique one-dimensional structure reduces the agglomeration and dissolution of particles and provides large surface area. The improved electron transport characteristics due to the structural anisotropy have facilitated the catalytic efficiency.

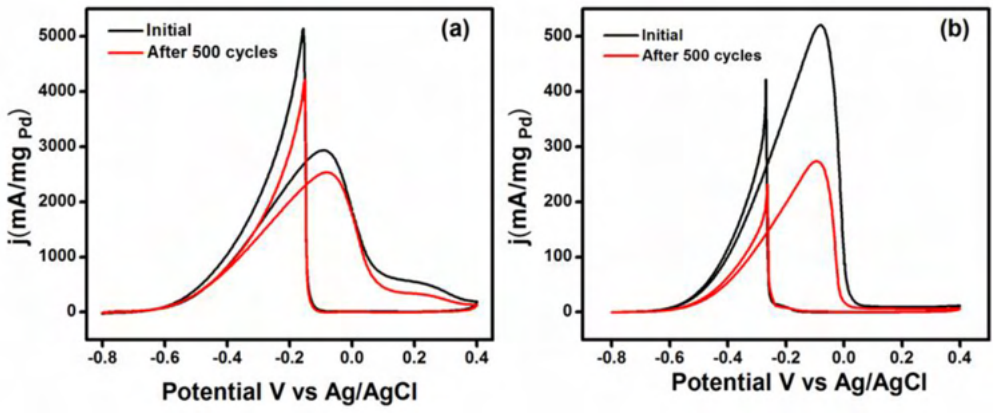

Fig. 7. CV curves of (a) 10%PdAu NW after 500 cycles in N_2 saturated 0.5 M KOH + 0.5 M C_2H_5OH solution (b) Pd catalyst after 500 cycles in N_2 saturated 0.5 M KOH + 0.5 M C_2H_5OH solution.

Table 2
Mass activity values of different PdAu catalysts.

Catalysts	Electrolyte	Mass activity (mA /mg $_{Pd/Pt}$)	Reference
Pd_2Au-180	1 M NaOH + 1 M Methanol	491.84	48
$Pd_{90}Au_{10}$	1 M KOH + 1 M Ethanol	1050.00	49
PdAu/C	0.5 M KOH + 0.5 M Ethanol	1700.00	70
Pd_5Au_1	1 M KOH + 1 M Ethanol	1739.93	56
Au@Pd/fuv-MWCNTs	0.5 M KOH + 2 M Methanol	785.70	71
NP- PdAu	0.5 M KOH + 1 M Methanol	866.5	72
$Pd_{30}Au_{70}$/C	1 M KOH + 1 M Methanol	950.6	73
PtNi/ceria	0.1 M $HClO_4$ + 0.5 M Methanol	1500.00	74
PtCo CNC	0.5 M H_2SO_4 + 1.0 M Methanol	692.00	75
Ru/Pt NWs	0.1 M $HClO_4$ + 1 M Methanol	570.00	76
3PtSn/C	0.5 M H_2SO_4 + 2 M Methanol	56.70	77
PtRu NWs	0.1 M $HClO_4$ + 0.5 M Methanol	820.00	78
10%PdAu NW	0.5 M KOH + 0.5 M Methanol	2256.9	This work
10%PdAu NW	0.5 M KOH + 0.5 M Ethanol	2932.5	This work

4. Conclusions

Au rich PdAu nano wires with different compositions were prepared by simple and speedy method. Well defined ultrathin nano wire morphology was analyzed by TEM analysis. The XRD and XPS analysis was employed to examine the incorporation of Pd and Au. The synthesized catalysts exhibited excellent catalytic activity and stability towards methanol and ethanol oxidation. The catalytic performance shown by 10% Pd incorporated Au wire was superior to other catalysts and pure Pd catalyst. The efficiency of the catalyst enhanced significantly even by reducing the amount of Pd to 90% owing to the unique structural features and bifunctional effects between Au and Pd. Ten times increase in the mass activity towards methanol and six times increment in the mass activity towards ethanol was observed.

Declaration of Competing Interest

None.

Credit authorship contribution statement

Roshima Kottayintavida: Formal analysis, Writing – original draft.

Acknowledgement

We gratefully acknowledge DST- Science & Engineering Research Board (SERB), Government of India (Grant No: EEQ //2016/000342) for financial support. Roshima K acknowledges CSIR, New Delhi for the award of Senior Research Fellowship.

Supplementary materials

Supplementary material associated with this article can be found, in the online version, at doi:10.1016/j.electacta.2021.138405.

References

[1] B.Y. Xia, H.B. Wu, X. Wang, X. Wen (David) Lou, One-pot synthesis of cubic $PtCu_3$ nano cages with enhanced electro catalytic activity for the methanol oxidation reaction, J. Am. Chem. Soc. 134 (34) (2012) 13934–13937, doi:10.1021/ja3051662.
[2] Z.Y. Shih, C.W. Wang, G. Xu, H.T. Chang, Porous palladium copper nanoparticles for the electro catalytic oxidation of methanol in direct methanol fuel cells, J. Mater. Chem. A (1) (2013) 4773–4778 https://doi.org /, doi:10.1039/C3TA01664A.
[3] C. Qiu, R. Shang, Y. Xie, Y. Bu, C. Li, H. Ma, Electro catalytic activity of bimetallic Pd-Ni thin films towards the oxidation of methanol and ethanol, Mater. Chem. Phys. 120 (23) (2010) 323–330, doi:10.1016/j.matchemphys.2009.11.014.
[4] H. Mao, T. Huang, A. Yu, Surface palladium rich CuxPdy/carbon catalysts for methanol and ethanol oxidation in alkaline media, Electrochim. Acta 174 (2015) 1–7, doi:10.1016/j.electacta.2015.05.160.
[5] Y. Zhang, F. Gao, C. Wang, Y. Shiraishi, Y. Du, Engineering spiny PtFePd@PtFe/Pt Core@multishell nanowires with enhanced performance for alcohols electrooxidation, ACS Appl. Mater. Interfaces 11 (34) (2019) 30880–30886, doi:10.1021/acsami.9b09110.
[6] K.G. Nishanth, P. Sridhar, S. Pitchumani, A.K. Shukla, A DMFC with methanol-tolerant-carbon-supported-pt-pd-alloy cathode, J. Electrochem. Soc. 158 (8) (2011) B871 –, doi:10.1149/1.3596542.
[7] Z. Qi, H. Geng, X. Wang, C. Zhao, H. Ji, C. Zhang, Z. Zhang, Novel nanocrystalline PdNi alloy catalyst for methanol and ethanol electro-oxidation in alkaline media, J. Power Sources 196 (14) (2011) 5823–5828, doi:10.1016/j.jpowsour.2011.02.083.
[8] Y. Zhao, X. Yang, J. Tian, F. Wang, L. Zhan, Methanol electro-oxidation on Ni@Pd core-shell nanoparticles supported on multi-walled carbon nanotubes in alkaline media, Int. J. Hydrog. Energy 35 (8) (2010) 3249–3257, doi:10.1016/j.ijhydene.2010.01.112.
[9] K.G. Nishanth, P. Sridhar, S. Pitchumani, Carbon-supported Pt encapsulated Pd nanostructure as methanol-tolerant oxygen reduction electro-catalyst, Int. J.

Hydrog. Energy 38 (1) (2013) 612–619 https://doi:, doi:10.1016/j.ijhydene.2012.06.116.
[10] Z. Chen, Y.C. He, J.H. Chen, X.Z. Fu, R. Sun, Y.X. Chen, C.P. Wong, PdCu alloy flower-like nano cages with high electro catalytic performance for methanol oxidation, J. Phys. Chem. C 122 (16) (2018) 8976–8983, doi:10.1021/acs.jpcc.8b01095.
[11] Z. Yang, S. Wang, J. Wang, et al., Pd supported on carbon containing nickel, nitrogen and sulfur for ethanol electro oxidation, Sci. Rep. 7 (2017) 15479, doi:10.1038/s41598-017-15060-x.
[12] R.S. Amin, R.M. Abdel Hameed, K.M. El-Khatib, M. Elsayed Youssef, Electrocatalytic activity of nanostructured Ni and Pd-Ni on Vulcan XC-72R carbon black for methanol oxidation in alkaline medium, Int. J. Hydrog. Energy 39 (5) (2014) 2026–2041, doi:10.1016/j.ijhydene.2013.11.033.
[13] B. Habibi, S. Mohammadyari, Facile synthesis of Pd nanoparticles on nano carbon supports and their application as an electrocatalyst for oxidation of ethanol in alkaline media: the effect of support, Int. J. Hydrog. Energy 40 (34) (2015) 10833–10846, doi:10.1016/j.ijhydene.2015.07.021.
[14] J.C. Calderón, M.J. Nieto-Monge, S. Pérez-Rodríguez, J.I. Pardo, R. Moliner, M.J. Lázaro, Palladium-nickel catalysts supported on different chemically-treated carbon blacks for methanol oxidation in alkaline media, Int. J. Hydrog. Energy 41 (43) (2016) 19556–19569, doi:10.1016/j.ijhydene.2016.07.121.
[15] J.L. Tan, A.M. De Jesus, S.L. Chua, J. Sanetuntikul, S. Shanmugam, B.J.V. Tongol, H. Kim, Preparation and characterization of palladium-nickel on graphene oxide support as anode catalyst for alkaline direct ethanol fuel cell, Appl. Catal. A Gen. 531 (2017) 29–35, doi:10.1016/j.apcata.2016.11.034.
[16] Y. Wang, X. Wang, C.M. Li, Electrocatalysis of Pd-Co supported on carbon black or ball-milled carbon nano tubes towards methanol oxidation in alkaline media, Appl. Catal. B Environ. 99 (1–2) (2010) 229–234, doi:10.1016/j.apcatb.2010.06.024.
[17] L.M. Luo, R.H. Zhang, D. Chen, Q.Y. Hu, X.W. Zhou, Synthesis of 3D thornbush-like trimetallic CoAuPd nanocatalysts and electrochemical dealloying for methanol oxidation and oxygen reduction reaction, ACS Appl. Energy Mater. 1 (6) (2018) 2619–2629, doi:10.1021/acsaem.8b00329.
[18] L. Yang, Y. Tang, D. Yan, T. Liu, C. Liu, S. Luo, Polyaniline-reduced graphene oxide hybrid nanosheets with nearly vertical orientation anchoring palladium nanoparticles for highly active and stable electrocatalysis, ACS Appl. Mater. Interfaces 8 (1) (2016) 169–176, doi:10.1021/acsami.5b08022.
[19] R. Kottayintavida, N.K. Gopalan, Nickel phosphate modified carbon supported Pd catalyst for enhanced alcohol electro oxidation, Int. J. Hydrog. Energy 45 (2020) 11116–11126, doi:10.1016/j.ijhydene.2020.02.050.
[20] M. Kübler, T. Jurzinsky, D. Ziegenbalg, C. Cremers, Methanol oxidation reaction on core-shell structured ruthenium-palladium nanoparticles: relationship between structure and electrochemical behavior, J. Power Sources 375 (2018) 320–334, doi:10.1039/C7TA07879J.
[21] W. Chen, Y. Zhang, X. Wei, Catalytic performances of PdNi/MWCNT for electrooxidations of methanol and ethanol in alkaline media, Int. J. Hydrog. Energy 40 (2) (2015) 1154–1162, doi:10.1016/j.ijhydene.2014.11.069.
[22] L.L. Carvalho, F. Colmati, A.A. Tanaka, Nickel-palladium electrocatalysts for methanol, ethanol, and glycerol oxidation reactions, Int. J. Hydrog. Energy 42 (25) (2017) 16118–16126, doi:10.1016/j.electacta.2012.08.080.
[23] J. Liujun, S. Hongyuan, S. Tongxin, G. Fei, Z. Yangping, W. Caiqin, W. Cheng, D. Yukou, Monodispersed bimetallic platinum-copper alloy nanospheres as efficient catalysts for ethylene glycol electrooxidation, J. Colloid Interface Sci. 551 (2019) 81–88 https://doi:, doi:10.1016/j.jcis.2019.04.097.
[24] F. Han, J. Xia, X. Zhang, Y. Fu, PdAu alloy nanoparticles supported on nitrogen-doped carbon black as highly active catalysts for Ullmann coupling and nitrophenol hydrogenation reactions, RSC Adv 9 (2019) 17812–17823, doi:10.1039/C9RA01685F.
[25] L. Wang, Y. Nemoto, Y. Yamauchi, Direct synthesis of spatially-controlled Pt-on-Pd bimetallic nanodendrites with superior electrocatalytic activity, J. Am. Chem. Soc. 133 (25) (2011) 9674–9677, doi:10.1021/ja202655j.
[26] J. Sheng, J. Kang, H. Ye, J. Xie, B. Zhao, X.-Z. Fu, C.-P. Wong, Porous octahedral PdCu nanocages as highly efficient electrocatalysts for the methanol oxidation reaction, J. Mater. Chem. A 6 (2018) 3906–3912, doi:10.1039/C7TA07879J.
[27] J. Sheng, J. Kang, Z. Hu, Y. Yu, X.-Z. Fu, R. Sun, C.-P. Wong, Octahedral Pd nano cages with porous shells converted from Co $(OH)_2$ nano cages with nano sheet surfaces as robust electrocatalysts for ethanol oxidation, J. Mater. Chem. A 6 (2018) 15789–15796, doi:10.1039/C8TA05000G.
[29] F. Han, C. Hu, X. Zhang, C. Jing, T. Hu, X. Yang, Mechanistic insights into the catalytic reduction of nitrophenols on noble metal nanoparticles/N-doped carbon black composites, Compos. Commun. 23 (2021) 100580 https://doi:, doi:10.1016/j.coco.2020.100580.
[28] Y. Hu, P. Wu, H. Zhang, C. Cai, Synthesis of graphene-supported hollow Pt–Ni nanocatalysts for highly active electrocatalysis toward the methanol oxidation reaction, Electrochim. Acta 85 (2012) 314–321, doi:10.1016/j.electacta.2012.08.080.
[30] C.M. Sánchez-Sánchez, J. Solla-Gullón, F.J. Vidal-Iglesias, A. Aldaz, V. Montiel, E. Herrero, Imaging structure sensitive catalysis on different shape-controlled platinum nanoparticles, J. Am. Chem. Soc 132 (16) (2010) 5622–5624, doi:10.1021/ja100922h.
[31] W. Hong, J. Wang, E.D Wang, Au/Pt and Au/PtCu Nanowires with enhanced electro catalytic activity for methanol electro oxidation, Small 10 (16) (2014) 3262–3265, doi:10.1002/smll.201400059.
[32] Y. Yin, Yu Lu, Y. Sun, Y. Xia, Silver nanowires can be directly coated with amorphous silica to generate well-controlled coaxial nanocables of silver/silica, Nano Lett. 2 (4) (2002) 427–430, doi:10.1021/nl025508.
[33] Y. Feng, L. Bu, S. Guo, J. Guo, X. Huang, 3D platinum-lead nanowire networks as highly efficient ethylene glycol oxidation electrocatalysts, Small 12 (33) (2016) 4464–4470, doi:10.1002/smll.201601620.
[34] H. Xu, J. Wei, M. Zhang, C. Wang, Y. Shiraishi, J. Guo, Y. Du, Solvent-mediated length tuning of ultrathin platinum–cobalt nanowires for efficient electrocatalysis, J. Mater. Chem. A 6 (2018) 24418–24424 https://doi:, doi:10.1039/c8ta08251k.
[35] Y. Lu, S. Du, R. Steinberger-Wilckens, One-dimensional nanostructured electrocatalysts for polymer electrolyte membrane fuel cells—a review, Appl. Catal. B Environ 199 (2016) 292–314, doi:10.1016/j.apcatb.2016.06.022.
[36] H. Falsig, B. Hvolbæk, I.S. Kristensen, T. Jiang, T. Bligaard, C.H. Christensen, J.K. Nørskov, Trends in the catalytic CO oxidation activity of nanoparticles, Angew. Chem. Int. Ed. 47 (26) (2008) 4835–4839, doi:10.1002/anie.200801479.
[37] C. Xu, J. Su, X. Xu, P. Liu, H. Zhao, F. Tian, Y. Ding, Low temperature CO oxidation over unsupported nanoporous gold, J. Am. Chem. Soc. 129 (1) (2007) 42–43, doi:10.1021/ja0675503.
[38] P. Song, S.-S. Li, L.-L. He, J.-J. Feng, L. Wu, S.-X. Zhong, A.-J. Wang, Facile large-scale synthesis of Au–Pt alloyed nanowire networks as efficient electrocatalysts for methanol oxidation and oxygen reduction reactions, RSC Adv. 5 (2015) 87061–87068, doi:10.1039/C5RA18133J.
[39] J. Luo, P.N. Njoki, Y. Lin, D. Mott, C.-J. Wang, Zhong, Characterization of carbon-supported AUPT nanoparticles for electrocatalytic methanol oxidation reaction, Langmuir 22 (6) (2006) 2892–2898, doi:10.1021/la0529557.
[40] A.A. Vega, R.C. Newman, Methanol electro-oxidation on nanoporous metals formed by dealloying of Ag–Au–Pt alloys, J.Appl. Electrochem. 46 (9) (2016) 995–1010, doi:10.1007/s10800-016-0978-5.
[41] M. Graf, M. Haensch, J. Carstens, G. Wittstock, J. Weissmüller, Electrocatalytic methanol oxidation with nanoporous gold: microstructure and selectivity, Nanoscale 9 (2017) 17839–17848, doi:10.1039/C7NR05124G.
[42] P. Rodriguez, Y. Kwon, M.T.M Koper, The promoting effect of adsorbed carbon monoxide on the oxidation of alcohols on a gold catalyst, Nat. Chem. 4 (3) (2011) 177–182, doi:10.1038/nchem.1221.
[43] B.B. Blizanac, M. Arenz, P.N. Ross, N.M. Marković, Surface electrochemistry of CO on reconstructed gold single crystal surfaces studied by infrared reflection absorption spectroscopy and rotating disk electrode, J. Am. Chem. Soc. 126 (32) (2004) 10130–10141, doi:10.1021/ja049038s.
[44] Y. Lu, J. Tu, C. Gu, X. Xia, X. Wang, S.X. Mao, Growth of and methanol electrooxidation by gold nanowires with high density stacking faults, J. Mater. Chem. 2011 (21) (2011) 4843–4849, doi:10.1039/C0JM04083E.
[45] P. Rodríguez, A.A. Koverga, M.T.M Koper, Carbon monoxide as a promoter for its own oxidation on a gold electrode, Angew. Chem. Int. Ed. 49 (7) (2010) 1241–1243, doi:10.1002/ange.200905387.
[46] N. Zanganeh, V.K. Guda, H. Toghiani, J.M. Keith, Sinter-resistant and highly active Sub-5nm Bimetallic Au–Cu nanoparticle catalysts encapsulated in silica for high-temperature carbon monoxide oxidation, ACS Appl. Mater. Interfaces 10 (5) (2018) 4776–4785, doi:10.1021/acsami.7b19299.
[47] C. Wang, Ke Zhang, H. Xu, Y. Du, M. Cynthia Goh, Anchoring Gold Nanoparticles on Poly(3,4-ethylenedioxythiophene) (PEDOT) Nanonet as Three-dimensional Electrocatalysts toward Ethanol and 2-propanol Oxidation, J. Colloid Interface Sci. 541 (2019) 258–268 https://doi:, doi:10.1016/j.jcis.2019.01.055.
[48] L.-M. Luo, R.-H. Zhang, D. Chen, Q.-Y. Hu, X. Zhang, C.-Y. Yang, X.-W. Zhou, Hydrothermal synthesis of Pd Aunanocatalysts with variable atom ratio for methanol oxidation, Electrochim. Acta 259 (2018) 284–292, doi:10.1016/j.electacta.2017.10.177.
[49] A. Caglar, H. Kivrak, Highly active carbon nanotube supported PdAu alloy catalysts for ethanol electrooxidation in alkaline environment, Int. J. Hydrogen Energy 44 (2019) 11734–11743, doi:10.1016/j.ijhydene.2019.03.118.
[50] W. Yang, Q. Zhang, C. Peng, E. Wu, S. Chen, Y. Ma, L. Deng, Au@PdAg core–shell nanotubes as advanced electrocatalysts for methanol electrooxidation in alkaline media, RSC Adv 9 (2019) 931–939, doi:10.1039/C8RA08781D.
[51] E. Wu, Q. Zhang, A. Xie, W. Yang, C. Peng, J. Hou, L. Deng, Synthesis of hollow echinus-like Au@PdAgNSs decorated reduced graphene oxide as an excellent electrocatalyst for enhanced ethanol electrooxidation, J. Alloys Compd. 789 (2019) 174–182, doi:10.1016/j.jallcom.2019.03.086.
[52] C. Liu, X. Cai, J. Wang, J. Liu, A. Riese, Z. Chen, S.-D. Wang, One-step synthesis of AuPd alloy nanoparticles on graphene as a stable catalyst for ethanol electro-oxidation, Int. J. Hydrogen Energy 41 (31) (2016) 13476–13484, doi:10.1016/j.ijhydene.2016.05.194.
[53] H.-Y. Chen, A.-J. Wang, L. Zhang, J. Yuan, Q.-L. Zhang, J.-J. Feng, One-pot wet-chemical synthesis of uniform AuPtPd nano dendrites as efficient electrocatalyst for boosting hydrogen evolution and oxygen reduction reactions, Int. J. Hydrogen Energy 43 (2018) 22187–22194, doi:10.1016/j.ijhydene.2018.10.120.
[54] J.S. Jirkovský, I. Panas, E. Ahlberg, M. Halasa, S. Romani, D.J. Schiffrin, Single atom hot-spots at Au–Pd nanoalloys for electrocatalytic H_2O_2 production, J. Am. Chem. Soc. 133 (48) (2011) 19432–19441, doi:10.1021/ja206477z.
[55] J. Liu, J. Wang, F. Kong, T. Huang, A. Yu, Facile preparation of three-dimensional porous Pd–Au films and their electrocatalytic activity for methanol oxidation, Catal. Commun. 73 (2016) 22–26, doi:10.1016/j.catcom.2015.09.033.
[56] J. Zhong, D. Bin, Y. Feng, K. Zhang, J. Wang, C. Wang, Y. Du, Synthesis and high electrocatalytic activity of Au-decorated Pd heterogeneous nanocube catalysts for ethanol electro-oxidation in alkaline media, Catal. Sci. Technol. 6 (2016) 5397–5404 10.1039/C6CY00140H.
[57] C. Zhu, S. Guo, S. Dong, PdM (M = Pt, Au) bimetallic alloy nanowires with enhanced electrocatalytic activity for electro-oxidation of small molecules, J. Adv. Mater 24 (17) (2012) 2326–2331, doi:10.1002/adma.201104951.

[58] Q.-.L. Wang, R. Fang, L.-.L. He, J.-.J. Feng, J. Yuan, A.-.J. Wang, Bimetallic PdAu alloyed nanowires: rapid synthesis via oriented attachment growth and their high electrocatalytic activity for methanol oxidation reaction, J. Alloys Compd. 684 (2016) 379–388, doi:10.1016/j.jallcom.2016.05.188.
[59] X. Jiang, X. Qiu, G. Fu, J. Sun, Z. Huang, D. Sun, Y. Tang, Highly simple and rapid synthesis of ultrathin gold nanowires with (111)-dominant facets and enhanced electrocatalytic properties, J. Mater. Chem. A 6 (2018) 17682–17687, doi:10.1039/C8TA06676K.
[60] R. Cao, T. Xia, R. Zhu, Z. Liu, J. Guo, G. Chang, Y. He, Novel synthesis of core-shell Au-Pt dendritic nanoparticles supported on carbon black for enhanced methanol electro-oxidation, Appl. Surf. Sci. 433 (2018) 840–846, doi:10.1016/j.apsusc.2017.10.104.
[61] K.H. Choi, K.S. Lee, T.Y. Jeon, H.Y. Park, N. Jung, Y.H. Chung, Y.E. Sung, High alloying degree of carbon supported Pt-Ru alloy nanoparticles applying anhydrous ethanol as a solvent, Electrochem. Sci. Technol. 1 (2010) 19–24.
[62] Y. Liang, J. Li, Q.C. Xu, R.Z. Hu, J.D. Lin, D.W. Liao, Characterization of composite carbon supported PtRu catalyst and its catalytic performance for methanol oxidation, J. Alloys Compd. 465 (2008) 296–304.
[63] Z.L. Wang, J.M. Yan, H.L. Wang, Y. Ping, Q. Jiang, Au@Pd core–shell nanoclusters growing on nitrogen doped mildly reduced graphene oxide with enhanced catalytic performance for hydrogen generation from formic acid, J. Mater. Chem. A (1) (2013) 12721–12725.
[64] J. Wang, P. Zhang, Y. Xiahou, D. Wang, H. Xia, H. Möhwald, Simple synthesis of Au–Pd alloy nanowire networks as macroscopic, flexible electrocatalysts with excellent performance, ACS Appl. Mater. Interfaces 10 (1) (2018) 602–613, doi:10.1021/acsami.7b14955.
[65] R. Kottayintavida, N.K. Gopalan, Pd modified Ni nanowire as an efficient electro-catalyst for alcohol oxidation reaction, Int. J. Hydrogen Energy 45 (2020) 8396–8404, doi:10.1016/j.ijhydene.2020.01.006.
[66] JL. T, J. D, M. Arvee, SL. Chua, J. S, S. S, BJV. T, H. Kim, Preparation and characterization of palladium-nickel on graphene oxide support as anode catalyst for alkaline direct ethanol fuel cell, Appl. Catal. A Gen. 531 (2017) 29–35 https:// doi:, doi:10.1016/j.apcata.2016.11.034.
[67] Y. Zhao, X. Yang, J. Tian, F. Wang, L. Zhan, Methanol electro-oxidation on Ni@Pd core-shell nanoparticles supported on multi-walled carbon nanotubes in alkaline media, Int. J. Hydrogen Energy 35 (8) (2010) 3249–3257, doi:10.1016/j.ijhydene.2010.01.112.
[68] A. Thota, K. Boga, R. Narayan, S. Bojja, C.R.K Rao, Synthesis of star shaped electroactive, LEB state aniline oligomer and its high performing Pt and Pt-Au nanocatalyst for MOR, Int. J. Hydrogen Energy. 44 (2019) 11066–11078, doi:10.1016/j.ijhydene.2019.02.207.
[69] R.T. Magal, V. Selvaraj, A comparative study for the electrocatalytic oxidation of alcohol on Pt-Au nanoparticle-supported copolymer-grafted graphene oxide composite for fuel cell application, Ionics (Kiel) 24 (5) (2017) 1439–1450, doi:10.1007/s11581-017-2295-3.
[70] H. Mao, T. Huang, A. Yu, Surface noble metal modified PdM/C (M = Ru, Pt, Au) as anode catalysts for direct ethanol fuel cells, J. Alloys Compd. 676 (2016) 390–396, doi:10.1016/j.jallcom.2016.03.200.
[71] M.-.L. Xu, X.-.K. Yang, Y.-.J. Zhang, S.-.B. Xia, P. Dong, G.-.T. Yang, Enhanced methanol oxidation activity of Au@Pd nanoparticles supported on MWCNTs functionalized by MB under ultraviolet irradiation, Rare Metals 34 (1) (2014) 12–16, doi:10.1007/s12598-014-0400-6.
[72] X. Wang, B. Tang, X. Huang, Y. Ma, Z. Zhang, High activity of novel nanoporous Pd–Au catalyst for methanol electro-oxidation in alkaline media, J. Alloys Compd. 565 (2013) 120–126, doi:10.1016/j.jallcom.2013.02.170.
[73] Z. Yin, M. Chi, Q. Zhu, D. Ma, J. Sun, X. Bao, Supported bimetallic PdAu nanoparticles with superior electrocatalytic activity towards methanol oxidation, J. Mater. Chem. A (1) (2013) 9157–9163, doi:10.1039/C3TA11592E.
[74] Y. Kwon, Y. Kim, J.W. Hong, Y. Whang, S. Kim, D.H. Wi, H.R. Byon, S.W. Han, One-pot production of ceria nanosheet-supported PtNi alloy nanodendrites with high catalytic performance toward methanol oxidation and oxygen reduction, J. Mater. Chem. A 8 (2020) 25842–25849 https://doi:, doi:10.1039/D0TA09310F.
[75] Z. Li, X. Jiang, X. Wang, J. Hu, Y. Liu, G. Fu, Y. Tang, Concave PtCo nanocrosses for methanol oxidation reaction, Appl. Catal. B Environ. (2020) 119135 https://doi:, doi:10.1016/j.apcatb.2020.119135.
[76] M. Li, Y. Wang, J. Cai, Y. Li, Y. Liu, Y. Dong, S. Li, X. Yuan, X. Zhang, X. Dai, Surface sites assembled-strategy on Pt–Ru nanowires for accelerated methanol oxidation, Dalton Trans. 49 (2020) 13999–14008, doi:10.1039/D0DT02567D.
[77] D.H. Lim, D. Choi, W.D. Lee, H.I. Lee, A new synthesis of a highly dispersed and CO tolerant PtSn/C electrocatalyst for low-temperature fuel cell; its electrocatalytic activity and long-term durability, Appl. Catal. B Environ 89 (2009) 484–493 https://doi:, doi:10.1016/j.apcatb.2009.01.011.
[78] L. Huang, X. Zhang, Q. Wang, Y. Han, Y. Fang, S. Dong, Shape-control of Pt-Ru nanocrystals: tuning surface structure for enhanced electrocatalytic methanol oxidation, J. Am. Chem. Soc. 140 (2018) 1142–1147 https:// doi:, doi:10.1021/jacs.7b12353.